THE SOUTHERN MARGIN OF FLEMISH CAP, OFFSHORE NEWFOUNDLAND: PROCESSING AND INTERPRETATION OF SEISMOLOGICAL DATA PROVIDE INSIGHTS INTO THE RIFTING EVOLUTION

JULIE ANN SMITH

THE SOUTHERN MARGIN OF FLEMISH CAP, OFFSHORE NEWFOUNDLAND: PROCESSING AND INTERPRETATION OF SEISMOLOGICAL DATA PROVIDE INSIGHTS INTO THE RIFTING EVOLUTION

by

© Julie Ann Smith

A thesis submitted to the

School of Graduate Studies

in partial fulfillment of the

requirements for the degree of

Masters of Science

Earth Science/Memorial University of Newfoundland/Faculty of Science

Memorial University of Newfoundland

April, 2008

St. John's Newfoundland

Abstract

The Newfoundland/Iberia conjugate continental margins developed during Jurassic and Cretaceous time. They are good places to study rifted margins since they are non-volcanic, so that extensional crustal structures are not altered or obscured by magmatic processes. The "ERABLE" seismic reflection survey was recorded in the Newfoundland basin by the Geological Survey of Canada and IFREMER in 1992. I have processed and interpreted three ERABLE profiles extending from the southern margin of Flemish Cap extending into the Newfoundland Basin. Various types of noise such as multiples and side scattered reflections posed challenges for producing a seismic section that represents subsurface reflectivity. F-k and radon filters improve the signal to noise ratio in deep water, but were less successful in the shelf region of the Flemish Cap.

The final processed lines have provided a more comprehensive data coverage along the southern margin of Flemish Cap. Combining these data with SCREECH seismic profiles, two ODP drill sites, and other geophysical data have allowed the mapping of distinct zones of continental, transitional, and oceanic crust in this region. I compare these results to crustal boundaries on the Iberia margin that are well constrained from detailed seismic and drilling.

My results indicate asymmetry in the conjugate pair, with the zone of extended continental crust and transitional crust being much wider on the Iberian margin compared to the Newfoundland margin. Also, there is evidence of possible detachment faulting on both margins, although less wide spread on the Newfoundland margin. I propose either a

simple shear or simple shear/pure shear combination model involving a westward dipping detachment fault, with the Newfoundland margin acting as the upper plate.

However, the Newfoundland margin has a long and complex rifting history that cannot be explained by only 2-D rifting models, thus a Late Jurassic to Early Cretaceous rifting and break-up model is presented as an attempt to account for the present day structure of the southern margin of Flemish Cap.

Acknowledgements

First and foremost, I would like to thank Dr. Jeremy Hall for all of his guidance and support that played a key role in the fabrication of my thesis. Without the immeasurable aid that he eagerly provided, the success of my research could not have been possible. Second, I would like to thank Sharon Deemer for the countless hours of one on one instruction that she so willingly offered her talent in seismic processing. I would also like to thank Dr. Charles Hurich, who is part of my supervisory committee. His suggestions and editing of my work has been an important step to producing a polished product.

I would like to thank Dr. Michael Enachescu, Dr. Charles Hurich, and Dr. Toby Rivers who taught courses as part of my Masters program and advanced my understanding of various tectonic regimes. Thank you to both Dr. Brian Tucholke and Dr. Shri Srivastava, who have a vast amount of knowledge in this project area, and contributed pertinent discussions and ideas. I greatly appreciate the technical computer support provided by Daniel Vasiliu, Clyde Clements, Phil Baluk, and Anthony Kocurko. Financial support provided by NSERC and the School of Graduate Studies has allowed the project to be undertaken and completed. Thanks to GSC (Dr. Dr. Shri Srivastava) and IFREMER (Dr. J. C. Sibuet) who kindly provided the ERABLE seismic data, and Landmark Graphics Corporation for the use of their 2D processing software.

Thanks to all my professors, TA's, and fellow students for making my experience at Memorial intellectually inspiring and fun. Finally, I would like to thank my parents

and friends for their support during this project. Everyone mentioned has played a vital role in my research presented here before you.

Table of Contents

List of Tables

List of Figures

List of Plates

List of Abbreviations

AGC:	Automatic Gain Control
CDP:	Common Depth Point
ER54:	Erable Line 54
ER 56:	Erable Line 56
EU:	Eurasia
FFID:	Field File Identification
FGP:	Frontier Geoscience Project
GSC:	Geological Survey of Canada
IB:	Iberia
IFP:	Institut Francais du Petrole
IFREMER:	French Research Institute for Exploitation of the Sea
MCS:	Multi-Channel Seismic
NMO:	Normal Moveout
ODP:	Ocean Drilling Program
PR:	Peridotite Ridge
RMS:	Root Mean Square
RRR:	Ridge-Ridge-Ridge type triple junction
S1:	Low roll off slope used for Butterworth filter in dB/octave
S2:	High roll off slope used for Butterworth filter in dB/octave
SCREECH:	Study of Continental Rifting and Extension on the Eastern Canadian Shelf
SCR1:	SCREECH Transect 1

SCR104: SCREECH Line 104

SCR2: SCREECH Transect 2

SCR3: SCREECH Transect 3

T1: Low relief and reflectivity transitional basement interpreted as containing exhumed serpentinized peridotite

T2: Moderate to high relief transitional basement interpreted as containing serpentinized peridotite ridges

T_{OC}: Transitional Thin Ocean Crust

S/N: Signal to Noise

TWT: Two Way Travel Time

UTM: Universal Transverse Mercator

List of Appendices

Chapter 1: Introduction and Background of Study Area

1.1 Introduction and Scope

The study of rifting and ocean spreading processes are of interest to the scientific community (e.g., Whitmarsh and Wallace, 2001; Hart and Blusztajn, 2006; Hopper et al., 2006; Lau et al., 2006a; Lau et al., 2006b; Müntener and Manatschal et al., 2006; Shillington et al., 2006; Van Avendonk et al., 2006). Understanding these processes requires a thorough study of lithospheric mechanical behavior on both sides of a conjugate margin. Magmatic activity can intrude and obscure pre-existing crustal structures, and also make seismic imaging of these structures difficult. Since the Newfoundland-Iberia conjugate margin (Figure 1.1) is for the most part non-volcanic, this makes it a desirable location to study rifting processes.

The transition zone between continental and oceanic crust is well constrained on the Iberia margin from both seismic and drilling data. The transition zone within the Newfoundland basin has been explored in less detail, but is the focus of recent studies (e.g. Funck et al., 2003; Hart and Blusztajn, 2006; Hopper et al., 2004; Hopper et al., 2006; Lau et al., 2006a; Lau et al., 2006b; Müntener and Manatschal et al., 2006; Sibuet et al., 2007; Shillington et al., 2006; Van Avendonk et al., 2006). It is the aim of this project to use various types of geophysical and drilling data to gain a better understanding of the evolution and formation of the Newfoundland Basin, with emphasis on the southern margin of Flemish Cap (Figure 1.2). Placing boundaries on continental, transitional, and oceanic crust is the first step in approaching this problem. Defining the boundaries of different crustal zones provides valuable geometrical constraints on rifting.

The results from this work will then be compared with those on the Iberian margin to investigate various styles of rifting.

The study area includes the eastern Grand Banks and the southern margin of Flemish Cap extending into the deeper waters of the Newfoundland Basin. The primary data set used in this study is from the "Erable" seismic reflection survey, which was

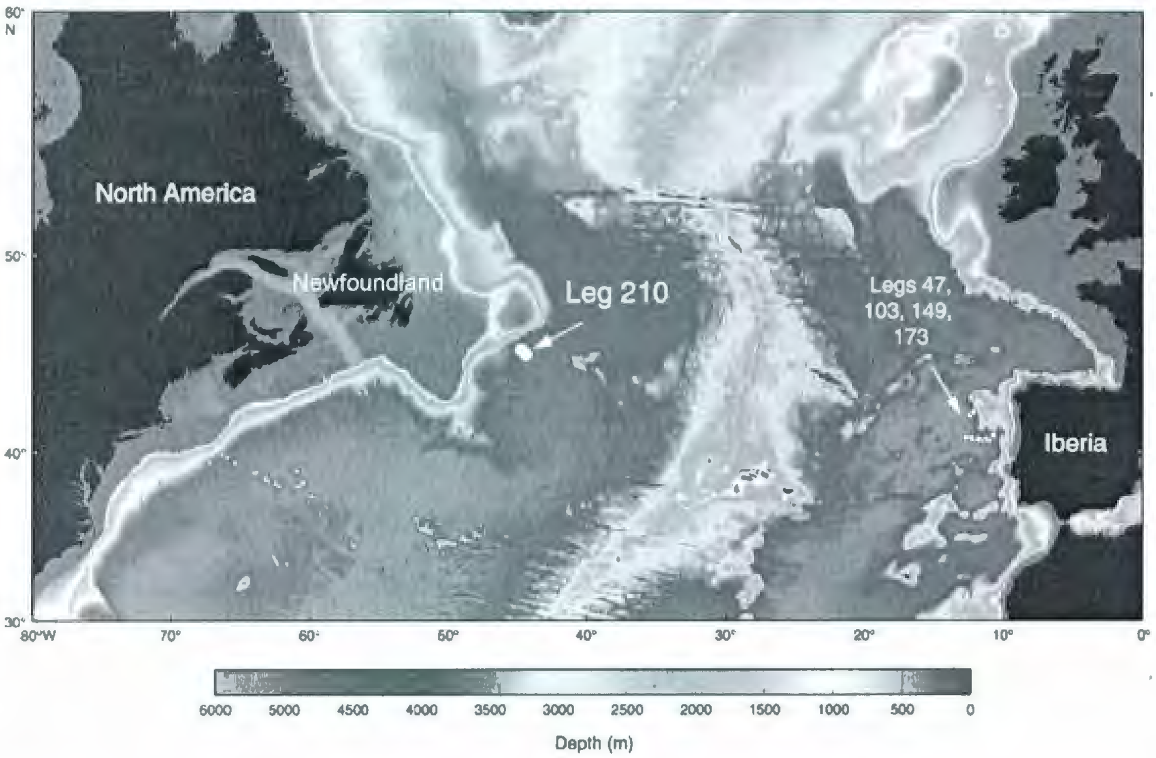

Figure 1.1: Map of North Atlantic Bathymetry showing the Newfoundland and Iberia conjugate margins (modified from Shipboard Scientific Party, 2004a). Ocean drilling locations from Leg 47, 103, 149, 173 (Iberia margin) and 210 (Newfoundland margin) are illustrated.

recorded by the Geological Survey of Canada (GSC) and IFREMER (French Research Institute for Exploitation of the Sea) in 1992 for the purposes of proposing a drill site for the Ocean Drilling Program (ODP). These seismic data have not been processed and published in open literature. Three lines of multi-channel seismic reflection data, totaling about 485 km, from this survey were processed using extensive multiple removal techniques: Line 53, 54, and 56. A detailed interpretation of these data adds to the existing data coverage within this area, which includes geophysical data from

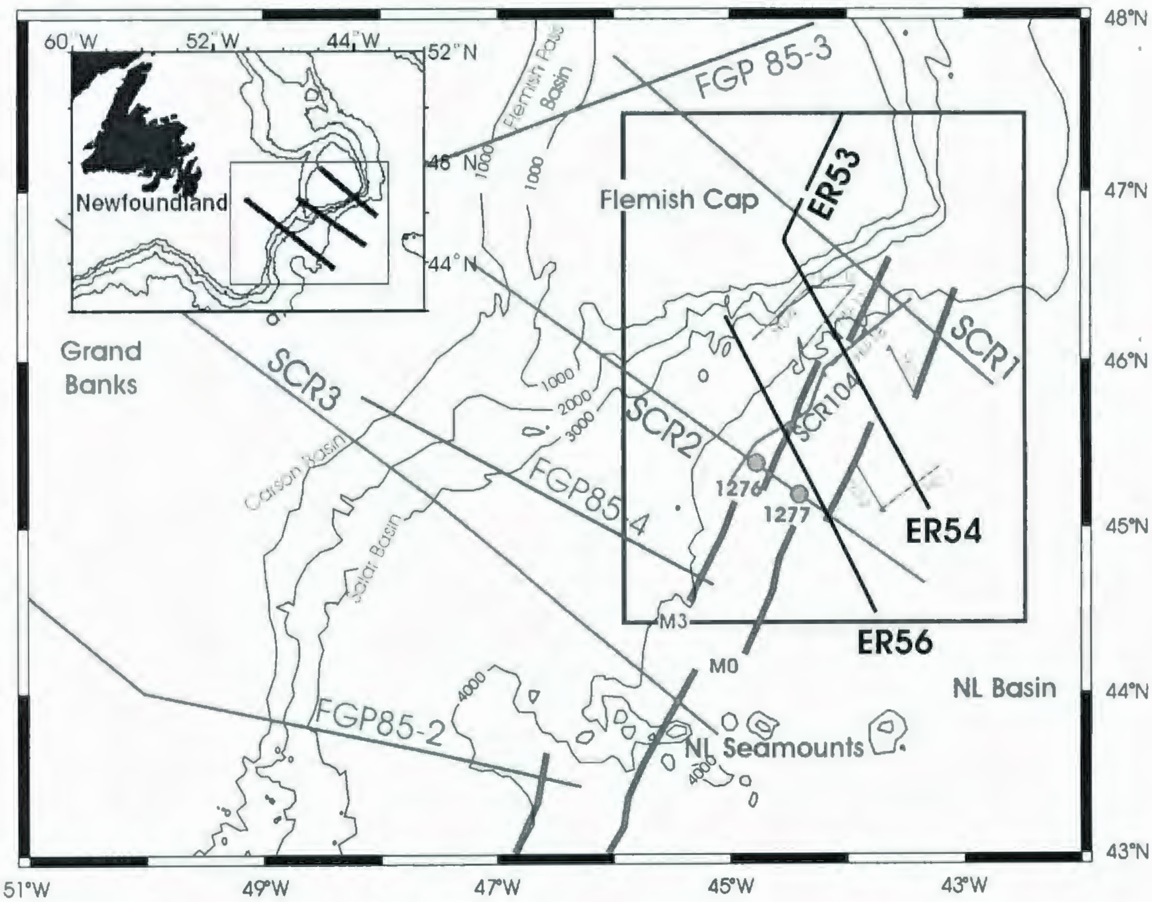

Figure 1.2: Map showing bathymetry and data coverage used for interpretation (Modified from Lau et al., 2006b) with the red rectangle outlining the project area. SCREECH survey transects are outlined in blue, Frontier Geoscience Project (FGP) transects are outlined in purple, GSC wide-angle refraction lines collected in the CSS Hudson 85-025 cruise are outlined in green, ODP drill sites from Leg 210 are outlined in orange, and Erable survey transects are outlined in black. Interpretation of magnetic anomalies M0 and M3 are taken from Srivastava et al. (2000) and shown with purple solid lines.

the SCREECH (Study of Continental Rifting and Extension on the Eastern Canadian Shelf) survey, wide-angle seismic refraction data collected by the GSC in 1985, and two sites (1276 and 1277) drilled by the Ocean Drilling Program (ODP) during Leg 210 in 2003 (Figure 1.2).

1.2 Geology of the Flemish Cap Continental Crust

Just east of the northern Grand Banks and southeast of the Orphan Basin lies a detached fragment of continental crust. This submarine knoll consists of Hadrynian (Late Proterozic) rocks that are exposed in its core, and otherwise are surrounded and onlapped by a very thin cover of Mesozoic and Cenozoic sediments (King et. al, 1985). These sediments are folded and faulted along the west to southwest edge of Flemish Cap, and are relatively undisturbed elsewhere. Flemish Cap has a sub-circular shape and is fairly flat along the top and covered by less than 200 m of water. Coring bedrock was performed by Bedford Institute of Oceanography using an electric drill that could penetrate up to 6 m. Samples were collected in areas of mapped acoustic basement and was unsuccessful in areas where basement had Quaternary surficial cover. Complete sample coverage of basement could not be obtained for this reason.

Sampling results did show that a large portion of Flemish Cap consists of pink, medium-grained granodiorite and minor granite (Figure 1.3; King et. al, 1985). However, not all cores recovered these types of rocks. One core recovered dacite and the other a volcanically-derived siltstone, suggesting that mapped acoustic basement is not homogeneous. Basement rocks of Flemish Cap are correlated with Hadrynian rocks of the Avalon terrane based on lithology. This is not surprising since much of the continental shelf off Newfoundland consists of Avalon terrane (King et al., 1986) that is the most easterly tectonostratigraphic zone of the Appalachian Orogeny (Williams and

Hatcher, 1982). Typically this terrane consists of "late Proterozoic volcanic, sedimentary, and intrusive rocks overlain by early to mid Paleozoic marine and terrestrial sediments" (King et al., 1986). Geochronological analysis of granodiorite from drill core does however suggest that these rocks represent an older part of the Avalon terrane (King et al., 1985).

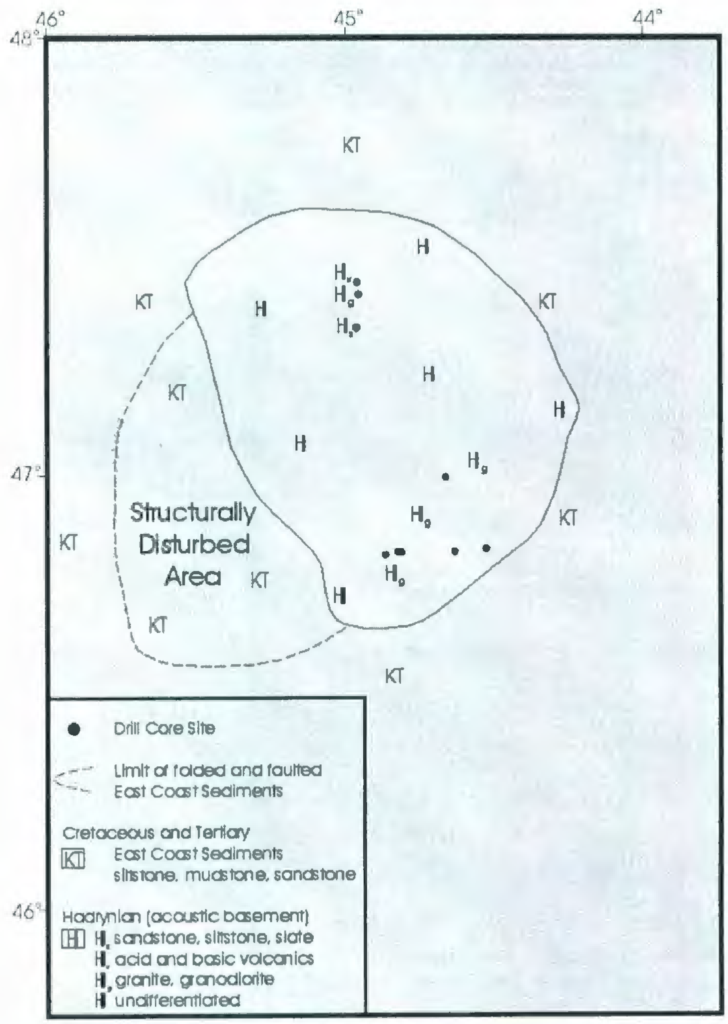

Figure 1.3: Geological map of the Flemish Cap area (after King et. al, 1985).

1.3 Rifting History

As illustrated in multiple plate reconstructions of M0 time, the southern margin of Flemish Cap is conjugate with Galicia Bank off the western Iberia margin (e.g., Srivastava et al., 2000). Opening of the North Atlantic occurred with progressive rifting moving to the north. The Flemish Cap continental block is affected by 3 phases of rifting, where the first two phases are significant with respect to the opening between the Grand Banks and Iberia (Tucholke et al., 1989; Hopper et al., 2006).

The first stage of rifting occurred in the Late Triassic to Early Jurassic between Nova Scotia and Africa while forming northeast-southwest trending basins on both the Grand Banks and Iberia Margin (Grant and McAlpine, 1990; Hopper et al., 2006). Final breakup between Nova Scotia and Africa occurred in the Middle Jurassic, where spreading was accommodated along the Newfoundland fracture zone until Early Cretaceous time (Tankard and Welsink, 1989).

The second major rifting phase started in the Late Jurassic (late Callovian or Kimmeridgian) between the Grand Banks and Iberia, and continued until final breakup occurred in the late Early Cretaceous (Barremian-Aptian) (Tucholke et al., 1989; Grant and McAlpine, 1990). At this time separation between the southwest margin of Flemish Cap and Galicia Bank occurred (Tucholke et al., 1989; Hopper et al., 2006). This rifting phase is associated with a period of uplift and erosion along the Grand Banks forming a number of unconformities (Tucholke et al., 1989). Since many of these unconformities tend to coalesce at basin margins, unconformities that are associated with this rifting phase are generally termed the Avalon Unconformity (Grant and McAlpine, 1990).

The third phase of rifting occured in the Late Cretaceous and is responsible for the opening of the Labrador Sea. It is during this period that final separation occured between the northeast margin of Flemish Cap and the Goban Spur (Graciansky et al., 1985; Tucholke et al., 1989; Hopper et al., 2006).

Sibuet et al. (2007a) hypothesize that Flemish Cap was located in the East Orphan Basin prior to the second stage of rifting. In fact, it is believed that Flemish Cap has rotated 43° clockwise (with respect to Iberia) and displaced 200-300 km southeast (with respect to NA) during M25-M0 time (Late Jurassic to early Aptian), yet has remained attached to North America (Sibuet et al., 2005). This idea is based on plate reconstructions at M0 time using Bouguer gravity anomalies from both sides of the Atlantic Ocean (Figure 1.4). Note that at chron M0, a major triple junction existed involving spreading in the North Atlantic and Bay of Biscay. This separated the North American (NA), Iberian (IB), and Eurasian (EU) tectonic plates into 3 rift branches: 1) NA/IB, 2) IB/EU (Bay of Biscay), and 3) NA/EU plates (e.g., Sibuet and Collette, 1991; Sibuet et al., 2004). Looking at the rift arm between NA/IB From Figure 1.4, the continental margin of Grand Banks and Iberia can be described as approximately parallel southwest of Flemish Cap (or have similar geometries) (Sibuet et al., 2007a). However, the southern margin of Flemish Cap makes a 43° angle with its conjugate Galicia Bank, providing evidence of its movement prior to chron M0 time. Since onset of rifting between the Grand Banks and Iberia occurred close to chron M25 time (Late Jurassic), this would allow one to constrain the movement of Flemish Cap to occur between the M25-M0 period.

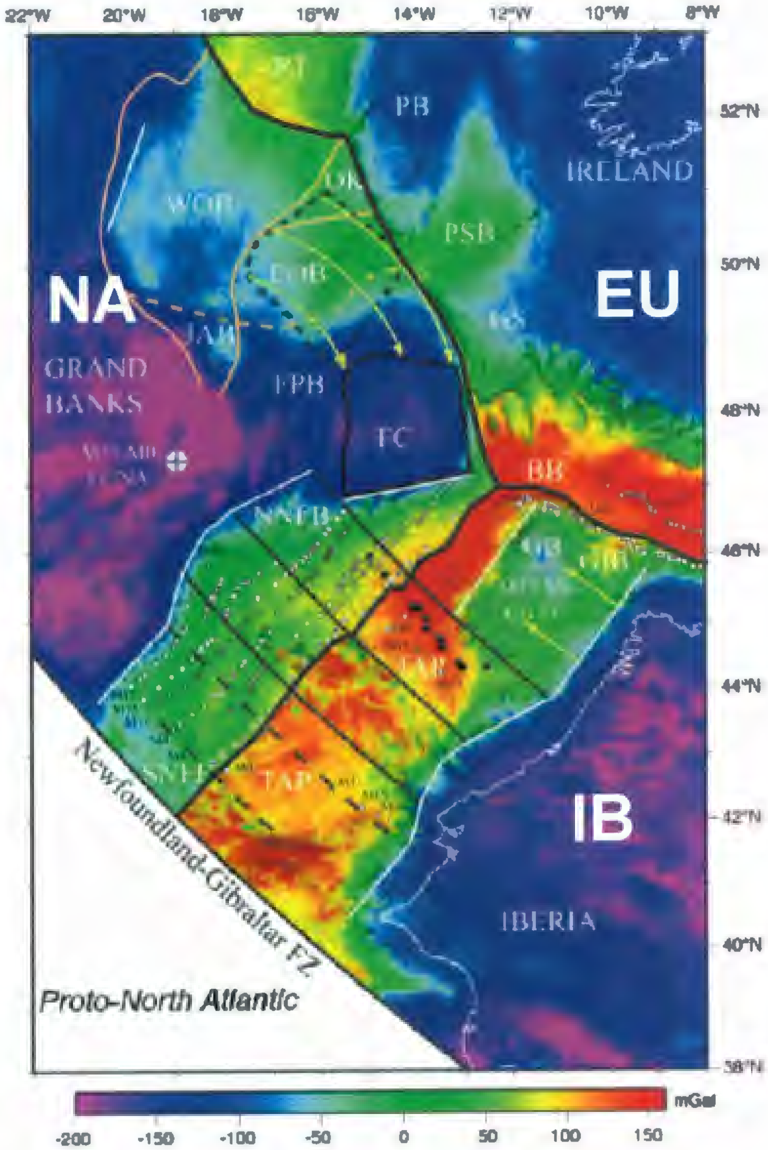

Figure 1.4: Modified after Enachescu et al. (2005). Plate reconstruction at M0 time using Bouguer gravity anomalies. Note the triple junction that exists between the North American (NA), Iberian (IB), and Eurasian (EU) tectonic plates.

1.4 Data from the Newfoundland Margin

1.4.1 FGP Multi-Channel Seismic and GSC Refraction/Wide-Angle Reflection

The GSC has obtained deep multi-channel seismic reflection data along offshore eastern Canada as part of the Frontier Geoscience Project (FGP). The FGP project involved the collection of over 6800 km of data between 1984 and 1990, where 3 lines, 85-2, 85-3, and 85-4 lie near or within this project area (Figure 1.5).

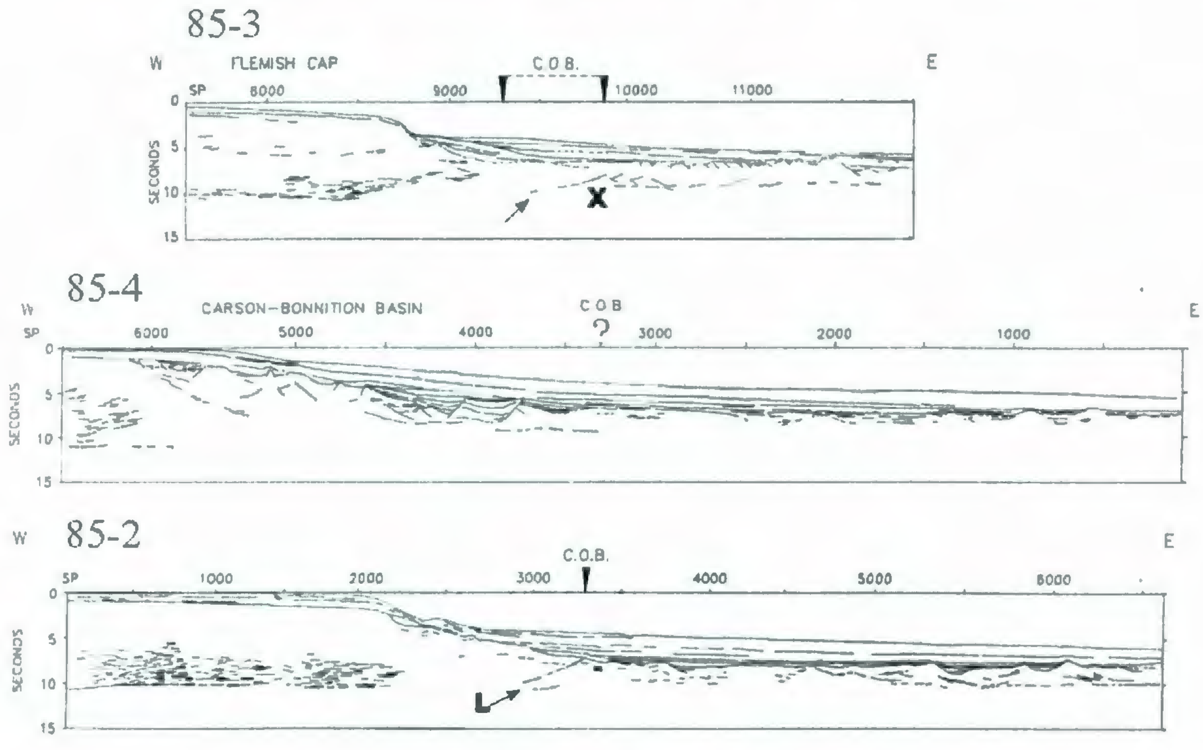

Figure 1.5: Line drawings of MCS reflection profiles 85-2, 85-3, and 85-4 from the Frontier Geoscience Project running perpendicular to the continental margin (from Keen and de Voogd, 1988). See Figure 1.2 for the location map of these profiles. Note the landward dipping reflector denoted L on profile 85-2. A landward dipping reflector is also imaged on profile 85-3. East of the landward dipping reflector on profile 85-3 are segmented dipping reflectors that are denoted X. C.O.B = Continent Ocean Boundary.

Between 1983 and 1992, the GSC has conducted multiple seismic refraction/wide-angle reflection surveys, and many of these surveys coincide with the location of FGP seismic reflection lines. This is done to provide velocity constraints for the seismic reflection data.

Previous interpretations suggested that the change from the continental to oceanic domain was represented by a sharp boundary (Keen and de Voogd, 1988), as opposed to present interpretations that recognize a transitional zone between the two (e.g., Funck et al., 2003; Hopper et al., 2004; Hopper et al., 2006; Lau et al., 2006a; Lau et al., 2006b; Shillington et al., 2006; Van Avendonk et al., 2006). Keen and de Voogd (1988) provided an interpretation of the FGP seismic reflection data collected along the Atlantic margin extending from the southeastern Grand Banks into the Orphan Basin. Here they use additional characteristics to help locate the continent-ocean boundary. These characteristics include defining ocean crust by the absence of syn-rift sediments, a rough basement surface with 0.5-1s relief, and crustal thickness less than 10 km thick (where 7-8 km is presently considered an average normal ocean crust thickness (Fowler, 2005, p.1)). They did recognize problems with using some of these characteristics, such as some ocean spreading environments produce smooth basement crust, and crust less than 10 km may simply represent thinned continental crust.

In addition to these criteria discussed above, a predominant landward dipping reflector was used locate the continent-ocean boundary on line 85-2 (Keen and de Voogd, 1988). This feature called the "L Reflector" is located at the base of the slope and appears to separate two regions that have very different seismic character, inferred to represent continental crust to the west, and ocean crust to the east (Figure 1.5). A similar feature is also recognized on the near by SCR3 seismic reflection line, where the lower part of the reflection corresponds with a increase in velocity to 7.6-7.9 km/s, interpreted as the top of partially serpentinized mantle (Lau et al., 2006a; Lau et al., 2006b). It is also possible that this reflection is produced by a shear zone that aids in the exhumation of mantle further seaward, as the thinned and faulted continental crust allows the penetration of seawater and serpentinization of upper mantle (Lau et al., 2006b).

Line 85-3 is collected across Flemish Cap extending northeastwards across the slope and into deep water (>5s) (Keen and de Voogd, 1988). Beneath the shelf, bright reflections from lower continental crust are well imaged, and rise beneath the slope where crust thins. Here the base of these reflections is interpreted to represent Moho. On this line, the location of the continent-ocean boundary was chosen based on the presence of a continuous landward dipping reflection that corresponds with a positive magnetic anomaly. East of this boundary within assumed oceanic crust lies a set of discontinuous landward dipping reflections, named "X-reflectors", that occur about 7 km below the top of basement.

A seismic refraction survey was undertaken over a section of FGP profile 85-3 to investigate the nature of these X-reflectors (Reid and Keen, 1990). Results from this experiment yield a 4.5 km/s velocity, likely representing the top of layer 2 oceanic crust, above a 7.4 km/s velocity that is associated with the strong X-reflections. Here it is assumed that these X-reflections are produced from the mafic lower crust.

The northeast margin of Flemish Cap was reconstructed with its conjugate margin, the Goban Spur located offshore United Kingdom, at the inferred time of rifting (Keen et al., 1989). This was achieved by joining the 85-3 profile with a deep multichannel seismic reflection profile, WAM, at the assumed continent-ocean boundaries for the Flemish Cap and Goban Spur margins respectively. Here rifting structures west of Flemish Cap are not included within the study using the assumption that these features were produced by an earlier failed rift system. Results from this study favored the interpretation that rifting was accommodated through ductile stretching of the lower lithosphere and brittle faulting in the upper lithosphere.

FGP profile 85-4 was acquired across the Carson-Bonnition Basin, which is a shelf edge basin, extending into the deep water of the Newfoundland Basin (Figure 1.6; Keen and de Voogd, 1988). Resolving deep crustal or Moho reflections in the slope area was unsuccessful, which may be a result of the inability to image through broken-up and discontinuous sediments. The inferred continent-ocean boundary is positioned where syn-rift sediments are no longer imaged. Seaward of this there is no evidence of rotated fault blocks and basement reflections are more typical of a rough basement surface supporting the interpretation of ocean crust in this area.

A further investigation of the Carson-Bonnition Basin was conducted by collecting seismic refraction data to provide velocity control within the basin (Reid and Keen, 1988). Results indicate a 4.5 km/s layer on top of a 6.0 km/s basement surface. It is postulated that the 4.5 km/s refracted arrivals are produced by either Mesozoic syn-rift sediments, or upper Paleozoic sediments.

1.4.1.1 GSC Seismic Refraction: CSS Hudson Cruise 85-025

The GSC conducted a seismic refraction survey in 1985 along the southern margin of Flemish Cap (see Figure 1.2 for location) for the purposes of providing deep crustal information on the structure of the ocean-continent boundary (Todd and Reid, 1989). This experiment utilized two 16.4 and 32.8 L air guns, and 6 ocean bottom seismometers (OBS). From these data, velocity-depth models where derived from iteratively fitting computed travel times to the refraction records to obtain the best fit with the most simplistic model (Figure 1.6).

Refraction lines HU-9, HU-10, and HU-11 all have a 6.0 km/s velocity layer with a low gradient, providing evidence of continental crust. Line HU-6 has a less than 4 km thick 4.0-4.5 km/s velocity layer, and is missing layer 3 velocities (Todd and Reid, 1989). From this observation, some have interpreted an oceanic fracture zone, despite the fact that there are no clear linear trends in the magnetic or gravity data (Todd and Reid, 1989). A strong 7.3 km/s refracted arrival is recognized on HU-18, HU-1, and HU-2, and these lines are interpreted to lie within the oceanic crust domain.

Results of the refraction experiment led to the interpretation that the southern margin of Flemish Cap formed an "oblique sheared margin", as Iberia moved eastward along the margin (Todd and Reid, 1989).

These refraction data were obtained in very close proximity to Erable Line 54, and will thus be used in Section 3.2.5 to provide velocity control on the seismic reflection data. Since final Erable lines are presented as time sections, velocity-depth models from Todd and Reid (1989) are converted to velocity-time models (Appendix 1). Location of

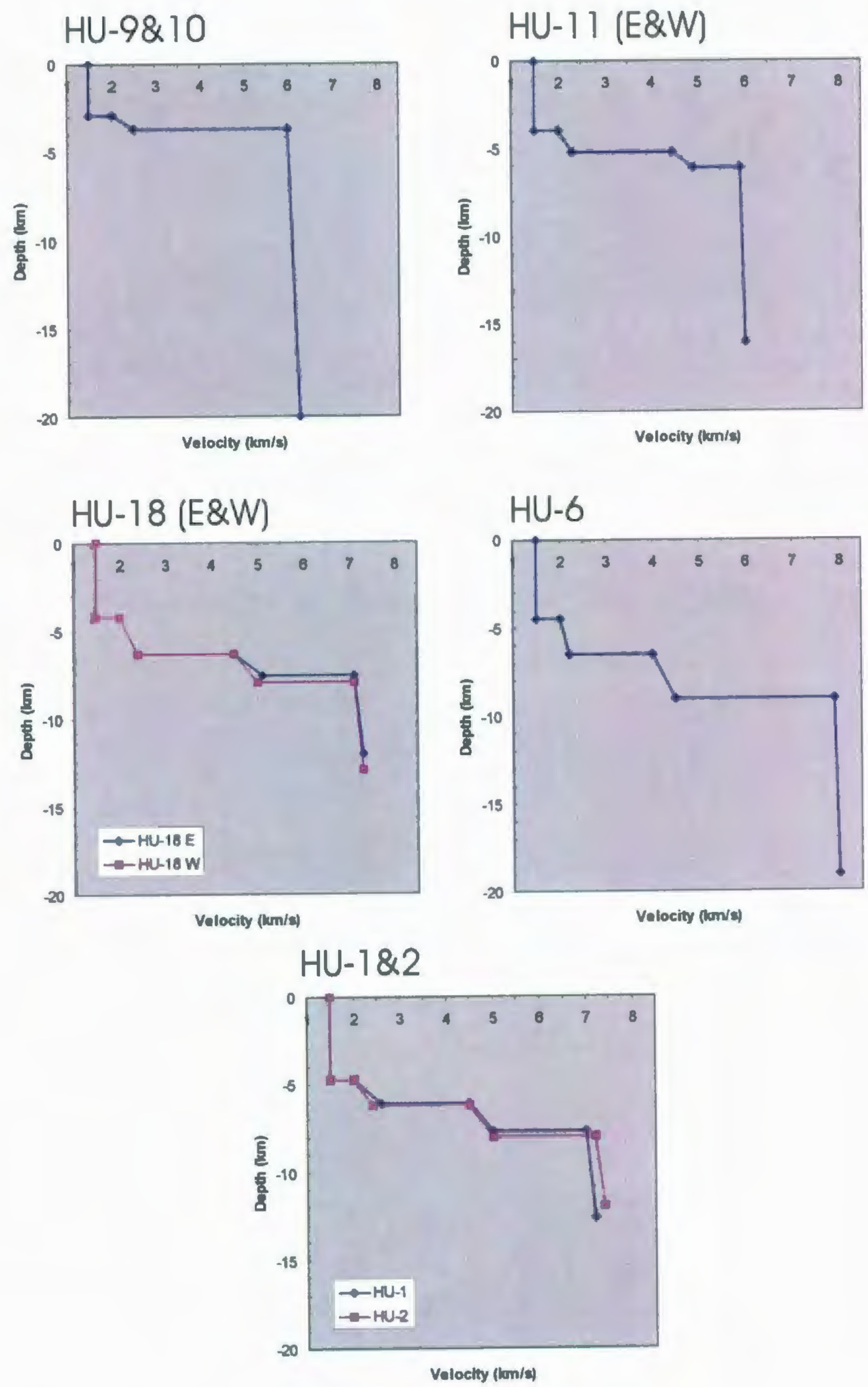

Figure 1.6: P-wave velocity verses depth models from the CSS Hudson Cruise 85-025 seismic refraction experiment (after Todd and Reid, 1989).

OBS's are projected onto the Erable Line 54 and corresponding velocity-time models are overlain onto final migrated sections (Plate 2e).

1.4.2 SCREECH Survey

The SCREECH survey collected seismic reflection and refraction, magnetic, gravity, and multi-beam bathymetric data along the eastern Grand Banks in July-August 2000 (Funck et al., 2003; Hopper et al., 2004; Hopper et al., 2006; Lau et al., 2006a; Lau et al., 2006b; Shillington et al., 2004; Shillington et al., 2006; Van Avendonk et al., 2006). Data from this survey were used to propose a site location for the Ocean Drilling

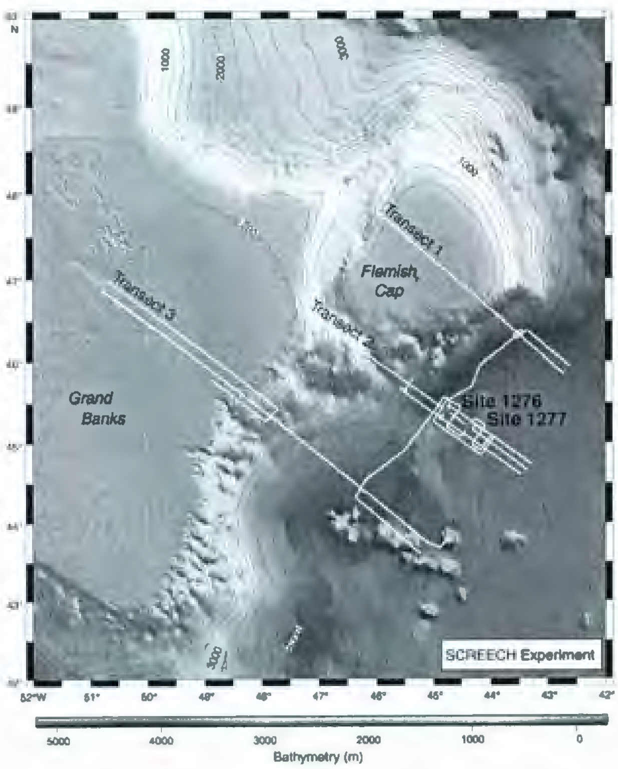

Figure 1.7: Bathymetric map of the Newfoundland margin showing location of Transect 1, 2, and 3 from SCREECH survey, and the two ODP locations that were subsequently drilled during Leg 210, Site 1276 and 1277 (From Shillington et al., 2004).

Program (ODP). There were 3 main objectives of the study, 1) to determine the composition of the transitional crust which lies between unequivocal ocean crust and continental crust, 2) to compare the crustal structures of the Newfoundland margin with the conjugate Iberia margin to gain a better understanding of the rifting process, and 3) acquire data for the purposes of selecting and proposing an ODP drill site within the Newfoundland Basin. These data were collected along 3 major transects (Figure 1.7), where transect 1 and 2 lie near the Erable profiles 54 and 56 and are used to aid in the interpretation of these lines. Transect 1 lies over the Flemish Cap extending into deep water on its southern margin, and Transect 2 lies over the location of the ODP drilling sites 1276 and 1277. An interpretation of the crustal boundaries of Screech Transects 1, 2, and 3 is given in Chapter 3.

1.4.3 Ocean Drilling Program Leg 210

1.4.3.1 Site 1276

The ODP drilled two sites on the Newfoundland margin during Leg 210 in 2003. The main objective was to examine deep basement structures to gain an understanding of the rifting evolution between Newfoundland and Iberia, with particular interest in the transitional crust (Tucholke et al., 2004). A secondary objective was to look at the shallower stratigraphy and postrift sedimentation to study the Cretaceous paleoceanography between Newfoundland and Iberia. The first location was drilled in a water depth of 4549.1 m on presumed transitional crust at Site 1276 (Figure 1.7). Here 85% core recovery was achieved over an interval of 800- 1736.9 mbsf. Sediments consisted of mostly bioturbated clay and mudstones, with interbedded gravity-flow deposits. Unfortunately drilling at this site did not reach basement, and bottomed out in diabase sills that have intruded Albian to Aptian sediments approximately 100-200 m above the anticipated depth of basement surface.

1.4.3.1.1 Mafic Sills: The U-Reflector

The diabase sills recovered from the ODP Site 1276 provide important information regarding the post rift magmatism history of the Newfoundland Basin (Tucholke and Sibuet, 2007). These mafic sills intrude uppermost Aptian to lowermost Albian sediment. Out of the two separate diabase sills recovered, the upper sills correspond with the U-reflector imaged on the SCR2 seismic reflection profile. The U-reflector is recognized as a high amplitude event that is widespread within the Newfoundland Basin, though the bright reflection is truncated by basement highs (as illustrated on Erable Line 56 (Plate 2d) SCREECH Transect 2 and Line 104 in (Plate 2b and f), also Tucholke et al., 1989). Imaging of basement or sediments below the U-event is most often unsuccessful, which could be a result of either: the seismic waves inability to penetrate through the sills, a weak impedance contrast at the basement surface, or a combination of both (Shillington et al., 2006).

In the past the U-reflector was described and mapped as an erosional unconformity or package of unconformities, that occur throughout the Aptian time, also refered to as the Avalon unconformity (Tucholke et al., 1989). In areas such as the southeastern Grand Banks and Salar Basin, the U-reflector clearly represents an unconformity (Tucholke et al., 1989), but drilling has shown that the U-reflection at Site 1276 is a result of the high impedance contrast between sediments and underlying mafic sills (Shipboard Scientific Party, 2004a). However, it is also possible that an unconformity exist at the level that the diabase sills intrude.

Geochronological dating of the sills was performed using a step-release $^{40}Ar/^{39}Ar$ method (Hart and Blusztajn, 2006). Results yield an age of ~105.3 Ma for the upper sill, and ~97.8 Ma for the lower sill, which is much younger than the assumed age of basement at this site of ~128 Ma.

1.4.3.2 Site 1277

Since basement was not penetrated at Site 1276, a second location was chosen, Site 1277 on a basement ridge named Mauzy Ridge (Shipboard Scientific Party, 2004a). This site was drilled in 4626.2 m of water in an area initially interpreted as oceanic crust (Shillington et al., 2004) and seaward of M1 (Shipboard Scientific Party, 2004a; M1 interpreted by Srivastava et al., 2000), where shallow basement penetration was successful. This site was chosen because of the thin sediment cover where the sediment thickness was estimated to be 132 m from multi-channel seismic. Because of time constraints, it was decided to drill through sediment and start coring at 100 mbsf. Drilling into hard layers coupled with recovering wash core containing gabbro and basalt fragments allows the suggestion that the basement surface could be as shallow as 85 mbsf.

Wash core and core recovered from Site 1277 has about a 60% core recovery yielding two lithological units (Müntener and Manatschal, 2006). First unit is mix of igneous and sedimentary rock from about 85-142.1 mbsf, where about half of the assemblage consists of basalt flows that are alternating with mass flows containing peridotite and serpentinized peridotite, somewhat deformed gabbroic rocks, and a small percentage of sandstones (Shipboard Scientific Party, 2004b; Müntener and Manatschal, 2006). Here the sedimentary material is interpreted as being sourced from the underlying rock units (Müntener and Manatschal, 2006). The second unit is recovered from 142.1-180.3 mbsf, representing serpentinized peridotite in-situ basement with minor veins of gabbro (Shipboard Scientific Party, 2004b; Müntener and Manatschal, 2006).

A recent geochemical study performed on the rocks recovered from Site 1277 concludes that the mafic rocks recovered from the upper unit are genetically unrelated to the underlying serpentinized peridotite basement (Müntener and Manatschal, 2006). They also suggest that the recovered serpentinized peridotites are not representative of a mid-ocean ridge environment, but acquired their geochemical signature pre-rift, and may be related to a subduction in the Caledonian, or an even older orogenic event. These rocks would have then later been exhumed to the seafloor during the rifting of the Atlantic.

1.5 Western Iberia Margin

1.5.1 Galicia Bank

ODP Leg 103 drilled Sites 637-641 in 1985 along the western margin of Galicia Bank (Shipboard Scientific Party, 1987a). Drilling at Site 637 recovered serpentinized peridotites along the North-South trending peridotite ridge (R2, Figure 1.8). This location was the first to sample mantle rocks from the ocean-continent transition zone (OCTZ), thus giving rise to theories of mantle exhumation occurring before seafloor spreading in the rifting process (Shipboard Scientific Party, 1998).

Initially the serpentinized peridotites recovered from Site 637 were interpreted to represent sub-oceanic mantle due to similarity in composition with other oceanic peridotites (Shipboard Scientific Party, 1987b), however a more detailed analysis of the petrology and structure of the sample was later performed. This led to the conclusion that these serpentinized peridotites were in fact subcontinental mantle that were exposed to the seafloor during the rifting process (Evans and Girardeau, 1988; Girardeau et al., 1988; Kornprobst and Tabit, 1988).

Multichannel seismic reflection data have been collected in the area of the Leg 103 drilling by the Institut Francais du Petrole (IFP) in 1975 and 1980. A line drawing of GP101 profile is presented in Figure 1.9 (Reston et al., 1996). From these data a prominent undulating reflection is observed called the S-reflector, first recognized by Boillot et al. (1988) and Boillot and Winterer (1988). Many different possibilities are given for the source of this reflection such as the brittle-ductile transition and the top of a large intrusion, however, the interpretation of a top to the west detachment fault is the most widely accepted (Winterer et al., 1988; Reston et al., 1996; Reston 1996; Whitmarsh et al., 1996). After combining seismic refraction data with the previously acquired reflection data, it was determined that the S-reflector is intracrustal at the eastern end of the line (landward), cuts deeper into the lower crust moving west, and nearing or reaching the crust-mantle boundary at the western end over a distance of about 20 km (Whitmarsh et al., 1996).

Adjacent to thinned continental crust is a peridotite ridge sampled during drilling Site 637 just to the north of GP101 (Figure 1.9). The dominant velocity for the

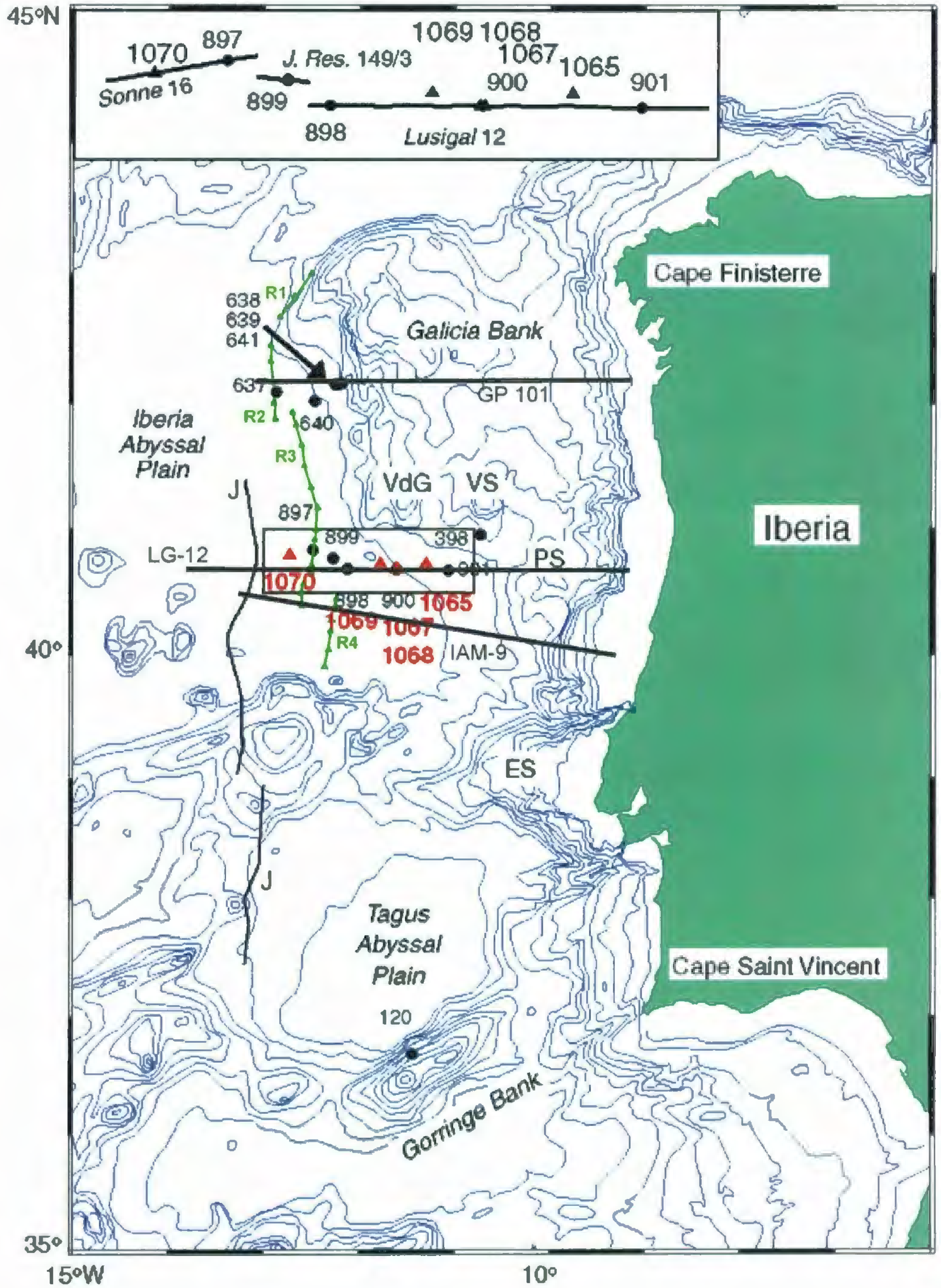

Figure 1.8: Bathymetry of the Iberia margin (After Beslier et al., 2001). Note the locations drilled by the DSDP/ODP illustrated by black circles: Site 398 from Leg 47B,

Sites 637-640 from Leg 103, and Sites 897-901 from Leg 149. Most recently, Sites 1065-1070 were drilled by the ODP during Leg 173 and are illustrated with red triangles. Inset shows the location of seismic reflection lines collected over Leg 149 and 173 drill sites used to construct line drawing in Figure 1.10. Bold lines are transects of seismic reflection and refraction data. Black line labeled J represents the J magnetic anomaly. R1, R2, R3, and R4 (in green) denote peridotite ridges sampled and identified on seismic data (Beslier et al., 1993). VdG = Vasco da Gama Seamount, VS = Vigo Seamount, PS = Porto Seamount, and ES = Estremadura Spur.

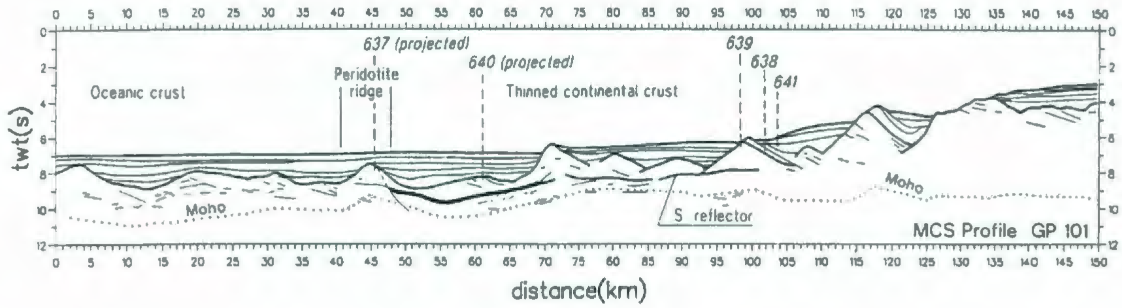

Figure 1.9: Line drawing of GP101 from a multichannel seismic reflection time profile (From Whitmarsh et al., 1996). Note the location of the S-reflector outlined with a bold line, and the location of ODP drilling sites either along the GP101 transect or projected on to it.

serpentinized peridotite ridge is 7.2-7.6 km/s, which underlies a ~4 km thick low velocity layer (Whitmarsh et al., 1996). This layer consists of a 3.5 km/s velocity at the very top, and a steep velocity gradient from 4.0-6.9 km/s below.

Just seaward of the peridotite ridge, inferred ocean crust has a thickness of about 2.5-3.5 km, and gradually thickens to about 7 km (normal ocean crust) over a width of ~20 km (Figure 1.9 Whitmarsh et al., 1996). Velocities in this area resemble that of normal ocean crust, however a crustal thickness of 2.5-3.5 km is much thinner than that of normal ocean crust. It is suggested that the initial oceanic crust produced is anomalously thin due to a limited magma supply created from the conductive cooling of the mantle during a long rifting stage.

1.5.2 Iberia Abyssal Plain

Various sites have been drilled in the Iberia Abyssal Plain by both the Ocean Drilling Program (ODP) and the Deep Sea Drilling Program (DSDP). The first hole was Site 398 drilled by the DSDP in 1976 during Leg 47B. In 1993, during ODP Leg 149, sites (897-901) were drilled along the margin to gain an understanding of the rifting and break-up history between Newfoundland and Iberia, and to better define the location and composition of transitional crust (Whitmarsh and Wallace, 2001; Pinheiro et al., 1996). From these results it was recommended that more drilling, mainly in the transitional zone, was necessary to obtain this goal. Consequently the ODP drilled Sites 1065-1070 in 1997 during Leg 173 in close proximity.

Results from these studies (Figure 1.10) were synthesized to propose that the thinning of continental crust was accommodated initially by pure shear of the entire lithosphere, followed by simple shear involving both low angle detachment faults and high angle normal faults (Whitmarsh et al., 2000; Whitmarsh and Wallace, 2001). Cores recovered from Sites 901, 1065, and 1069 were drilled on rotated fault blocks and did not penetrate basement. These sites sampled sediments and fossils that imply a shallow water environment and indirect evidence of underlying continental crust (Dean et al., 2000; Whitmarsh and Wallace, 2001).

Basement was cored from three sites (900, 1067, and 1068) on Hobby High, which is a north-south trending basement ridge. Here lower continental crust and mantle rocks have been exhumed, likely from the later stage of faulting in the rifting process (Whitmarsh and Wallace, 2001).

Exhumed serpentinized peridotites where recovered from basement rock of Sites 897, 1068, and 1070 (Whitmarsh and Wallace, 2001). Basement was not penetrated at Site 899, however serpentinized peridotites were also recovered from this location. Site 1070 is located just east (~30 km) of the magnetic J-anomaly, where the J-anomaly is assumed to indicate ocean crust. This site was assumed to lie within the oceanic domain because of its rough basement morphology and close proximity to the J-anomaly, yet pegmatitic gabbros and overlying serpentinized peridotite breccias were recovered from drilling. The lack of extrusive basalts gives evidence against an oceanic affinity for these rocks, but it may be possible that rocks recovered from this site are not representative of the surrounding geology.

Analysis of the petrology and geochemistry of the peridotites from Sites 1068 (Hobby High) and 1070 (near J-anomaly) have been performed to determine whether these peridotites are derived from sub-oceanic or sub-continental mantle (Abe, 2001; Hébert et al., 2001). Results from both studies suggest the peridotites from Sites 1068 and 1070 represent subcontinental mantle.

Analysis of seismic reflection data including the LG-12 profile allows the identification of strong intracrustal reflections (labeled L, FB, H, and F in Figure 1.11), where some are interpreted as detachment faults (Krawczyk et al., 1996). The H-reflector is a fairly continuous reflection that originates on the western flank of the basement high (where Site 1065 is drilled) dipping seaward, then flattens and turns upward and onlaps the eastern flank of Hobby High (Sites 900, 1067, 1068). Another seaward dipping reflector, the F-Reflector, originates on the western flank of Hobby High, and is interpreted as a detachment fault that is responsible for exposing the lower crust and mantle rocks on the western flank of Hobby High (Whitmarsh et al., 2000). These low-angle normal or detachment faults appear to sole at different depths within the mantle, in contrast to the Galicia Bank S-reflector.

A 350 km multi-channel seismic reflection profile IAM-9 (Figure 1.12) was collected on the western Iberia margin just south of Leg 149 and 173 ODP drilling sites (Pickup et al., 1996). The velocity structure of IAM-9 reflection data is constrained by 3 older seismic refraction lines that intersect the profile, and run parallel to the Iberia margin (Whitmarsh et al., 1990). More recently improved seismic refraction data was collected directly along the IAM-9 Transect, where the results are in good agreement with the previous data set (Dean et al., 2000).

The IAM-9 profile shows a different marginal environment compared to that farther to the north (Dean et al., 2000). Continental crust is thinned through rotated faulted blocks similar to the north; however, there is no evidence of seaward dipping detachment faults similar to the H and S reflector imaged to the north on seismic lines LG-12 and GP101 respectively (Dean et al., 2000). The upper layer of basement within this area is modeled with a velocity between 5.5-6.8 km/s.

Adjacent to rotated fault blocks of thinned continental crust lies a 120 km wide section within the transitional zone, which is characterized by low basement relief and low top-of-basement reflectivity (Pickup et al., 1996; Dean et al., 2000). Here the upper

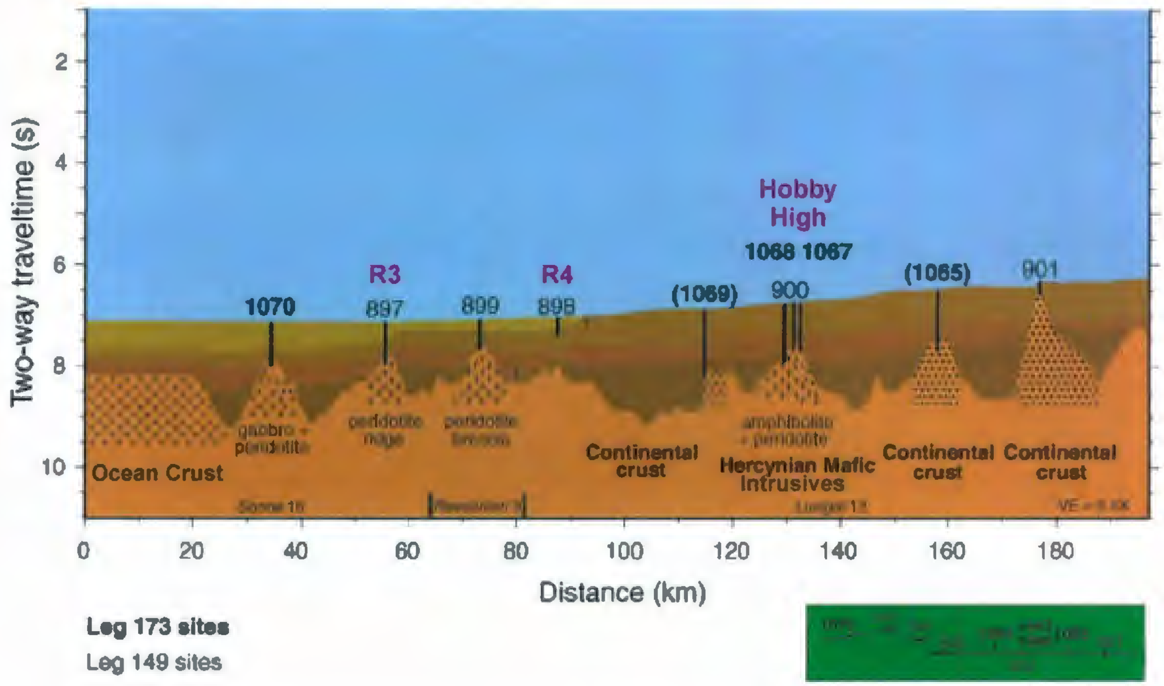

Figure 1.10: Summary of drilling results from ODP Leg 149 and 173 projected or overlain on line drawing of MCS reflection data from east to west: Lusigal 12, Resolution 3, and Sonne 16 (Modified from Concheryo and Wise, 2001).

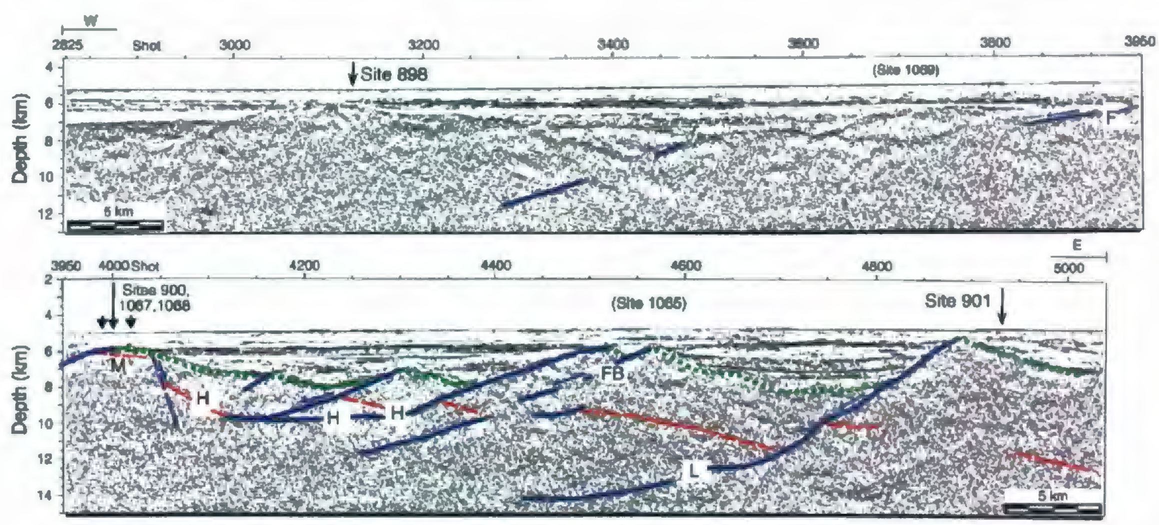

Figure 1.11: LG-12 seismic reflection profile (From Whitmarsh and Wallace, 2001). Note the location of L, FB, H, and F reflectors representing low angle faults. Top of basement outlined in green, and assumed depth of Moho outlined in red.

basement unreflective layer is about 2 km thick, and has 5.2 km/s velocity at its top (Dean et al., 2000). Below this is a 1 km thick, 6.4-7.0 km/s layer. Further seaward within the transitional zone is a 50 km wide section of increased basement relief and reflectivity, which includes two peridotite ridges (R3 and R4). Here basement velocity structure is also divided into two layers but the velocities are reduced: a ~1 km thick layer with a 4.3 km/s velocity at its top, and a raised 5.7-7.3 km/s layer with a thickness of about 2 km. A 7.3-7.9 km/s velocity layer underlies the whole of the transitional zone, with a thickness up to 4 km.

An interpretation for the transitional region is that it contains exhumed mantle that has been highly serpentinized through faulting and the influx of seawater (Pickup et al., 1996; Dean et al., 2000). This zone includes the area of increased basement relief likely representing peridotites ridges (R3 and R4) that have been identified to the north. The top of basement velocity in the section of inferred peridotite ridges does have a velocity of ~4.3 km/s, which is lower than what is expected for 100% serpentinized peridotite (Dean et al., 2000). However, this is still a reasonable interpretation if the top of acoustic basement is highly faulted and brecciated, which would further reduce the seismic velocity.

West of R3 in the vicinity of both M3 and the J-anomaly, a two-layer velocity structure that is typical for normal layer 2 and 3 oceanic crust is observed with velocities of 4.5-6.5 km/s and 6.7 and 7.2 km/s respectively (Dean et al., 2000).

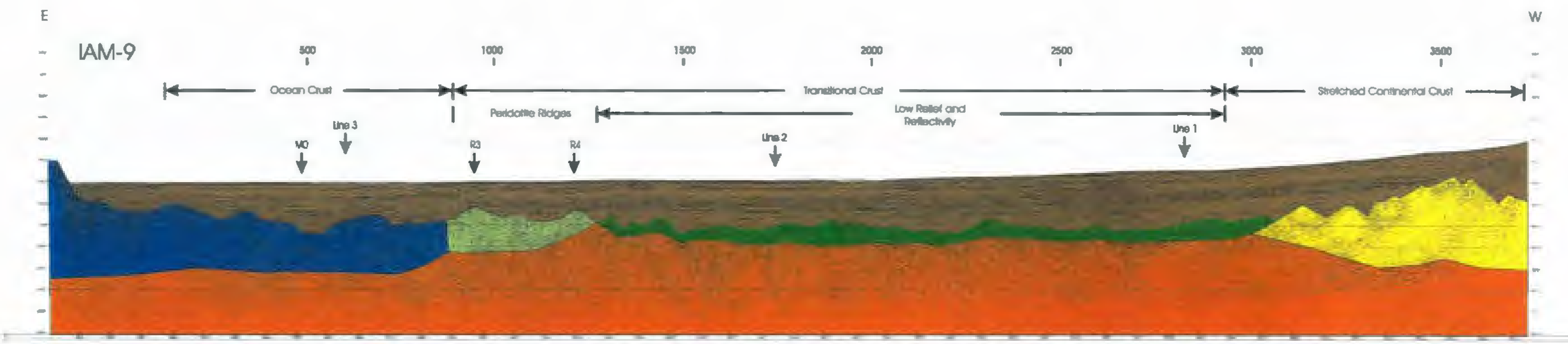

Figure 1.12: Multi-channel seismic reflection profile IAM-9 outlining the areas interpreted as ocean crust, transitional crust, and stretched continental crust. Orange = mantle, blue = ocean crust, light green = sampled peridotite ridges, green = serpentinized mantle, yellow = continental crust, and brown = sediments.

1.6 Objectives

Despite the extensive investigation of both the Newfoundland and Iberia margin, questions remain regarding the relationship between this conjugate pair. Some of these questions include:

1) Where are the boundaries of continental, transitional, and oceanic crust located on the southern margin of Flemish Cap, and how does this relate to the Iberia margin?
2) What is the dominant mode of rifting that accommodated separation between Newfoundland and Iberia?
3) As the continental margin bends around the edges of Flemish Cap, how is rifting and seafloor spreading accommodated?

I have applied extensive processing efforts to lines 53, 54, and 56 from the Erable survey, providing more comprehensive data coverage along the southern margin of Flemish Cap. A detailed comparison of the Newfoundland and Iberia margin discussing symmetrical and asymmetrical features will be explored to aid in answering some of the above questions. A model will be provided in order to provide insights on rifting and break-up processes that led to the formation of the present day Flemish Cap southern margin.

Chapter 2: Processing Methods

2.1 Data Acquisition and Geometry Set-up

The Erable cruise report, field notes, and navigation file were used to set up the geometry for the processed lines. See Figure 2.1 for a schematic of the field geometry used for the Erable multi-channel seismic (MCS) reflection survey. The following *Regional Survey Acquisition Parameters* for the survey were obtained from the Erable cruse report:

Source:	
Type:	8 Bolt air guns
Total Capacity:	5700 cu
Depth:	15-17 m
Shot interval:	~100 m (Once every 19.4 sec at cruising speed 5 knots)
Streamer:	
Length:	2400 m
Channels:	96
Spacing:	25 m
Elements:	24 hydrophones per channel
Channel 1 offset:	300 m
Streamer depth:	17-35 m (Varied for survey due to extreme temperature variations)
Recording:	
System:	SERCEL SN358
Format:	SEGD 9 Track 6250 bpi
Filter:	0-77 Hz
Record length:	0-17.408 s
Sampling rate:	4 ms

The navigation file provided a set of latitude and longitude readings with corresponding time and field file identification (FFID) readings. It should be noted that the navigation coordinates where taken at set time interval and thus every shot does not have a corresponding navigation reading. This poses a problem since ProMAX requires a UTM coordinate for every FFID. Therefore, it was decided that the best approach was to pick a set of latitude and longitude coordinates and convert these to UTM coordinates (Appendix 2 and 4). This set of UTM coordinates can then be used to interpolate UTM coordinates for every FFID, and correctly represents the location of the data so long as the ship speed is fairly constant (Appendix 3 and 5).

About 10 evenly spaced points were initially chosen for interpolation, and additional points were added where shot spacing appeared to change rapidly. The latitude-longitude points were first converted from decimal degree to degrees, minutes, and seconds. Then the points were converted to UTM using the Geographic to UTM conversion calculator from the *Natural Resources Canada* website. A station number is assigned to every CDP and is calculated for each FFID location using the assumption that there is a station every 12.5 m (CDP spacing).

Line 53 deviated from its course between FFID's 3712 and 3786 to avoid a fishing ship, and this created a sharp kink in the line. One option is to process this section using crooked line geometry. However, this piece of data is collected over Flemish Cap where there water is shallow and there is almost no sediment cover. These conditions produce reverberations with very strong amplitudes in the data. It is not likely that good quality data will be recovered from this section. Another option that is much less computationally intensive is to assume that there is no kink in the line. This is done by deleting every second FFID where the kink exists to account for the reduced distance that the straight line encompasses, projecting the FFID coordinates onto the straight line, and assigning the appropriate shot spacing. The data within these FFID's will not have geological significance, but will allow the data to remain continuous which is beneficial when applying processing tools that have problems with edges such as migrations.

Field notes were accessed to acquire the nominal source and receiver depths for the lines 53, 54, and 56. The following parameters where used for the geometry setup of Line 53, 54, and 56:

Nominal Receiver Source Interval:	25 m
Nominal Shot Spacing:	100 m
Nominal Source Depth:	16 m
Nominal Receiver Depth:	18 m
Channel Spacing:	25 m
X Channel Offset:	300 m
Y Channel Offset:	0
CDP spacing:	12.5 m

It is likely that the nominal source and receiver depth obtained from field notes was chosen based on the assumption that the dominant frequencies recovered will be approximately 20-23 Hz. Within seawater with a velocity ~1480 m/s, this corresponds to a seismic wavelength of about 64 m ($v = f\lambda$). The seismic wave reflected from or below the seafloor heads upward toward the sea surface to be recorded by the hydrophones. The waves received by the hydrophones include: 1) the upcoming wave that is directly recorded by the hydrophones, and 2) upcoming wave that travels an extra distance x to the water surface, reflects of the air-water interface producing a $\lambda/2$ phase shift, which then returns to the hydrophone at a depth x below the water surface. The optimal result is for the two groups of seismic waves to have constructive interference, so that signal is not lost. This can be achieved by placing both the source and receiver at a depth of about $x = \lambda/4$, or ~16 m.

There was some ambiguity over what the near channel (Channel 1) offset was for the survey. The cruise report says 300 m in the general description of the streamer (pg 38, Erable cruise report). However, processing parameters are given for lines 8, 16, and 54, and a near offset of 330 m, 300 m, and 330 m are denoted respectively. Because of

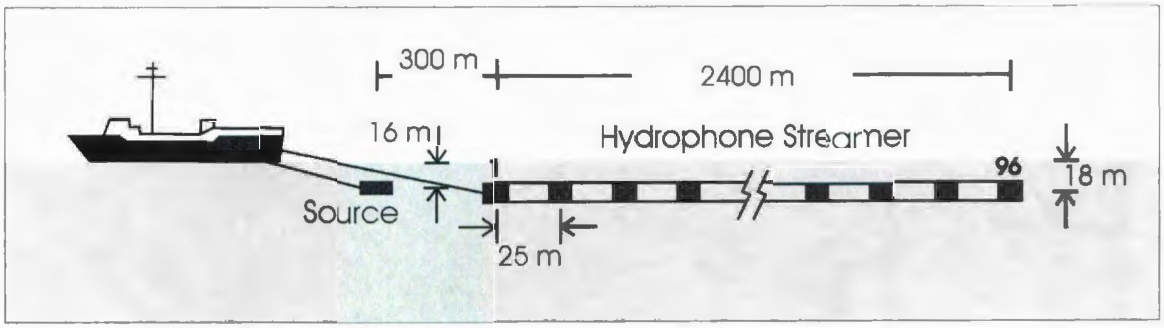

Figure 2.1: Schematic of field geometry used for lines 53, 54, and 56 Erable MCS data.

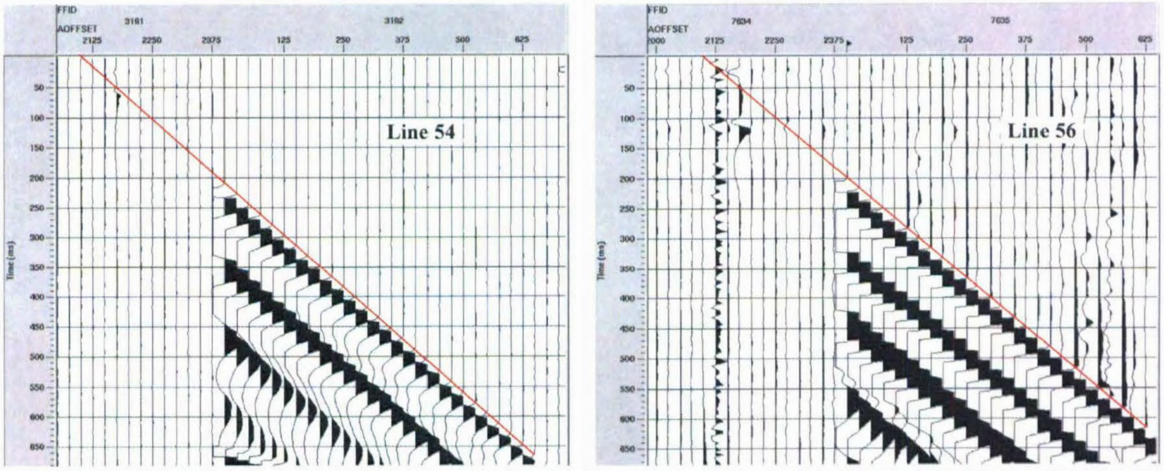

Figure 2.2: A section of a shot gather from Line 54 and 56 expanded. The direct wave is extrapolated back to time zero to measure the offset of the first channel.

the inconsistency between the general description and processing parameters, a shot gather for lines 54 and 56 (Figure 2.2) was looked at in close detail to determine what the offset of the near channel is. The first arrival of the direct wave on each channel was traced back to zero time to estimate what the distance was between the gun and near channel. Knowing that the trace spacing on the shot record (channel spacing) is 25 m and there are 12 traces between the near channel and the point where we cross the time axis, this gives an offset of 300 m for both lines.

2.2 Trace Editing

Channel 86 from lines 53, 54, and 56 was killed because this channel appeared noisy on Line 53 and beginning of Line 54, and was dead on the end of Line 54 and all of Line 56.

Shot 4391 was a dead shot and was also deleted. Data from Line 53 and 54 are continuous and written to one file. *For the remainder of Chapter 2, Line 54 will refer to both Line 53 and 54.*

2.3 Frequency Spectrum Analysis and Testing of Bandpass Filters

The frequency content of the data was examined for the shelf, slope, and deep water regions for Line 54 and Line 56 using the *Frequency spectrum analysis* program in ProMAX (Figures 2.3 and 2.4). For each region on both lines there is little signal amplitude content above about 40 Hz. Also, there is a very low frequency noise spike that occurs on all spectrum analyses, but is strongest within the shelf region, getting weaker moving into deep water. It appears that the frequency range of the signal is between approximately 5-35 Hz, so a bandpass filter may be applied to remove unwanted frequency content above and below this specified range.

Testing of band pass filters was used to examine how each filter removes high and low frequency noise, but also observing how the filters degrade the quality of the data. Bandpass filters such as the Ormsby and Butterworth create a ringing wavelet, and also can decrease temporal resolution. The undesirable ringing in the wavelet can be explained by Gibbs phenomenon. This occurs due to a truncation of the Fourier series that is induced by the design of the filter with a steep slope on the cut off frequencies. This effect is decreased as the slope of the cut of frequencies become gentler. Band-limiting the data also decreases the vertical resolution, and so it is important to remove only the minimal range of frequencies from the spectrum when trying to achieve desirable noise attenuation. The effect of the bandpass filters can be tested on real data, but to understand simply the effect of bandpass filters, a synthetic spike was generated (Figure 2.5) and various bandpass filters applied (Figures 2.6-2.8).

Figure 2.6 compares the effects of the Ormsby and Butterworth filter, using the same cut off frequencies and a similar slope on the cut off. Frequencies for Ormsby filter are denoted in an f1-f2-f3-f4 format, with f1 and f2 representing the 0% and 100% points respectively of the low cut ramp, and f3 and f4 representing the 100% and 0% points of the high cut ramp (Landmark ProMAX Software Manual). In contrast, frequencies cutoffs of the Butterworth filter are denoted in a f1-S1-f2-S2 format. This produces a filter that accepts 100% of frequencies between f1 and f2, and creates a low roll off slope (S1) and and a high roll off slope (S2) in dB/octave.

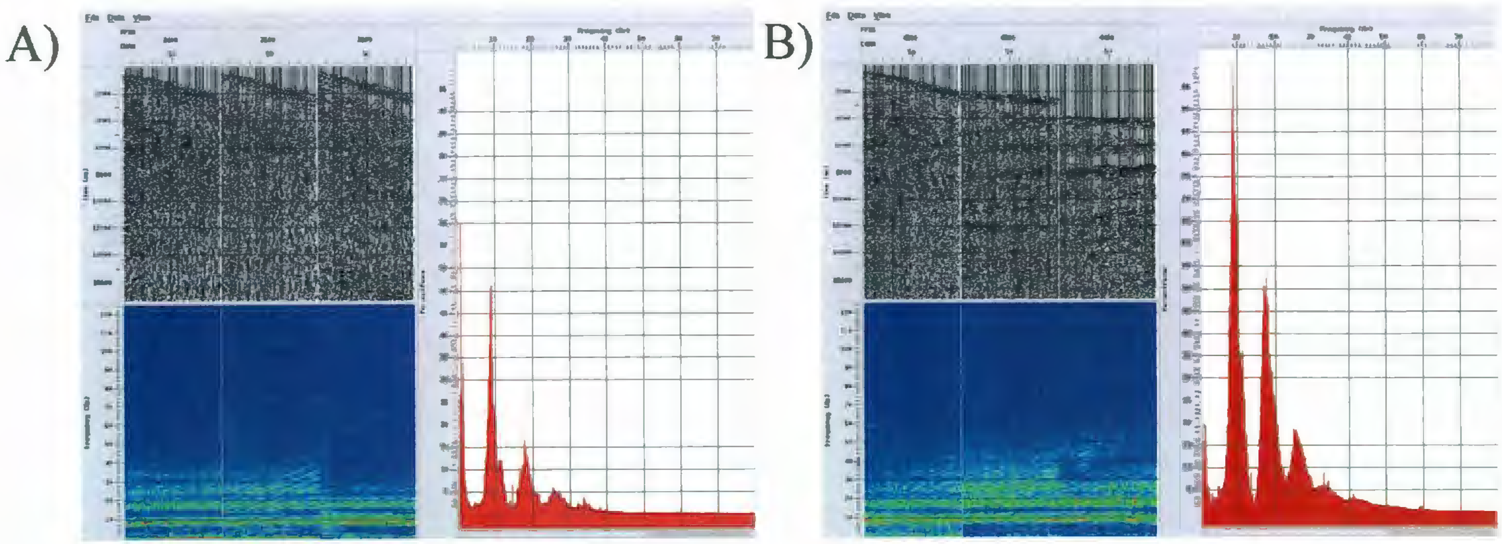

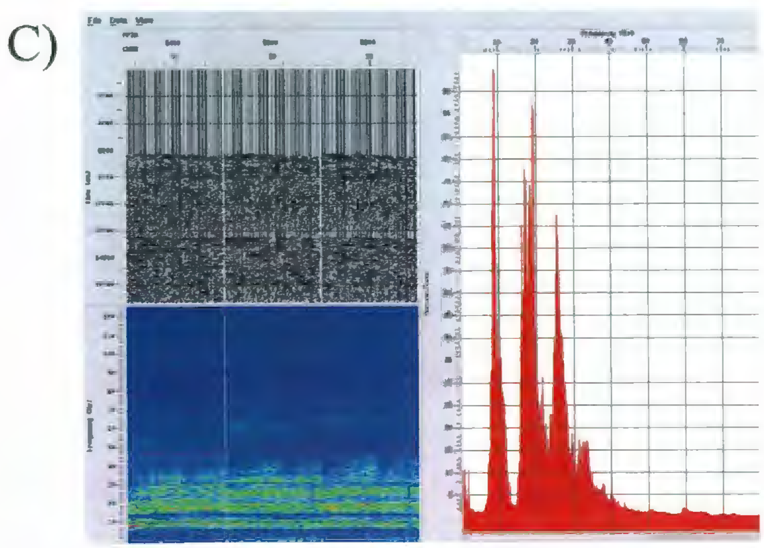

Figure 2.3: Frequency spectrum analysis of shot gathers from Line 54 with the direct and refracted waves muted. Each analysis contains three shot gathers taken from the (a) shelf (b) slope, and (c) deep water regions.

A) B)

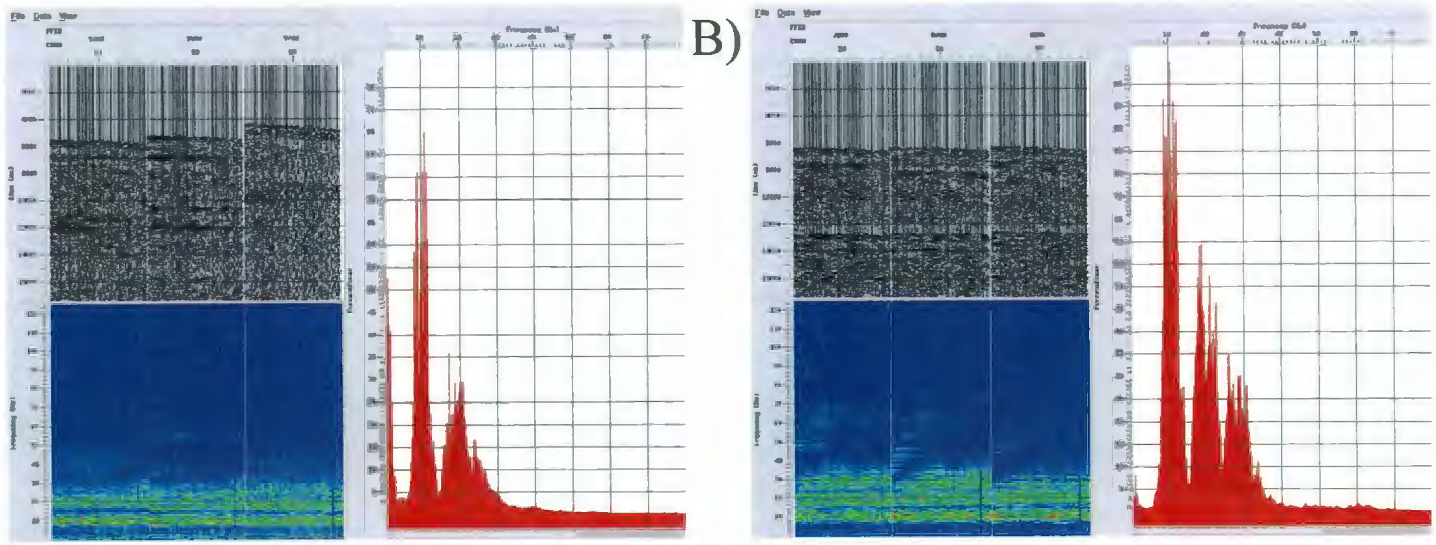

Figure 2.4: Frequency spectrum analysis of shot gathers from Line 56 with the direct and refracted waves muted. Each analysis contains three shot gathers taken from the (a) slope and (b) deep water regions.

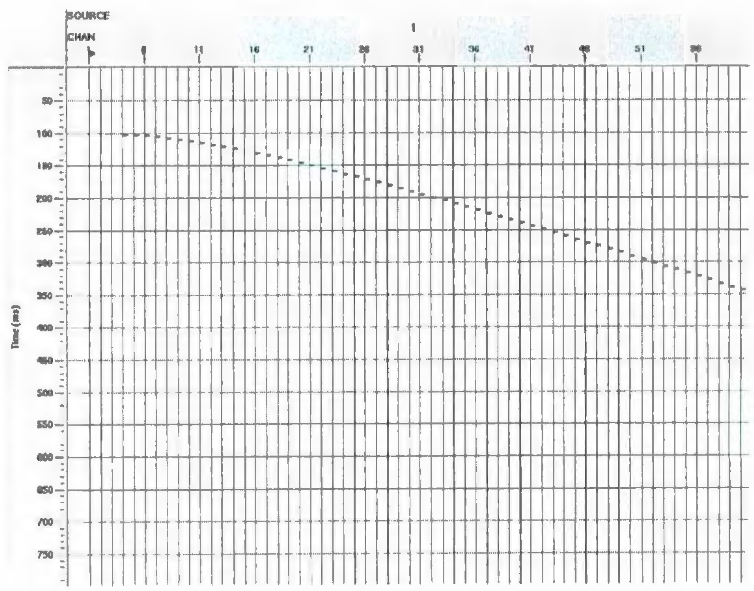

Figure 2.5: A synthetic shot gather created using a spike. This will be used to test different bandpass filters and observe the effects.

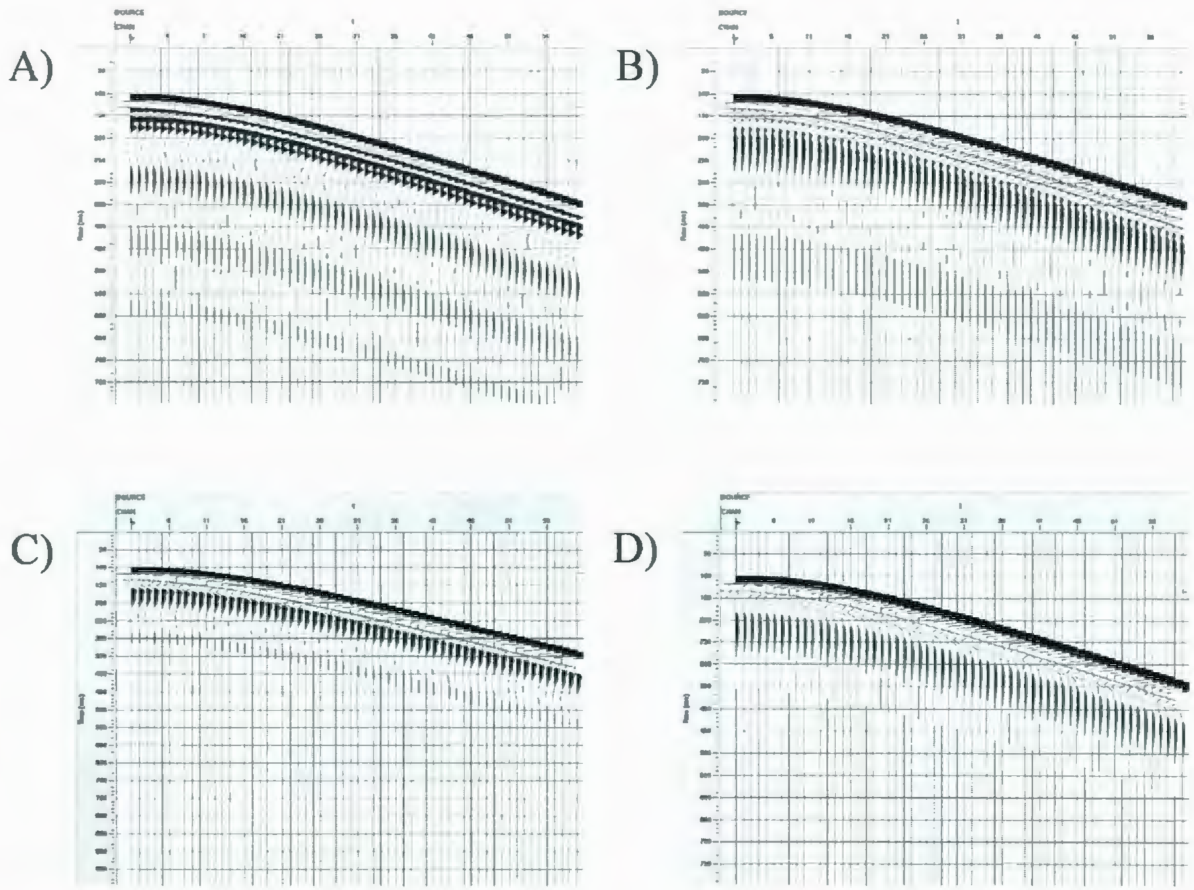

Figure 2.6: Synthetic shot gathers created using a spike and various minimum phase bandpass filters are applied in the frequency domain to observe the effect of each filter. (a) Ormsby filter of 5-8-40-60, (b) Ormsby filter of 2-5-40-60 (c) Butterworth filter of 8-12-40-24, and (d) Butterworth filter of 5-12-40-24.

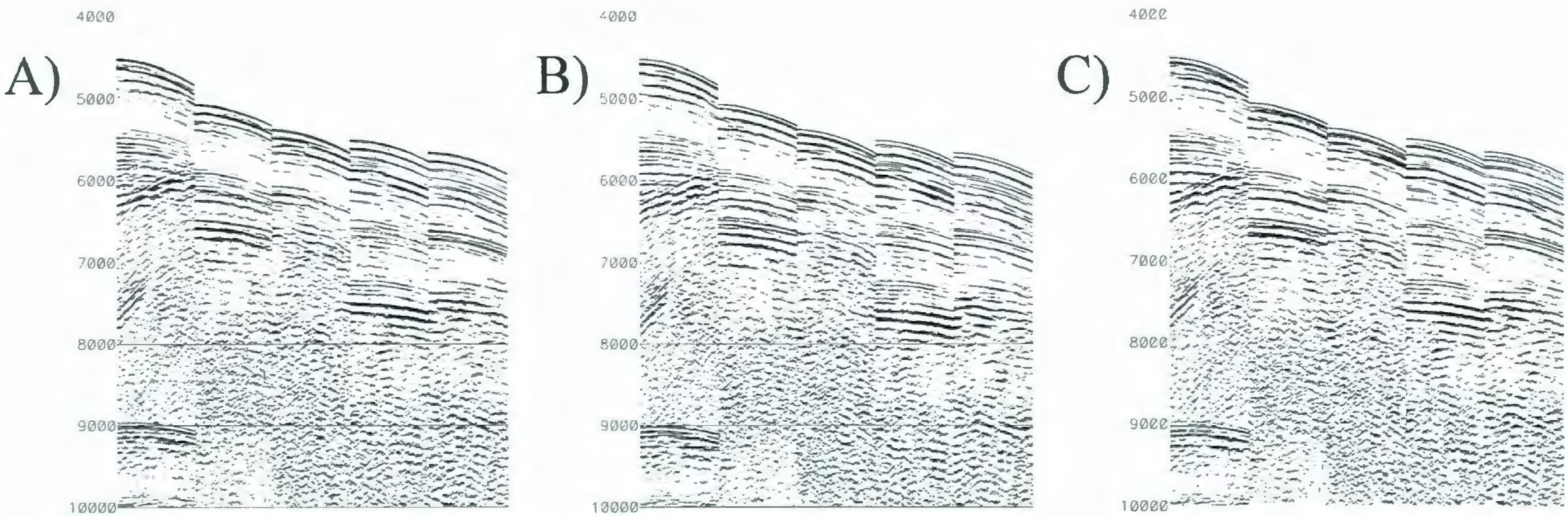

Figure 2.7: Display of every 100th shot gather ranging from FFID 4491 - 4891. (a) No band pass filter has been applied, (b) Ormsby bandpass filter of 5-8-40-60 applied, and (c) Ormsby bandpass filter of 2-5-40-60 applied. An AGC with a 2000 ms window is used for amplitude balancing in all sections. Note the effect each bandpass filter has on the water bottom reflection.

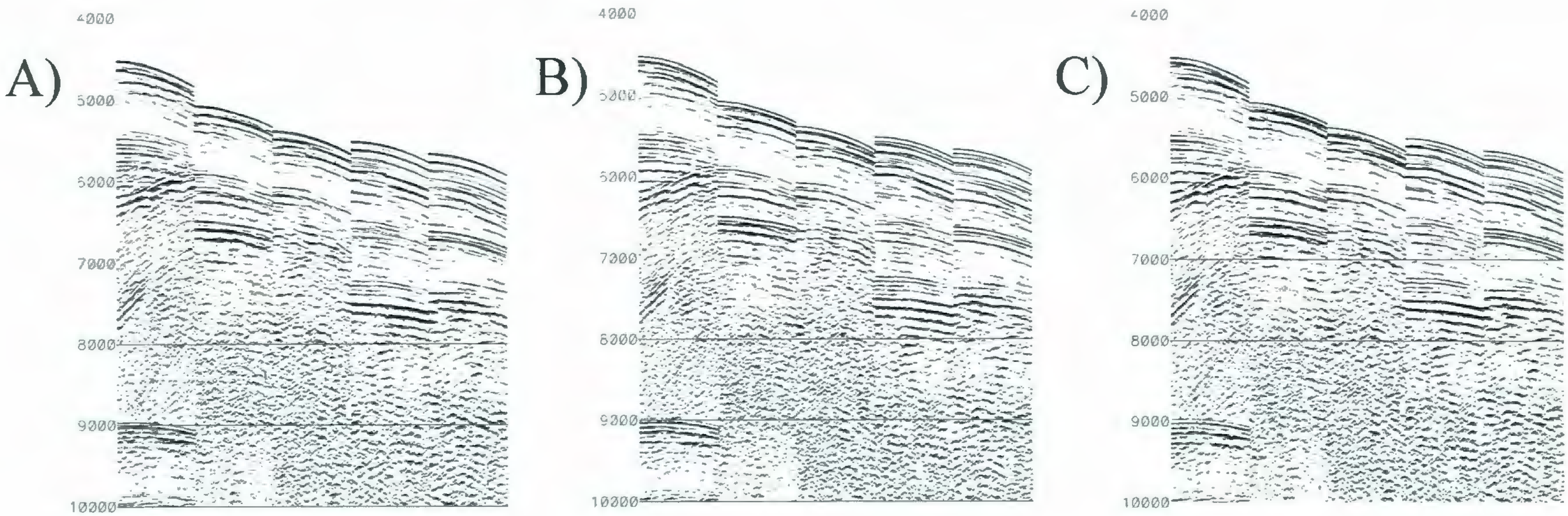

Figure 2.8: Display of every 100th shot gather ranging from FFID 4491 - 4891. (a) No band pass filter has been applied, (b) Butterworth bandpass filter of 8-12-40-24 applied, and (c) Butterworth bandpass filter of 5-12-40-24 applied. An AGC with a 2000 ms window is used for amplitude balancing in all sections. Note the effect each bandpass filter has on the water bottom reflection.

Note that the Ormsby filter (Figure 2.6 a) gives a complicated first arrival wavelet, and the ringing gives a false impression that a second, third, and fourth reflector are present. In comparison, the Butterworth filter (Figure 2.6 c) first arrival wavelet has a more simple shape and the ringing produces only one event that could be mistaken for a reflector that does not exist, and it is very low in amplitude. Figure 2.6 (a) and (b) can be compared to observe the effect of changing the cut off frequencies of the Ormsby filter from 8-40 to 5-40 respectively. Here we see that increasing the frequency bandwidth and creating a gentler slope on the low frequency cut reduces the ringing (Figure 2.6 b). This creates a lower frequency wavelet with a larger period, but now only one event can be mistaken for a non-existent reflector. Comparing the two Butterworth filters with cut off frequencies of 8-40 and 5-40 (Figures 2.6 c and d), there is an improvement of the wavelet quality using the wider frequency bandwidth, which is similar to that of the Ormsby filter. Lastly, when comparing the Ormsby and Butterworth filters with the larger bandwidth (Figures 2.6 b and c), we see the Butterworth filter, the initial wavelet for both are very similar. However the Ormsby filter produces an extra peak that is not seen in the Butterworth filter.

This exercise has reinforced the idea that using a higher bandwidth of frequencies increases vertical resolution and reduces ringing in the spectrum. Also, it has also showed us that the Butterworth filter appears to produce less ringing compared to the Ormsby filter. Before making any judgements, one must observe the effect of these filters on real data, where the source wavelet is unknown.

Figure 2.7 and 2.8 illustrate the effect of the Ormsby and Butterworth bandpass filters respectively on shot gathers from the slope area of Line 54. These data are in agreement with the finding from testing performed on the synthetic spike. Here we observe that including lower frequencies produces less ringing on strong reflectors, particularly the basement reflection. There is little difference between the Ormsby and Butterworth filtered sections with the same cut off frequencies (Figures 2.7 c and 2.8 c). But, since the Butterworth did a much better job on the synthetic spike, it is chosen for the processing flow.

2.4 Brute Stack

A bandpass filter has been applied to improve the signal to noise ratio. Now that the geometry has been set up, the data can be sorted into CDP (common mid-point) gathers. At this point we can make a first pass at picking velocities to use for a NMO (normal moveout) correction, and then sum the traces to create a brute stack. Producing a brute stack at this stage will enable one to identify different types of noise that still contaminate the section, and also create a plan to remove this noise. The following processing scheme was applied to the brute stack given illustrated in Figure 2.9:

1. Butterworth bandpass filter 5-12-40-24 (using f1-S1-f2-S2 format)
2. AGC 2000 ms
3. Direct and refracted wave top mute
4. NMO correction
5. CDP stack

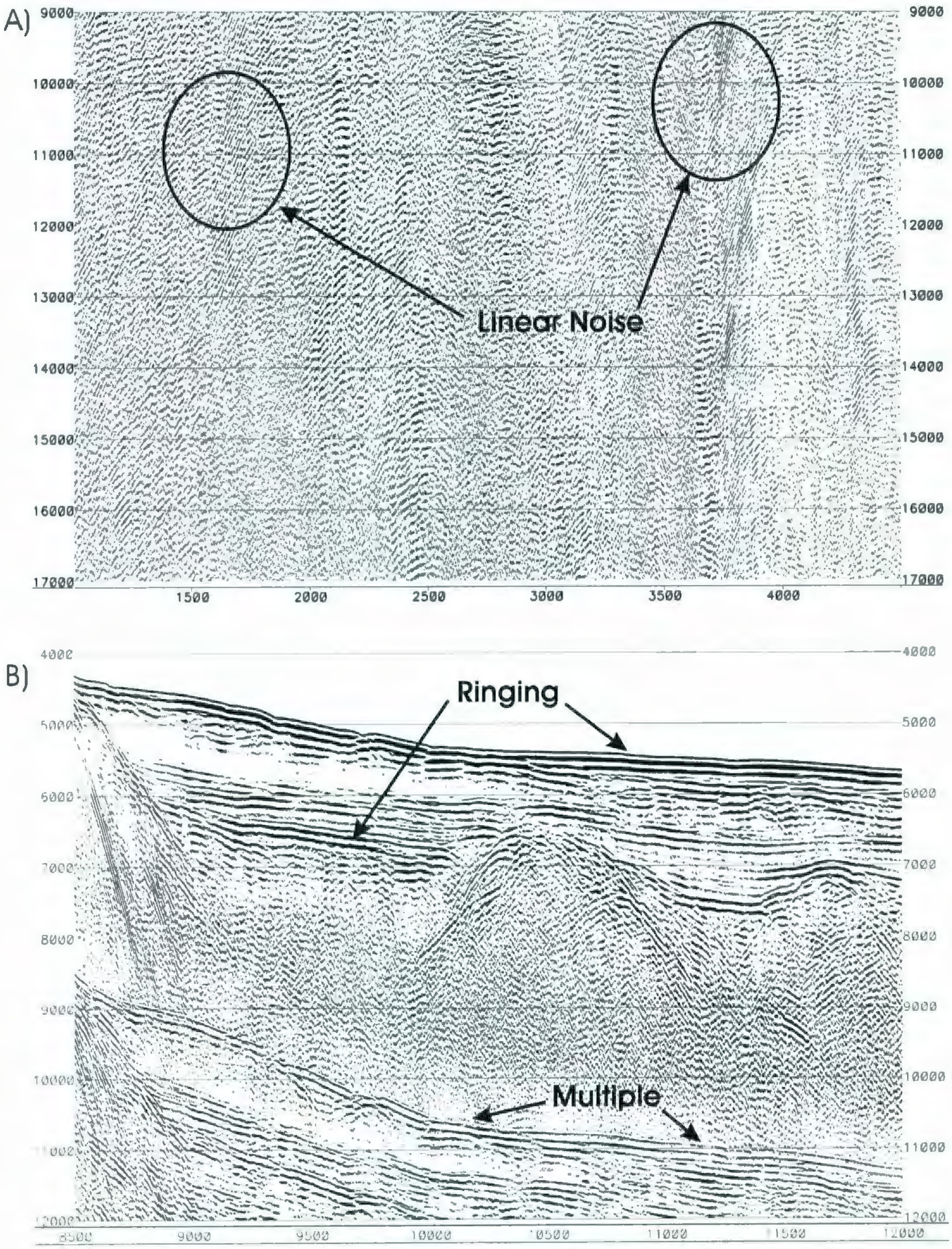

Figure 2.9: Line 54 brute stack from a) the later travel times of the shelf (CDPs 1000-4500), and b) the slope moving into deeper water (CDPs 8500-12000), illustrating various types of noise discussed in text.

Some of the obvious sources of noise in this section are 1) linear noise that dominates in the shelf section, 2) multiple reflections created from energy bouncing in the water column, and 3) the reverberatory nature or "ringy" character of reflections reducing temporal resolution.

2.5 Velocity Analysis

2.5.1 Velocity Control on Shelf Using Refraction Data

The Flemish Cap shelf is an area where the multiple reflections are very strong, and primary reflections create weak or ambiguous semblance peaks in the velocity analysis. It is desirable to have some velocity control on the shelf so that any primary reflections from within the thin sediment cover or within the top section of basement may be flattened with the proper NMO correction, and sum together within the stack. At later recording time, the NMO correction is less sensitive to small changes in velocity; therefore a detailed velocity analysis is only necessary for the upper 5 seconds or so of the data. Looking at refraction and reflections on shot gathers of the raw data is one way to derive velocity information on the shelf.

Figure 2.10 is a shot gather showing the first arrivals from left to right, a direct wave (traveling through water), refraction from the water bottom, and refraction from the top of basement. On some shot gathers the reflections from the water bottom and top of basement are visible, and thus velocities are measured. A number of shot gathers, including the shot gather in Figure 2.10, have direct and refracted waves interfering with the reflection. However, the reflection from the water bottom is bounded by the sediment refraction, and asymptotically approaches the direct wave. Similarly, the reflection from the base of sediments is bounded by the basement refraction and asymptotically approaches the sediment refraction. Therefore the direct waves and refracted waves can help with making estimates of reflection velocities on shot gathers where reflections cannot be directly measured. The velocities measured from the reflections are apparent velocities, but since the shelf is relatively flat, we assume that they approximate the interval velocities of the layers.

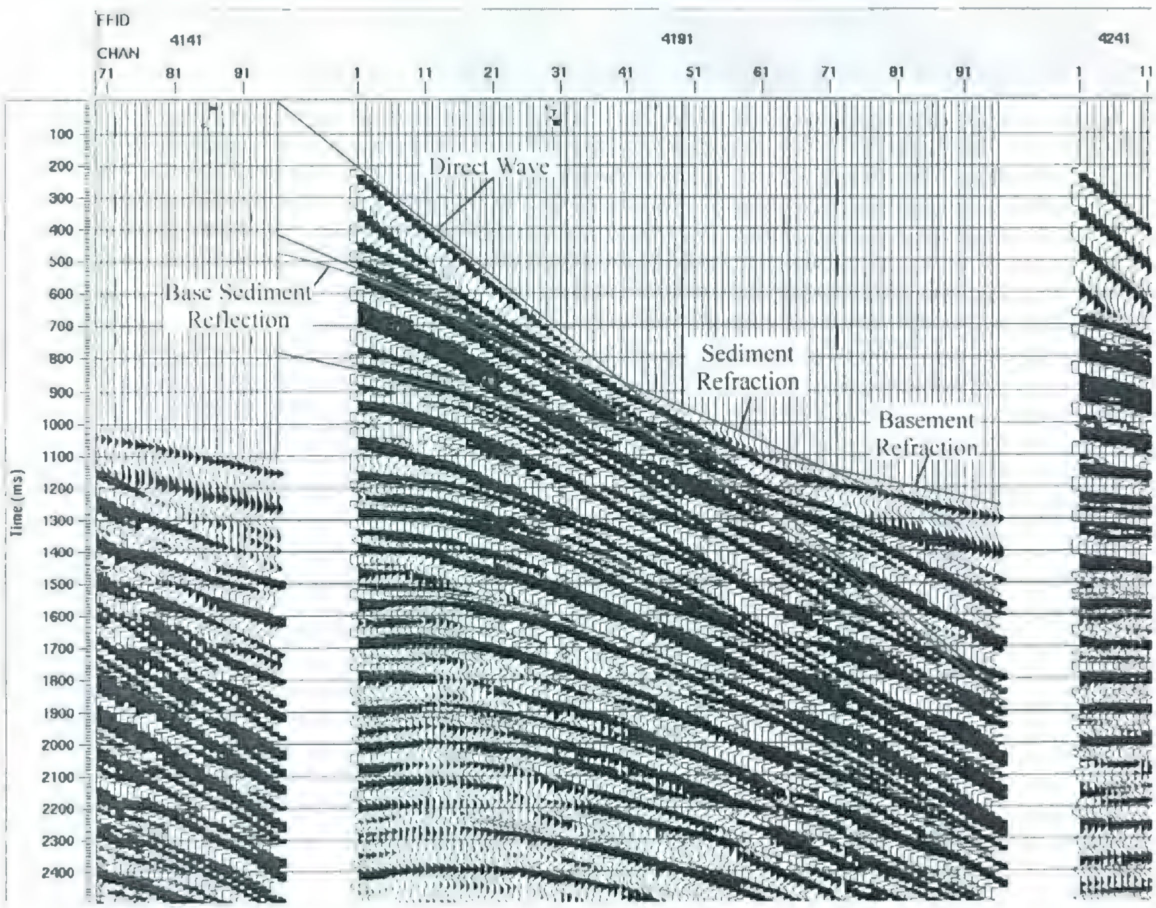

Figure 2.10: Shot gather with some reflections and refractions highlighted in blue and red respectively.

ProMAX uses rms (root mean square) reflections velocities for NMO corrections, so it is necessary to convert the interval velocities (V_{int}) to rms velocities (V_{rms}) which is done using Dix's equation:

$$V_{int} = [(T_i\, V_{rms(i)}^{\;2} - T_{(i-1)}\, V_{rms\,(i-1)}^{\;2})/(T_i - T_{(i-1)})]^{1/2} \qquad (2.1)$$

This equation can be rearranged to solve for the rms velocity:

$$V_{rms\,(i)} = [(V_{int}^{\;2} * (T_i - T_{(i-1)}) + T_{(i-1)}\, V_{rms\,(i-1)}^{\;2}) \,/\, T_{(i-1)}]^{1/2} \qquad (2.2)$$

Where T represents the zero offset two way travel time of the reflected wave. T_1 and T_2 are measured by extrapolating the hyberbolic shape of the waterbottom and top of basement reflected waves back to zero offset. No first arrival refractions are observed from within the basement from the shot gathers, so T_3, T_4 and T_5 were arbitrarily chosen at 1, 2 and 4 seconds two way time, and it is assumed that the interval velocity remains constant between T_2 and T_4. These measurements were recorded and 5 rms velocities calculated at every 50th shot gather along the shelf to gain lateral velocity control (Table 2.1). There is a great amount of uncertainty associated with the calculated rms velocities and these are only used in combination with other velocity control.

A test piece was selected from the shelf in an area where a weak primary reflection is observed from base of sediment. This section is stacked over a range of constant stacking velocities to observe which velocity best images reflections within sediments. NMO stretch (discussed in Section 2.6) obscured any primary reflections and only peg leg multiples were imaged. An NMO stretch mute can be designed for each constant velocity stack, however it is time intensive to adequately remove the distorted zone from each section without removing the signal, so this method is not used for these data.

Individual CDP gathers input into the velocity analysis program do not provide sufficient S/N (signal to noise) ratio to produce well defined semblance peaks in the velocity spectra (Figure 2.12 a). However, the S/N ratio is considerably improved when adjacent CDP's are combined and input into the velocity analysis, which can be done using a supergather. Since shot spacing is 100 m and CDP spacing is 12.5 m, at least 8 adjacent CDP's are required to provide a full range of offsets. However, ProMAX requires the user to input an odd number of gathers into the supergather program.

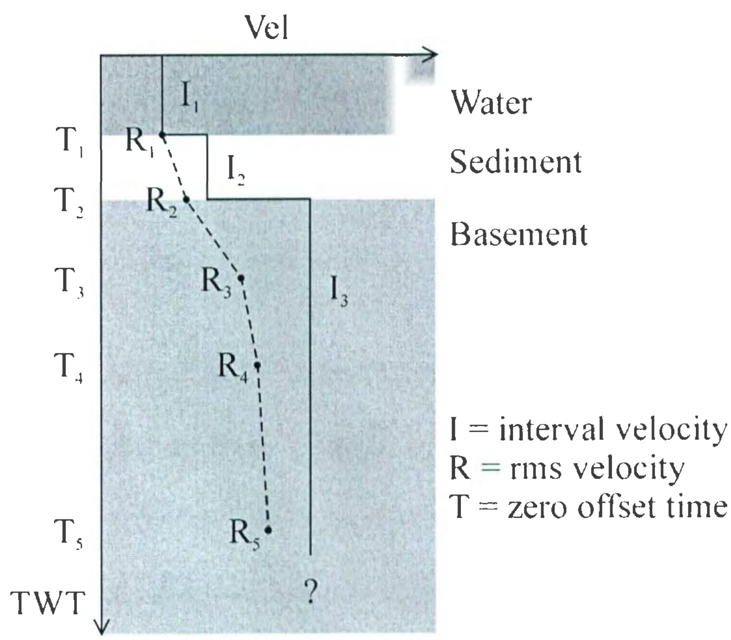

Figure 2.11: Schematic illustrating the arrangement of the interval and rms velocities that are recorded in Table 2.1. Note that T_3 = 1s, T_4 = 2s and T_5 = 4s.

Table 2.1: RMS Velocities derived from shot gathers for the upper crust of the Flemish Cap. T is normal incidence two way travel time of the reflection, and R represents the corresponding rms velocity of the reflected wave. "No Sed" indicates shot gathers where no reflection or refraction from the sediment later is observed. See text and Figure 2.11 for further detail.

FFID	CDP	T1	R1	T2	R2	T3	R3	T4	R4	T5	R5
3191	102	608	1458	868	1654	1000	2289	2000	3669	4000	4192
3241	447	540	1459	832	1749	1000	2698	2000	4210	4000	4791
3291	742	492	1467	768	1775	1000	2805	2000	3959	4000	4425
3341	1035	456	1451	660	1725	1000	3136	2000	4061	4000	4452
3391	1330	416	1467	768	1794	1000	2922	2000	4165	4000	4664
3441	1633	388	1467	No Sed		1000	4156	2000	4698	4000	4946
3491	1936	392	1448	No Sed		1000	4053	2000	4587	4000	4833
3541	2243	382	1445	No Sed		1000	3529	2000	3957	4000	4154
3591	2549	372	1462	No Sed		1000	3621	2000	4045	4000	4242
3641	2854	352	1460	424	1857	1000	4433	2000	5062	4000	5348
3691	3157	304	1460	464	2217	1000	4198	2000	4809	4000	5087
3741	3432	300	1464	424	2067	1000	4439	2000	5038	4000	5312
3791	3700	276	1482	436	2199	1000	4329	2000	4910	4000	5177
3841	4000	240	1463	424	2287	1000	4178	2000	4686	4000	4920
3891	4299	244	1470	412	2346	1000	4433	2000	4960	4000	5204
3941	4606	272	1476	336	1963	1000	4913	2000	5411	4000	5643
3991	4942	296	1467	No Sed		1000	4921	2000	5371	4000	5583
4041	5253	292	1461	440	1960	1000	4772	2000	5496	4000	5824
4091	5629	316	1470	556	1945	1000	4106	2000	5005	4000	5398
4141	6031	352	1465	780	2153	1000	3213	2000	4517	4000	5044
4191	6433	380	1462	476	1681	1000	4366	2000	5142	4000	5489

Because of this, 9 adjacent CDP's are combined into a supergather and used to perform the velocity analysis (Figure 2.12 b). The velocities estimated from the shot gathers (Table 2.1) and velocity models derived from previous work within the Flemish Cap region (Funck, 2003) are both used in combination with the supergather velocity analysis to produce a first pass at the stacking velocity function.

2.5.2 Velocity Analysis Slope and Deep Water

Moving from the shelf into the slope and deep water area, the sediment cover and water depth progressively increase allowing for improved signal to noise ratio, and thus the velocity analysis becomes more precise as semblance peaks become better defined (Figure 2.13).

2.6 NMO Stretch

Figure 2.14 illustrates a CDP gather from the shelf with and without a NMO correction applied. Note the distortion on the NMO corrected CDP gather that is most predominant at large offsets and low reflection time. This distortion is a product of the NMO correction, where events are stretched along the time axis, producing events shifted into lower frequencies (Yilmaz, 1987, p. 48 and 161). Most NMO correction programs allow the user to input a percentage of the NMO stretch to be removed. A 15% stretch mute has been applied in the slope and deep water sections and has worked quite successfully. However this method did not work well within the shelf region of shallow water where refracted waves greatly interfere with the reflected waves. Also, a near trace mute will be applied later in the processing sequence to increase the success of filters used for demultipling, which in turn decreases the fold of the data. A NMO stretch mute is carefully picked so that enough traces are left to retain a portion of the primary events while removing the distortion (Figure 2.14 b).

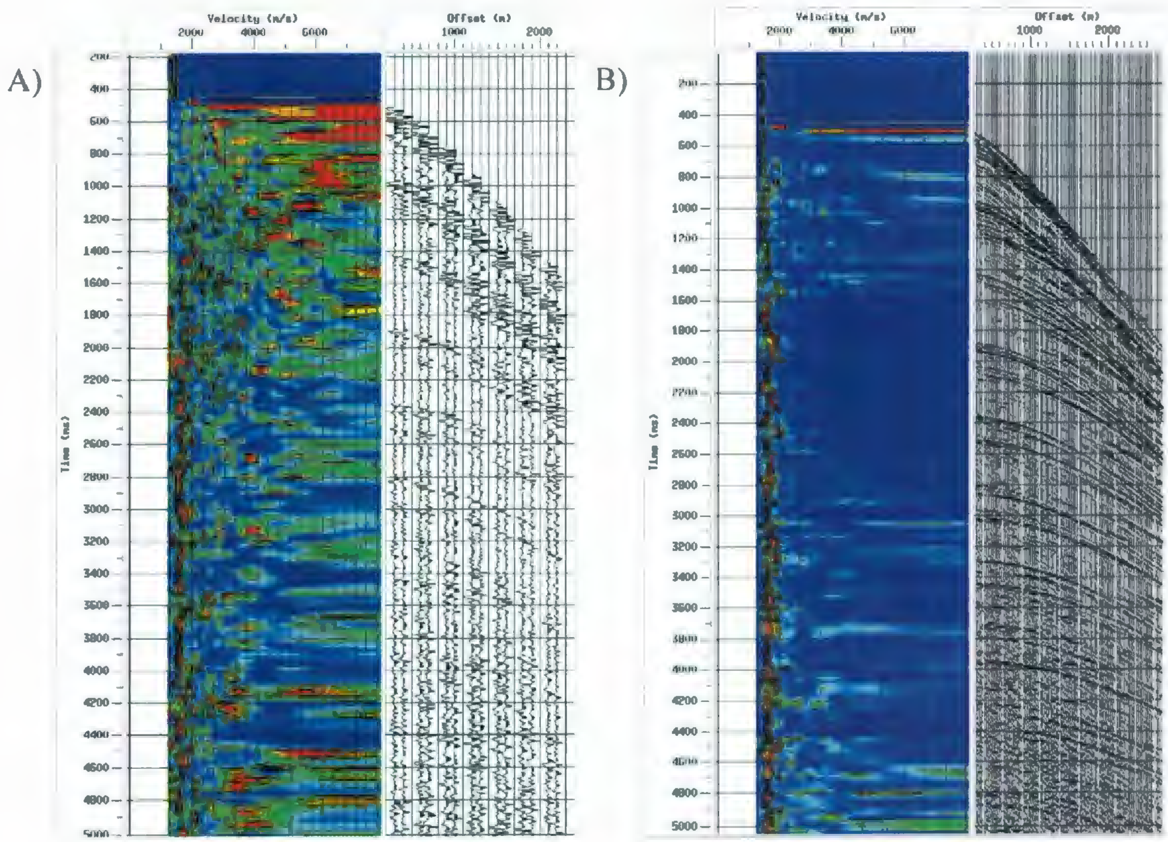

Figure 2.12: a) Velocity analysis of single CDP gather taken from shelf region of Line 54. b) Velocity analysis of supergather consisting of nine adjacent CDP gathers to improve the S/N ratio.

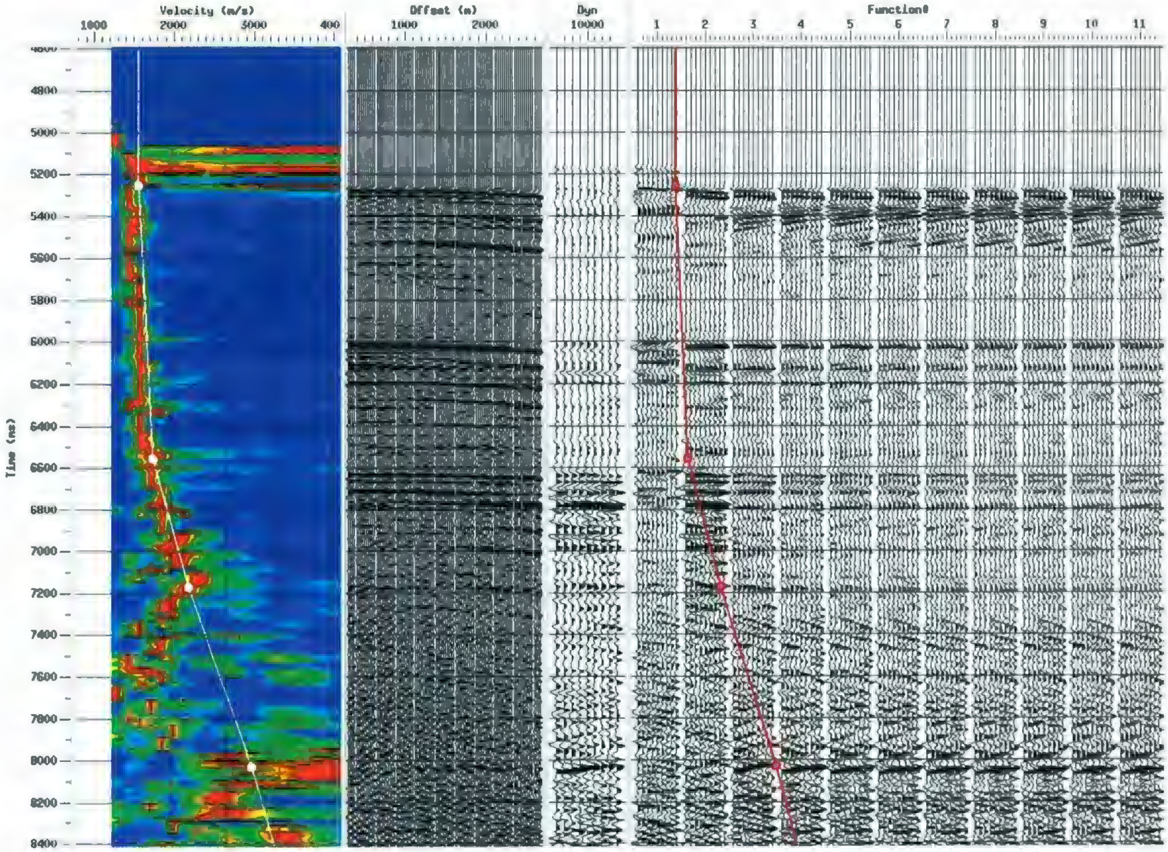

Figure 2.13: Velocity analysis of CDP gather taken from deep water section of Line 54. Note the improvement of the semblance peaks when picking a stacking velocity function.

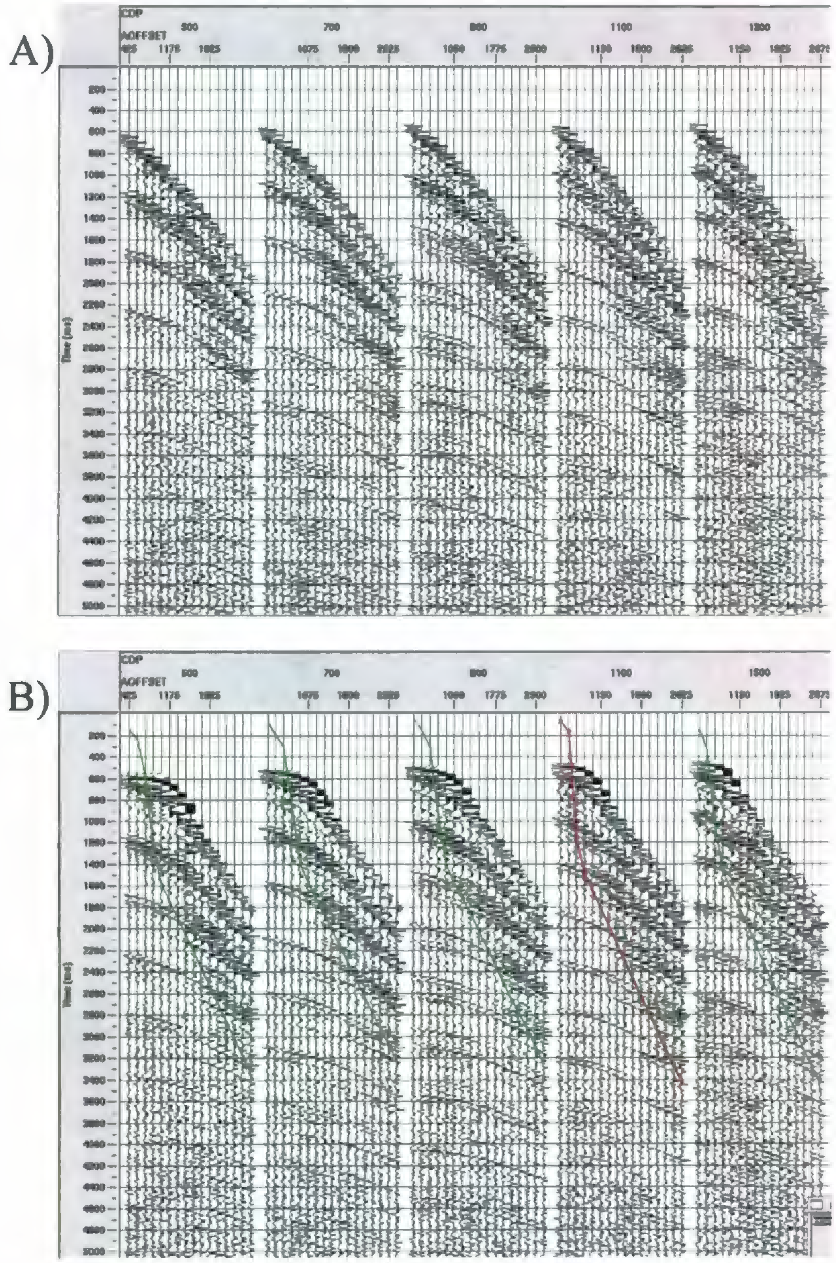

Figure 2.14: CDP gathers from shelf a) without and b) with NMO correction applied. Note the top NMO stretch mute in b) that is applied before stacking to remove NMO Stretch.

2.7 Deconvolution

Deconvolution is a process that may be applied pre- or post-stack to improve the temporal resolution of the data (Yilmaz, 1987, p. 83). Generally there are two types of deconvolution filters used in seismic processing: deconvolution and predictive deconvolution. The first filter compresses the seismic wavelet giving the section a much less "ringy" appearance. The second filter is used for multiple attenuation, which is applied by using the periodic rate of the multiples to predict when they will occur. Both filters are applied in such a way that a prediction lag gap (α) and a prediction filter length (n) are chosen in milliseconds, where the first α lags of the autocorrelation that are preserved, and the remaining n lags are reduced to zero. The difference between a spiking and prediction deconvolution filter lies in the length of the prediction filter and

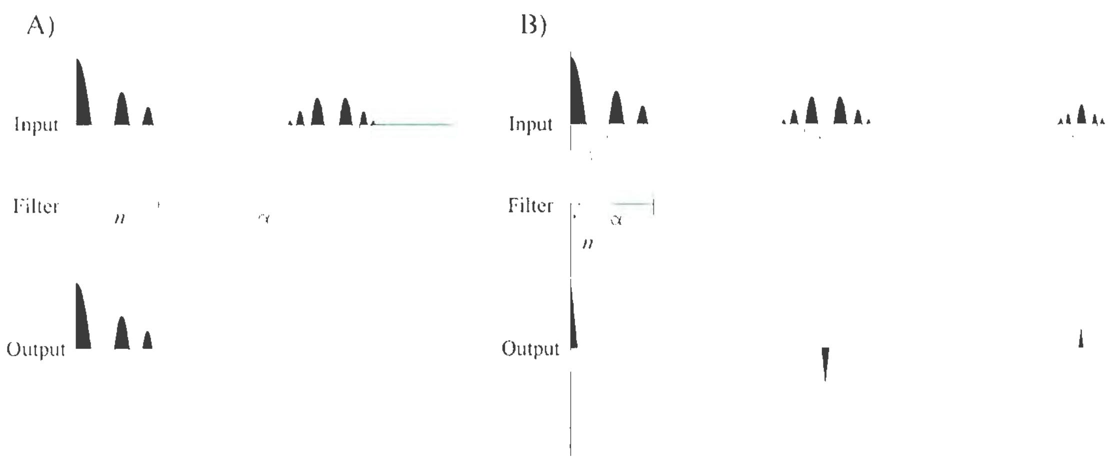

Figure 2.15: a) Autocorrelations of a seismogram illustrating the length of n and α used to design a predictive deconvolution filter, and below the autocorrelation of the output of the filter. b) Autocorrelations of a seismogram illustrating the length of n and α used to design a spiking deconvolution filter, and below the autocorrelation of the output of the filter.

prediction gap. The spiking deconvolution filter uses a prediction lag gap of 1 time sample period with a prediction filter length that encompasses the ringing of the wavelet. A prediction deconvolution filter uses a gap that is just shorter than the multiple period, and the prediction filter length encompasses the first multiple (Figure 2.15).

2.7.1 Spiking Deconvolution

Figure 2.16 is a brute stack seismic section. Note the waveform of the water bottom reflection contains 3 peaks, and this section is characterized by having a "ringy" appearance. The auto correlation function was calculated for this section of the line (Figure 2.17). There is a strong continuous peak at approximately 100 ms lag, a second less continuous peak at 230 ms lag. The peak is repeated in parts of the lower section, but progressively becomes less continuous laterally. From this several spiking deconvolutions were tested. Spiking deconvolution attempts to balance the amplitude and power spectra, and since the data contains low frequency noise, it is useful to remove this noise before applying the deconvolution. If the low frequency noise is not removed, the deconvolution will dramatically boost the high frequencies to balance the low frequency noise, thus producing a section with over compensated high frequencies. A Butterworth filter of 5-12-70-36 was chosen to remove the low frequency noise based on the discussion in *Bandpass filtering* above. An additional bandpass filter is necessary after the spiking deconvolution to remove initial high frequency noise as well as noise produced from the spiking deconvolution filter.

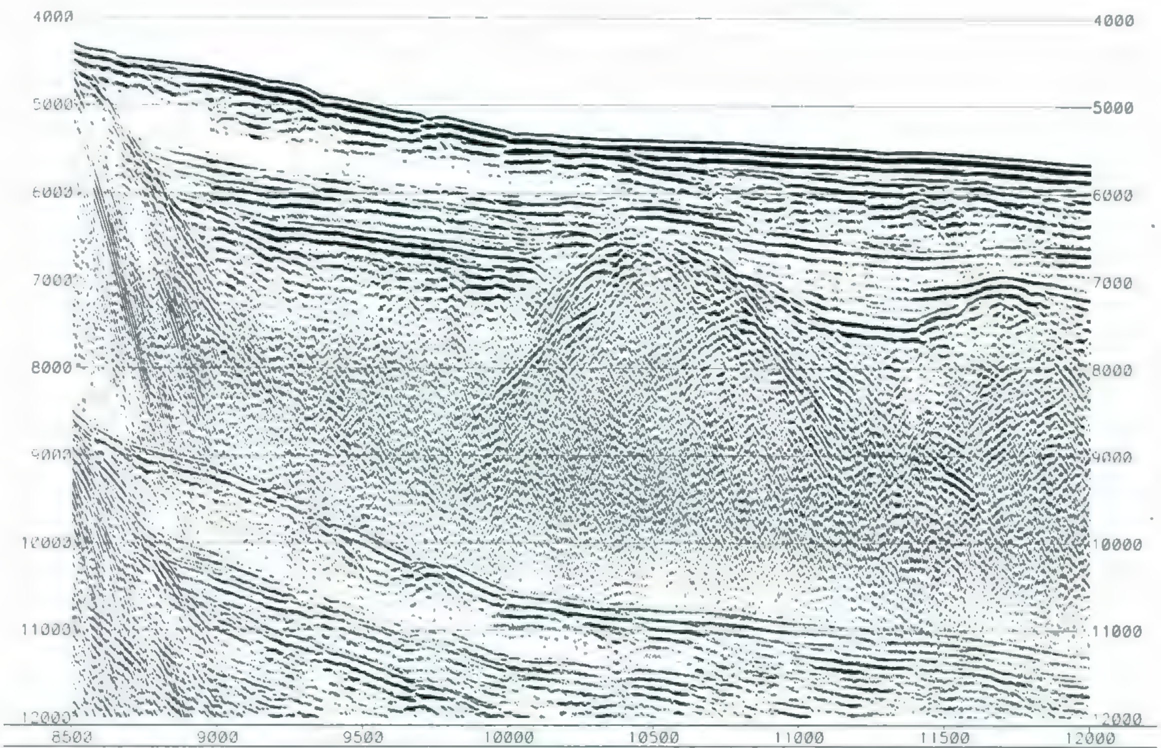

Figure 2.16: Brute stack of CDPs 8500-12000 from Line 54.

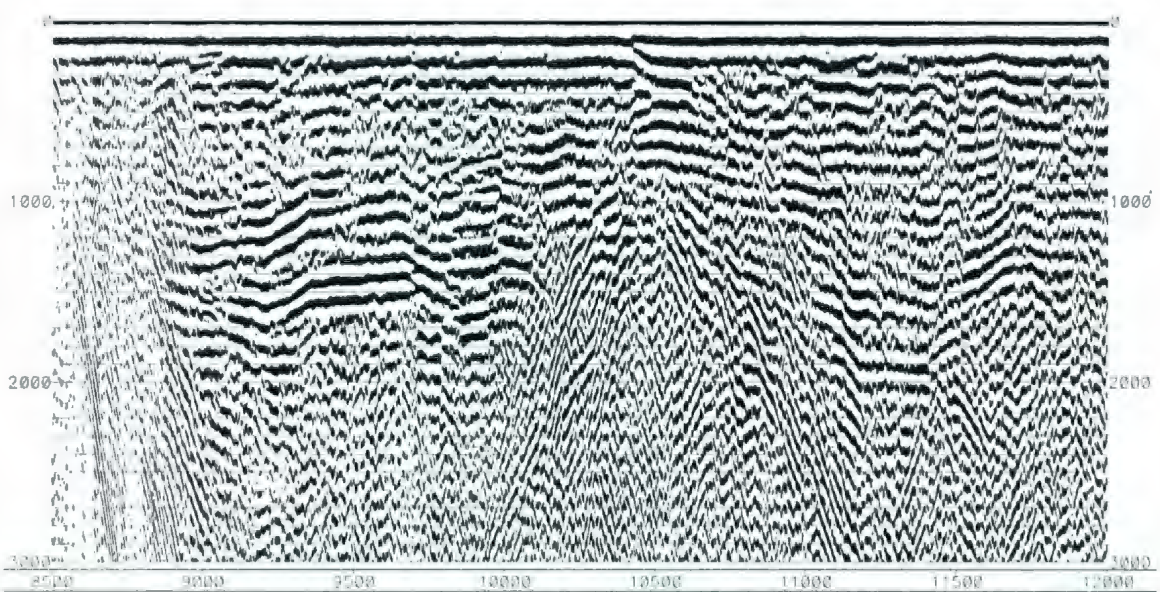

Figure 2.17: Autocorrelation of of CDPs 8500-12000 Line 54.

Various parameters for the spiking deconvolution operator length and bandpass filters were tested and compared. Initially an operator length of 150 ms was used based on the strong continuous peak in the autocorrelation. A Butterworth filter (5-12-40-24) was tested post deconvolution and pre-stack (Figure 2.18). These processing parameters produced a stack with a sharper waterbottom reflection, however there was a substantial amount of ringing of the wavelet produced by the Butterworth filter. In ProMAX there is an option within the spiking/predictive deconvolution program to apply a bandpass filter. Figure 2.19 illustrates a stack with the same operator length of the spiking deconvolution filter (150 ms), but with the bandpass filter (4-8-35-70 Hz) applied within the spiking deconvolution program. Here the ringing of the wavelet is reduced, but the water bottom refection does produce a double peak. Longer operator lengths (200 and 300 ms) in combination with the bandpass filter where tested on the data (Figures 2.20 and 2.21). Comparing the top of basement reflection on the test panels presented thus far, the 300 ms operator length produces a refection that has the least amount of ringing, which is expected based on the autocorrelation (Figure 2.17). In some cases, a predictive deconvolution filter can be used to spike the data. This is done by using a very small prediction gap and an operator length, which encompasses the ringy wavelet. The first zero crossing in the autocorrelation occurs at approximately 25 ms. So to retain the initial peak of the waterbottom refection, we use a predictive deconvolution filter with a gap of 25 ms in combination with a 300 ms operator length (Figure 2.22). The results from the spiking and predictive deconvolution using a 300 ms operator length are quite similar

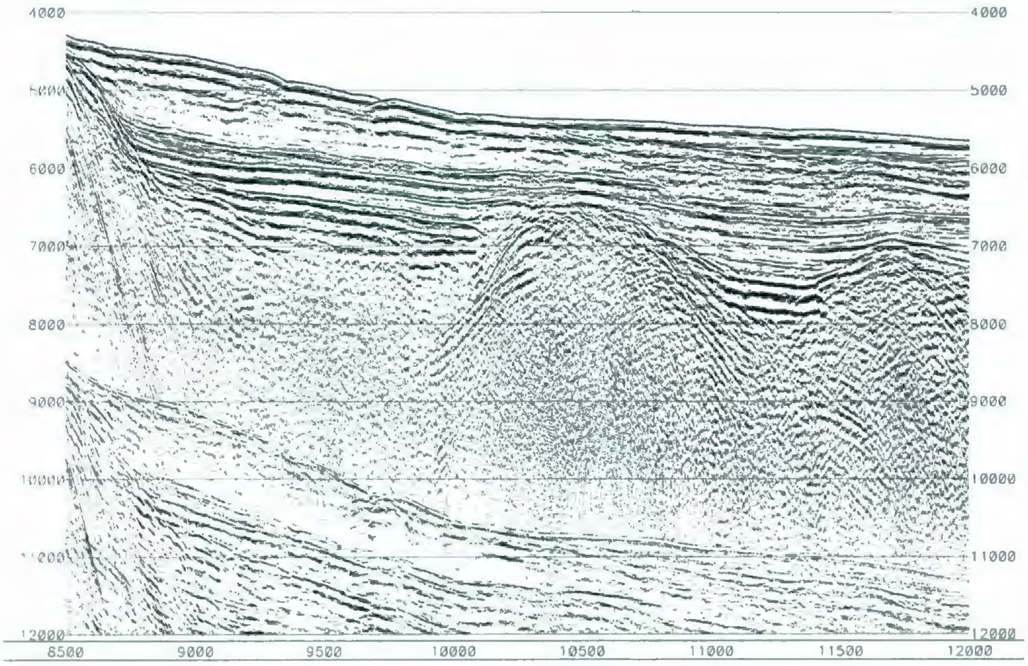

Figure 2.18: Stack with spiking deconvolution with operator length 150 and a Butterworth filter (5-12-40-24) applied pre-stack.

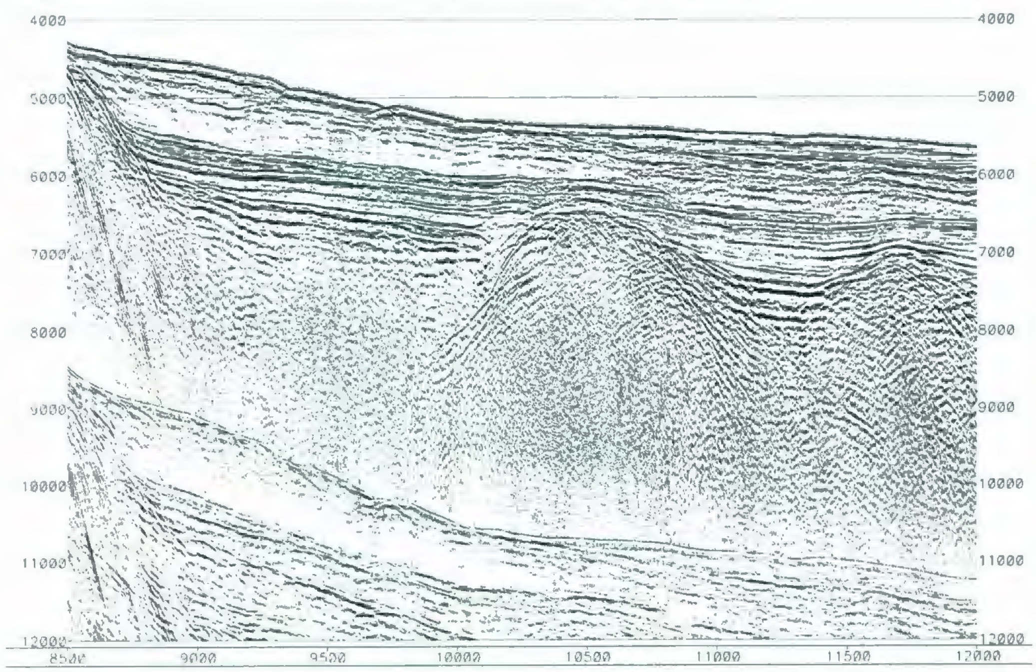

Figure 2.19: Stack with spiking deconvolution with operator length 150 and an Ormsby filter (4-8-35-70) applied pre-stack.

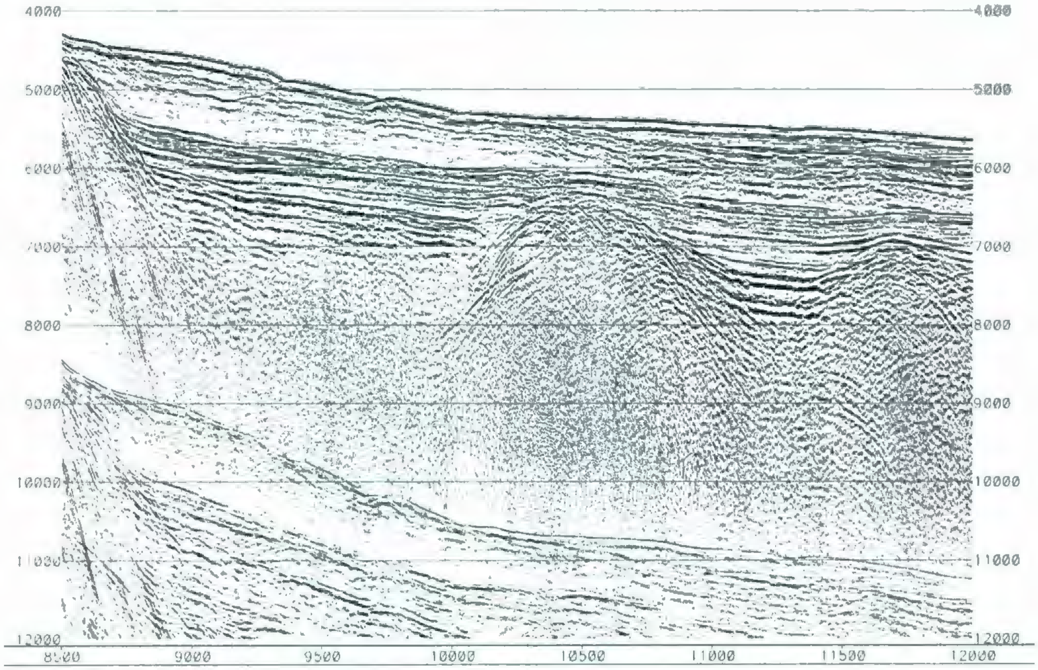

Figure 2.20: Stack with spiking deconvolution with operator length 200 and an Ormsby filter (4-8-35-70) applied pre-stack.

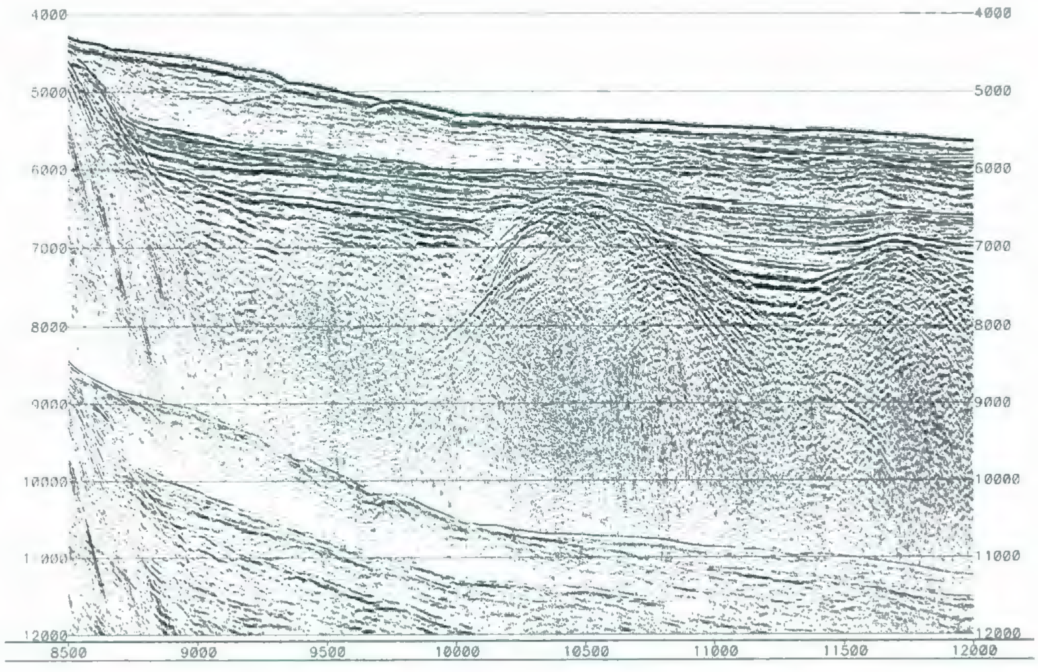

Figure 2.21: Stack with spiking deconvolution with operator length 300 and an Ormsby filter (4-8-35-70) applied pre-stack.

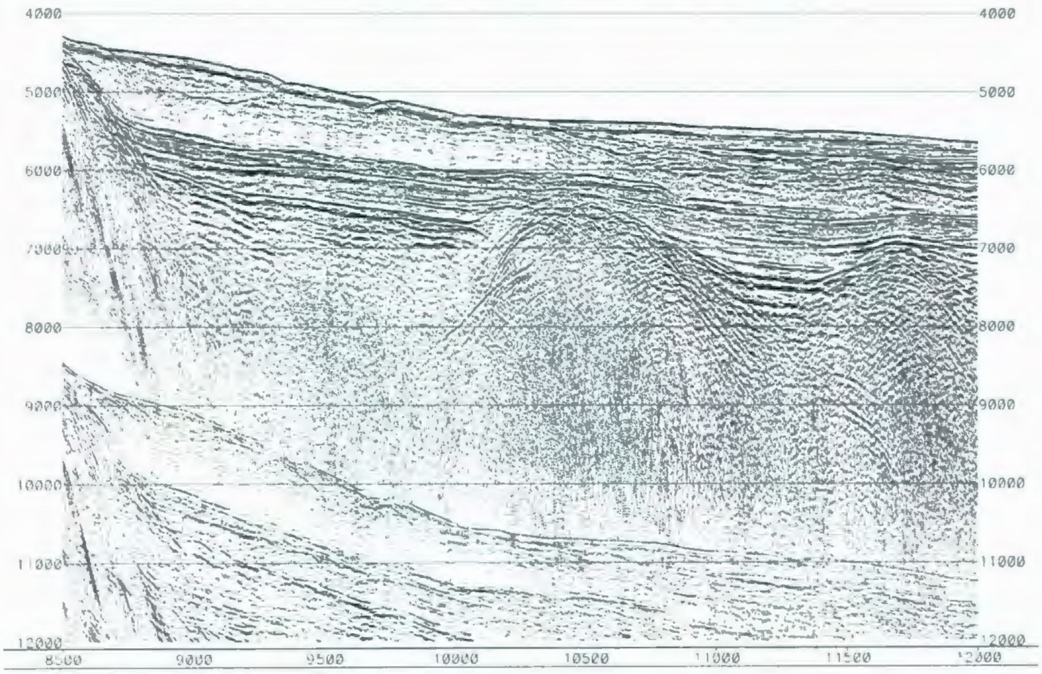

Figure 2.22: Stack with a predictive deconvolution applied to act as a spiking deconvolution. A gap of 25 ms and operator length 300 ms is used and an Ormsby filter (4-8-35-70). Both the deconvolution and Ormsby filter are applied pre-stack.

(Figures 2.21 and 2.22), except for the fact that the spiking deconvolution produces a slight doublet on the water bottom reflection, where as the predictive deconvolution section produces a clean wavelet, thus, a prediction deconvolution with an operator gap and length of 25 and 300 ms respectively is chosen to spike the data.

2.8 F-K Filter Used to Remove Linear Noise

The brute stack in Figure 2.9 illustrates the presence of linear noise that dominates the late travel times in the shelf region. Shot gathers and CDP gathers where taken from this region and are illustrated in Figure 2.23. This noise is particularly strong in the shot gathers, and less dominant in the CDP gathers. The moveout of the linear noise is measured from the shot gathers and seems that it can dominantly be separated into two groups based on velocity and frequency (Figure 2.23). The first group (N1) exhibits very low frequencies, less than 1 Hz, and velocities ranging between 1250-1390 m/s

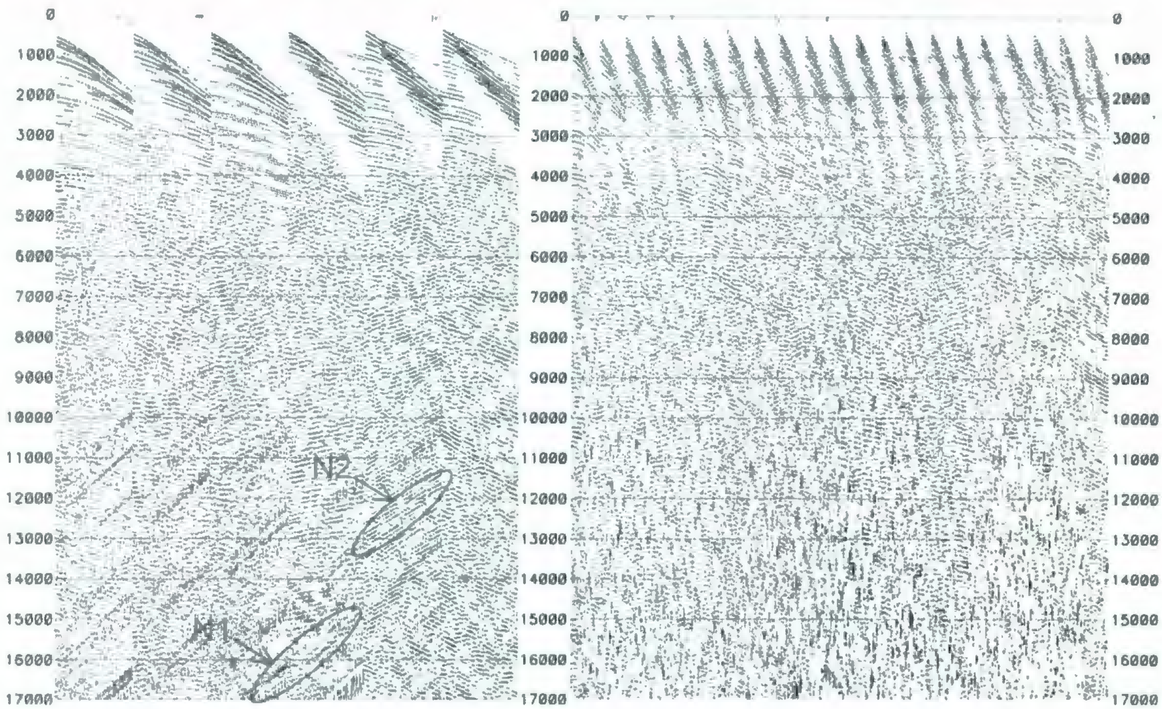

Figure 2.23: *Left:* Shot gathers 3291-3791(100), *Right:* CDP gathers 1000-3000 (100). N1 represents low frequency noise with a velocity of ~1380 m/s, and N2 represents variable frequency range noise with a velocity of ~2100 m/s.

(nominally 1380 m/s). The second group (N2) has a variable frequency range, and velocities ranging from 1950-2600 m/s (nominally 2100 m/s). Generally, there are three main types of noise that may produce linear coherent noise: 1) direct waves, or waves created by the source that travel through the water straight to the hydrophones, 2) vibrations of the cable caused by effects such as yanking of the cable from the pull of the boat, 3) waves scattered from irregularities in the waterbottom or subsurface from objects located out of the plane of the survey (Larner et. al, 1983). Direct wave noise is expected to have a velocity close to 1450-1500 m/s in seawater, and will exhibit a linear pattern in both the shot and CDP domain. Here the 1380 m/s velocity noise (N1) has a velocity slower than that typical of sound traveling through seawater, and the noise does not remain linear when sorted into CDP gathers. Also, application of a low cut bandpass filter successfully removes N1 as seen in Figure 2.24. The frequency dependency of this noise coupled with the low velocity suggests that this noise is likely

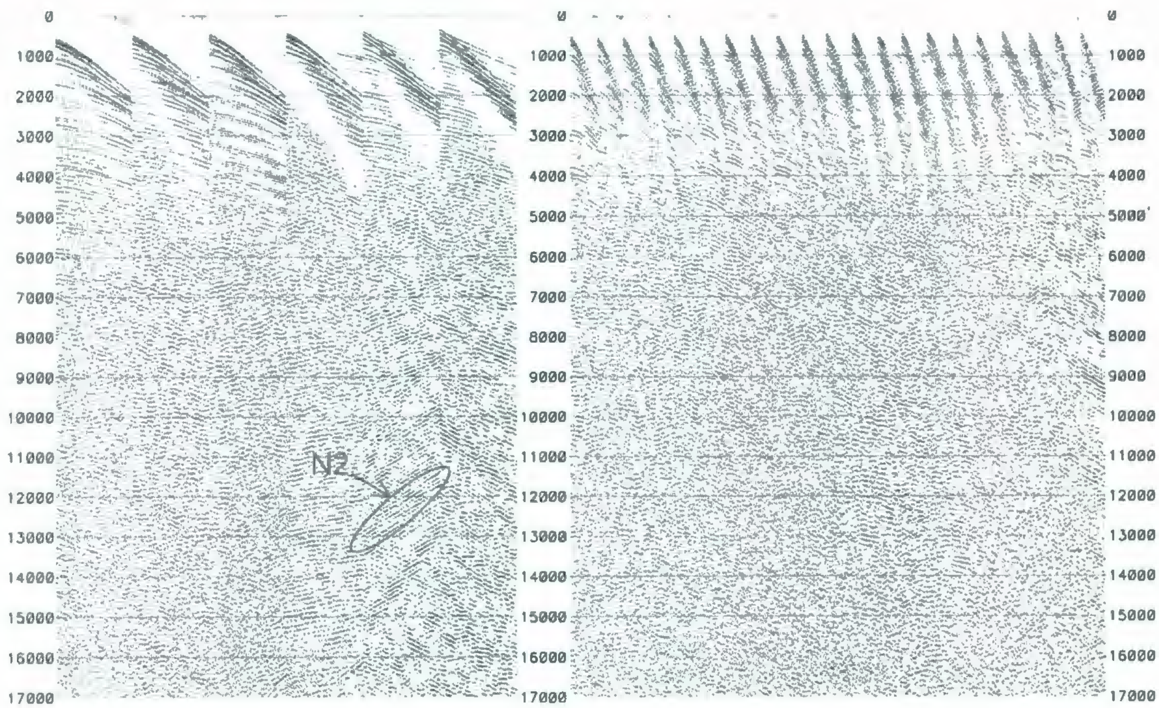

Figure 2.24: *Left:* Shot gathers of FFID's 3291-3791(100), *Right:* CDP gathers 1000-3000 (100). Both have a 5-12-70-36 Butterworth bandpass filter applied. The bandpass filter has done an excellent job of removing N1, but N2 still remains.

derived from mechanical cable motion (Larner et. al, 1983). However, these velocities are slightly higher than what is expected when comparing with results found by Weichart (1973). This paper suggests that pulsed waves traveling through the streamer have a velocity that is about 15% lower than that of water velocity. From Figure 2.24 it is apparent that there still remains noise, dominantly with a 2100 m/s moveout. This noise has a higher apparent velocity than would be expected from direct waves or cable motion, and is assumed to be caused by side-scattered waves. Note that the hyperbolic reflections asymptotically approach a straight line moving away from the apex. If the scatter lies substantially in front or behind the streamer, the apex of the refection will not appear on the shot gather, and thus the refection moveout will appear linear (Larner et. al, 1983).

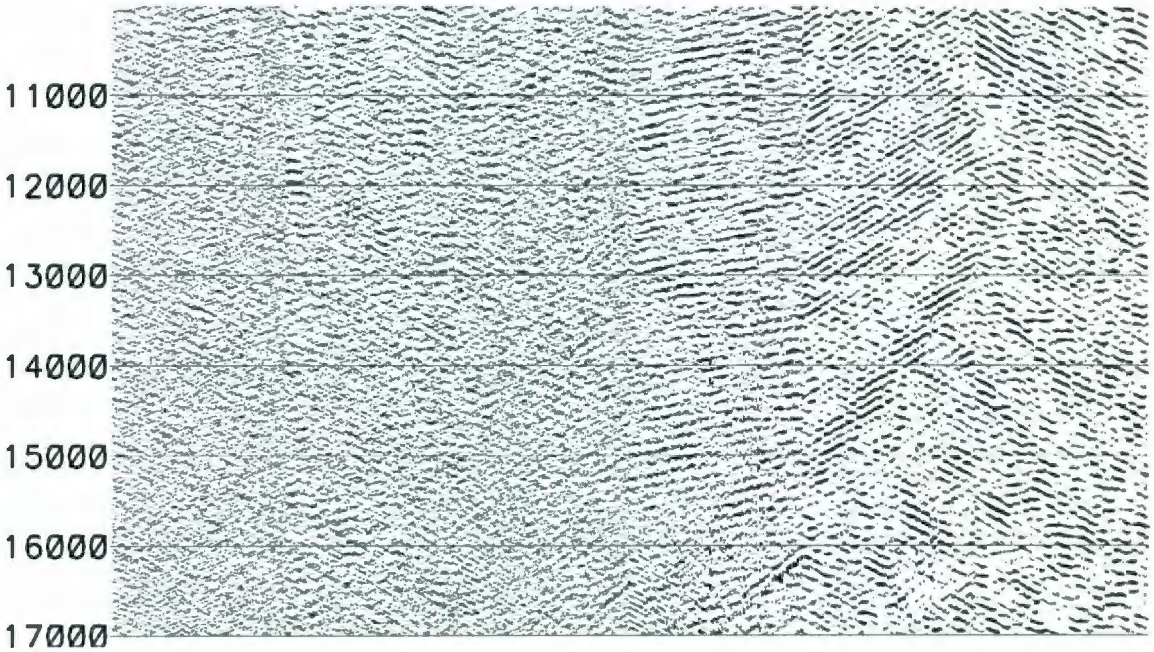

Figure 2.25: A zoomed in view of the bottom section of FFID's 3291-3791(100) shown in Figure 2.24. A 5-12-70-36 Butterworth bandpass filter has been applied.

The bottom 10-17 sec is blown up from Figure 2.24 shot gathers to take a closer look at the frequency content of the remaining noise that has not been removed from the bandpass filter (Figure 2.25). The linear noise on the first 4 shot gathers (from right to left) contains high frequencies, while the linear noise on the last two shot gathers are dominated with low frequencies. Here the linear noise is represented by a large range of frequencies that overlap with signal. Thus, attempting to remove the noise using the bandpass filter to pass a smaller range of frequencies would also result in removing some primary reflectivity.

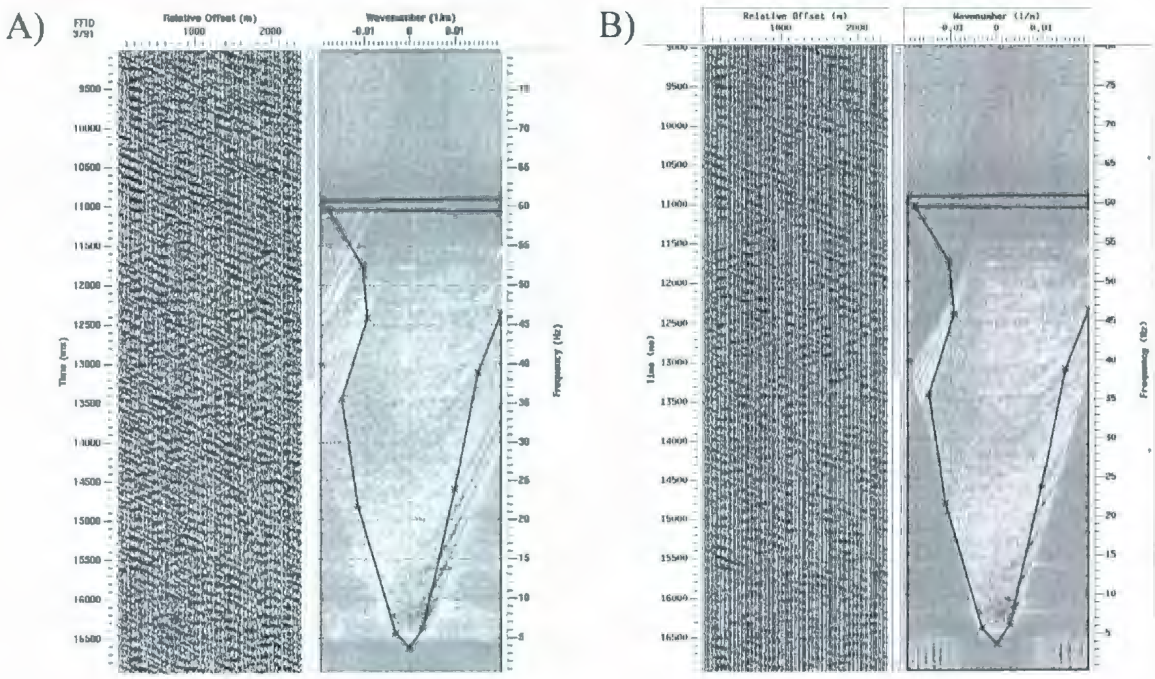

Figure 2.26: a) F-k analysis of shot gather (FFID 3791) from shelf region and b) output of filter.

Since the remaining noise dominantly has a velocity close to, or less than 2100 m/s, the noise can be separated based on its slope in the t-x domain. The shot gathers (time-offset domain) can be 2-D Fourier transformed into the frequency and wavenumber domain (f-k domain), where the inverse slope of an event in the t-x domain is equal to the slope of an event in the f-k domain (Yilmaz, 1987, p. 63). A polygon filter is designed to remove the linear noise, and then the data is 2-D inverse Fourier transformed back to the t-x domain (Figure 2.26). This filter is successful in attenuating the linear noise, but has not completely removed it. In parts of the data where only noise is present without any primary reflections, removing steep linear slopes causes new shallower slopes to align.

2.9 F-K Demultipling

2.9.1 Continental Shelf

The shelf of Flemish Cap is an area where the water is very shallow, and thus a large number of multiple reflections dominate the first 5 seconds or so of data. The f-k filter can be a useful tool for separating the multiple and primary energy. In the f-k domain, events with negative dip plot in one quadrant of the f-k spectrum, events with positive dip plot in the other quadrant, and flat events plot along the zero wave number axis. Multiple reflections have a velocity slower than primary reflections, and can be separated based on the NMO corrections to CDP gathers. However, the CDP gathers have a maximum fold of 12 traces, which is not enough samples for the f-k filter to work with, hence the data becomes aliased. Since the shelf is a flat area where the lateral variation is gradual, adjacent CDP gathers can be combined into super gathers which increase signal to noise ratio and reduce aliasing. 8 adjacent CDP's are combined to give the full range of offsets for the f-k filter to work with.

It is a common practice to use the f-k filter for multiple removal on CDP gathers, or supergathers in this case. This is done by applying a NMO correction with a velocity function greater than that of the multiple reflections but lower than that of the primary reflections (Yilmaz, 2001, pg. 911). This produces primary reflections that are over corrected (positive dip), and the multiple reflections that are under corrected (negative dip), thus separating the reflections into different quadrants when the data is transformed from the t-x into the f-k domain (Figure 2.27and 2.28).

The energy from the multiple reflections now plots on the right side of the f-k spectrum, which is removed (zeroed). Once the data are transformed back into the t-x domain, the NMO correction used for the f-k filter is removed, and the super gathers are resorted into CDP gathers using inline sort. At this point a new NMO correction is applied to the CDP gathers to flatten primary reflections for stacking. However, it should be noted that multiple reflections were not successfully removed by this process from the near offset traces (Figure 2.29).

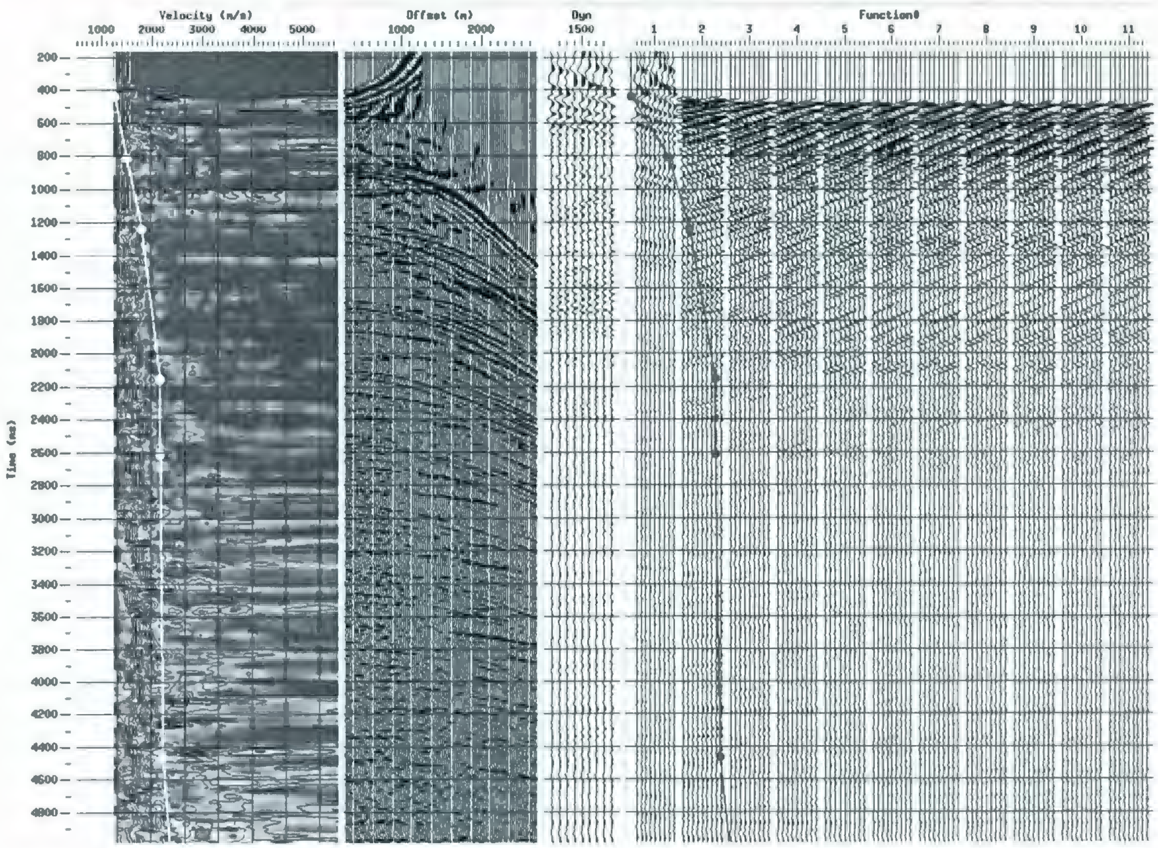

Figure 2.27: Velocity semblance illustrating CDP gather that has NMO correction that over corrects the primary reflections and under corrects the multiple reflections.

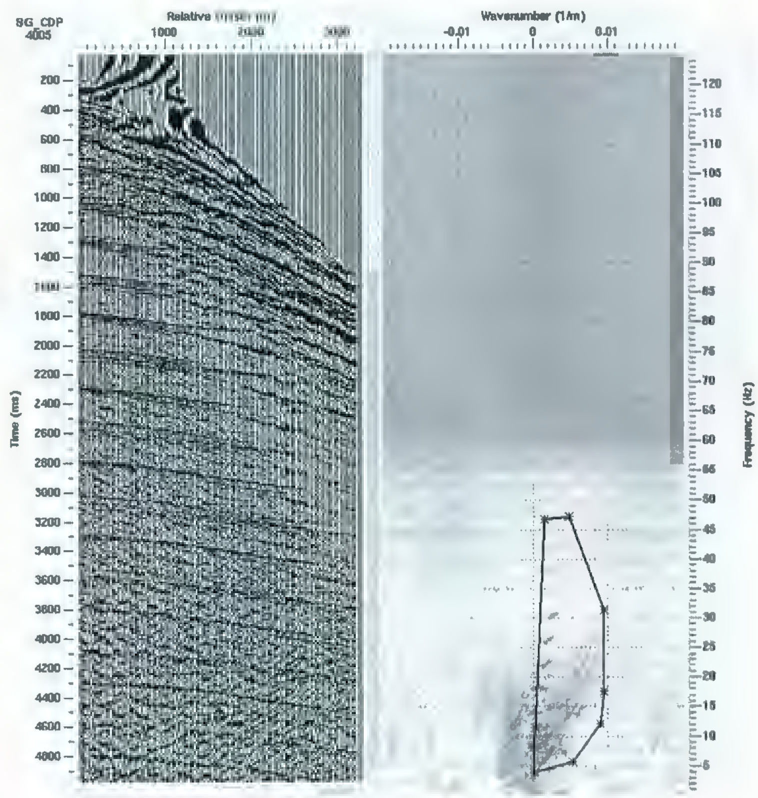

Figure 2.28: CDP gather that is 2-D Fourier Transformed from the t-x domain to the f-k domain. The region enclosed by polygon is removed to attenuate multiple reflections.

Recall that reflections plot on CDP gathers as hyperbolic functions, so that the event dip on the near offset traces are very shallow, perhaps flat in areas, and the dip increase moving into farther offsets. This means that the near traces of the reflections plot near k=0 within the f-k domain, and the k value increases as offset increases. It is undesirable to use the f-k filter to remove energy very close to k=0 because this will also include energy from primary reflections. A solution to this problem is to mute the near traces. A near trace mute was designed (Figure 2.29) and applied to the f-k filtered CDP gathers before stacking. Figure 2.30 compares a stack of the upper shelf section with and without the f-k filter (and near trace mute), where the f-k filtered section shows improvement.

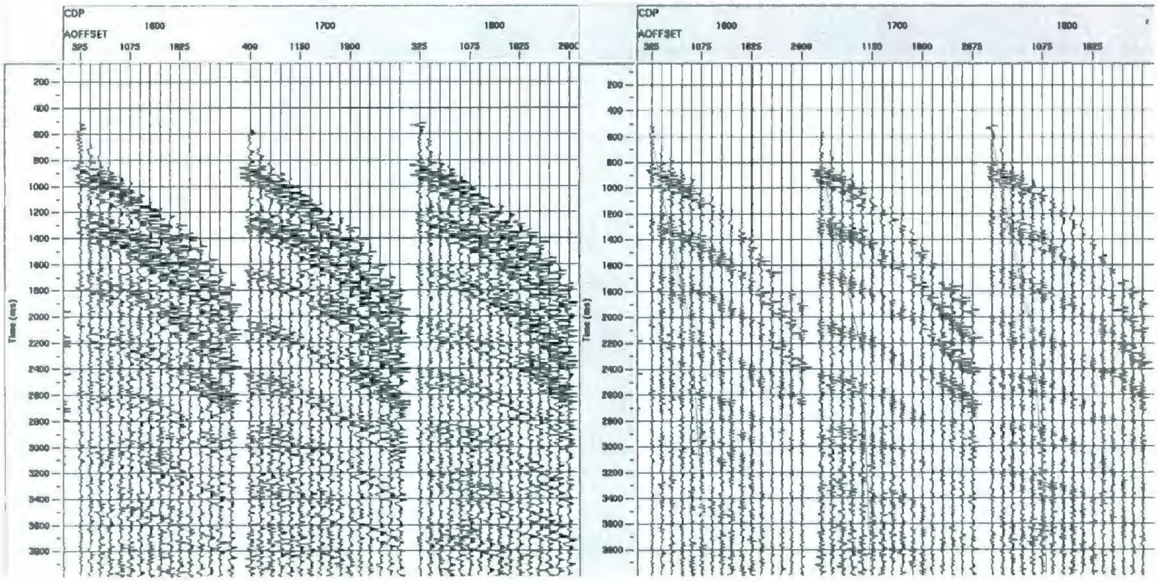

Figure 2.29: CDP gather before (right) and after (left) application of f-k filter for multiple reflection removal. The green line to the left represents the near trace bottom mute applied before stack.

Since multiple energy is strongest in the first 5 seconds of data, the f-k filter is only applied to this section of data using the windowed processing tool. Appling the near trace mute to the entire section reduces the signal of the Moho reflection, so the near trace mute was only applied to the f-k filtered section of data (first 5 seconds of data), also using the windowed processing tool. Attenuating the multiples improves the accuracy of picking velocities within the velocity analysis, thus stacking velocities along the shelf are re-picked at this point (Figure 2.31).

A)

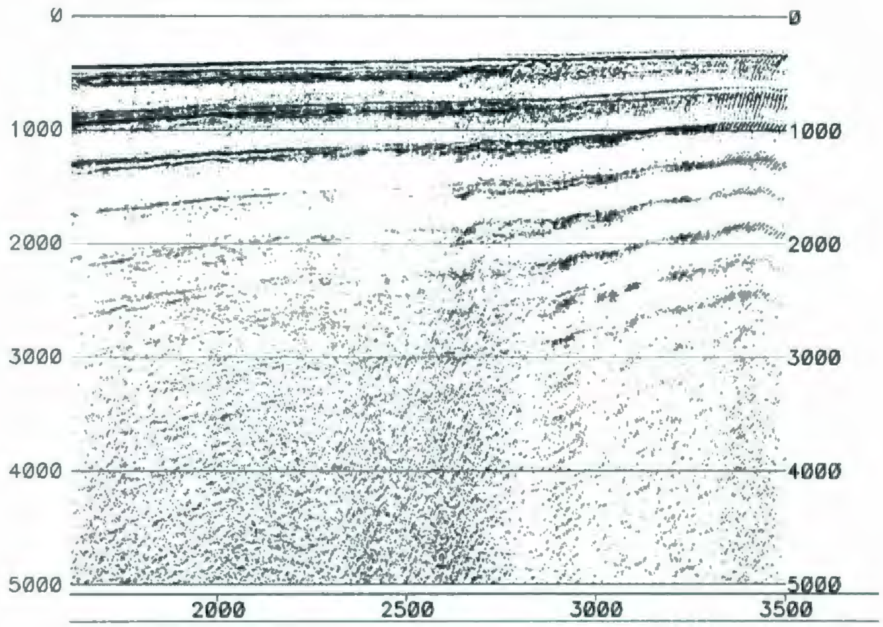

B)

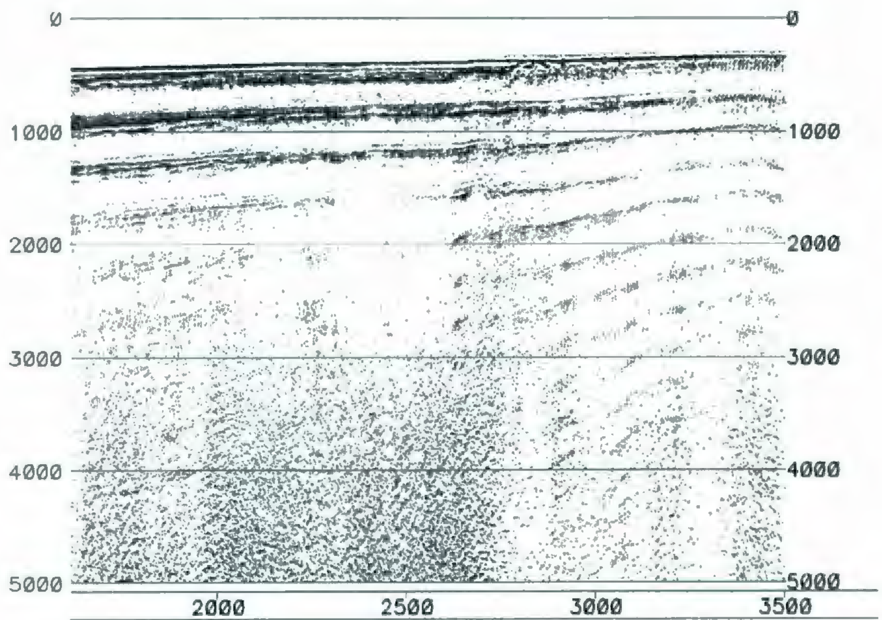

Figure 2.30: Stacked section a) before and b) after application of f-k filter and near trace mute for multiple reflection attenuation.

A)

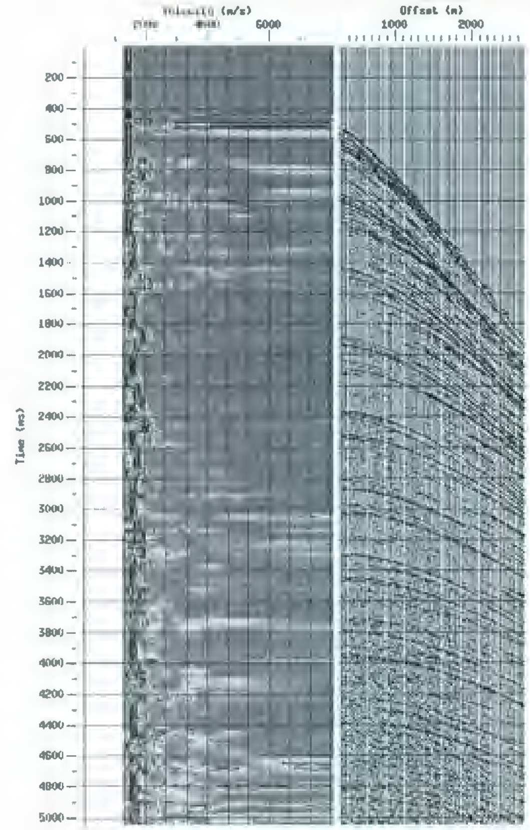

B)

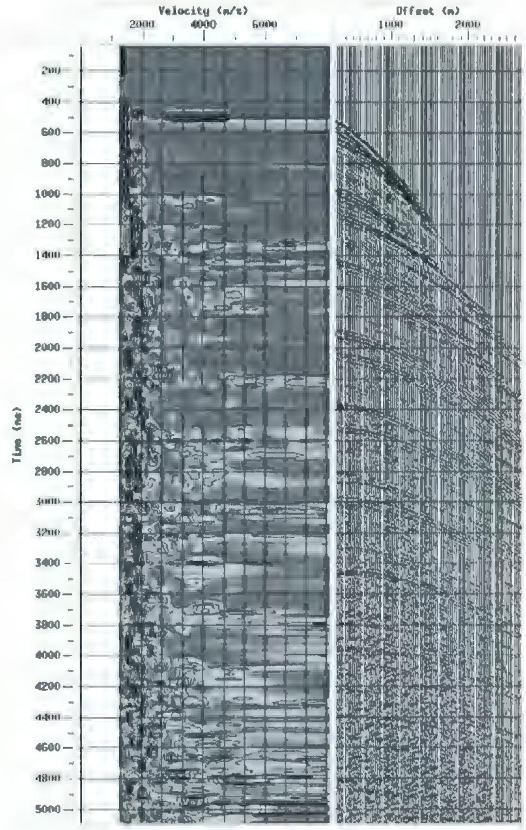

Figure 2.31: a) Velocity analysis of CDP gather before and b) after application of f-k filter used to attenuate multiple reflections. Note that the semblance peaks are stronger in the f-k filtered CDP gather.

2.9.2 Continental Slope

The f-k filter was also tested on the slope to remove multiples, however it was unsuccessful in this region. The slope is an area where the depth of sea-bottom is changing very rapidly, and also has very rugged topography. Combination of 8 adjacent CDP's to form super gathers including a full range of offsets was tested in this region. This produced very incoherent (jagged) reflections that could not be removed by f-k filter (Figure 2.32).

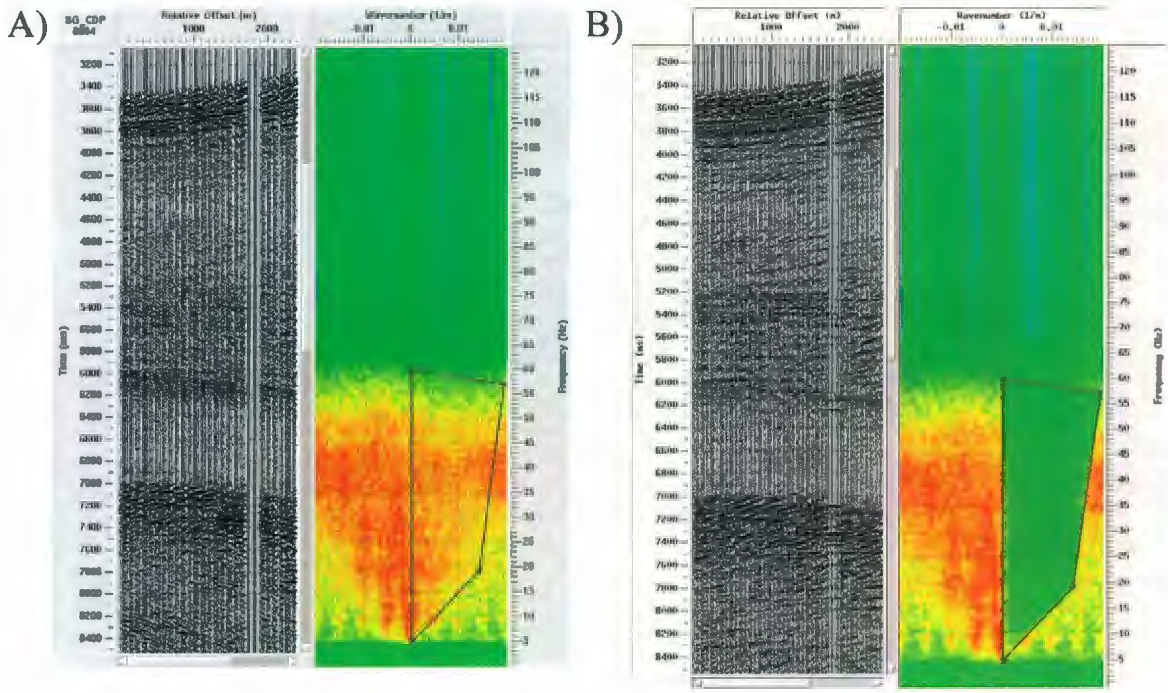

Figure 2.32: (a) F-k analysis of super gathers on slope (b) and output of f-k filter. Note the jagged character of reflections where overall shape of multiple is down-dip, but individual sections align up-dip. This plots the multiple energy on the left side of the f-k spectrum, explaining why the multiple is not attenuated.

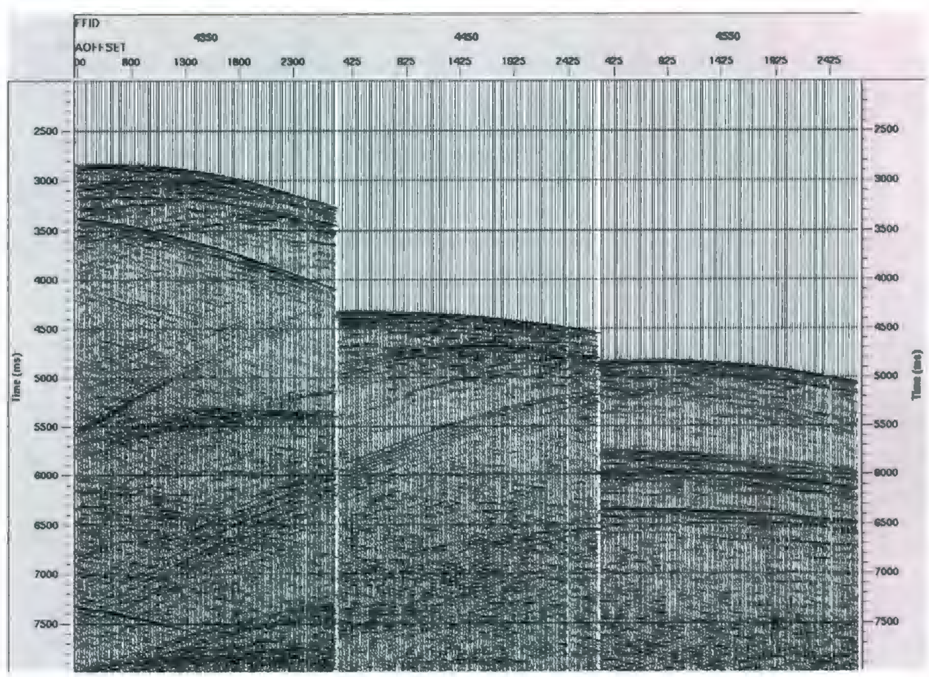

Figure 2.33: Shot gathers illustrating the wide range of dips on the primary reflections.

Interpolation of traces was also tested before f-k filtering. The traces were interpolated in the shot domain, since there are more traces and hence more samples for the interpolation to work with, then resorted into CDP gathers. The f-k filter was applied to the interpolated CDP gathers, and the interpolated traces were then removed, leaving only the original traces with the f-k filter applied. Unfortunately this process was also unsuccessful in removing much of the multiple reflections.

Another possibility explored was to apply the f-k filter to the shot gathers. However there were many shots in the slope area that occurred on steeply dipping surfaces that caused primary reflections to have both positive and negative dips, making it difficult to separate primaries and multiples in the f-k domain (Figure 2.33). Receiver gathers were also considered but had the same problem (Figure 2.34).

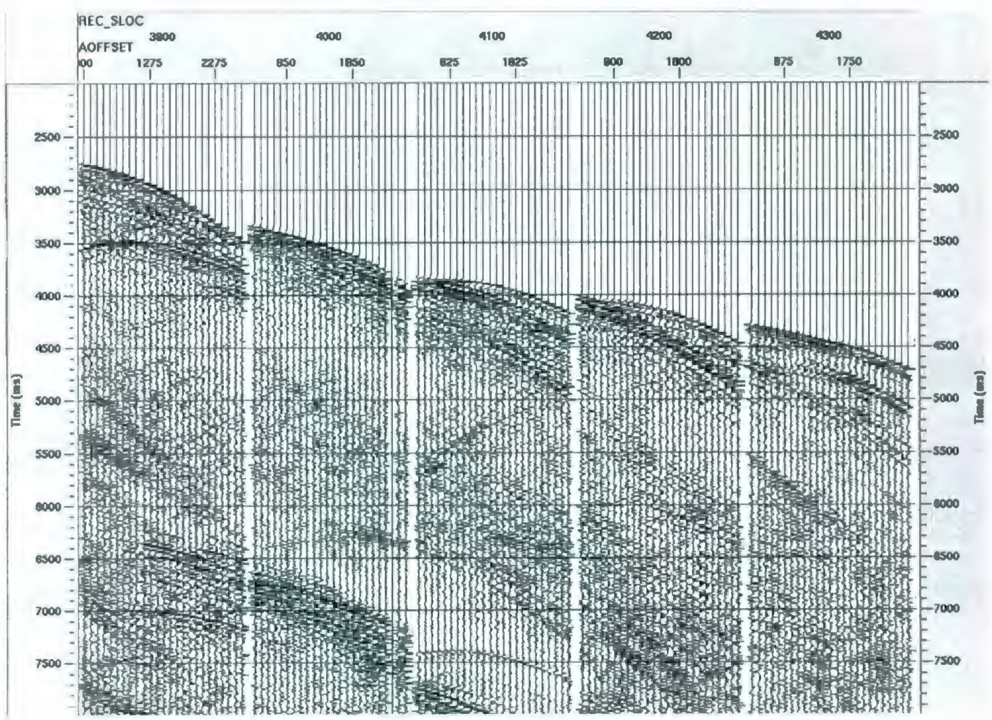

Figure 2.34: Receiver gathers illustrating the wide range of dips on the primary reflections.

2.10 Radon Filter

The slope is a section where we would like to carefully remove the water bottom multiple in hopes of recovering any deep primary reflections. This must be done with care so that removing the multiple does not diminish the signal of any primary

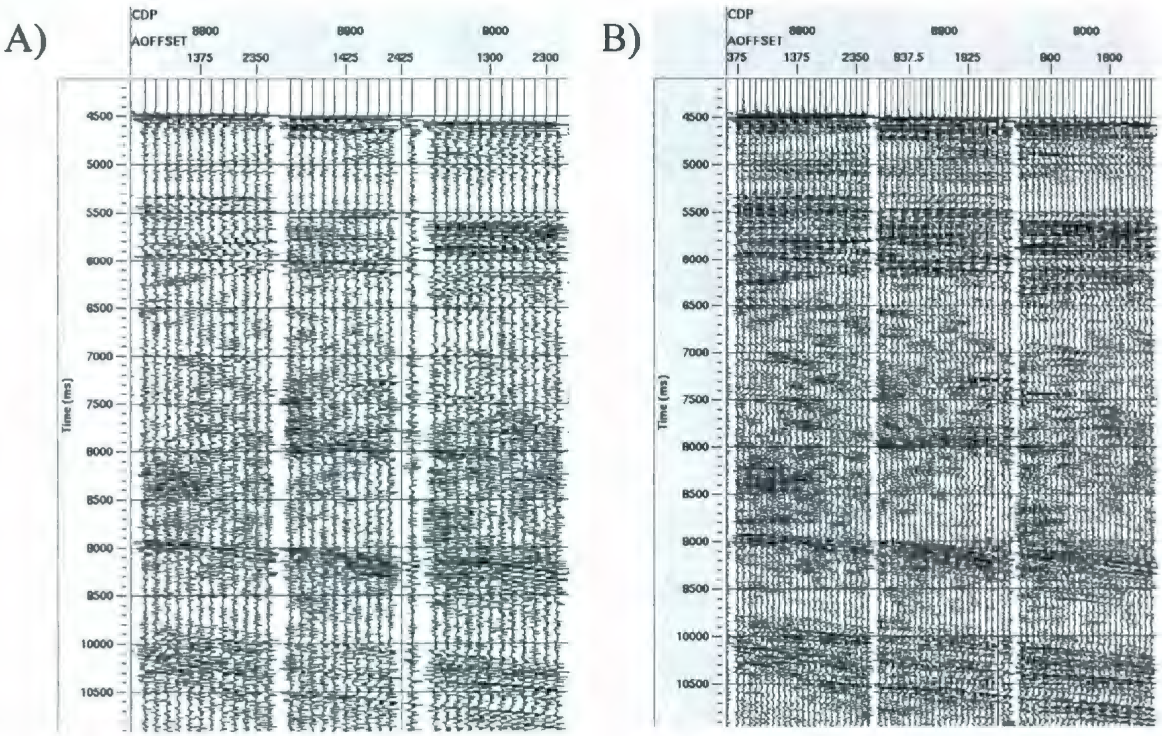

Figure 2.35: NMO corrected CDP gathers a) before and b) after Beam and Steer interpolation.

reflections. The radon filter is a common technique used for multiple reflection removal. This technique works on the principle that multiples have a hyperbolic travel time moveout different from that of the primary events that occur at the same arrival time (Foster and Mosher, 1992). As mentioned earlier, CDP gathers alone do not provide enough samples for the radon filter to work with, and combination of adjacent CDP's does not work in this area due to rapid changes in water bottom depth and dip.

Interpolation of CDP's was tested in combination with the radon filter. Various interpolation programs were tested, yet the Beam and Steer interpolation proved to work the best and was chosen for this reason (Figure 2.35).

Before applying a Radon filter, a NMO correction is applied to the CDP gathers using a velocity function that flattens the primary events, but under corrects the multiples. Next we transform the data in such a way that the data is stacked over a range of different hyperbolic or parabolic surfaces, so that primary and multiple events (with different moveout) plot in different regions (Foster and Mosher, 1992). ProMAX allows you to chose either a hyperbolic or parabolic surface to fit to the reflections, where a hyperbolic surface is recommended for deep water sections (Landmark ProMAX Software Manual) and is chosen for these data. Figure 2.36 is an illustration of a CDP gather transformed to the radon domain.

Now that the primary reflections are separated from the multiples, a top mute is applied to remove the primary reflections. The multiple reflections are then inverse transformed from the Radon domain to the t-x domain, and subtracted from the original data (Figure 2.37). This in theory should leave only the primary reflections remaining. Since the Radon filter is fitting reflections to hyperbola as opposed to the f-k filter which is fitting reflections to straight lines, it should also do a better job of removing multiples at near offsets.

However, it should be noted that there is somewhat of an overlap between the primary and multiple energy within the Radon domain. Removing most of the multiple

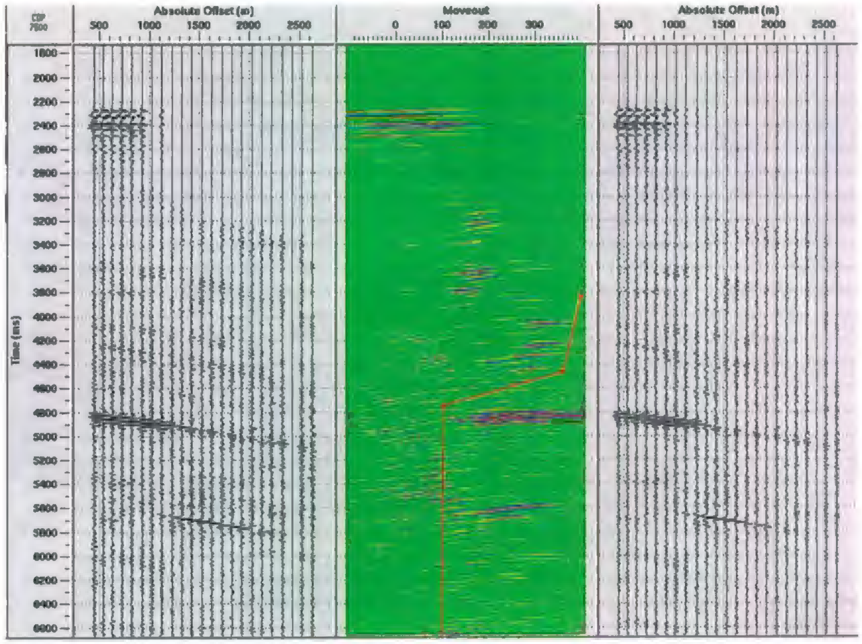

Figure 2.36: On the left is the input CDP gather, the middle is the radon transform of the CDP gather, and on the right is the inverse radon transform to get back the original CDP gather.

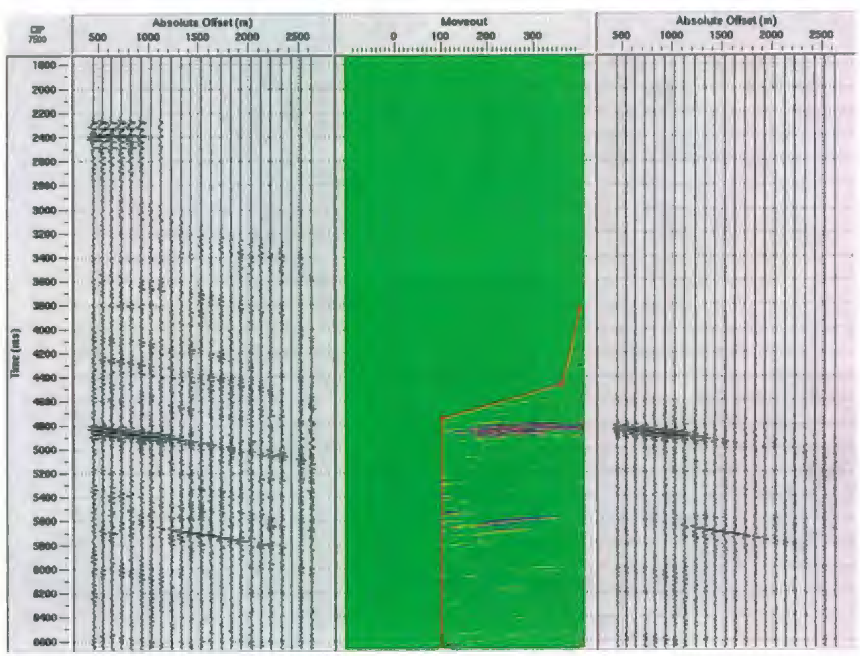

Figure 2.37: On the left is the input CDP gather, the middle is the radon transform of the CDP gather with the primary reflections removed, and on the right is the inverse radon transform to get back the multiple reflections. See Figure 2.38 for results of radon filtered CDP gathers.

reflections causes a problem, being that this diminishes weak primary reflections that are cut by the water bottom multiple. Because of this various primary mutes were tested, and the mute which yielded the best signal to noise ratio of primary reflections cut by the water bottom multiple was chosen. The remaining multiple energy does pose a problem during the stacking process. Multiple reflections keep their hyperbolic shape while primary reflections are flattened after a NMO correction has been applied for stacking. Although multiple reflections have a considerable amount of curvature at large offsets, they are quite flat at near offsets, meaning remaining noise from multiples will sum together at near offsets and cancel at far offsets. Because of this, a mute was designed to remove the near traces after the first water bottom multiple (Figure 2.38).

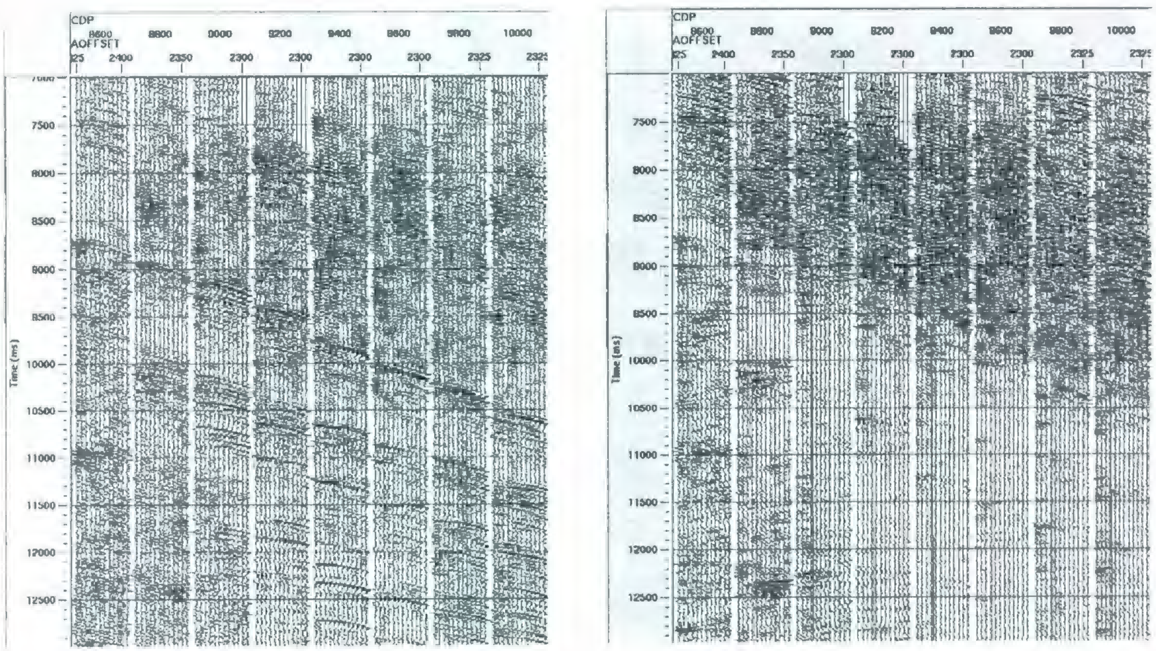

Figure 2.38: *Left*: CDP gathers before application of radon filter. *Right*: CDP gathers after application of radon filter with interpolated traces removed. Red and green lines on right indicate where near trace bottom mute is chosen to remove remaining noise at near offsets. Figure 2.39 illustrates the stack of both sets of CDP gathers, where the radon filter did a good job of suppressing the water bottom multiple.

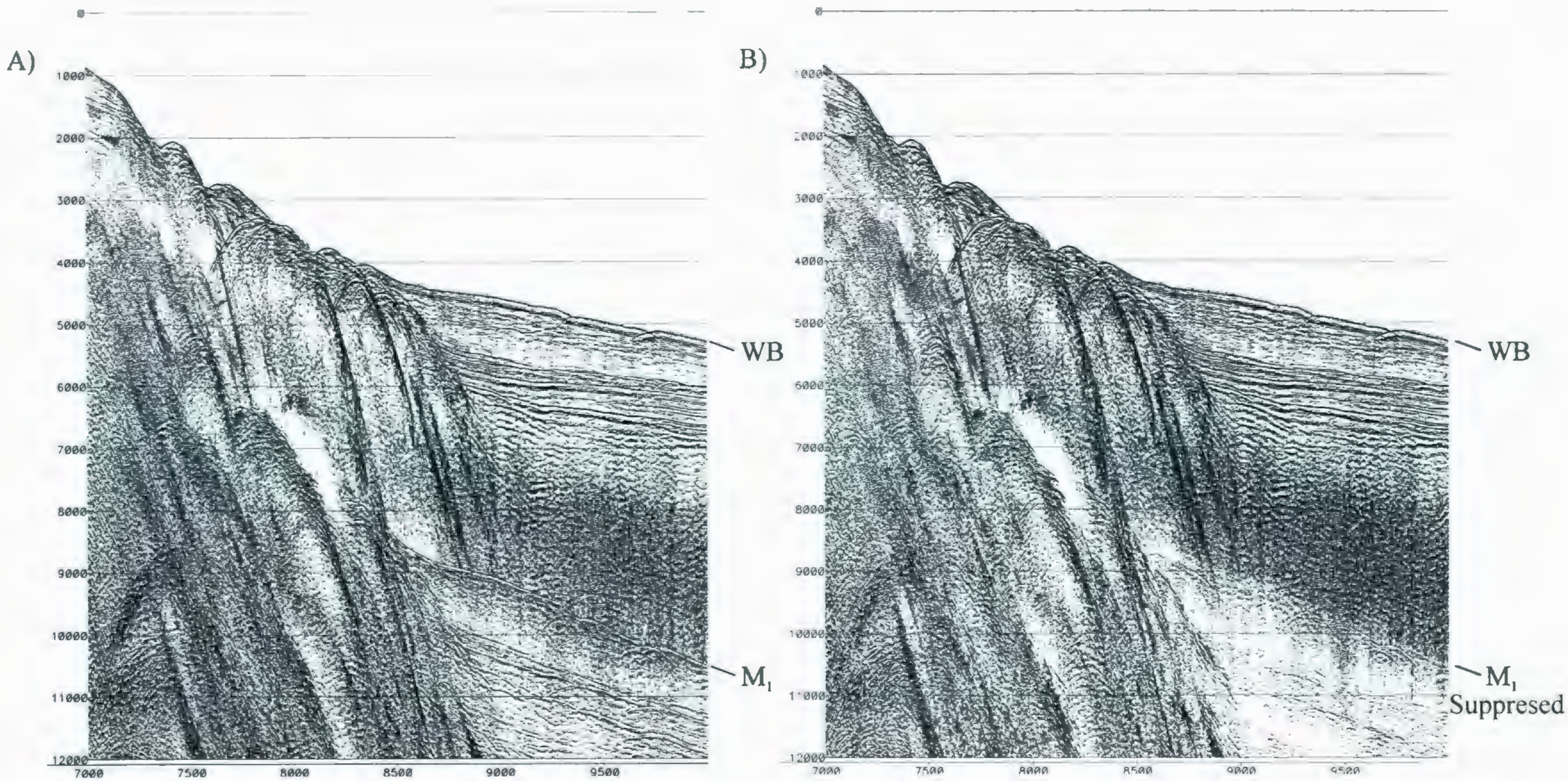

Figure 2.39: a) Stack of slope without radon filter. b) Stack of slope with radon filter and near trace mute applied before stack.

2.11 Post Stack Processing

2.11.1 Predictive and Adaptive Deconvolution

ProMAX contains several processors that predict and attenuate multiple reflections. Testing has been performed with a predictive deconvolution filter, and also an adaptive deconvolution filter, where both take advantage of the periodic and predictive nature of the water bottom multiples to remove them. This water-born noise appears in the seismic section at a two way time that is a multiple of the water bottom time. It is desirable to vary the deconvolution prediction gap onset as the water bottom time varies. This is achieved by picking a horizon that follows the water bottom. The horizon can then be transferred to the database as a water bottom header, and the header attached to the data to which the deconvolutional filters will be applied. ProMAX allows both the predictive deconvolution and adaptive deconvolution prediction gap to be applied water bottom relative. It is recommended to input a negative prediction gap of a few milliseconds since the multiple may not occur at exactly twice the water bottom time (Landmark ProMAX Software Manual).

The predictive deconvolution filter allows for definition a window of data from which the filter is designed. ProMAX also allows defining more than one design window, meaning that more than one filter can be designed. In this case, each filter is designed and applied within that time gate, and the program will interpolate or extrapolate between or outside each specified time gate. This is useful since the frequency content and character of the wavelet changes within the section.

The adaptive deconvolution filter works differently in that it does not use time gates to design the filter, and works with the full seismic trace. Within this program there is a parameter that can be varied to change the amount of the multiple energy removed, and this parameter is referred to as the rate of adaptivity (Landmark ProMAX Software Manual). This is a ratio that represents the degree to which the filter adapts itself to be similar to the section of multiple energy. A very low adaptive rate would mean that the filter used for deconvolution would only remove multiples that are almost exact duplicates of the primaries, where a very high adaptive rate would mean that the filter would adapt itself to be similar to that of the multiple, thus removing a great portion of the multiple within the given operating length. The ProMAX manual suggests that an adaptive rate of 0.1 is a good starting point. Extensive testing is performed with both filters on shelf, slope, and deep water sections of the data as discussed below.

2.11.1.1 Shelf (Line 54: CDP's 102-6999)

Trial and error tests were performed with both the predictive and adaptive deconvolution filters. The predictive deconvolution filter was tested with various different design windows. Two design windows worked better than one, yet there was no difference in data quality when comparing design windows that were separated versus overlapping. Similarly, various adaptation rates were tested for the adaptive deconvolution filter. Testing showed that a -25 ms prediction gap and 300 ms operator length was optimal for both filters. Figure 2.40 illustrates that the adaptive deconvolution did a better job of removing multiple reflections, particularly the first water bottom

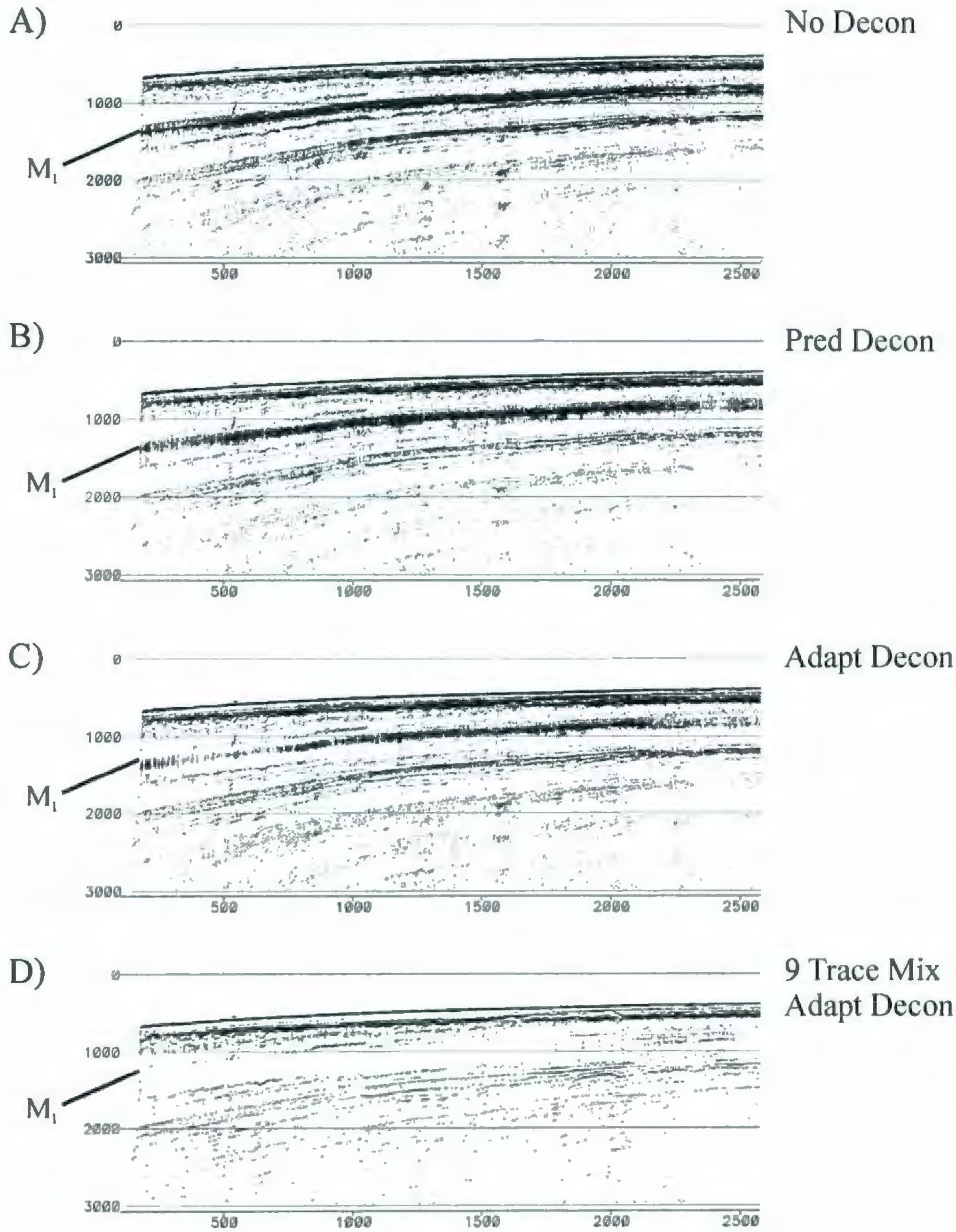

Figure 2.40: a) Stack of shelf without a predictive or adaptive deconvolution filter applied. b) Predictive deconvolution filtered stack with a –25 ms prediction gap and 300 ms operator length. The Predictive Deconvolution filtered stack has two design windows that overlap. c) adaptive deconvolution filtered stack similarly with a –25 ms prediction gap and 300 ms operator length. The adaptive rate used for the adaptive deconvolution filtered stack is 0.05. d) Here a tapered 9-trace mix was applied to the stack followed by the same deconvolution filter that is applied in c). Note that d) yields the most favorable results.

multiple (M1) in the shelf region. For this reason the adaptive deconvolution filter is preferred over the predictive deconvolution filter.

The character of the multiples on the stacked section before (and also after) an adaptive deconvolutional filter is applied is quite nebulous and non-continuous. This will impair the ability of the deconvolution filter since it is looking to remove a seismic wavelet with similar character to the wavelet created by the water bottom reflection. A tapered 9-trace mix was chosen to obtain a more coherent wavelet of the multiples. Applying this process to the stack that is input into the adaptive deconvolution filter improves its success (Figure 2.40 d).

2.11.1.2 Slope (Line 54: CDP's 7000-9500, Line 56: CDP's 15500-18096)

Between 9 and 10 seconds and CDPs 9000-9500, there are weak primary reflections that cut the seabottom multiple. These reflectors likely represent the base of the crust rising as the crust thins seaward. Testing within the slope region with both predictive and adaptive deconvolution has yielded undesirable results. Both filters did attenuate the seabed multiple, but also attenuated the primary reflectors that cut it, giving no improvement of the S/N ratio. Various parameters for each were tested, and the best one is chosen to compare to the radon filtered section (Figure 2.41). The radon filtered section did a much better job of preserving the primary reflector below the onset of the multiple, and thus neither the adaptive nor predictive deconvolution filters were applied in the slope section.

A)

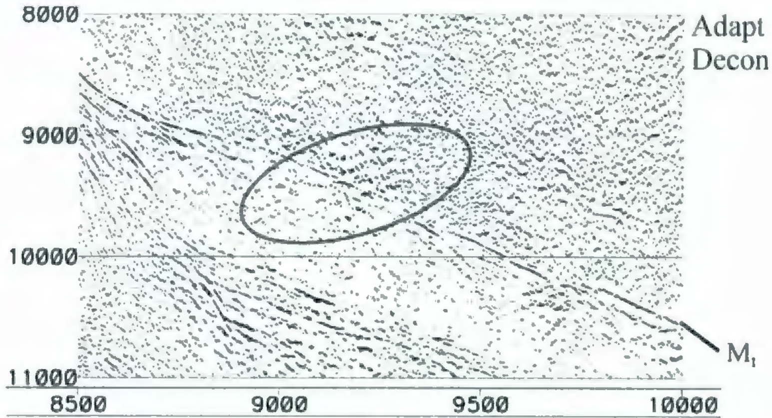

B)

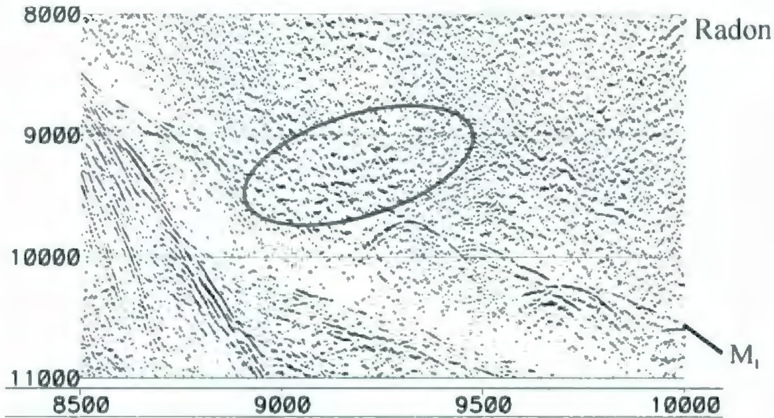

Figure 2.41: Expanded view of possible primary reflection that is cut by the multiple (Line 54). In both sections a 2000ms AGC is applied to enhance the signal of the primary. a) adaptive deconvolution (0.3 rate, -50 ms gap, and 5000 ms operator length) is applied to reduce the multiple energy, but also reduces the amplitude of the primary below the onset of the multiple. b) The radon filter also reduces the multiple energy. However the primary energy below the onset of the multiple is preserved.

2.11.1.3 Deep Water (Line 54: CDP's 9501-20865, Line 56: CDP's 1-14499)

The deep-water section is an area where we expect to see a Moho reflection at a two way travel time (TWT) that is less than the TWT of the water bottom multiple. The boundary between mantle and crust occurs at a more shallow depth in this region since this area contains both highly thinned continental crust, and oceanic crust that is typically between 3-5 km thick. For this reason it is not necessary to remove the water bottom multiple reflection, and this multiple will be muted from the final stack. However, it is desirable to remove the multiple reflection from the stacked section that will be used for migration.

Choosing to completely mute the multiple from the stack before migration may cut off some of the diffracted energy from deep reflectors. Another point that should be noted is that the resolution of migrated seismic sections decreases along the edges of the section. If the multiple is muted before stack, this would decrease resolution of deep

Table 2.2: Rate of adaptation used for each range of CDP's to remove water bottom reflection.

Line 54

CDP Range	Rate of Adaptation
9000-10500	0.3
10501-13500	0.4
13501-17750	0.3
17751-20865	0.6

Line 56

CDP Range	Rate of Adaptation
1-5000	0.6
5001-10500	0.5
10501-15500	0.4
15501-18096	0.3

reflectors. It is also undesirable to migrate a section with a strong sea bed multiple because the multiple will produce over-migration smiles that may obscure shallow primary reflections. A post stack adaptive deconvolution is a quick and effective way to remove multiple reflections. Since there are no expected reflectors below the multiple, a very high rate of adaptation is used in this section. The strength of the multiple varies along this section of the line, so the rate of adaptation is also varied using if statements as illustrated in Table 2.2. Testing is performed with various prediction gaps and operator lengths. A prediction gap of ~50 ms is necessary to include the onset of the multiple. Much larger prediction distance is required to remove the full period of the multiple in areas of deep water, where 5000 ms has achieved this.

2.11.2 Final Pre-Migration Processing, Display, and Plot Parameters

This section provides final processing applied to the stack to reduce noise before migration (Tables 2.3 and 2.5). Additional processes (Tables 2.4 and 2.6) are applied to improve the display of the stack (Plates 1a and 1b), but are not included in the final processing flow.

2.11.2.1 Line 54 (Plate 1a)

Table 2.3: Final processing applied to Erable Line 54 before migration.

Shelf CDPs 102-6999	<u>Ormsby bandpass filter (4-8-25-40)</u> Applied using windowed processing to a ~ 12 to 17 s time window with 3000 ms edge taper ramp and 5000 trace blend.
Slope and deep water CDPs 7000-20685	<u>Trace mix</u> 5 trace equal weighted mix

Table 2.4: Final display and plot parameters for Erable Line 54 final stack.

AGC	2 s
Gain	0.9
Trace plot mode	variable area only
Bias	-80%
Clip limit	2

2.11.2.2 Line 56 (Plate 1b)

Table 2.5: Final processing applied to Erable Line 56 before migration.

Slope CDPs 18096-15000	Trace mix 5 trace equal weighted mix

Table 2.6: Final display and plot parameters for Erable Line 56 final stack.

AGC	2 s
Ormsby bandpass filter	4-8-20-35 using time window given in Appendix 6
Gain	0.9
Trace plot mode	variable area only
Bias	-80%
Clip limit	2

2.11.3 Migration

A migration algorithm must be chosen to collapse diffractions and move dipping reflectors up-dip, where the objective is to obtain a seismic image that is closest to an image of the true subsurface (Yilmaz, 2001, pg. 463). For these data, lateral velocity variations are for the most part moderate, justifying the use of a time migration versus a depth migration algorithm. However, there are situations that arise in areas of deep oceanic crust where conflicting dips of primary events have different hyperbolic moveout, thus different stacking velocities. To properly image these conflicting diffractions, a pre-stack migration is necessary. In other areas, the inability to image deep reflectors could be the result of either strong lateral velocity variations, or recording events that originate from outside the 2-D survey profile (out of the plane, or sideswiping). For the first case a depth migration is required to properly image the events. Likewise, a 3-D migration is required for the second case. It is not uncommon for a combination of these effects to occur in areas that are structurally complex, where a pre-stack 3-D depth migration would provide the best results. This process requires 3D data, and abundant computing time and cost, making it an unfavorable option.

A post stack Kirchhoff time migration algorithm is initially attempted for the entire section. This technique applies amplitude and phase corrections to the data (Yilmaz, 2001, pg. 484-485). It then sums the amplitudes that fall along a particular diffraction hyperbola, whose curvature is dependent on the velocity function. This summation is then mapped as a point in the $x - \tau$ plane, where τ represents the time that the event occurs in the migrated position.

Two main parameters that control the performance of the Kirchhoff migration are the aperture width of migration and the maximum dip to migrate (Yilmaz, 2001, pg. 474). Aperture width can be defined as horizontal range over which the summation path extends. Theoretically, the tail of the diffraction hyperbola has an infinite length, thus an infinitely long aperture width would produce the best results. In reality, the signal of the diffraction pattern diminishes as it increases with time and depth, and the longer the aperture width, the longer the processing time and cost. A migration aperture of 12000 m is chosen to include the majority of the energy included in the diffraction pattern. The second parameter, maximum dip angle, works in such a way that any dipping reflectors with a dip larger than the maximum dip angle will not be properly migrated. Since there are very steep dips present along the slope, a maximum dip of 90° was chosen.

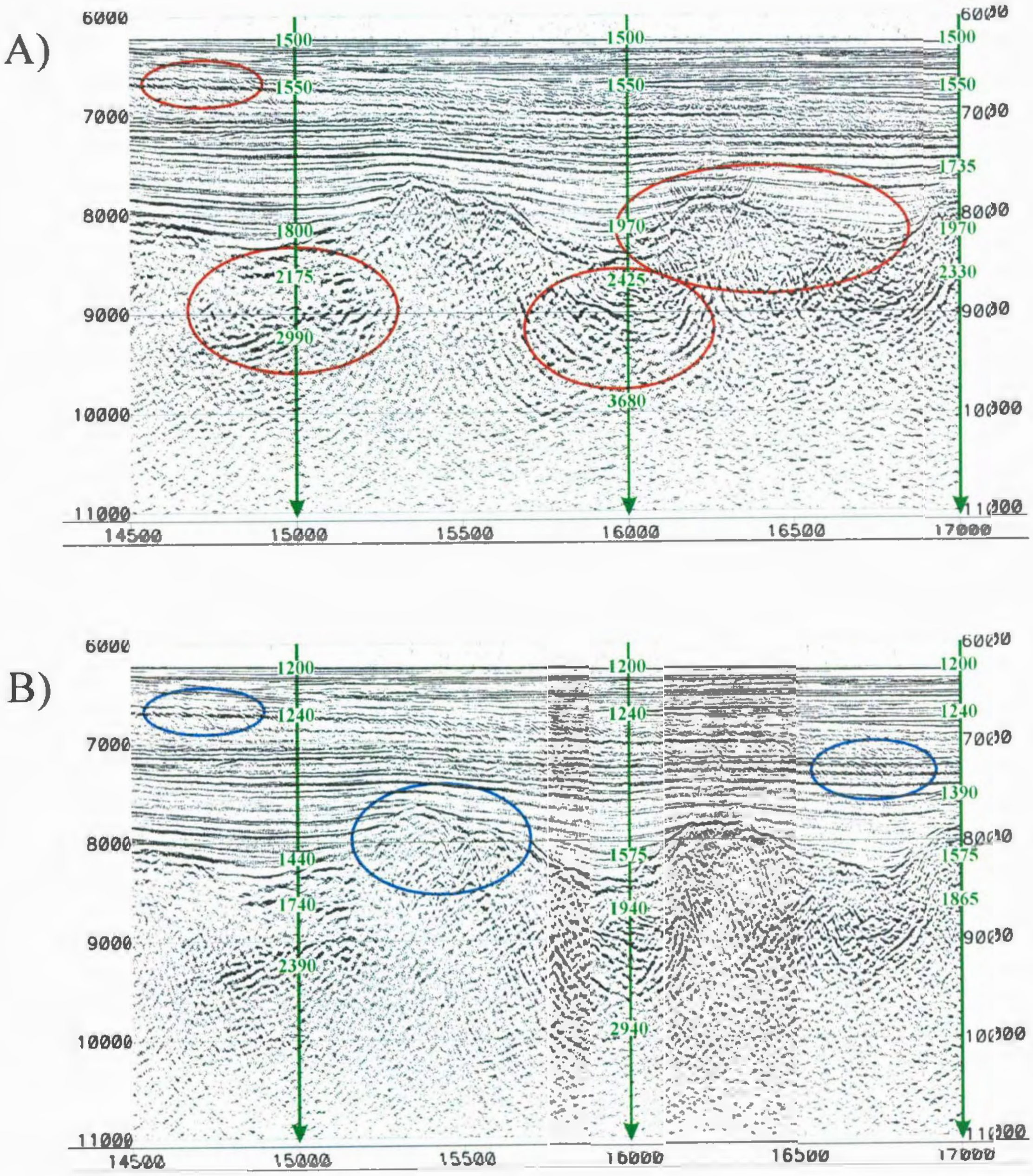

Figure 2.42: a) A post-stack time Kirchoff migration of a deep-water section using rms stacking velocities as a first pass. Note that section is generally over-migrated, where the areas that are circled red exhibit a "smile" appearance. b) Post-stack time Kirchoff migration using a velocity function that is 20% lower than the rms stacking velocities. Here the section is generally under-migrated, where the areas that are circled blue exhibit a "frown" appearance. However, imaging of deep reflectors is improved.

The rms stacking velocity function is used as a first pass at migrating the data (Figure 2.42 a). The result was a section that was generally over migrated giving a "smile" appearance where each diffraction hyperbola is inverted, especially prominent in those at the sediment/basement interface. The velocity function was then simply reduced by 20%, and the section was migrated again (Figure 2.42 b). This generated a section that was generally under migrated giving a "frown" appearance where the diffraction hyperbola is not completely collapsed. However there are some sections where the imaging of the sediment/basement surface is improved. Imaging of sub-basement reflectors that may represent Moho is also improved.

Based on whether events appeared over or under migrated, the rms velocity function was iteratively adjusted and used to migrate the stack. For the most part the section is successfully resolved (Figure 2.43). The inability to focus some sediment reflectors is likely because the sediments here are very anisotropic and non-homogeneous both vertically and laterally. There may be no migration velocity that can bring this into focus using the post-stack time migration algorithm. Sub-basement reflections that most likely represent Moho also are not imaged.

2.11.4 Post Migration F-K Filtering for Shelf

Although extensive multiple removal techniques were used in attempt to remove strong reverberatory multiple reflections, little to almost no primary intracrustal reflections were recovered from the continental shelf area. Multiple energy remaining on the stack is low velocity. Migration velocities are chosen such to represent the subsurface geology and increase with depth, thus multiple reflections become severely

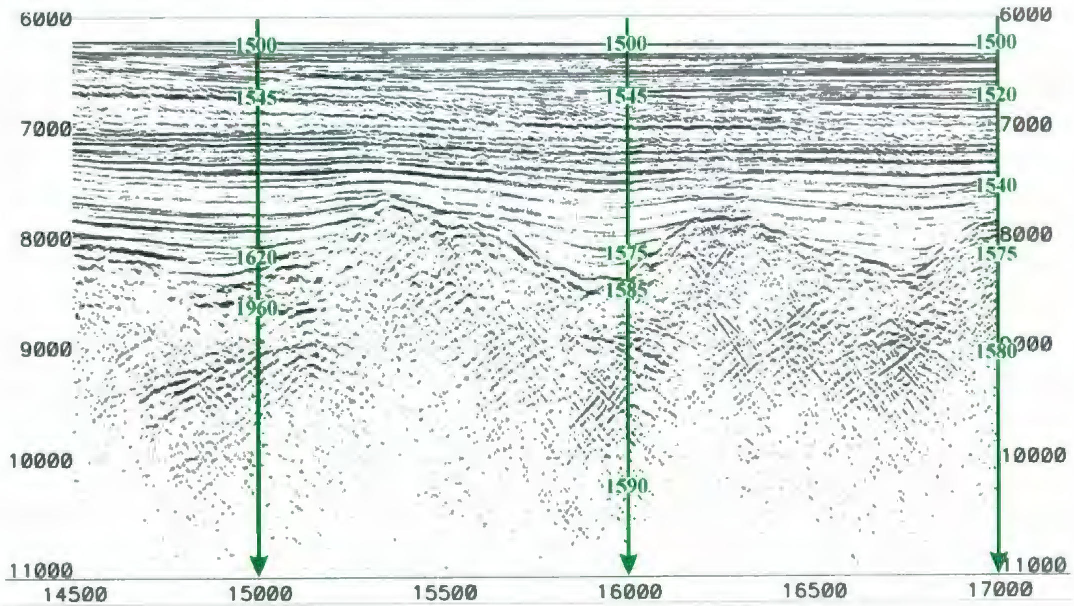

Figure 2.43: A post-stack time Kirchoff migration of the deep-water section. The rms velocity function is iteratively adjusted to achieve optimal ~~resolution~~ RESULTS, although imaging of deep reflectors is unsuccessful.

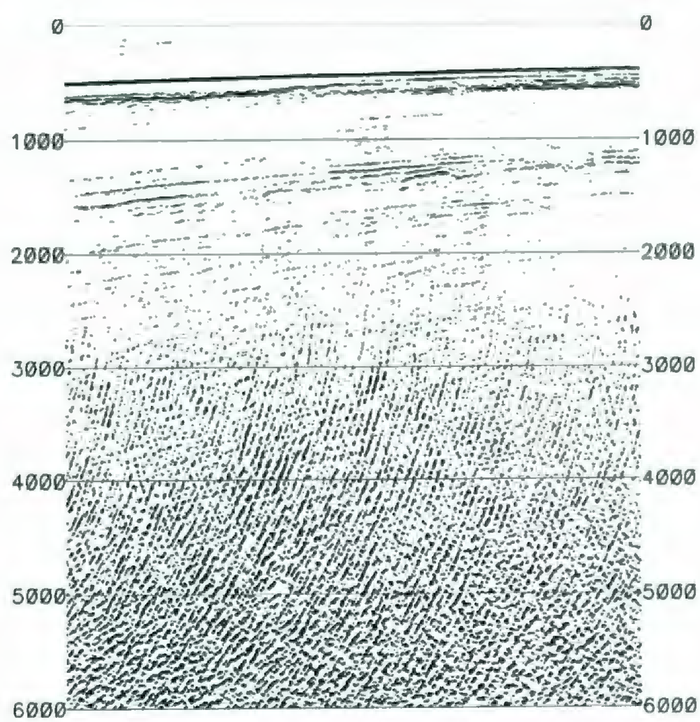

Figure 2.44: Migrated section of the shelf CDPs 1000-2500. Remaining noise from low velocity waterbottom multiples is severely over migrated producing steeply dipping "smiles".

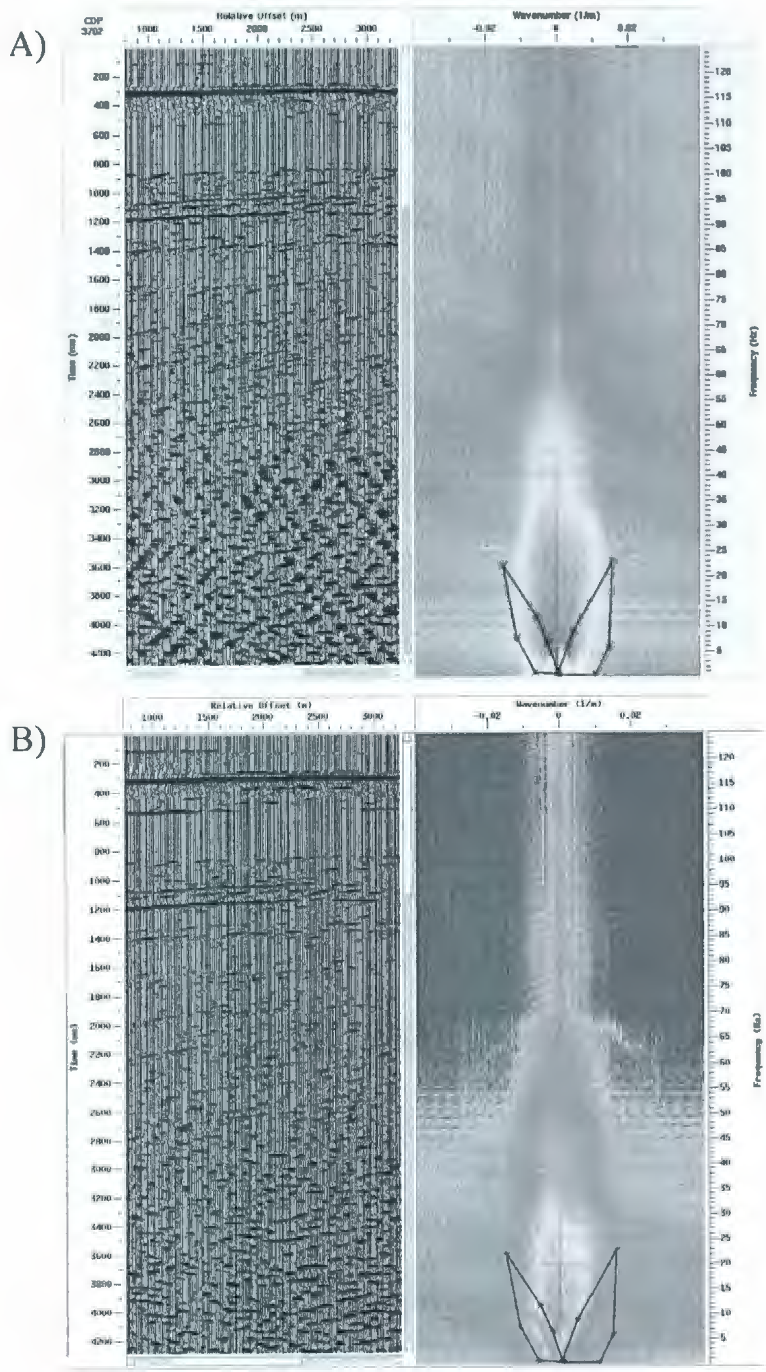

Figure 2.45: F-K analysis showing a) the input that is a stacked section of the shelf on the left and corresponding rejection region chosen for the F-K filter to the right, and b) the output of this selected F-K filter.

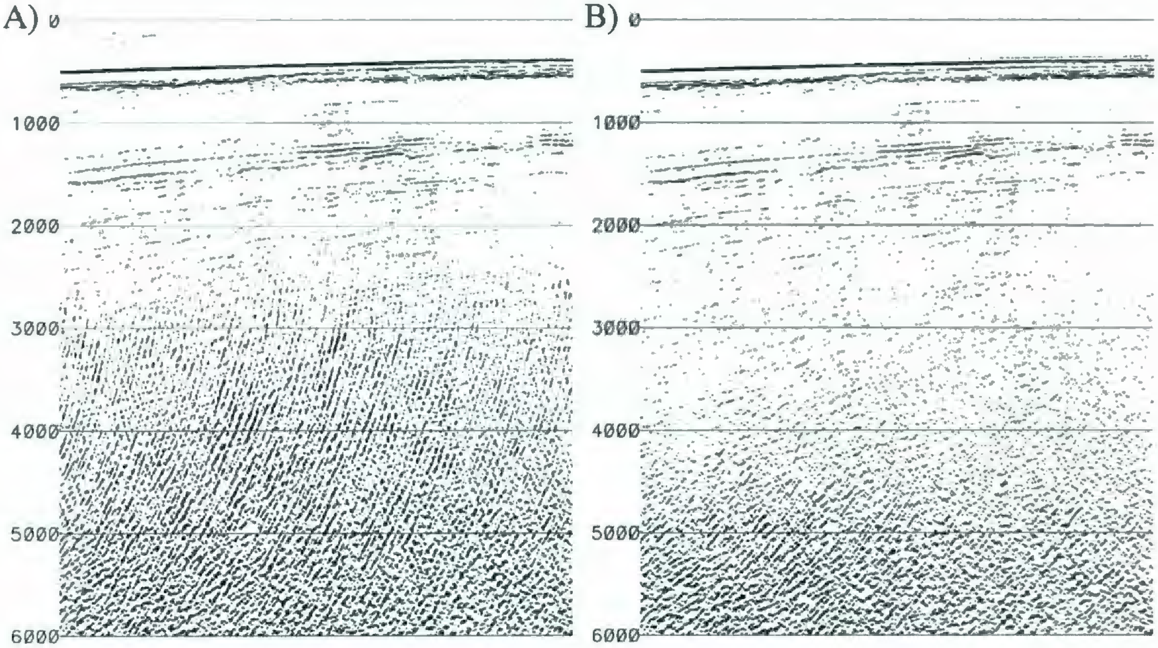

Figure 2.46: a) Migrated section of the shelf CDPs 1000-2500 as shown in Figure 2.44. b) Also showing the Migrated section of the shelf CDPs 1000-2500 with the addition of an F-K filter to remove most of the steeply dipping "smiles" from over-migration of waterbottom multiples (F-K filter rejection region illustrated in Figure 2.45). Some shallower dips of the migration "smiles" have not been removed because it degrades primary Moho reflections.

over migrated producing steeply dipping migration "smiles" as illustrated in Figure 2.44. Most primary reflections on the in the shelf region are sub-horizontal in contrast to this steeply dipping noise, where the F-K filter can separate the two based on the dip. Figure 2.45 illustrates the region polygon used to remove this noise, and Figure 2.46 shows the result of applying this filter. The region was chosen such that it did not remove shallow dipping migration "smiles" because making the F-K rejection region larger degraded the signal of the primary Moho reflection.

2.11.5 Final Migration Display and Plot Parameters

This section provides final processing applied to time migrated data to enhance display (Tables 2.7 and 2.9). Plot parameters are also given in Table 2.8 and 2.10.

2.11.5.1 Line 54 (Plate 1c)

Table 2.7: Final processing applied to Erable Line 54 for improved display.

Shelf CDPs 102-6999	<u>Power exponent f-k filter (1.25)</u> Data transformed to the f-k domain, raised to the power of 1.25, and transformed back to the t-x domain. This is done to enhance the continuity of the Moho reflection. <u>Time variant scalar (user input values)</u> Four time windows outlined with a different gain applied to each to create a more balanced section. See Appendix 7 and 8 for time windows and gains respectively. <u>Trace mix</u> 9 trace tapered weighted mix <u>17 s AGC</u> To balance amplitudes laterally across the section.
Slope and deep water CDPs 7000-20865	<u>Ormsby bandpass filter (4-8-20-35)</u> Applied to CDPs 7000-11115 within a time window outlined in Appendix 9 with 1000 ms edge taper ramp and 2000 trace blend. <u>Time variant scalar (user input values)</u> Four time windows outlined with a different gain applied to each to create a more balanced section. See Appendix 7 and 8 for time windows and gains respectively. <u>Trace mix</u> 9 trace tapered weighted mix <u>12 s AGC</u> To balance amplitudes laterally across the section.

Table 2.8: Final plot parameters for the time migrated Line 54.

Gain	0.9
Trace plot mode	variable area only
Bias	-60% for shelf, -85% for slope and deep water
Clip limit	2

2.11.5.1 Line 56 (Plate 1d)

Table 2.9: Final processing applied to Erable Line 56 for improved display.

Deep CDPs 15499-1	Trace mix 5 trace equal weighted mix Ormsby bandpass filter (4-8-20-35) Applied to a time window outlined in Appendix 6 with 1000 ms edge taper ramp and 1000 trace blend.

Table 2.10: Final plot parameters for the time migrated Line 56.

Gain	0.9
Trace plot mode	variable area only
Bias	-75% for slope, -90% for deep water
Clip limit	2

2.12 Summary of Processing Flow

1. Geometry
2. Velocity Analysis
3. Pre Stack Data Enhancement
    a) Direct wave top mute
    b) Butterworth filter 5-12-70-36 (using f1-S1-f2-S2 format, where S1 and S2 are slopes)
    c) Shelf (Line 54 only): FK filter on shot gathers to remove linear noise
    d) 2s AGC
    e) Spiking deconvolution (25ms gap, 300ms length)
    f) Ormsby filter 4-8-40-70
    g) Direct wave top mute
4. Pre Stack Multiple Removal
    Shelf (Line 54 only): FK filter on CDP gathers
    Slope: Radon Filter
5. Edit Velocity Analysis
6. Stack
7. Post Stack Processing

    Line 54:
    Shelf (CDPs 102-6999):
    a) Trace mix (9 taper weighted mix)

b) Adaptive deconvolution
c) Windowed processing Ormsby bandpass filter
d) Migration
e) Post stack F-K filter
f) Power exponent F-K filter
g) Time variant scalar gain
h) Trace Mix (9 taper weighted mix)
i) 17 s AGC

Slope (CDPs 7000-9500):

a) Trace mix (5 equal weight mix)
b) Migration
c) Windowed processing Ormsby bandpass filter
d) Time variant scalar gain
e) Trace mix (9 taper weighted mix)
f) 12 s AGC

Deep (CDP 9501-20865):

a) Adaptive deconvolution
b) Trace Mix (5 equal weight mix)
c) Migration
d) Windowed processing Ormsby bandpass filter (CDPs 9501-11115 only)
e) Time variant scalar gain
f) Trace mix (9 taper weighted mix)
g) 12 s AGC

Line56:

Slope (CDPs 18096-15500):

a) Trace mix (5 equal weight mix)
b) Migration

Deep (CDPs 15499-1):

a) Adaptive deconvolution
b) Migration
c) Trace mix (5 equal weight mix)
d) Windowed processing Ormsby bandpass filter

Chapter 3: Recognizing Crustal Domains and Placing of the Crustal Boundaries

3.1 Recognizing Crustal Domains

Before placing boundaries on continental, transitional, and oceanic crust, it is necessary to identify and distinguish these domains from one another. This section will explore the typical composition and morphology of each crustal domain, and how we can recognize this from seismic reflection and refraction data.

3.1.1 Continental Crust

Continental crust has a variable composition and thickness, which is dependent on its tectonic and metamorphic history. Continental crust in an extensional regime (excluding thinned crust on continental margins) has an average crustal thickness of ~30 km, where as crust in an orogenic regime has an average of ~46 km (Christensen and Mooney, 1995). Even though the composition is heterogeneous and complex, it is distinguishable from ocean crust in that it is much more silica rich (Fowler, 2005, p. 514). Generally speaking, average upper continental crust is composed of granodiorite and the lower continental crust is closer to a gabbro composition.

Similarly, the P-wave velocity through the crust is variable since the seismic velocity through the crust is dependent on its composition. However, typical crustal velocities are summarized in Table 3.1 based on average velocities measured from seismic refraction studies within various tectonic settings globally. Upper crustal P-wave velocities usually fall between 5.9-6.3 km/s (Fowler, 2005, p. 511). The middle crust velocities are more variable, between 6.0-7.1 km/s, with the normal range between 6.4-6.8 km/s. Average lower continental crust has a bimodal distribution, with most values falling either between 6.6-6.8 km/s, or 7.0-7.2 km/s (Christensen and Mooney, 1995; Fowler, 2005, p. 512). The higher velocity range is found in areas with magmatic underplating, such as passive margins (Fowler, 2005, p. 513). Overall, the velocity structure can be described as having a low velocity gradient, between 0.02 and 0.03 s^{-1} based on an average crustal thickness of 38 km.

Table 3.1: A summary of typical P-wave velocities for continental crust (From Fowler, 2005, p. 511-513) and velocities of the Flemish Cap crust from seismic refraction experiments (Funck et al., 2003).

Section of Continental Crust	**Typical Velocity**	**Velocities Measured from Flemish Cap**
Upper crust	6.0-6.3 km/s	6.0-6.2 km/s
Middle crust	6.4-6.8 km/s	6.3-6.4 km/s
Lower crust		
High temperature	6.6-6.8 km/s	6.6-6.7 km/s
High grade metamorphism/ Magmatic underplating	7.0-7.2 km/s	

In addition to average continental crust velocities, we will also take in consideration the crustal velocities measured from seismic refraction experiments over Flemish Cap (Funck et al., 2003), which we would expect to be present, yet distributed over a smaller thickness, within the extended continental crust region (Table 3.1).

Continental crust is extended during the rifting process, and commonly exhibits rotated fault blocks capped with pre-rift sediments (Figure 3.1). Syn-rift sediments can exhibit growth towards the normal faults that accommodate the movement of the rotated crustal blocks. However imaging rotated fault blocks alone is not enough evidence to suggest a continental crust affinity, because these features are sometimes imaged in ultra-slow spreading ocean crust, such as the Labrador Sea (Srivastava and Keen, 1995), and the southeast margin of Flemish Cap (Hopper et al., 2004; Hopper et al., 2006). But observing rotated fault blocks in addition to seismic velocities typical of continental crust can provide evidence of a continental crust domain. See Section 3.1.2 for a discussion on what velocities are expected for sediments and subcontinental mantle.

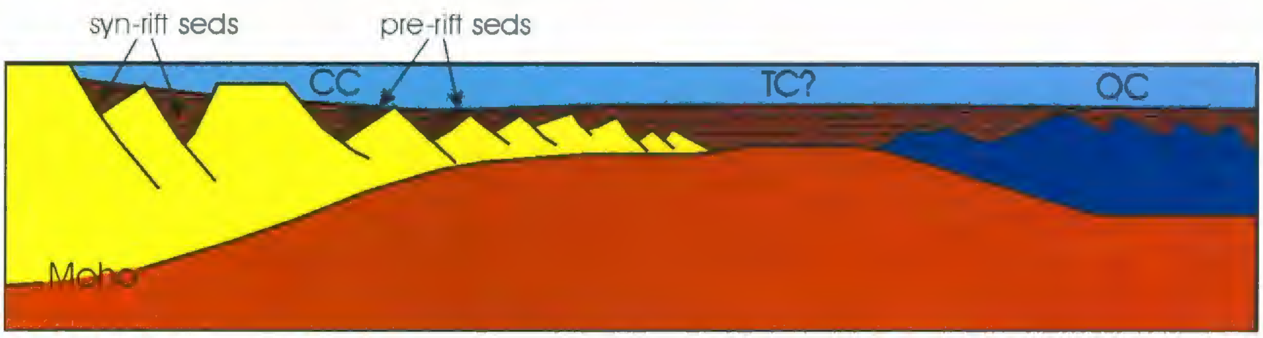

Figure 3.1: Schematic of a rifted continental margin extending from the continental slope on the left, into the deep ocean abyssal to the right. CC = Continental Crust, TC = Transitional Crust, OC = Ocean Crust. Note that the continental crust has been extended through rotated fault blocks, and is capped with pre-rift sediments in areas. Also note the syn-rift sediments that accumulated during the movement of the crustal blocks exhibiting growth towards major normal faults.

3.1.2 Oceanic Crust

Oceanic crust has a very recognizable velocity structure, controlled by a compositional layering that occurs in a normal seafloor-spreading environment. A four-layer classification has been developed for the oceanic domain as given in Table 3.2.

Sediments (Layer 1) have a an average P-wave velocity of about 2.0 km/s (Fowler, 2005, p. 401), where sediment velocities are as low as 1.5 km/s at the sea bottom, and increase with depth as they become more consolidated. In fact, pre-rift or syn-rift sediments (located above continental crust) can have velocities up to about 5.2

km/s, as obtained in the Carson Basin. Upper mantle (Layer 4) velocity both beneath continental and oceanic crust has an average velocity of about 8.1 km/s (Fowler, 2005; Christensen and Mooney, 1995), but this velocity is reduced if mantle rocks undergo serpentinization (discussed in Section 3.1.3.1).

Table 3.2: A four-layer classification scheme for the sediments and crust beneath ocean basins providing the typical velocity range for each (After Fowler, 2005, p. 399)

Layer	**Composition**	**Velocity (km/s)**
Layer 1	Sediments	2.0 (Average)
Layer 2	Basalts and sheeted dykes	3.5-6.6
Layer 3	Gabbro	6.5-7.2
Layer 4	Upper Mantle	7.9-8.1

The crustal layer typically consisting of basalts and sheeted dikes (Layer 2) with P-wave velocities between 3.5-6.6 km/s, and gabbro (Layer 3) with velocities between 6.5-7.2 km/s (Fowler, 2005, p. 401-402). Since the average crustal thickness of oceanic crust is about 7-8 km (Fowler, 2005, p. 326), this yields a velocity gradient of about 0.5 s^{-1}, which is much higher compared to that of continental crust (~0.025 s^{-1} for average continental crust thickness).

Ocean crust in slow spreading environments can be recognized on seismic reflection data from its usually rough and high amplitude basement surface, in contrast to the smoother basement surface produced at fast spreading ridges (Shillington et al., 2006). Rough basement topography produces diffraction patterns on the stacked seismic section that can be resolved by applying a migration algorithm to the data.

During sea-floor spreading, magnetic minerals in volcanic rocks extruded to the ocean floor align themselves with Earth's magnetic field, where the rock then cools and crystallizes setting the magnetization (Fowler, 2005, p. 51-57). This process produces linear magnetic anomaly strips parallel to the spreading axis that have amplitudes on the order of ± 500 nT, depending on whether the Earth's magnetic field polarity was normal or reversed at the time oceanic rocks acquired their thermoremanent magnetization. These high amplitude magnetic anomalies can aid in identifying an ocean crust domain.

3.1.3 Transitional Crust

For the purpose of this paper, transitional crust is defined to represent the domain between inferred extended continental crust, and oceanic crust (where the features discussed in Sections 3.1.1 and 3.1.2 are used to provide evidence of the boundaries of the continental and ocean crust respectively). There are four hypotheses proposed for the crust within the transitional zone: 1) highly extended continental crust (Tucholke et al., 1989; Enachescu, 1992), 2) thin oceanic crust formed by slow or ultra-slow seafloor spreading (Reid, 1994; Keen and de Voogd, 1988; Srivastava et al., 2000), 3) exhumed serpentinized mantle (e.g., Boillot et al., 1987; Dean et al., 2000), and 4) a combination of any of the above (e.g., Lau et al., 2006b).

The Iberia margin has been extensively studied through seismic studies and drilling. Within this margin it has been established that the transitional crust contains exhumed serpentinized mantle (e.g., Boillot et al., 1987; Whitmarsh et al., 1996; Pickup et al., 1996; Dean et al., 2000), and this hypothesis has also been proposed for the transitional crust on the conjugate Newfoundland margin (e.g., Lau et al., 2006b; Tucholke and Sibuet, 2007; Sibuet et al., 2007b).

3.1.3.1 Exhumed Serpentinized Mantle

During rifting, continental crust becomes extensively thinned and faulted, possibly to the point where the peridotites of the upper mantle become completely exposed at the sea floor. The extensional faulting allows for seawater to penetrate the upper layer of the mantle, where the seawater reacts with the peridotites and alters a percentage of the olivine minerals to serpentine (Eq. 3.1; Schroeder et al., 2002). The hydration of peridotite rocks to form serpentinite is a process known as serpentinization (Fowler, 2005, p. 663). The following is one possible exothermic reaction that can occur from serpentinization below 500 °C:

$$\underset{\text{olivine}}{6(Mg, Fe)_2SiO_4} + 7H_2O = \underset{\text{serpentine}}{3(Mg, Fe)_3Si_2O_5(OH)_4} + \underset{\text{magnetite}}{Fe_3O_4} + H_2 \quad (3.1)$$

Serpentinization of peridotites changes the physical properties of the rock, producing an increase in volume and decrease in density and strength. As a result, this decreases the P-wave velocity. The higher the degree of serpentinization, the more the P-wave velocity is reduced. For example, the seismic P-wave velocity of peridotites with no serpentinization is about 8.1 km/s (Fowler, 2005; Christensen and Mooney, 1995), for 10-15% serpentinization the velocity is ~7.5-7.8 km/s (Escartin et al., 2001), and for 100% serpentinization it is ~5 km/s (Schroeder et al., 2002).

The serpentinization reaction has a significant effect on the rheological behavior of the mantle. Deformation experiments performed by Escartin et al. (2001) suggest that peridotite with more than 10% serpentine has reduced strength, and its volumetric strain behavior is comparable of pure serpentinite. It is also stated that strength is not a linear function of serpentinization, but rather decreases abruptly at approximately 9-15%

serpentinization. The reasoning for this is that the deformation is accommodated by the serpentine, leaving the olivine un-deformed.

As illustrated in Eq. 3.1, magnetite is a commonly a product of the serpentinization reaction. Consequently, peridotites that undergo a high degree of serpentinization in turn have a higher magnetic susceptibility and ferromagnetic properties, unlike unaltered peridotites, which have a weak magnetic susceptibility and paramagnetic properties (Oufi et al., 2002). In fact, a recent study performed by Oufi et al. (2002) has shown that a non-linear relationship exists between the two, where magnetic susceptibilities remain modest until about 75% serpentinization (corresponding to a P-wave velocity between 5-5.5 km/s), and above this value the magnetic susceptibility increases rapidly. The natural remnant magnetization (NRM) of serpentinized peridotites can be quite variable, and depends on the formation of magnetite grains. Typically, elongated grains that form concentrated veins produce a high NRM, and irregular alignment and concentrations produce a low NRM (Sibuet et al., 2007b).

Various studies on the magnetic properties of oceanic serpentinized peridotites show that they may make a contribution to oceanic magnetic anomalies (Nazarova, 1994; Dyment et al., 1997; Oufi et al., 2001). Dyment et al. (1997) recognize that the marine magnetic anomalies at slow- to intermediate-spreading ridges are skewed or have a "hook shape", and this effect decreases as the spreading rate increases. Similarly, drilling and dredging results confirm that serpentinized peridotites are most often recovered from slow and intermediate spreading ridges and this is not a common process at fast spreading ridges (Dyment et al., 1997).

A high amplitude magnetic anomaly has been identified within the transition zone on the Iberian Margin over Site 899 (Zhao, 2001). Serpentinized peridotites recovered from this site possess a strong magnetization intensity, which suggests that these rocks significantly influence the observed magnetic anomaly. A recent study performed by Sibuet et al. (2007) of ODP sites from both the Newfoundland and Iberia margin suggest that the oldest identified M-Sequence anomalies (M17-M3 or younger; M-sequence identified by Srivastava et al., 2000), located in the zone of thinned continental crust and transitional crust, are created by exhumed serpentinized mantle. They also suggest that serpentinization of upper mantle rocks as they are gradually exhumed can form magnetic lineations in a similar fashion as basalts from seafloor spreading, with the difference being that the resulting magnetic anomalies may have weaker amplitudes.

3.2 Placing Crustal Boundaries

Using the above summary describing features of continental crust, oceanic crust, and transitional crust, data from the Newfoundland margin are examined in detail to place boundaries of the crustal domains, and explore the possible hypothese for the transitional crust. The main data sets used for interpretation are the SCREECH seismic reflection and refraction data, drilling results from the ODP Leg 210, refraction data from the CSS Hudson Cruise 85-025, and the MCS reflection lines 53, 54 and 56 processed for this study from the Erable survey. The discussion will begin with the SCREECH data set, starting on the southwestern edge of the project area on the Grand Banks, working to the northeast edge of Flemish Cap. Various authors' interpretations will be drawn upon for the SCREECH data set and ODP Leg 210 drilling results (Funck et al., 2003; Hart and Blusztajn, 2006; Hopper et al., 2004; Hopper et al., 2006; Lau et al., 2006a; Lau et al., 2006b; Müntener and Manatschal et al., 2006; Shillington et al., 2006; Van Avendonk et al., 2006). An interpretation for the Erable data and overlapping CSS Hudson refraction data is then discussed. Lastly, Line 104 from the SCREECH survey lies sub- parallel to the margin and connects all of the dip lines discussed above. This profile will be used to tie the interpretation of all lines together. SCREECH Transects 1, 2, 3 and Line 104 will be referred to as SCR1, SCR2, SCR3, and SCR104 respectively. Erable lines 53, 54, and 56 will be referred to as ER53, ER54, and ER56. SCREECH Transect 3 is not located on the southern margin of Flemish Cap, and thus not in the project area. However the interpretation of the crustal boundaries on this profile is used to illustrate how the boundary geometries change from the Grand Banks to the southern margin of Flemish Cap.

3.2.1 SCREECH Transect 3 (Plate 2a)

A ray tracing technique was used on OBS data to forward model travel times, and a velocity model was created (Lau et al., 2006a). Between CDPs 509000-513000 in section C1, strong landward dipping intra-crustal reflections are identified and named 'L' (Lau et al., 2006b) based on its similarity to the 'L' reflection first observed on the 85-2 profile (Keen and de Voogd, 1988). The seaward lower section of these reflectors is coincident with a 7.6-7.9 km/s p-wave velocity hence these reflectors are interpreted as separating crust from underlying serpentinized mantle (Lau et al., 2006a; Lau et al., 2006b).

The edge of the thinned continental crust zone is hard to interpret in areas where there is a lack of basement reflectivity on seismic reflection data, perhaps created by the overlying U-reflector (Lau et al., 2006a). The OBS data does however model a ~5.6-6.0 km/s low-gradient layer within this low-reflectivity zone, consequently it is interpreted as continental crust (C2). The zone interpreted as continental crust (C1 and C2) is much wider compared to those of SCR1 and SCR2, thinning over a distance of about 170 km.

Adjacent to the thinned continental crust lies an 80 km wide zone (sections T1a, T1b, and T2) that is characterized by a high velocity gradient, and is interpreted as transitional crust (Lau et al., 2006a). Here a ~4.4-7.8 km/s basement layer is modeled from the refraction data, however velocity resolution within this area is poor. The high velocity gradient suggest that this area does not contain continental crust, and is most likely produced by either: 1) layer 2 and 3 thin oceanic crust or 2) exhumed serpentinized mantle, where serpentinization decreases with depth (Lau et al., 2006a).

Basement relief and character within the transitional zone is quite variable. A rounded basement high with disturbance in the overlying sediments marks the landward edge (T1a) (Lau et al., 2006b). This disturbance in the above sediments suggests uplift in this area and a diapiric nature for the basement high. This area also has a high velocity gradient in the upper basement, thus the interpretation of a serpentinized peridotite diapir is indicated. Further seaward is a low relief area where the basement surface is not clearly imaged (T1b). This is likely a result of the weak impedance contrast at top of basement or the inability to image below the strong U-reflector. This basement character is very similar to the serpentinized mantle identified on the IAM-9 profile from the conjugate Iberian margin (Pickup et al., 1996), and quite different from the high basement reflectivity and relief representing thin ocean crust identified on SCR1 (Hopper et al., 2004; Hopper et al., 2006), supporting the interpretation of exhumed serpentinized mantle for this region. At the seaward edge of this zone there are two moderate relief basements highs where top of basement is weakly imaged (T2). Within this section the refraction data does not provide sufficient evidence to distinguish between the interpretation of either exhumed serpentinized mantle or ocean crust for this region (Lau et al., 2006b). However Lau et al. (2006a) prefer the interpretation of exhumed serpentinized mantle. This is because 1) magnetic anomalies in this area are very weak (M-Sequence anomalies older than M4 interpreted by Srivastava et al., 2000), 2) and basement relief is moderate with weak reflectivity; both features are uncharacteristic of ocean crust.

Velocity-depth models VD1, VD2, and VD3 are provided for locations at CDPs 545500, 548750, and 551875 respectively (Figure 3.2; Lau et al., 2006a). Results indicate that these velocity models are representative of normal oceanic crust, with an uncertainty for the most seaward model VD3 (CDP 551875) (Lau et al., 2006a). Here the interpreted layer 3 ocean crust has a velocity <0.3 km/s higher than what is expected, although it should also be noted that the resolution of the velocity-depth model at this location is estimated to be accurate within ±0.2 km/s. The velocity information, together with the relative roughness of the basement surface, leads to the interpretation of this zone as oceanic crust (O1, Plate 2a).

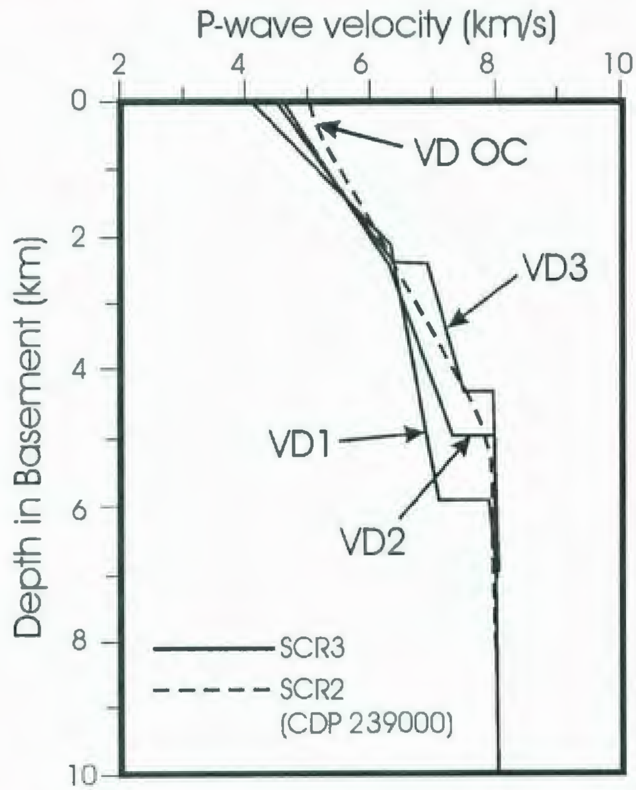

Figure 3.2: Velocity versus depth models from SCR3 (Lau et al., 2006a), SCR2 (Van Avendonk et al., 2006), taken with the interpreted oceanic crust region and overlain on velocities of typical Atlantic oceanic crust illustrated by shaded gray area (White et al., 1992) modified from Lau et al. (2006a). Velocity models from SCR3 are labeled VD1, VD2, and VD3 representing locations at CDPs 545500, 548750, and 551875 respectively. Velocity model from in the interpreted ocean crust domain on the SCR2 profile at CDP 239000 is labeled VD OC.

Adjacent to the seaward edge of transitional crust (T2), the most landward continuous sub-horizontal crustal reflections are imaged, which are interpreted to represent oceanic Moho (Lau et al., 2006b), and thus defining the landward limit of oceanic crust (O1). Further seaward between CDPs 545000-550000 there is an increase in basement relief and rotated fault blocks are imaged, which may indicate an extensional phase during early seafloor spreading (Lau et al. 2006b). Section O2 has a continued rough basement surface, but differs from section O1 in that there is a reduction in basement topography, and an absence of rotated fault blocks.

3.2.2 SCREECH Transect 2 (Plate 2b)

A velocity model has been constructed for SCR2 using an iterative tomographic inversion of recorded OBS data (Van Avendonk et al., 2006). The continental slope (CDPs 211000-214000) was modeled with a 14 km thick 5.5-6.0 km/s crustal layer over a deep 7.0-7.5 km/s layer. Although a 7.0-7.5 km/s layer is interpreted as serpentinized peridotite in areas such as the Iberian margin, this is not the case here. Since the crust is not thinned to less than 10 km, it is highly unlikely that serpentinization will occur (Perez-Gussinye and Reston, 2001), thus, the 7.0-7.5 km/s layer is interpreted to represent magmatic underplating or intruded mafic melt prior to rifting (Van Avendonk et al., 2006). A large crustal block at the foot of the continental slope (CDPs 218000-220000) displays evidence of dipping sediments, likely pre-rift, lying directly above the basement surface (Shillington et al., 2006). The Moho is clearly imaged beneath this crustal block and illustrates an interesting shape consisting of both a landward and seaward dip.

Three velocity-depth models from Van Avendonk et al. (2006) located at CDP 224800, 232800, and 239000 (Figure 3.2 and 3.3; Appendix 10) are converted to time (Appendix 11) and overlain on the SCR2 profile given in Plate 2b. These velocity models are labeled VD T1, VD T2, and VD OC representing velocity-depth models from the interpreted T1, T2, and ocean crust domains respectively, as discussed below.

The onset of transitional crust is located seaward of CDP 220000 and is separated into two domains. The first domain is characterized by a wide flat area, containing ODP drill Site 1276, where basement is not imaged (Shillington et al., 2006). This domain is named T1 and extends to CDP 230000. The inability to image a reflection from the top of basement may be because reflections are obscured by the U-reflector (discussed in Section 1.4.3.1.1). Velocities modeled within zone T1 show a 6 km thick layer on the landward end with crustal velocities between ~5.5-6.5 km/s that thins to 2 km on the seaward edge of this section, where the crust layer overlies velocities that steeply increase to > 8.0 km/s throughout this section, indicating the inferred top of unaltered mantle (Shillington et al., 2006). A velocity versus depth model from zone T1 (VD T1; CDP 232800) is illustrated in Figure 3.3. Based on the velocity of this crustal layer, Van Avendonk et al. (2006) interpret this crustal layer as highly thinned continental crust. Similarly, Shillington et al. (2006) interpret this zone as thinned continental crust, but add that it may be modified by "magmatic intrusions and/or mantle exhumation/initial oceanic accretion." However there is no evidence of rotated fault blocks or pre-rift sediments within this section, and the 5.5-6.5 km/s P-wave velocities can also be produced by 50-90% serpentinization of peridotites (Escartin et al., 2001). Thus, my interpretation of exhumed serpentinized mantle is equally plausible for this transitional domain, similar to that imaged on the conjugate IAM-9 profile (Pickup et al., 1996; Dean et al., 2000), and sampled there during ODP legs 149 and 173 (e.g., Whitmarsh and Wallace, 2001).

Seaward of zone T1 there is a sudden increase in basement relief and reflectivity (CDP 230000), where a 6.0-7.6 km/s layer in the top 5-6 km of basement is modeled, extending to the location of Site 1277 (Van Avendonk et al., 2006). This defines the T2 domain. A velocity versus depth model from zone T2 (VD T2; CDP 224800) is shown in Figure 3.3. Due to the presence of the M3 anomaly located in the landward limit of section T2, and the sudden change in basement reflectivity and relief, this area was initially interpreted to represent the onset of seafloor spreading (Shipboard Party, 2004a). However, recent work by Müntener and Manatschal (2006) on rocks recovered from Site 1277 suggest that these rocks likely represent subcontinental mantle that was exhumed during rifting. If this interpretation is correct, then the 5-6 km thick 6.0-7.6 km/s layer that is modeled within this region represents mantle peridotites that have been serpentinized by about 15-60% (Van Avendonk et al., 2006).

Velocity-depth models from both the T1 (VD T1; CDP 224800) and T2 (VD T2; CDP 232800) domains along the SCR2 profile are compared with a velocity-depth model from the peridotite ridge domain on profile IAM-9 from the Iberian margin (Dean et al., 2000) in Figure 3.3. Although the velocity structure within zone T1 on the SCR2 profile does not fit that of the IAM-9 profile, this does not dismiss the possibility of serpentinized peridotites for this area. Drilling results indicate that the zone T2 on the SCR2 profile likely contains serpentinized peridotites (Müntener and Manatschal, 2006), yet velocities modeled here are also quite different from those from the IAM-9 profile. The variation among all three models may simply represent the effect of varying degrees of serpentinization with depth, and not necessarily the presence of continental basement within the T1 region on the SCR2 profile.

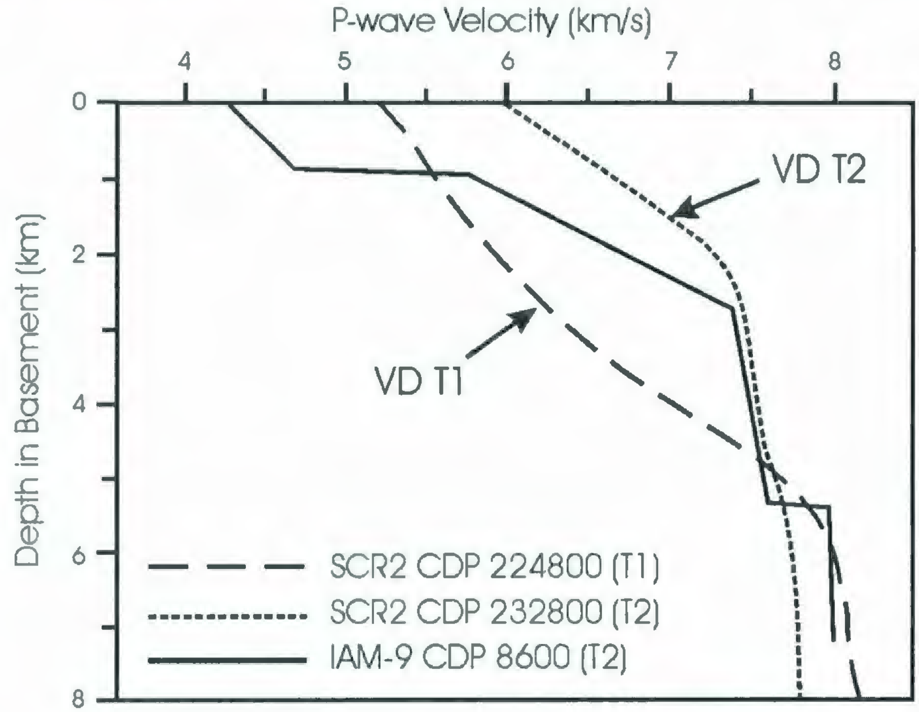

Figure 3.3: Velocity verses depth models taken within the interpreted transitional crust region of the SCR2 indicated with dotted lines, and the IAM-9 profile from the Iberian margin indicated with a solid line. For SCR2, the velocity model located at CDP 224800 is taken within the T1 domain (VD T1) characterized by unreflective low relief basement, and the second location at CDP 232800 is taken within the T2 domain (VD T2) between Sites 1276 and 1277 where basement is imaged as rough with high relief. The velocity model of the IAM-9 profile is taken within the overlapping peridotite region at CDP 8600 (T2).

Seaward of Site 1277 the velocity gradient in the first 5 km of basement increases (Van Avendonk et al., 2006). This change in P-wave velocity gradients occurs near the location of the M0 magnetic anomaly, which is a positive anomaly that is stronger compared to the older M-Sequence anomalies, and in the past has been regarded as undisputedly being formed by seafloor spreading (Sibuet et al., 2007b). A velocity versus depth model in the location of the M0 anomaly (VD OC; CDP 239000) is presented in Figure 3.2 and compared to velocities of typical Atlantic Ocean crust, showing a similar velocity structure. As a result this region is interpreted as ocean crust (Van Avendonk et al., 2006).

3.2.3 SCREECH Transect 1 (Plate 2c)

The continental crust along the SCR1 profile thins very abruptly, from about 30 km to 3 km thickness over a distance of 80 km (Hopper et al., 2006), as illustrated by the steep continental slope (CDPs 50000-56000). Interesting deep reflections imaged beneath the foot of the continental slope between CDPs 54000-58000 include landward and seaward dipping reflections. Reflections V and W are interpreted as intracrustal, with V possibly representing the top of middle crust which truncates against W, where W has a dip of about 45° and possibly represents a fault (Hopper et al., 2004). Reflection M is interpreted to represent the crust-mantle boundary.

Seaward dipping reflections below the slope appear to continue from the lower crust into the mantle (Hopper et al., 2006). At a first look these reflections may be peg-leg multiples or out-of-the-plane energy, where both would be low velocity. However depth migration performed by Hopper et al. (2006) successfully migrated most of these reflections using a velocity between 6.4-6.8 km/s, so these reflections are interpreted as primary. It is uncertain what produces this observed reflectivity but it appears to be unrelated to rifting and spreading of the North Atlantic, and more likely caused by a collapse structure or an older orogenic structure.

Between CDPs 58500-60000, a high crustal block is present with high reflectivity in the upper section exhibiting velocities between 3.8-5 km/s. Reflectivity decreases below this, as the velocity increases to about 6.5 km/s. There are no observed Moho reflections in this area but modeling of OBS data show a 7.6-8.0 km/s velocity layer, interpreted as serpentinized mantle. This crustal block is interpreted as continental crust because of the lack of high velocity gradient, and smooth basement surface, and weak stratigraphic layering (Funck et al., 2003; Hopper et al., 2004). A recent interpretation suggests that this crustal block cannot be considered unambiguous continental crust and that an interpretation of exhumed serpentinized mantle is also possible, which would place the seaward limit of continental crust near CDP 58000 (Hopper et al., 2006). Peridotite ridges can exhibit smooth basement surfaces, as serpentinization weakens peridotites, leading to erosion (Hopper et al., 2006; Tucholke et al., 2006). Also it is argued that the velocity structure of this crustal block is not well resolved because it is a small feature (Hopper et al., 2006). Here the interpretation of continental crust presented by Funck et al. (2003) and Hopper et al. (2004) is favored based on their arguments outlined above, and also based on comparison of ER54 as discussed in Section 3.2.5.

The ocean-continent transitional area is 55 km wide and located between stretched continental crust, and somewhat normal thickness (5-8 km) of oceanic crust (Funk et al., 2003). A fault separates the crustal block at CDPs 58500-60000 from crust at CDPs >60000 with a very different velocity structure and reflection character. This crust appears to be layer 2 and 3 oceanic crust with velocities of ~4.7-4.9 km/s and ~6.8-7.0 km/s respectively, and a total thickness between ~2-3 km. In fact layer 3 appears to pinch out and is absent between CDPs 65500-67550, where crust thins to only ~1-1.5 km (Hopper et al., 2006). Rotated fault blocks are imaged between CDPs 66000-70500 exhibiting stratified layers within. Some authors explore the possibility of a continental affinity for these crustal blocks, which would require a jump in the spreading axis (Hopper et al., 2004). However, there is little variation in the interpreted layer 2 velocities across this region providing the sense that this is a continuous layer throughout the transitional region. Also, rotated crustal blocks have been recognized in the ultra-slow spreading ocean crust in the Labrador Sea (Srivastava and Keen, 1995). Thus these rotated crustal blocks are similarly interpreted as ocean crust being formed in an ultra-slow spreading environment (Funck et al., 2003; Hopper et al., 2004; Hopper et al., 2006).

A strong 'Z' reflection is imaged below thinned ocean crust between CDPs 66500-67700 (Hopper et al., 2004; Hopper et al., 2006). This reflection occurs near the top of serpentinized mantle (Funck et al., 2003), and has been modeled as a detachment that accommodated mantle exhumation, and was later covered by flood basalts (Hopper et al., 2004). However, this strong reflection is not present on SCREECH Line 101 seismic reflection profile collected only 10 km to the northeast, suggesting that this is not a continuous regional feature (Hopper et al., 2006).

The region of thin continental and oceanic crust between CDPs 57500-69000 is underlain with a 7.6-8.0 km/s velocity layer, and normal mantle velocity of 8.0 km/s is observed elsewhere along the profile (Funck et al., 2003). The 7.6-8.0 km/s layer is interpreted as serpentinized mantle, where faulting within the thin brittle crust allows a passage of seawater to react with the upper mantle. This velocity is consistent with about 10% serpentinization at the top that gradually reduces with depth to unaltered mantle.

3.2.4 Erable 56 (Plate 2d)

The ER56 profile is located in very close proximity to SCR2, and has a very similar seismic reflection character. There appears to be some evidence of rotated fault blocks along the continental slope, although these features are poorly imaged. Extending seaward from the foot of the slope is a section where these features are not imaged (CDPs 15500-14000), however deeper landward dipping to sub-horizontal reflections are successfully imaged. These reflections may represent the crust mantle boundary. A crustal block located between CDPs 14000-13500 is fairly angular, and appears to have stratigraphic layering that parallels its surface. It also correlates with a crustal block on SCR2 between CDPs 218000-220000, which is interpreted as continental crust. Thus, these features allow for a similar interpretation, where this crustal block defines the seaward limit of thinned continental crust.

Farther seaward, zone T1 (CDPs 13500-10000) is defined by the dramatic change in basement reflectivity and relief. Here the basement surface is not well imaged because it is partly obscured by the U and associated strong reflections (discussed in Section 1.4.3.1.1), but does appear not to have much relief. At CDP 11000 there is a slight increase in relief, where this feature correlates with the area drilled on ODP Site 1276. This zone of unreflective basement with a low relief is only about 30 km wide compared to ~60 km on SCR2, and ~100 km on the conjugate IAM-9 profile on the Iberia margin.

There is no velocity control from seismic refraction data to aid in the interpretation of these crustal zones. But considering ER56 is in close proximity to SCR2 that does have velocity control and two drilling locations along the profile, we can use this information to aid in its interpretation. As discussed in Section 3.2.2, the unreflective low relief basement area on SCR2 is modeled with crustal velocities between ~5.5-6.5 km/s that steeply increase to > 8.0 km/s. Some authors interpret this as thinned continental crust (Van Avendonk et al., 2006) or a combination of continental crust with magmatic intrusions/exhumed mantle/thin ocean crust (Shillington et al., 2006). However, there is no evidence of rotated fault blocks or pre-rift sediments imaged in this area (T1) on either the SCR2 or ER56 profiles. Thus, these velocities can also be attributed to serpentinization of exhumed mantle rocks (discussed in Section 3.2.2) as observed on the conjugate Iberia margin (e.g., Pickup et al., 1996; Dean et al., 2000; Whitmarsh and Wallace, 2001), and this interpretation is chosen here for the affinity of the crust within zone T1. It is also possible that the transitional zone is composed of a mix of various crustal types. Hypotheses made by other authors discussed above are viable (Van Avendonk et al., 2006; Shillington et al., 2006), however the interpretation that zone T1 consists of mainly exhumed serpentinized mantle is accepted here for profile ER56.

Moving further seaward between CDPs 10000-8500, basement relief becomes moderate and the basement surface is imaged, similar to the moderate relief area imaged on SCR2 (CDPs 229500-234000). This section contains the M3 magnetic anomaly that was once considered as a seafloor-spreading anomaly in this region (e.g., Srivastava et al., 2000; Shipboard Scientific Party, 2004a), but now is hypothesized to be produced by serpentinized peridotites (Sibuet et al., 2007b). Basement relief becomes very high

(CDPs 8500-5500), where the basement ridge located at CDP 8000 correlates well to Mauzy Ridge where Site 1277 was drilled.

The zone of moderate- moving into higher-basement relief is named zone T2 (CDPs 10000-7000), and is very similar to the T2 domain on the SCR2 profile. A 6.0-7.6 km/s velocity characterizes this zone on the SCR2 profile (Van Avendonk et al., 2006), and drilling from Site 1277 suggests that these rocks represent exhumed serpentinized subcontinental mantle (Müntener and Manatschal, 2006). This crustal domain is correlated with T2 on SCR2, and is most likely formed through exhumation and serpentinization of mantle rocks.

Basement becomes relatively smooth near the M0 magnetic anomaly (CDP 6000) and this continues extending seaward to the end of the profile, and illustrates a more moderate yet variable basement relief. The M0 is located over a basement low on both the ER56 and SCR2 profile, where this basement feature is likely correlated across both lines. As discussed in Section 3.2.2, a change in the velocity gradient along the SCR2 profile occurs at M0 (Van Avendonk et al., 2006), and modeled velocities at this location resemble those of typical Atlantic Ocean crust (VD OC; Figure 3.2). The landward limit of oceanic crust is similarly placed just landward of the M0 anomaly on the ER56 profile.

3.2.5 Erable 53 and 54 CSS Hudson 85-025 (Plate 2e)

ER 53 images the continental shelf of Flemish Cap is between CDPs 102-7000. Here shallow water depth combined with a hard water bottom reflection makes noise from multiple reflections a severe problem. Although various multiple removal techniques were used in the processing flow, the signal to noise ratio remains very low.

There appears to be a thin layer of sediments, approximately 175 m thick between CDPs ~102-3000. Refracted waves from the sediment layer gives apparent velocities between ~2040-2220 m/s, which is a good approximation of the true velocity since the shelf area is flat. These velocities may be indicative of Mesozoic or Quaternary glacial sediments, both of which have been sampled over Flemish Cap through dredging and shallow drilling (Grant, 1973; King et al., 1985). This sediment layer becomes very thin between CDPs ~3000-5000, and refracted waves from sediments illustrate a velocity increase to ~3040-3300 m/s. The increase in velocity may represent indurated Mesozoic or Cenozoic sediments, or perhaps older Paleozoic sediments. The sediment layer becomes thicker near CDP ~5000 and continues to thicken towards the slope break (CDP ~7000), with refracted arrivals between ~2350-2690 m/s.

Below the thin sediment layer, the top of continental basement is confirmed from refracted arrivals between ~4800-6100 m/s. No intracrustal reflections have been successfully imaged along the shelf. A package of horizontal reflections between 9-11 seconds (~32 km thick using average crustal velocity of 6.35 km/s) corresponds with the expected depth of the Moho, and continues south across the shelf raising to 8-10 seconds near the slope break (~29 km thick).

The CSS Hudson 85-025 seismic refraction experiment (Todd and Reid, 1989) was conducted near the ER54 profile, and resulting velocity-versus-time models (discussed in Section 1.4.1.1) are used to provide velocity control on the reflection data. All velocity models provide a good match between the water bottom and top of basement reflections. Along the continental slope there is little evidence of rotated fault blocks as observed on Galicia Bank (Reston et al., 1996) and the Iberian Abyssal Plain (Whitmarsh et al., 2000; Pickup et al., 1996). However, velocity models HU-9&10, and HU-11 confirm the presence of continental crust, modeling velocities of 6.0-6.1 km/s and 5.9-6.0 km/s respectively. The crustal block at HU-11 (CDPs 10000-11000) may represent a smaller westward dipping fault block adjacent to a horst that is bounded by a high angle landward dipping normal fault to the west, and a seaward dipping normal fault to the east.

Seaward, a crustal block of unknown origin is present between CDPs 11500-12000. Adjacent to this crustal block there is a change in the top of basement reflectivity character, and deeper reflections are more predominant. A seaward dipping reflection, that likely represents a fault, coincides with this change in basement character. The basement surface of this block is very angular, demonstrating a similar shape to the top of a rotated fault block. Also, two crustal blocks near the foot of the slope on the SCR1 profile (CDPs 56000-60000) that lies just north of ER54, have been interpreted as continental crust by some authors (Funck et al., 2003; Hopper et al., 2004). Two crustal blocks also lie near the foot of the continental slope on ER54 (CDPs 10000-12000), and may correlate with those identified on SCR1. Thus, based on the angular shape and correlation to features on SCR1, this crustal block is assumed to be a block of continental crust.

Immediately seaward of this block the velocity model from HU-18 has been projected onto the profile (~ CDP 12000). Profiles shot from both east and west indicate a 4.5-5.0 or 5.1 km/s layer that is about 1.5 km thick above a layer with a velocity of 7.0 km/s that increases to about 7.3 km/s within 5 km depth. This provides a high velocity gradient of about 0.4 s^{-1}, which is not typical of continental crust, and could represent either 1) layer 2 and 3 ocean crust, 2) highly serpentinized and brecciated peridotites (similarly interpreted on IAM-9; Dean et al., 2000) over moderately serpentinized peridotites (25-35%; serpentinization values from Escartín et al., 2001), or 3) layer 2 ocean crust over moderately serpentinized peridotite. The velocity model from HU-1, 2, and 18 have all been interpreted by Todd and Reid (1989) as being produced oceanic crust. Similarly on SCR1, thin ocean crust is interpreted to lie just seaward of the two crustal blocks interpreted as continental crust (CDP 60000) extending for about 60 km until normal ocean crust thickness is reached (Funck et al., 2003; Hopper et al., 2004; Hopper et al., 2006). The interpretation of thin ocean crust is also adopted for this region on the ER54 profile.

The HU-6 refraction profile has an interesting crustal velocity structure, where a 2.5 km thick 4.0-4.5 km/s layer, presumed to be layer 2 ocean crust, is modeled above unaltered mantle velocities of 7.9-8.0 km/s. It is possible that another layer is present between the two, but too thin to be resolved by the refraction experiment. It is observed on SCR1 that layer 3 crust pinches out and is absent over a distance of about 10 km (Funck et al., 2003; Hopper et al., 2004; Hopper et al., 2006). This interpretation is similarly accepted to explain the HU-6 velocity model. Just seaward of the HU-6 projection at CDP 13500, a possible stratified rotated block is imaged. Similar features have been imaged within the thinned oceanic crust region of SCR1 (Hopper et al., 2004; Hopper et al., 2006).

Basement relief and reflectivity is moderate between CDPs13000-16500, and then becomes more reflective extending seaward to the end of the profile maintaining a moderate relief. This change in the basement reflectivity occurs near the M0 magnetic anomaly (Srivastava et al., 2000) located at ~CDP 17500. Below the basement surface, deep reflectors are imaged from CDP13000 to the end of the profile. Note the package of reflectors between CDPs 13500-14000 at 8.5-9.0 s. The base of these reflector correlates with the unaltered mantle velocities (7.9-8.0 km/s) modeled at HU-6. These possible Moho reflections where present are imaged as sub-horizontal relatively continuous features, until CDP 16000, where the reflection become discontinuous and form "criss-cross" features up to CDP 17500. A strong lateral velocity contrast may explain the inability to image these reflections, where a pre-stack depth migration would be required to successfully resolve them. The change in basement reflectivity near the M0 magnetic anomaly may coincide with a more normal thickness of ocean crust produced by a faster spreading rate.

Both HU-1 and HU-2 display normal oceanic crust layer 2 and 3 velocities up to a depth of 6 and 6.5 km below basement surface, and no mantle arrivals where recorded to constrain the total thickness of the crust. This region has a crustal thickness that is likely close to, or within the range of normal ocean crust thickness (7-8 km; Fowler, 2005, p. 326). Thus, the region between CDPs 12000-17500 is interpreted as thin ocean crust, and CDPs > 17500 are interpreted as normal thickness ocean crust.

3.2.6 SCREECH Line 104 (Plate 2f)

Low basement relief, and an unreflective basement surface characterize the area extending from the SW end of SCR104, to CDP 124500. Here the U-reflection is present (Shillington et al., 2004), and appears to terminate near CDP 124500. This zone is interpreted as transitional crust (T1), and includes intersection points with SCR2 and ER56 at CDPs 137200 and 133750 respectively. The SCR2 and ER56 profiles are similarly interpreted as transitional crust at the SCR104 intersections.

A flat basement surface is imaged, with little intra-crustal reflectivity between CDPs 124500-122000. It is uncertain what crustal type this area represents. However this zone is in close proximity to both ER54 where continental crust is interpreted to lie adjacent to thin ocean crust, and this also applies to SCR1 to the northeast. Therefore this area most likely contains either thinned continental crust, or thin ocean crust.

Just northeast of this section at CDP 121900 is the intersection with ER54, corresponding with the boundary of continental crust and thin ocean crust interpreted on the ER54 profile (CDP ~12000). This area also corresponds with an increase in intra-crustal reflectivity extending northeast to the end of the profile. The velocity model from HU-18 is projected onto SCR104 at CDP12000. The 4.5-5.0 or 5.1 and 7.1-7.3 km/s are interpreted as layer 2 and 3 thin ocean crust (as discussed in Section 3.2.5). This zone is similarly interpreted as thin ocean crust (T_{OC}). Basement topography increases slightly between CDPs 117500-11300 also supporting this interpretation.

3.3 Results

A detailed map with the SCREECH and Erable transects is provided in Plate 3 that includes CDP numbers for each profile. Taking the crustal boundaries outlined in Section 3.2, we can overlay them onto the map of the project area, and observe the relationship between all profiles (Figure 3.4 and Plate 3). Straight line interpolation between the various profiles provide shapes for these crustal domains (Figure 3.5), and aids in the understanding of how rifting and seafloor spreading spatially changed along the southern margin of Flemish Cap. The region southwest of the shaded crustal domains has not been interpreted for this project, however crustal domains have been placed on profile FGP 85-2 by Lau et al. (2006b). Likewise, a sense of the crustal boundary trend south of profile FGP 85-2 is taken from Tucholke et al. (1989), where these boundaries are outlined with dashed lines. A discussion on what mechanisms that could allow for the bend in these boundaries is given in Chapter 4.

The dominantly low relief, unreflective transitional crust (T1), is interpreted as exhumed serpentinized mantle on the SCR3 profile (Lau et al., 2006a; Lau et al., 2006b). However this zone is interpreted as dominantly thinned continental crust on the SCR2 profile by Shillington et al. (2006) and Van Avendonk et al. (2006), because of correlation with the modeled ~5.5-6.5 km/s layer from the wide-angle data. Low relief and unreflective transitional crust is also observed on the ER56 profile (T1). There is no evidence of rotated fault blocks or pre-rift sediments imaged in the T1 domain on either of the ER56, SCR2, or SCR3 profiles. Also, a 5.5-6.5 km/s layer can also be attributed to serpentinization of exhumed mantle rocks. Thus, we hypothesize that the T1 domain consists of dominantly exhumed serpentinized mantle similar to the conjugate Iberian margin (e.g., Pickup et al., 1996; Dean et al., 2000; Whitmarsh and Wallace, 2001).

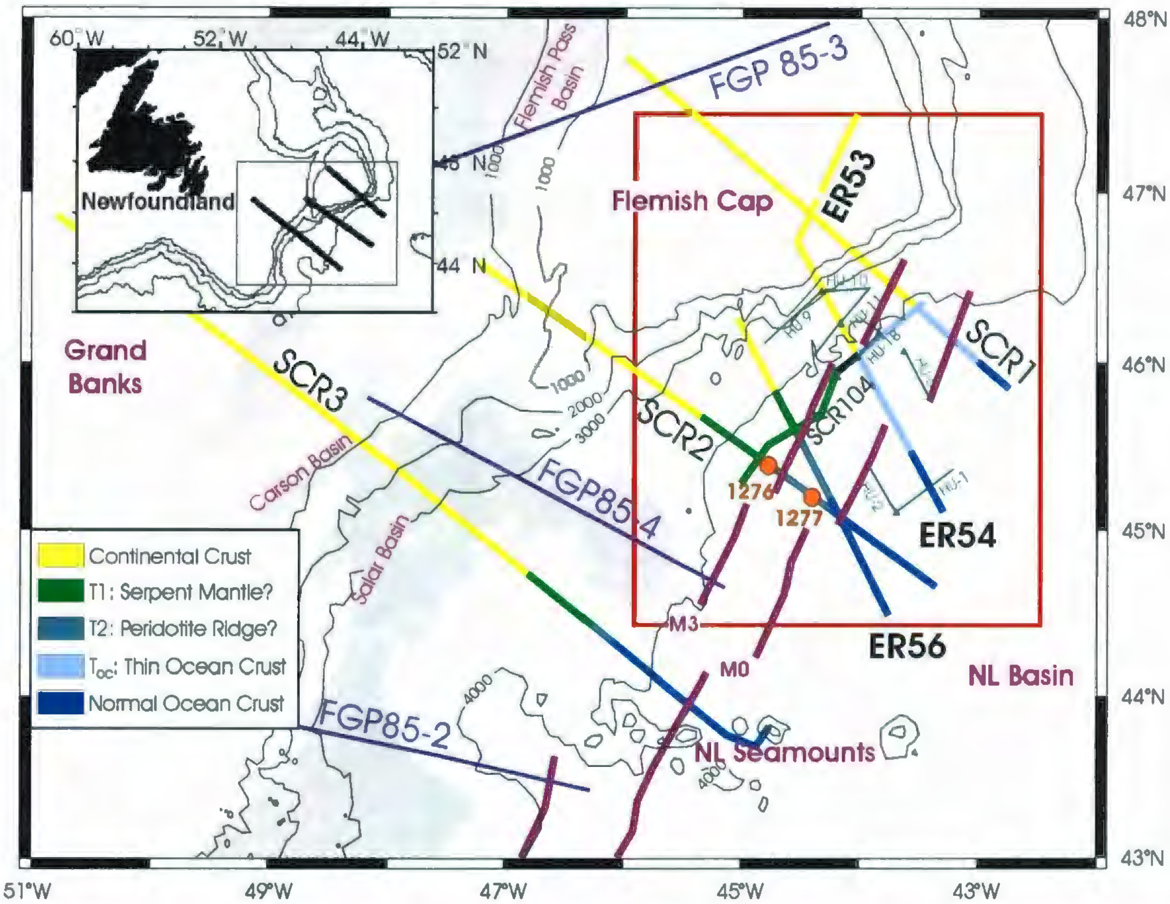

Figure 3.4: Map showing bathymetry and data coverage used for interpretation (Modified from Lau et al., 2006b) with the red rectangle outlining the project area. Interpretation of crustal boundaries and domains are placed on SCREECH and Erable profiles (as discussed in Section 3.2), where each domain is represented by a color as outlined in the legend on the bottom left corner. Frontier Geoscience Project (FGP) transects are outlined in purple, GSC wide-angle refraction lines collected in the CSS Hudson 85-025 cruise are outlined in green, and ODP drill sites from Leg 210 are outlined in orange. Interpretation of magnetic anomalies M0 and M3 are taken from Srivastava et al. (2000).

Profiles ER56, SCR2, and SCR3 all exhibit a moderate to high basement relief transitional crust (T2). From interpretation of the SCR3 profile, there remains some uncertainty whether this area represents exhumed mantle, or thin ocean crust (Lau et al., 2006a; Lau et al., 2006b). However drilling results from ODP Site 1277 show that the T2 domain on the SCR2 profile clearly contains serpentinized mantle (e.g., Shipboard Scientific Party, 2004b; Müntener and Manatschal, 2006). Thus, we hypothesize that zone T2 is dominantly composed of serpentinized peridotite ridges, similar to those observed on the conjugate Iberian margin (e.g., e.g., Pickup et al., 1996; Whitmarsh et al., 1996; Dean et al., 2000; Whitmarsh and Wallace, 2001).

The peridotites recovered from ODP Site 1277 are interpreted as subcontinental mantle rocks (Müntener and Manatschal, 2006). Similarly, geochemical analysis of rocks recovered from peridotite ridges on both the Galicia and Iberian margin have also been interpreted as subcontinental mantle (Evans and Girardeau, 1988; Girardeau et al., 1988; Kornprobst and Tabit, 1988; Abe, 2001; Hébert et al., 2001). Thus the proposed interpretation of the T2 peridotite ridge domain is subcontinental mantle exposed by rifting mechanisms. Since the low relief transitional domain (T1, interpreted as serpentinized mantle) is located landward of zone T2, this domain would similarly be interpreted as subcontinental mantle exposed during rifting. However, it should be noted that Site 1277 is the only drilling location that has sampled basement within the transitional crust of the Newfoundland margin. Although evidence described above supports the hypothesis that subcontinental mantle dominates the T2 region, there may be along strike variation of this zone, possibly containing some suboceanic mantle or melt products.

The T1 domain interpreted as exhumed serpentinized mantle dominates to the southeast pinching out moving northeast (Figure 3.5). The T2 domain interpreted

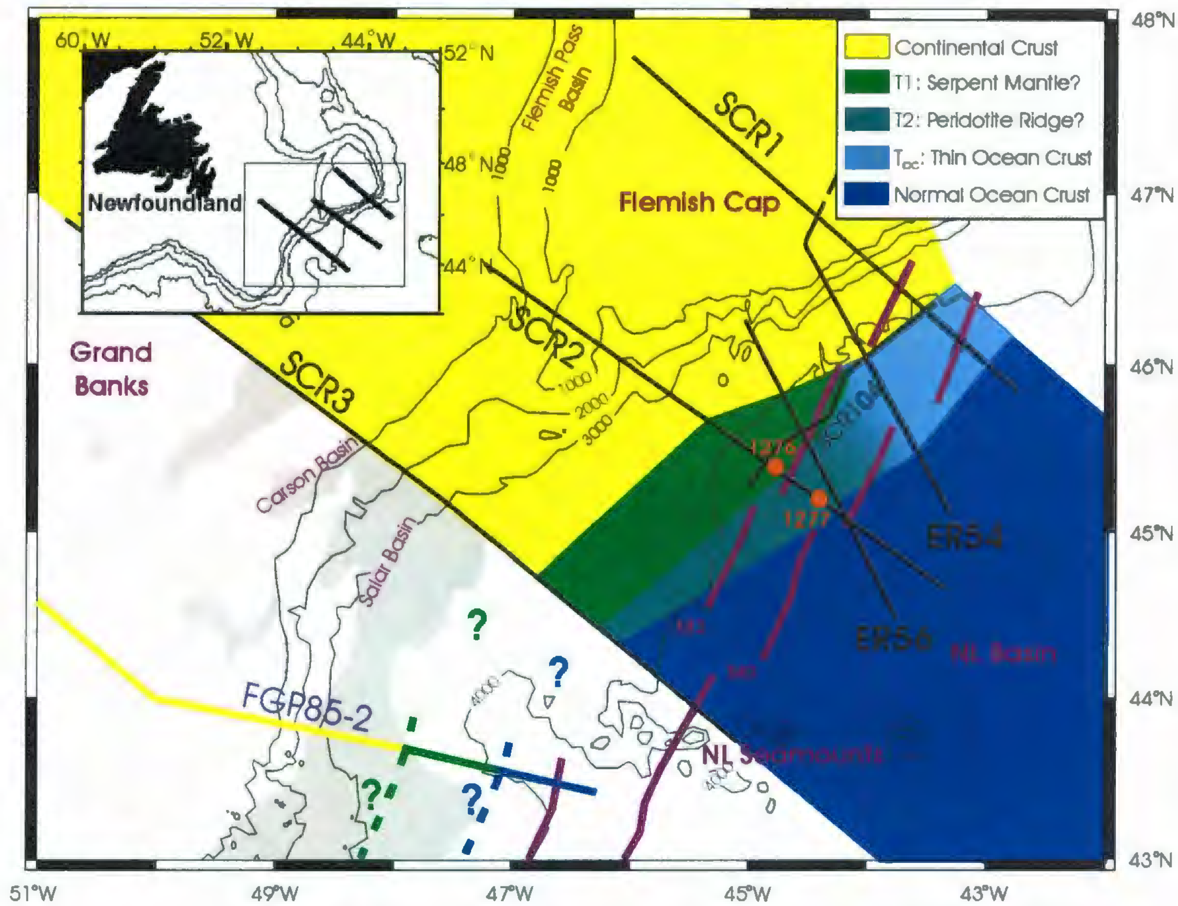

Figure 3.5: Map of project area showing bathymetry (Modified from Lau et al., 2006b). Interpretation of crustal boundaries and domains from SCREECH and Erable profiles as shown in Figure 3.4 are filled in to observe geometries of each domain. Interpretation of each crustal domain is represented by a color as outlined in the legend on the bottom left corner. ODP drill sites from Leg 210 are outlined in orange. Interpretation of magnetic anomalies M0 and M3 are taken from Srivastava et al. (2000) and shown with purple solid lines. Dashed line indicates assumed crustal boundaries from Lau et al. (2006b) and Tucholke et al., 1989.

peridotite ridges are also present to the southwest, and this zone widens as the former zone thins, but is not present on the eastern most edge of Flemish Cap. The transition from low relief exhumed mantle/peridotite ridges into thin ocean crust occurs between profile ER56 and ER54. Northeast of ER54, the transition from thinned continental crust to normal ocean crust is dominated by the formation of thinned ocean crust (T_{OC}), where

Layer 3 is absent in some areas. Thus a change occurs in the transitional zone moving from southwest to northeast, where the southwest appears to be developed by rifting of continental crust, and the northeast is formed by anomalous seafloor-spreading. This is also in agreement with the extended continental crust zone, where the width of thinned continental crust decreases moving to the northeast.

As illustrated in Figure 3.5, there is no correlation between magnetic lineations interpreted by Srivastava et al. (2000) and the various mapped crustal domains. This is likely because of the uncertainty associated with the weakness of the anomalies and along strike discontinuity.

A discussion of how rifting and sea floor spreading processes change moving along the margin is given in Chapter 4, along with possible rifting models for the Newfoundland and Iberian conjugate margins.

Chapter 4: Discussion

4.1 Basic Rifting Models

Pure shear extension is an early model proposed by McKenzie (1978) for the development of rifted continental margins. This model involves rapid uniform stretching throughout the continental lithosphere, with small-scale listric faulting occurring in the upper brittle crust, and ductile stretching in the lower crust (Figure 4.1 a). As the crust thins due to stretching there is an upwelling of the hot asthenosphere. This stage is associated with initial subsidence accommodated by fault block movement. Once stretching ends, heat is conducted to the surface and the lithosphere then thickens and cools, leading to a second slow stage of subsidence. Rifting accommodated by this pure shear uniform stretching would result in symmetrical conjugate margins.

However, asymmetries in continental margins are commonly observed, and cannot be represented by the pure shear rifting model (Lister et al., 1986). Wernicke (1985) proposed a simple shear model to explain this phenomenon, with a low angle normal fault that penetrates the entire lithosphere (Figure 4.1 b). In this scenario, crustal thinning is accommodated in the upper crust on the "break away side" (left as illustrated in Figure 4.1 b). As the detachment fault penetrates deeper, moving away from the "break away side" (right as illustrated in Figure 4.1 b) thinning of the lithosphere occurs within the lower crust and mantle, until only the mantle lithosphere is thinned. During rifting, uplift is produced in the area associated with the rising asthenosphere, while subsidence occurs below the area of crustal faulting. Hence, the asymmetry in the lithospheric response.

Lister et al. (1986) modified the simple shear rifting model so that it involves the delamination of the lithosphere, with the detachment fault becoming horizontal at the brittle-ductile transition, steeping, then again becoming horizontal at the crust mantle boundary (Figure 4.1 c). This would also produce asymmetrical plate margins, where the upper and lower plates are defined by rocks that originally lay above and below the detachment fault respectively. The lower plate is typically composed of rocks that have undergone extensive faulting and rotation, in comparison to the upper margin, which is much less structurally complex exhibiting some normal faulting with little rotation. Lister et al. (1986) also commented that the upper plate might be uplifted relative to the lower plate as a result of the rising asthenosphere and possible magmatic underplating.

Various models exist that combine the pure and simple shear models (e.g., Keen et al., 1989; Lister et al., 1991). These models are such that simple shear extension is accommodated along a detachment fault, and ductile pure shear stretching occurs below this in the lower crust and/or upper mantle (Figure 4.1 d). Some varieties of the combination model include: whether or not the detachment fault has multiple ramps and flats, the level at which the detachment fault soles (mid crustal or mantle depth), whether or not the zone of brittle extension in the upper crust is laterally offset from the zone of ductile stretching (Lister et al., 1991). The combination model shown in Figure 4.1 d illustrates a detachment fault that soles into the ductile lower crust, where the brittle faulting in the upper crust is not laterally offset from the zone of ductile stretching.

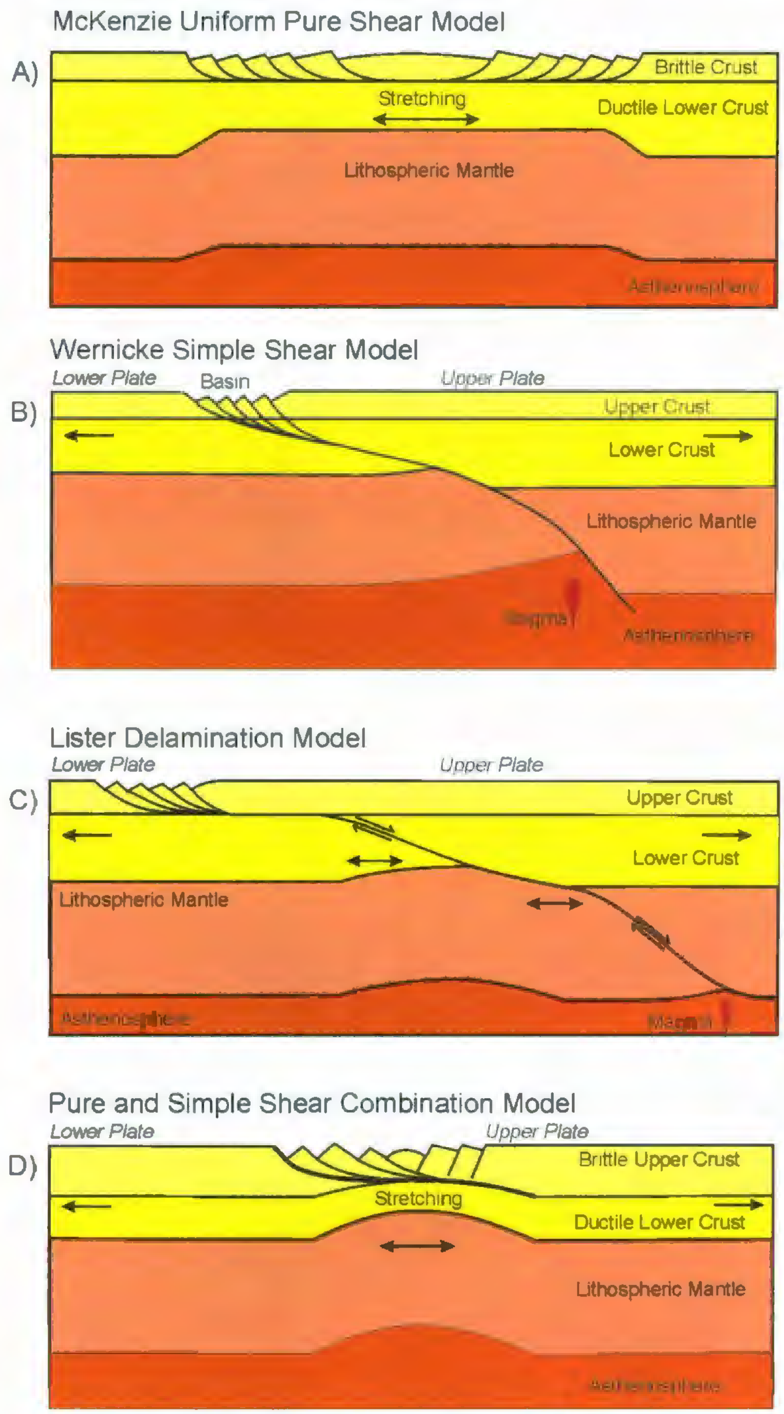

Figure 4.1: a) McKenzie (1978) pure shear extension model, b) Wernicke (1985) simple shear extension model, c) Lister delamination model (Lister et al., 1986), and d) pure and simple shear combination model with no lateral transfer (eg. Keen et al., 1989; Lister et al., 1991) (top three illustrations modified from Lister et al., 1986; and bottom illustration modified from Keen et al., 1989). Note that thickness of layers is not drawn to scale.

4.2 Newfoundland-Iberia Comparison

A comparison of conjugate profiles from the Newfoundland and Iberia margin is performed to provide insights into which rifting model best suits the structures observed along the margins, and to observe any lateral changes along the margin. A reconstruction at M0 (~118 Ma using Kent and Gradstein's, 1986, time scale; ~125 using the current Gradstein and Ogg, 2004, time scale) is given in Figure 4.2 (Van Avendonk et al., 2006),

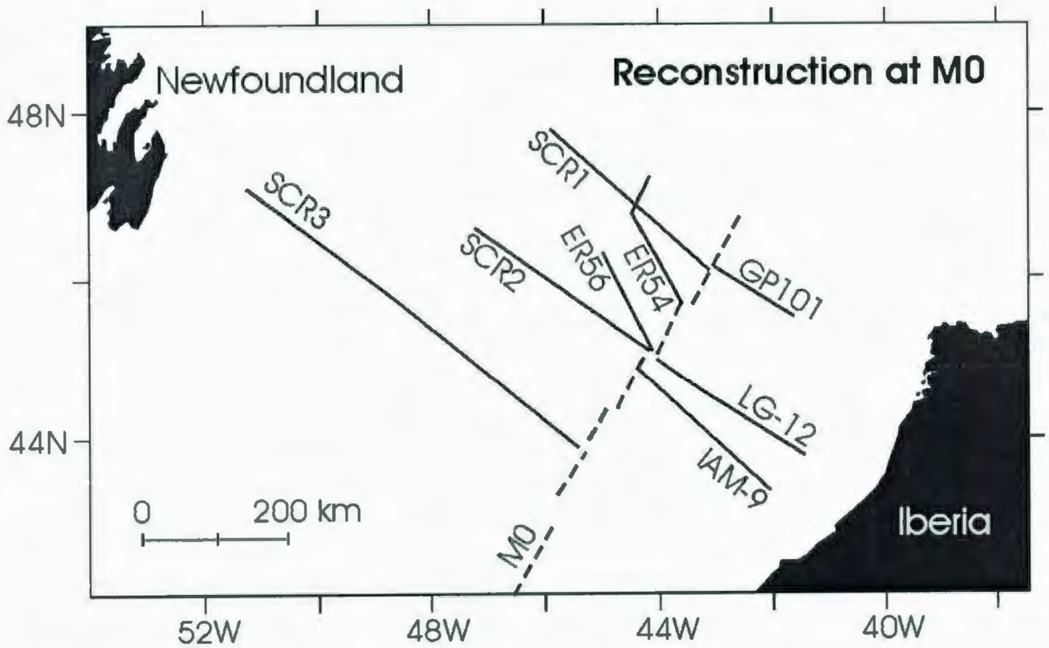

Figure 4.2: Reconstruction between Newfoundland and Iberia at M0 (~118 Ma using Kent and Gradstein, 1986, time scale; ~125 using the current Gradstein and Ogg, 2004, time scale) (After Van Avendonk et al., 2006). Latitude and longitude coordinates are fixed with respect to Newfoundland.

where M0 has in the past been interpreted as an undisputed oceanic magnetic anomaly being formed through seafloor spreading (Sibuet et al., 2007b). The SCREECH profiles are assumed to be approximately perpendicular to the direction of extension (Van Avendonk et al., 2006), as are the GP101, LG-12, and IAM-9 profiles from the Iberia margin. The Erable profiles 54 and 56 oblique to the SCREECH profiles, yet are approximately perpendicular to the strike of the Flemish Cap margin, and so lie in the optimal direction for imaging structures within this margin.

As illustrated in Figure 4.2, the SCR1 profile is conjugate with the GP101 profile. Although ER54 is slightly oblique to both of these profiles, it is also assumed to be approximately conjugate with GP101. The LG-12 profile and Leg 149/173 drilling sites are both conjugate to the SCR2 profile. These profiles also align with the most southern end of profile ER56, and are thus assumed to be approximately conjugate to this profile. The IAM-9 profile is located only 30 km to the south of LG-12, and within this 30 km the structure of the Iberia margin changes dramatically. Because the IAM-9 profile is in close conjugate proximity to the ER56 and SCR2 profiles in the M0 reconstruction, it will also be used for conjugate profile comparison.

4.2.1 Southwest Flemish Cap Margin and Southern Iberia Abyssal Plain

Figure 4.3 is a comparison of the ER56 and SCR2 profiles from the southwest Flemish Cap and Central Grand Banks margin with the southern Iberian Abyssal Plain. The zone of extended continental crust is about 55 km on both the ER56 and SCR2 profiles. This zone of thinning of crust beyond the shelf break is not as wide as that observed on the LG-12 and IAM-9 profiles. The full zone of extended continental crust extends further landward of the most landward edge of both the LG-12 and IAM-9 profiles. However measuring from the edge of the shelf break, the width of extended continental crust is about 330 km on both profiles. The thinning of the crust is clearly accommodated by multiple low angle listric faults on both Iberian profiles. A possible detachment fault is imaged on the LG-12 profile as discussed in Section 1.5.2, but not on the IAM-9 profile. In sharp contrast, faulting on the slope of the ER56 and SCR2 profiles is not as clearly imaged, and there is little to almost no evidence of crustal scale normal faulting or detachment faulting (Shillington et al., 2006).

The IAM-9 profile images a low relief transitional basement interpreted as exhumed serpentinized mantle (Pickup et al., 1996; Dean et al., 2000) that is about 120 km wide (T1), followed by a peridotite ridge region about 50 km wide (T2). The area around the LG-12 profile and Leg 149/173 drilling does not contain a low relief transitional region, but a zone of peridotite ridges about 80 km wide lies adjacent to the most seaward block of continental crust.

A low relief transitional region (T1) has been identified on both ER56 and SCR2 profiles with widths of 40 and 60 km respectively (Figure 4.2 for broad features or Plates 2b and 3b for detailed illustration). This is less than half the width of the low relief and reflectivity zone illustrated on the IAM-9 profile. Adjacent to the low relief unreflective transitional basement, there is a change to a more reflective, moderate to high relief transitional basement (T2), with widths of 50 and 55 km respectively. This zone is interpreted as serpentinized peridotite ridges, similar to the peridotite ridges located in the Iberia Abyssal Plain. The width of this zone off the southwestern margin of Flemish Cap is approximately the same as that observed from the IAM-9 profile. Comparison of the transitional regions of ER56 and IAM-9 (Figure 4.4) shows that the reflectivity is quite different. No top of basement reflection is observed from the low relief transitional region on the ER56 profile. An event named the U-reflector is widespread in this area

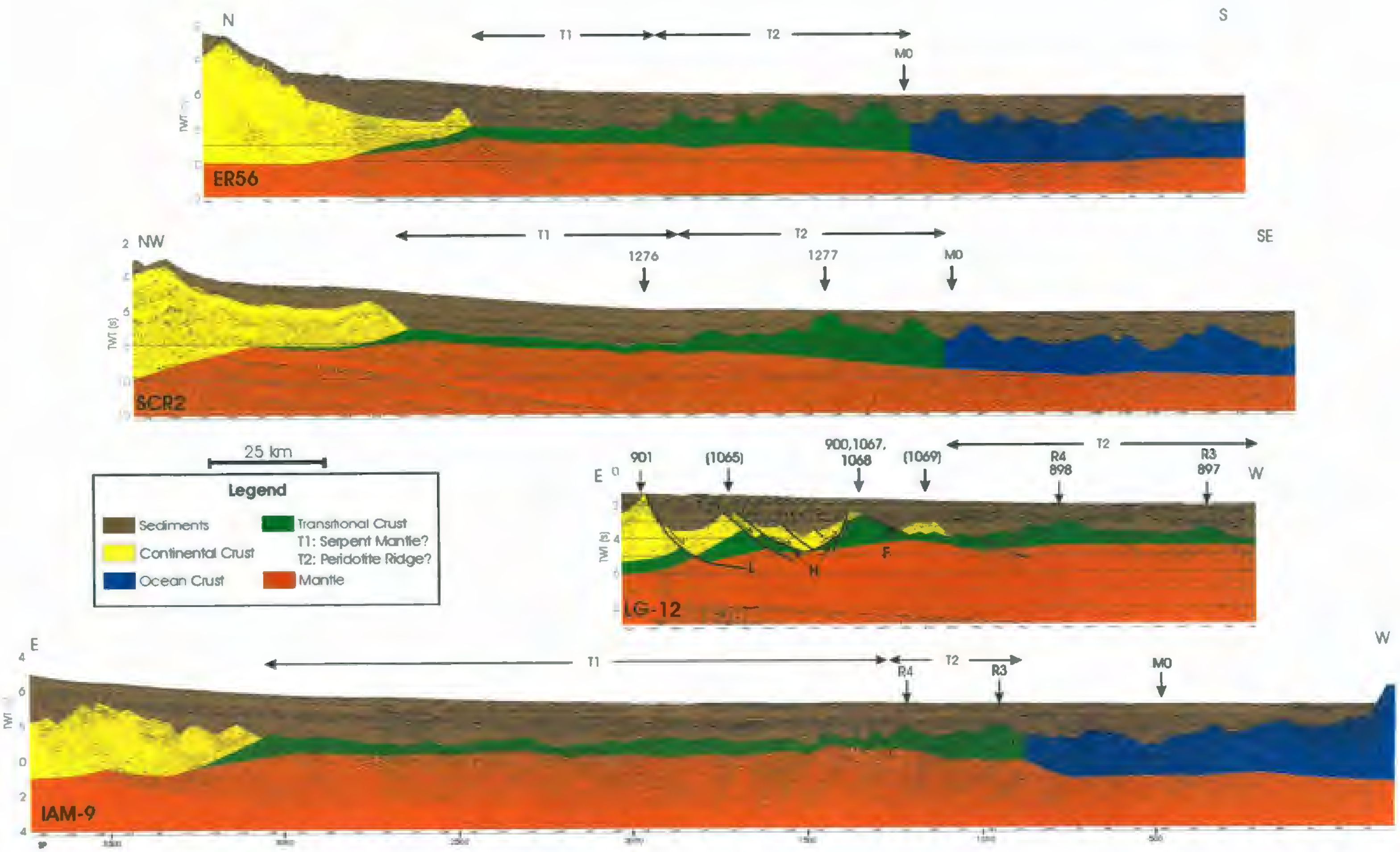

Figure 4.3: A comparison of ER56 and SCR2 from the southwest Flemish Cap margin with conjugate profiles LG-12 and IAM-9 from the southern Iberia Abyssal Plain. Both the LG-12 and IAM-9 profiles have been flipped for easy comparison to the Newfoundland profiles. See Figure 4.2 for a reconstruction between Newfoundland and Iberia at M0 for approximate profile locations at that time. ODP drill locations are labeled with drill site numbers, where numbers in brackets are sites that have been projected onto the profile. Interpretation of LG-12 and IAM-9 profiles taken from Pickup et al. (1996), Dean et al. (2000), Whitmarsh et al. (2000), Concheryo and Wise (2001), and Whitmarsh and Wallace (2001).

and is created by intrusion of mafic sills into sediments just above the assumed basement surface (see Section 1.4.3.1.1 for a full discussion). The lack of a visible basement reflection is likely a result of the inability of seismic waves to penetrate through the sills, a weak impedance contrast at the basement surface, or both (Shillington et al., 2006). In contrast, basement surface reflectivity on the IAM-9 profile in the low relief transitional is visible (yet of low reflectivity) and increases with depth. However, a widespread event comparable to the U-reflection on the Newfoundland margin is not present on the Iberian margin, so the difference in reflectivity may not be a result of different basement types.

The transitional region of increased basement relief has been identified as containing peridotite ridges on the IAM-9 profile (Figure 4.4), and a similar interpretation is given to this zone on the ER56 profile (see Section 3.2.4 for discussion on interpretation of crustal types). Amplitude and height of basement topography are very similar. The main difference between the Newfoundland and Iberia profile in this section, is that the basement highs are fairly angular on the IAM-9 profile, and more smooth on the ER56 profile. However studies have shown that serpentinization weakens peridotite rocks (Escartin et al., 2001), where serpentinization at the top of peridotite ridges would make them more susceptible to erosion, producing a more rounded basement surface (Tucholke et al., 2006), so the interpretation of a peridotite ridge for this region cannot be dismissed.

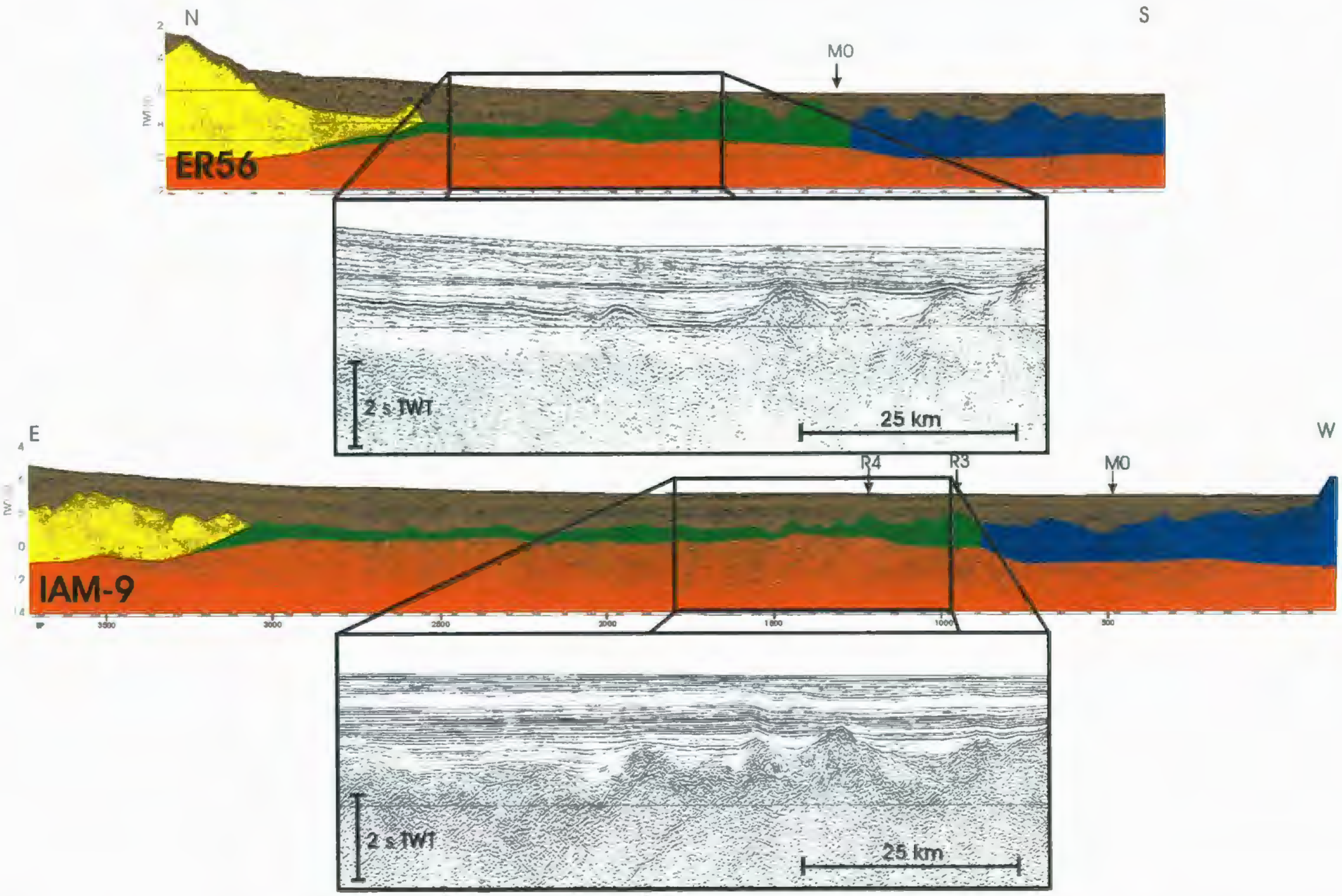

Figure 4.4: A comparison of the transitional crust of ER56 from the southwest Flemish Cap margin with transitional crust from the approximate conjugate IAM-9 profile within the southern Iberia Abyssal Plain. The IAM-9 profile has been flipped for easy comparison to the Newfoundland profile.

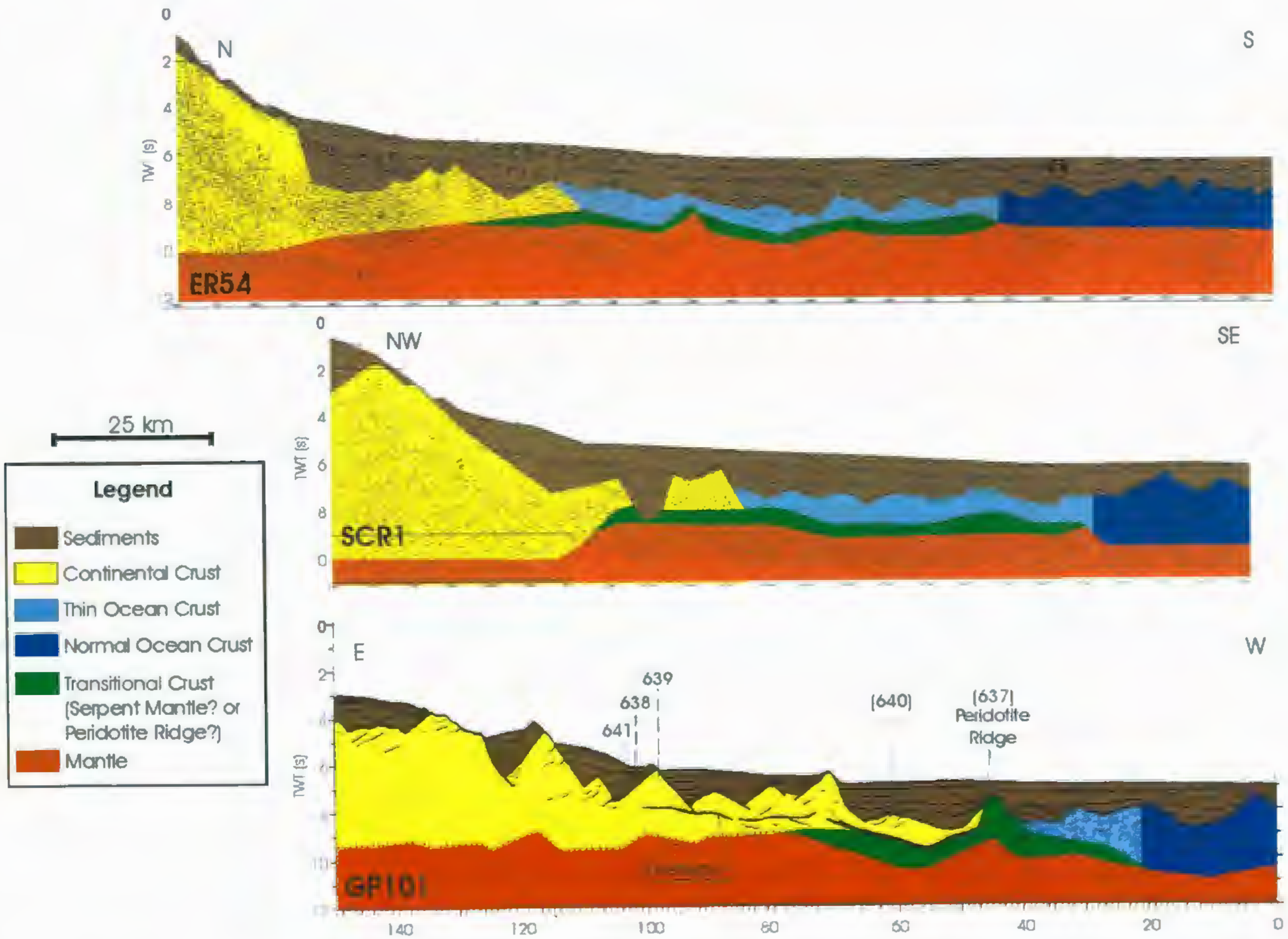

Figure 4.5: A comparison of ER54 and SCR1 from the southeast Flemish Cap margin with conjugate profile GP101 from the Galicia Bank margin. The GP101 profile has been flipped for easy comparison to the Newfoundland profiles. See Figure 4.2 for a reconstruction between Newfoundland and Iberia at M0 for approximate profile locations at that time. ODP drill locations are labeled with drill site numbers, where numbers in brackets are sites that have been projected onto the profile. Interpretation of the GP101 profile is taken from Reston et al. (1996) and Whitmarsh et al. (1996).

4.2.2 Southeast Flemish Cap Margin and the Galicia Bank

Figure 4.3 is a comparison of the ER54 and SCR1 profiles from the southeast Flemish Cap margin with the GP101 profile from the Galicia Bank margin. The zone of extended continental crust beyond the shelf break is about 80 km wide on the SCR1 profile (Hopper et al., 2006), and 70 km wide on the ER54 profile. The landward edge of continental crust is not included in the GP101 profile, but this profile does show continental crust thinning from 16 to 3 km over a distance of about 100 km suggesting that the zone of extended continental crust is much greater on the Galicia Bank margin. A strong continuous reflection named the S-reflector is imaged off Galicia Bank and is interpreted to represent a detachment fault (e.g., Boillot et al.1988a; Boillot et al., 1988b; Reston et al., 1996). There is no evidence of detachment faulting on the southeast margin of Flemish Cap. Also there is little evidence of highly rotated fault blocks as imaged on the Galicia Bank margin.

Neither the southeast Flemish Cap nor Galicia Bank margins contain a zone of low-relief transitional basement as observed just to the south (ER56, SCR2, and IAM-9 profiles). The GP101 profile has a narrow zone of transitional crust containing a peridotite ridge that was sampled at Site 637 by the ODP during Leg 103. This peridotite ridge abuts thin ocean crust that extents for about 20 km until it reaches normal ocean crust thickness. In contrast, no peridotite ridges are interpreted on the ER54 or SCR1 profiles, where thin ocean crust lies adjacent to the most seaward limit of continental crust. This zone of thin ocean crust is much wider on the southeast Flemish Cap margin, extending for about 70 and 60 km on the ER54 and SCR1 profiles respectively, and it also exhibits rotated fault blocks.

4.3 What Rifting Model is the Best Fit?

Starting with the southwest Flemish Cap and southern Iberia Abyssal Plain conjugate pair, the asymmetries of each margin provide evidence of a simple shear extension. Simple shear extension is typically accommodated through detachment faulting, where low angle major faults, which have been interpreted as detachment faults (Krawczyk et al., 1996; Whitmarsh et al., 2000), have been imaged on the LG-12 profile. The zone of extended continental crust is wider in the southern Iberia Abyssal Plain compared with the southwest Flemish Cap margin. Also highly-rotated fault blocks have been imaged in the southern Iberia Abyssal Plain, but not on the southwest Flemish Cap margin, suggesting that Iberia would be the lower plate, and Newfoundland the upper plate using the simple shear rifting model.

Similarly, the Galicia Bank margin also exhibits a wide zone of extended continental crust accommodated by low angle normal faults that sole near the S-reflector, a proposed detachment fault (eg. Boillot et al., 1988a; Boillot et al., 1988b; Reston et al., 1996). This is quite different from the abrupt thinning of the continental crust on the southeast Flemish Cap margin observed on both the SCR1 (Funck et al., 2003; Hopper et al., 2004; Hopper et al., 2006) and ER54 profiles. This provides further evidence that the Newfoundland shelf lies on the upper plate, and Iberia on the lower plate, as rifting is accommodated by a westward dipping detachment fault in a simple shear rift model.

Various authors have proposed simple shear models for the Newfoundland – Iberia conjugate pair, where both a westward (Winterer et al., 1988; Krawczyk et al., 1996; Whitmarsh et al., 2000) and eastward (Boillot et al., 1988b) dipping detachment fault has been modeled for the Iberian margin. However, extensive study has been performed on the nature of the S-reflector from multiple seismic reflection lines collected off Galicia Bank (Reston et al., 1996). Although these seismic reflection profiles image S as an undulating surface that, in different places, dips to the west, is sub-horizontal, and also gently to the east, the dominant dip direction is clearly to the west. The present day dip of a detachment surface does not always indicate the sense of shear, since it may have later become tilted. However there is no evidence of opposing dips observed within either the syn-rift or post rift sediments, so it is assumed that the predominant westerly dip of the S-reflector is a true indication of normal-slip shear motion (Reston et al., 1996). Also, overlying block-bounding faults also dip to the west, and evidence from detachment terranes is that faults overlying detachments are most often synthetic to the detachment (Lister and Davis, 1989), providing further evidence to support this theory. Sections of the S-reflector that dip eastward may simply represent area where the detachment fault bowed up as a result of removal of the load of the upper plate (Reston et al., 1996).

A similar bowing-upward feature is recognized on the H-reflector imaged on the LG-12 profile in the southern Iberia Abyssal Plain, where H is a proposed detachment fault separating crust and mantle rocks (Krawczyk et al., 1996) (Figure 1.10 and 4.3). In contrast, a comparison of seismic refraction and reflection results from Galicia Bank have determined that the S-reflector is intracrustal at the landward edge of Galicia Bank, and gradually cuts into the lower crust moving seaward (Whitmarsh et al. 1996). This suggests that there is variation along the Iberian margin in how these low angle (proposed detachment) faults form. Overall, evidence from dips of proposed detachment faults on the Iberian margin suggest that Iberia lies on the lower plate.

Although no detachment faulting has been imaged on the southern Flemish Cap margin, further south west on the Central Grand Banks, a package of westward dipping reflectors are imaged beneath the base of the continental slope on both the FGP 85-2 (Keen and de Voogd, 1988) and SCR3 (Lau et al., 2006b) profiles. It is uncertain what produces this strong L-reflection. Initially it was thought to be produced by magmatic material that underplated extended lower continental crust (Keen and de Voogd, 1988). A recent seismic refraction experiment conducted along the SCR3 profile has shown that the lower section of this package of reflectors is coincident with a 7.6-7.9 km/s P-wave velocity hence these reflectors are interpreted as separating crust from underlying serpentinized mantle (Lau et al., 2006a; Lau et al., 2006b). It is also proposed that the L-reflection represents a shear zone that aids in the exhumation of mantle further seaward (Lau et al., 2006b). It is possible that the shear zone could be remnants of a westward dipping detachment fault (Tankard and Welsink, 1987) as similarly suggested for the southern Iberia Abyssal Plain (Krawczyk et al., 1996; Whitmarsh et al., 2000) and Galicia Bank (Winterer et al., 1988; Reston et al., 1996; Reston 1996; Whitmarsh et al., 1996). It should be noted that intra-cratonic and continental slope rift basins located on the Grand Banks, such as the Jeanne D'Arc Basin and Carson-Bonnition Basin, have east-dipping basin-bounding faults (e.g., Enachescu, 1987; Enachescu, 1988), which would be antithetic to the proposed westward dipping detachment fault (Lister et al., 1991). However, the main rifting phase that affected many of these basins occurred in the Late Triassic to Early Jurassic (e.g., Enachescu, 1988; Enachescu, 1992), prior to the assumed final rifting that lead to continental break-up. Therefore, these extensional features may not be directly related (Keen et al., 1989).

In reality, rifting is not likely accommodated by solely simple shear or solely pure shear, but may involve a combination of both (e.g., Coward, 1986; Keen et al., 1989; Etheridge et al., 1989; Kusznir and Egan , 1989; Lister et al., 1991; Sibuet, 1992; Brun and Beslier, 1996). One such model is proposed for the Flemish Cap-Galicia Bank pair by Sibuet (1992). Here extension values were calculated based on the geometry of tilted fault blocks from the Galicia Margin, and compared to the expected subsidence function for a 125 Ma year old margin that has undergone pure shear extension. Landward, most tilted blocks fit the assumed subsidence function, but seaward, tilted blocks did not, and this led to the hypothesis that the main rifting mechanism for the entire lithosphere is pure shear, with simple shear occurring in more localized areas in the upper brittle crust of the Flemish Cap margin, and the seaward most-extended upper crust of the Galicia Bank.

One model evoked for the southern Iberia Abyssal Plain involves the recognition of four separate layers that are from top to bottom: brittle crust, ductile crust, brittle mantle, and ductile mantle (Brun and Beslier, 1996). Here it is suggested that rifting of the lithosphere occurs mostly by pure shear extension, producing mainly symmetrical features. However, some asymmetries are formed through heterogeneous boudinage and/or faulting of the brittle layers, where shear stretching occurs in the ductile lower crust and mantle layers.

4.4 Proposed Rifting and Break-up Models (Cross Section)

Here the hypothesis is accepted that rifting was accommodated by a west-dipping detachment fault, and is represented by both the S- and L-reflectors on the Iberian and Newfoundland margins respectively. Two different models of continental break-up are proposed in Figures 4.6 and 4.7.

Where the S-reflector is imaged, comparison of seismic reflection and refraction data has shown that it lies in mid-crust at its eastern edge, cuts into lower continental crust moving westward, and then comes close to, or reaches, the crust-mantle boundary (Whitmarsh et al., 1996). Similarly, modeling of seismic refraction data from the SCR3 profile shows that the base of the L-reflectors corresponds with the top of a modeled serpentinized mantle layer, at the western edge of the layer (Lau et al., 2006a; Lau et al., 2006b). These features condition both models presented (Figure 4.6 and 4.7).

ODP drilling from Legs 103 and 173 on the Iberian margin, and Leg 210 on the Newfoundland margin suggest that recovered serpentinized peridotites represent exhumed subcontinental mantle (Evans and Girardeau, 1988; Girardeau et al., 1988; Kornprobst and Tabit, 1988; Abe, 2001; Hébert et al., 2001; Müntener and Manatschal, 2006). This is the second condition set for both models illustrated in Figure 4.6 and 4.7.

The first model assumes a brittle lithosphere, with a detachment fault that penetrates the entire lithosphere as proposed by Wernicke (1985) (Figure 4.6 a). The

Iberian margin acts as the lower plate, and experiences dominantly upper crustal thinning, whereas the Newfoundland margin acts as the upper plate, and experiences dominantly lower crust and lithospheric mantle thinning. A slow and cold phase of rifting allows the crust to be thinned until it reaches zero thickness, and subcontinental mantle exhumation occurs (Figure 4.6 b). Faulting allows penetration of seawater into the peridotite rocks, so that serpentinization occurs. This is accompanied by a rising asthenosphere, which eventually penetrates to separate the two plates as seafloor spreading commences to form ocean crust (Figure 4.6 c). Here the breakup point is such that a section of subcontinental mantle from the Iberian upper plate is stranded on the Newfoundland margin. The detachment fault is now inactive. On the Newfoundland margin, the inactive detachment fault separates continental crust from mantle on its seaward side, and mantle from deeper mantle on its landward side. Seismic reflection and refraction data provide no evidence for a continuation of the detachment fault, separating mantle from mantle. It may be possible that the faulted mantle/mantle boundary does not possess an impedance contrast high enough to image a reflection. As seafloor spreading continues, the isotherms near the continental margins equilibrate, the asthenosphere level drops, and sub-oceanic mantle forms (Figure 4.6 c).

The second model proposed involves simple shear in the crust, and pure shear below (e.g., Keen et al., 1989; Lister et al., 1991). Here a detachment fault penetrates the entire crust and soles at the crust mantle boundary (Figure 4.7 a). The underlying mantle undergoes ductile pure-shear stretching. Similarly to the mantle exhumation stage in the simple shear model (Figure 4.6 b), crustal thinning is accommodated along this

Simple Shear (Brittle Lithosphere) Model

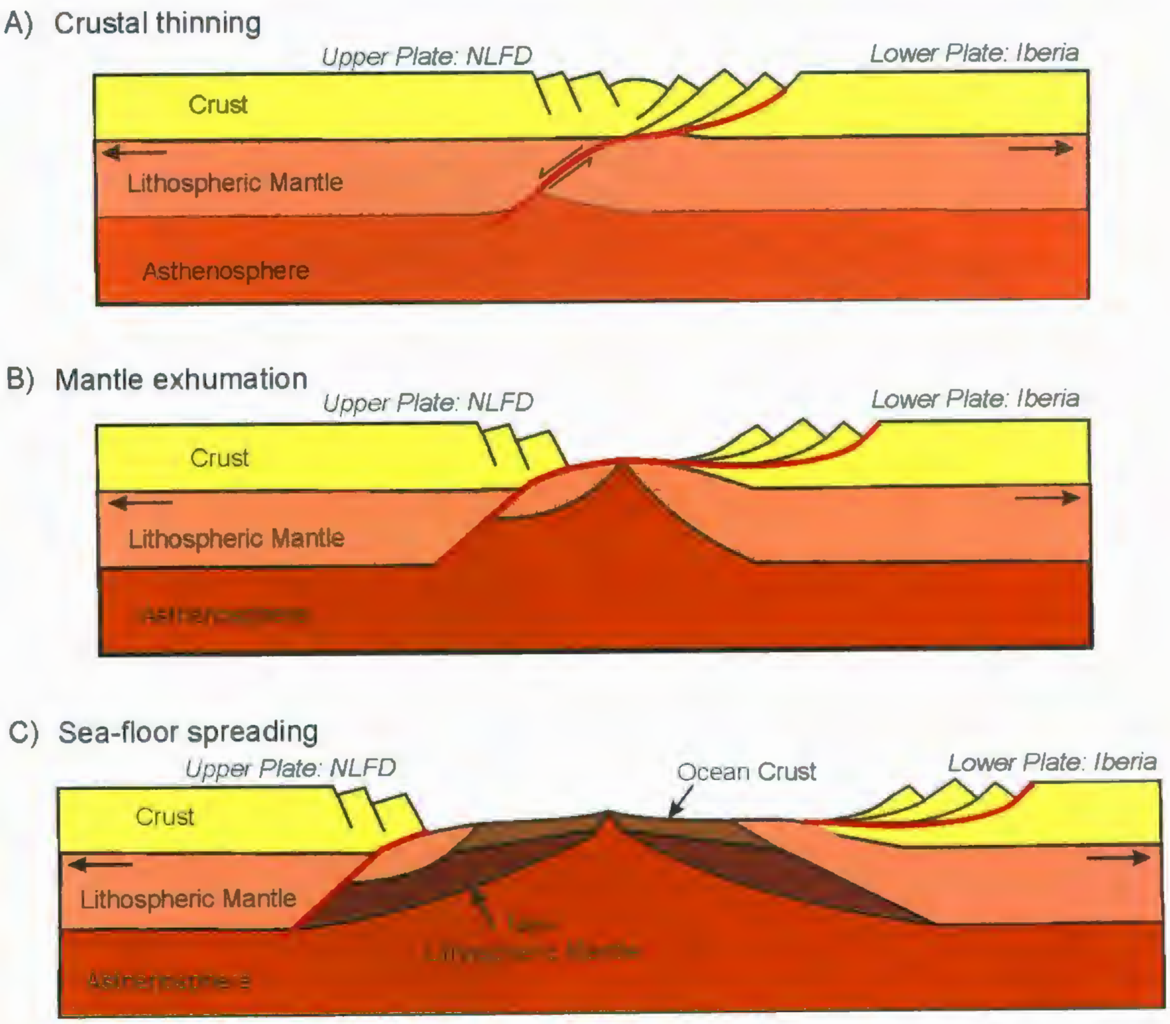

Figure 4.6: Simple shear model with a detachment fault (outlined in red) that penetrates the entire lithosphere (modified from Wernicke, 1985 and Lister et al., 1991). Note that thickness of layers is not drawn to scale.

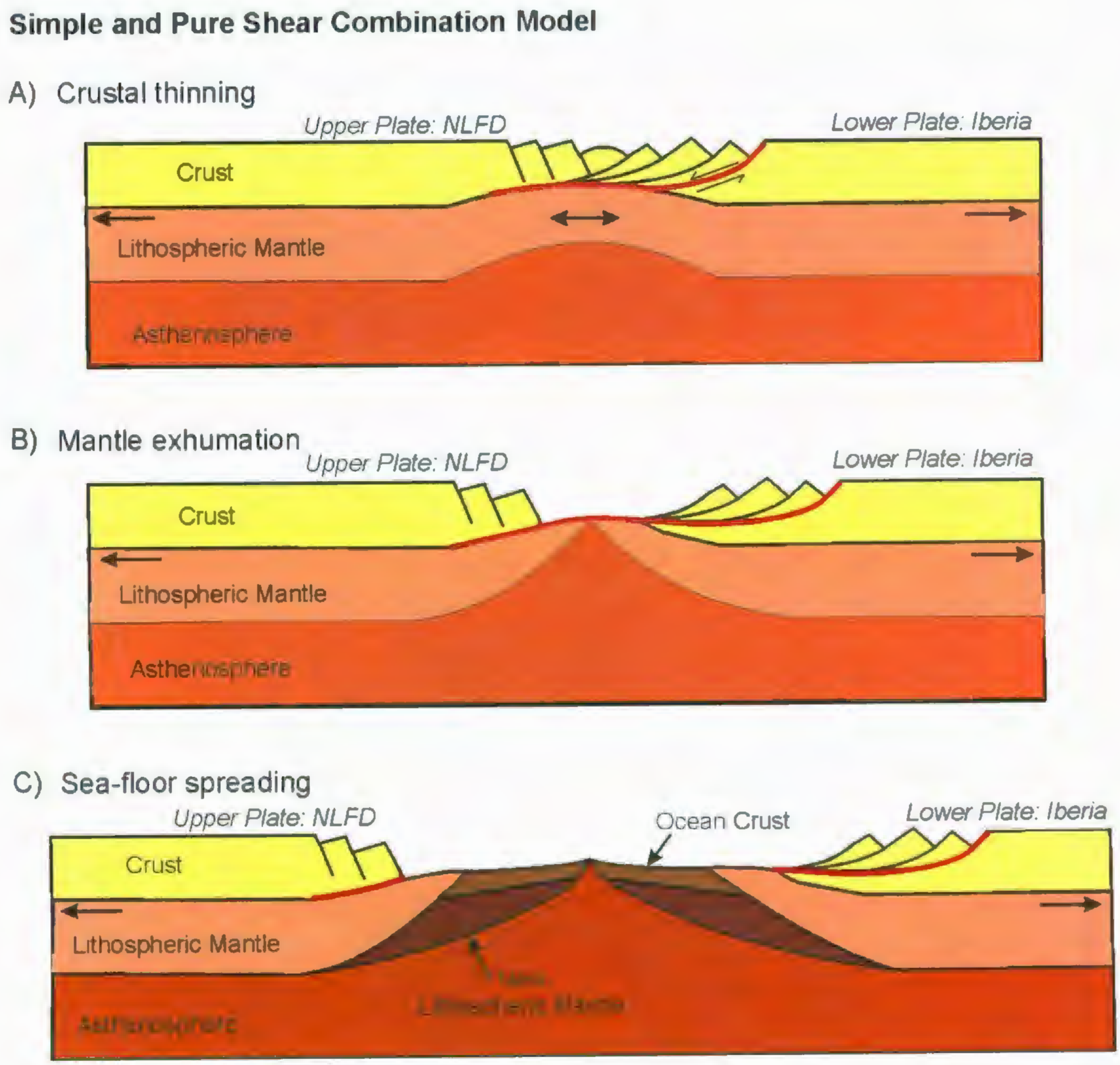

Figure 4.7: Simple shear and pure shear combination model, where a detachment fault (outlined in red) penetrates the crust and soles at the crust/mantle boundary (modified from Keen et al., 1989 and Lister et al., 1991). Pure shear stretching accommodates sub-crustal extension. Note that thickness of layers is not drawn to scale.

detachment fault, subcontinental mantle becomes exposed, and faulting and hydration forms serpentinized peridotites (Figure 4.7 b). The rising asthenosphere finally penetrates the seafloor separating the two plates and initiating seafloor spreading (Figure 4.7 c).

Based on the data presented thus far, we cannot discriminate between the two proposed models. Also, it should be noted that there is along-strike variation of the two conjugate margins that is not accounted for in these models. For example, there is no detachment fault imaged on the southeast margin of Flemish Cap, conjugate to S-reflector imaged on the Galicia margin. Similarly, there is no detachment fault imaged on the IAM-9 profile conjugate to the L-reflector imaged on the Central Grand Banks. Both models presented fit well for the southwest Flemish Cap/southern Iberia Abyssal Plain conjugate margin pair, where both margins have a zone interpreted as exhumed mantle. However the southeast Flemish Cap margin does not have a zone of exhumed mantle, where thinned continental crust lies adjacent to thin ocean crust, and the conjugate Galicia margin has a narrow zone of exhumed mantle. For this region, a slight modification of the two models would be necessary. Here the exhumation of mantle stage shown in Figure 4.6 b and 4.7 b would not last as long as farther south. The point of asthenospheric penetration would occur to the west of the zone of exhumed mantle. This would produce no exhumed mantle on the southeast Flemish Cap margin, with a narrow zone of exhumed mantle on the Galicia margin.

4.5 Developing a Rifting and Break-up Model (Plan View)

4.5.1 Objective

The objective is to provide a relatively simple geological model that illustrates how rifting and breakup between Newfoundland and Iberia changes with time, and produces the shapes of the various crustal domains observed on the present day southern margin of Flemish Cap. However, this model does not take into account detailed crustal geometries from Iberia, Europe, or north of the Flemish Cap margin, since this is outside the scope of this project. Instead, attempts are made to give a rough estimate of progressive motions that led to the formation of the southern Flemish Cap margin (following de Graciansky et al., 1985; de Graciansky and Poag, 1985; Sibuet and Collette, 1991; Sibuet et al., 2004; Enachescu et al., 2004a; Enachescu et al., 2004b; Enachescu et al., 2004c; Skogseid et al., 2004; Sibuet et al., 2007a; Tucholke and Sibuet, 2007; Tucholke et al., 2007).

4.5.2 Approach

In order to construct this model, it is necessary to clearly define the regions influenced by rifting versus seafloor spreading processes. Figure 3.5 illustrates the regions of continental crust, transitional crusts, and ocean crust. These regions need to be further extrapolated and interpolated to define the geometries that we are trying to re-produce for our model. There is a clear change in the orientation of the crustal boundaries from an approximately north-south trend on the Central Grand Banks, to a northeast-southwest trend along the southern margin of Flemish Cap (Figure 3.5). The bend in the crustal boundaries occurs south of the SCR3 profile, and north of the FGP

85-2 profile, but the exact location is uncertain because of lack of seismic coverage in this area. An interesting feature is that the Newfoundland Seamounts fall within the zone where the bend occurs, and they also line up with the Collector Anomaly (Haworth and MacIntyre, 1975; Haworth and Keen, 1979; Figure 4.8) as discussed in Section 4.5.4. We chose to place the bend in crustal boundaries at this location to constrain this section of our model (Figure 4.8), however any other location between SCR3 and FGP-85-2 is also possible.

As discussed in Section 3.3, both sections of transitional crust interpreted as low relief exhumed mantle and peridotite ridges (T1 and T2 respectively) are believed to have a subcontinental affinity, thus representing an area that has experienced rifting (represented by the grey section in Figure 4.9). Note that a lack of drill sites located within transitional crust does create an uncertainty in the interpretation that the entire region represents subcontinental mantle. Thus, some areas of the transitional crust may consist of suboceanic mantle or melt products. For the purposes of this model, we assume the hypothesis that the transitional crust containing exhumed subcontinental mantle is correct.

The area of extended continental crust has been formed through rifting. The most landward edge of the extended continental crust is approximated by the outline of the 600 m bathymetry contour, and it is assumed that crust located inside this boundary is relatively undeformed. However, it should be noted that this is used as a rough estimate since there is a small amount of internal deformation within Flemish Cap, and more deformation landward on the Grand Banks in basins such as the Jeanne d'Arc Basin.

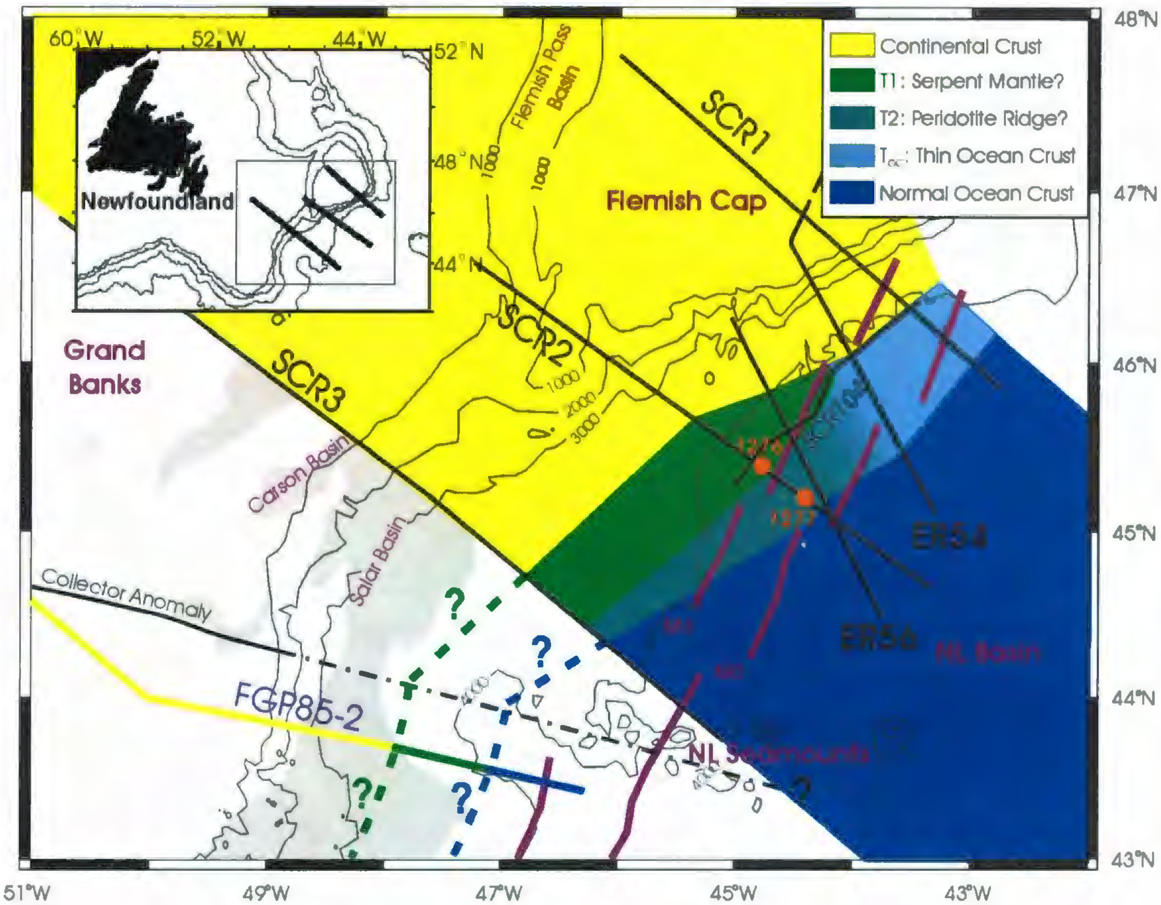

Figure 4.8: Map of project area showing bathymetry (Modified from Lau et al., 2006b). Interpretation of crustal boundaries and domains from SCREECH and Erable profiles as shown in Figure 3.4 are filled in to observe geometries of each domain. Interpretation of each crustal domain is represented by a color as outlined in the legend on the bottom left corner. ODP drill sites from Leg 210 are outlined in orange. Interpretation of magnetic anomalies M0 and M3 are taken from Srivastava et al. (2000) and shown with purple solid lines. Collector Anomaly outlined by black solid line and is extrapolated offshore as indicated by black dashed line (Haworth and MacIntyre, 1975; Haworth and Keen, 1979). Crustal boundaries of FGP 85-2 are taken from Lau et al., 2006b, and dashed blue and green lines indicates assumed crustal boundaries from Tucholke et al., 1989.

However crustal extension values are modest (Tankard and Welsink, 1987), so not accounting for these features in the model is reasonable. Thus, continental crust area outside the 600 m bathymetry contour is assumed to be the extended crust deformed during the Late Jurassic-Early Cretaceous rifting phase (also represented by grey area on Figure 4.9).

In contrast, both the normal ocean crust domain and the thin ocean crust (T_{OC}) domain located on the southeastern edge of Flemish Cap, represent the seafloor-spreading region (represented by blue regions on Figure 4.9). For the purposes of this paper, break-up is referred to as the end of the rifting phase (which produces either thin crust or exhumed subcontinental mantle), and the beginning of seafloor spreading. To constrain the timing and pattern of breakup, we look for evidence of seafloor spreading lineations within the magnetic data.

4.5.3 Constraints on Late Jurassic to Early Cretaceous Plate Motion

This section provides a discussion on various authors' interpretations of the rifting history on the Newfoundland margin, and corresponding movement of the Iberian plate that led to the break-up between the two. A summary of these events is provided in Figure 4.10. Many of these concepts are used as constraints to develop a model illustrating the rifting and break-up between Newfoundland and Iberia during the Late-Jurassic to Early Cretaceous presented in Section 4.6.

4.5.3.1 Newfoundland Margin

To model the time interval from Early Jurassic – Late Cretaceous, it is necessary to recognize the extension that occurred prior to this time. The Late Triassic – Early Jurassic rifting phase initiated the formation of many basins on both the Newfoundland and Iberian margin. These basins from the Newfoundland margin are dominantly located on the Southern and Central Grand Banks such as the Jeanne d'Arc, Flemish Pass, Salar and

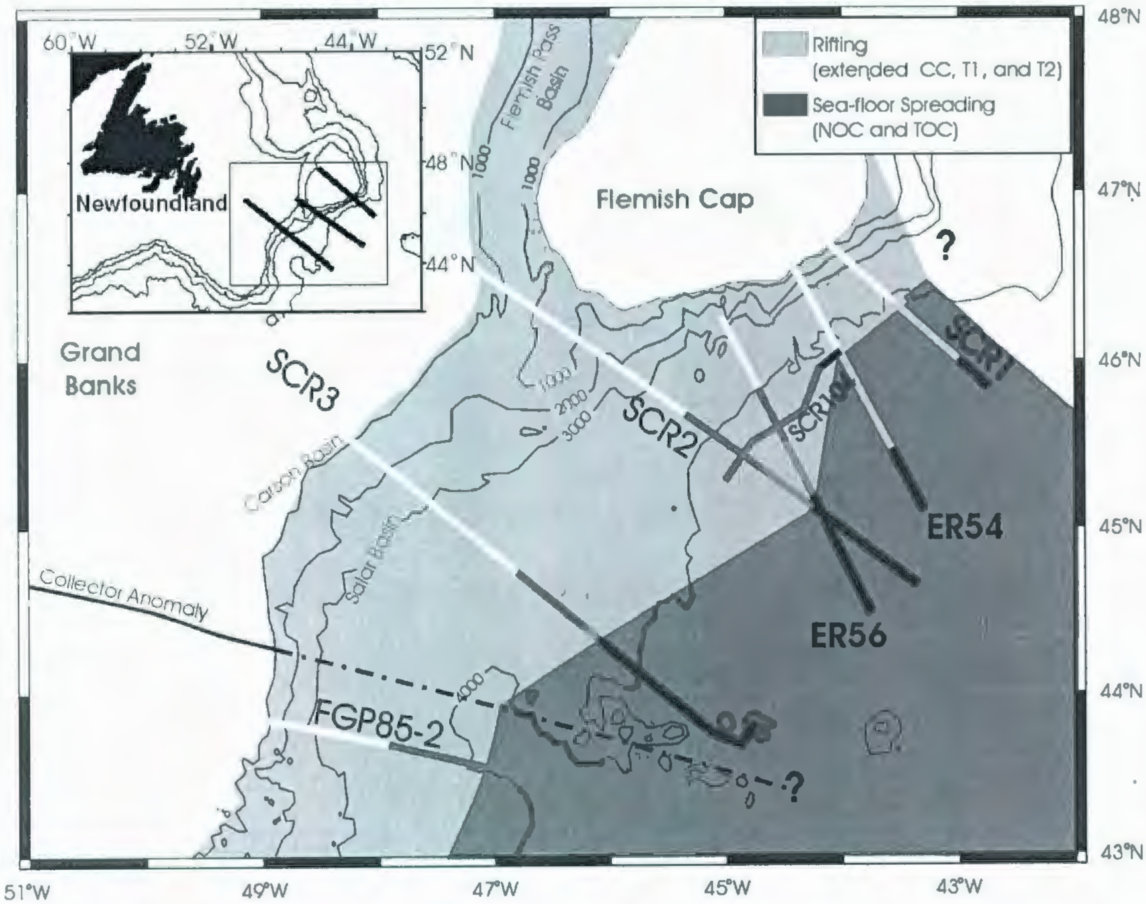

Figure 4.9: Map of project area illustrating regions formed through rifting (grey area), and regions formed through seafloor spreading (blue area) (Modified after Lau et al., 2006b). Interpretation of crustal boundaries from SCREECH and Erable profiles are taken from Figure 3.4. Landward boundary of extended continental crust is estimated by the 600 m bathymetry contour. Rifted crust area contains extended continental crust (extended CC), and transitional crust (T1 and T2). Seafloor spreading region contains both normal ocean crust (NOC) and thin ocean crust (TOC).

Carson Basins (e.g., Enachescu, 1988; Sibuet et al., 2007a). The Late Jurassic – Early Cretaceous rifting phase also created additional extension within these basins, although to a lesser extent relative to the previous rifting phase (Enachescu, 1987; Sibuet et al., 2007a).

Late Triassic – Early Jurassic rifting was followed by a phase of epeirogenic subsidence throughout the Middle Jurassic (Tankard and Welsink, 1987), with a small amount of extension as recorded in both the Jeanne d'Arc and Whale Basin (Tankard et al, 1989; Balkwill and Legall, 1989; Tucholke and Sibuet, 2007). Extension on both the Newfoundland and Iberian margin becomes much stronger during the Late Jurassic and eventually leads to continental break-up in the Late Cretaceous (e.g., Tucholke et al., 2007). More specifically, Tucholke and Sibuet (2007) have suggested a strong extensional phase likely affecting the entire length of the Newfoundland-Iberian rift throughout the Tithonian-Berriasian to early Valanginian time (using Gradstein and Ogg, 2004, time scale). This was followed by a Valanginian to Early Barremian extensional phase that created strong rifting and thinning of continental crust between the southern Flemish Cap – Galicia Bank conjugate pair, and produced exhumed mantle to the south.

When reconstructing plates prior to breakup, many authors have recognized a misfit where there is an overlap in the Flemish Cap – Galicia Bank area (e.g., Keen and Barrett 1981; Masson and Miles 1984; Srivastava and Tapscott, 1986; Sibuet et al., 2004). M0 (~118 Ma using Kent and Gradstein, 1986, time scale; ~125 Ma using current Gradstein and Ogg, 2004, time scale) reconstructions show that regions just south of the Flemish Cap – Galicia Bank conjugate pair have continental margins with similar geometries that parallel each other (Figure 1.3) (Sibuet et al., 2007a). A study performed by Sibuet et al. (2007a) has utilized Bouguer gravity anomalies to identify hinge zones along Flemish Cap and Galicia Bank. These outlined hinges have approximately the same length, and are oblique to one another at an angle of 43° (Figure 1.3). Interior

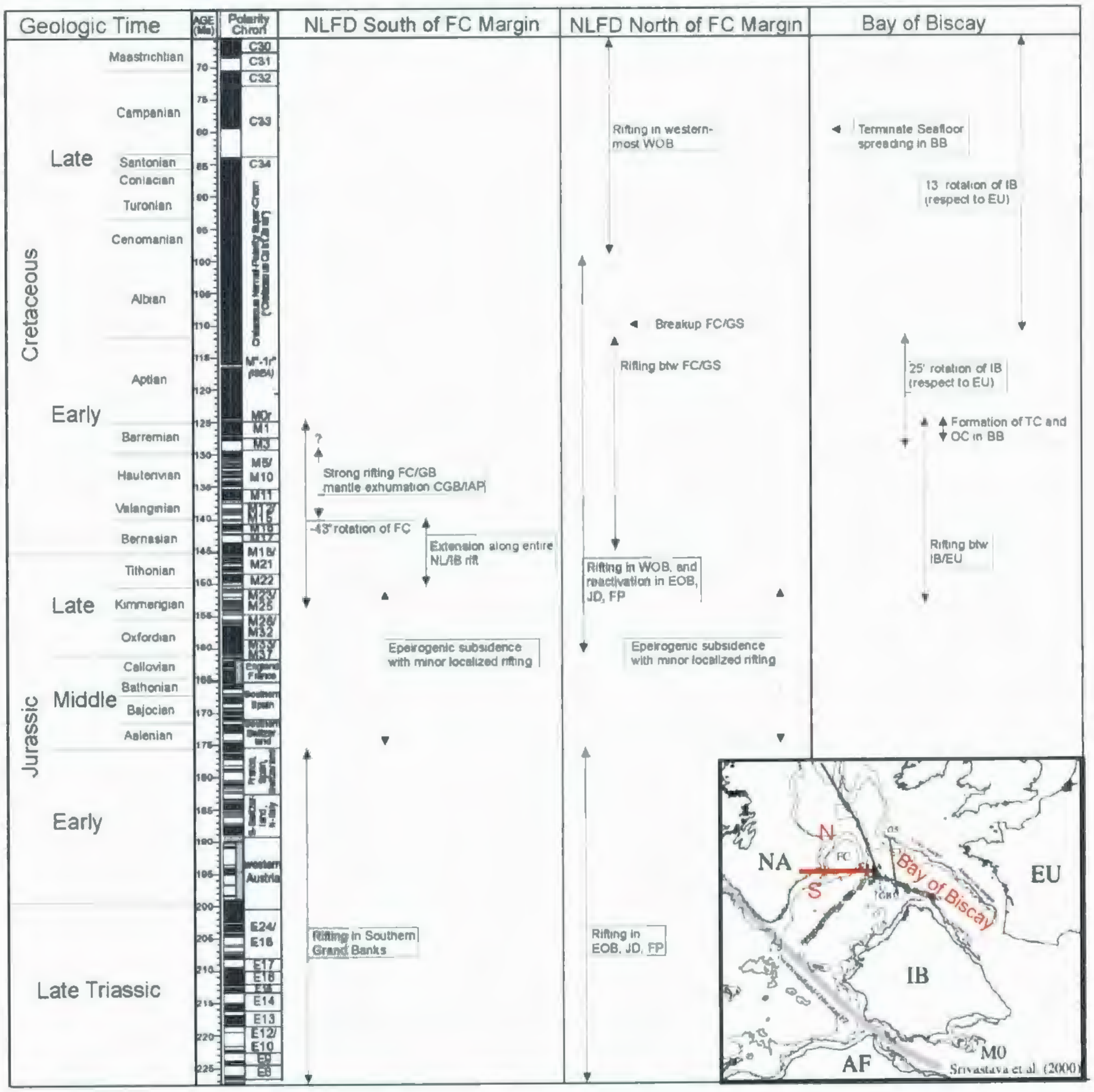

Figure 4.10: A summary of geological events as described throughout Section 4.5.3 used to constrain the proposed rifting and break-up model in Section 4.6 using Gradstein and Ogg, 2004, time scale. BB=Bay of Biscay, CGB=Central Grand Banks, EOB=East Orphan Basin, EU=Eurasia, FC=Flemish Cap, FP=Flemish Pass Basin, GB=Galicia Bank, GS=Goban Spur, IAP=Iberia Abyssal Plain, IB=Iberia, JD= Jeanne d'Arc, NLFD=Newfoundland, OC= Ocean Crust, TC= Transitional Crust, WOB=West Orphan Basin. Arrows indicate a time range for the corresponding event, but the limits of the ranges are approximate. Geological events on the Newfoundland margin and within the Bay of Biscay are separated into columns based on location. Inset on both right corner is M0 reconstruction taken from Sibuet et al., 2004 (after Srivastava et al., 2000) to illustrate the location described in each column.

basins of the Galicia Bank hinge zone have approximately the same width along their length, thus it is assumed that Galicia Bank did not rotate with respect to Iberia. Results from this study suggest that prior to the Late Jurassic – Early Cretaceous rifting phase, these hinge zones were parallel, and that Flemish Cap acted as a micro-plate, between M25 and M0 (~156-118 Ma using Kent and Gradstein, 1986, time scale; ~154-125 Ma using current Gradstein and Ogg, 2004, time scale) time, that rotated 43° clockwise (pole of rotation at 46.17°N, 49.09°W) relative to the North America (NA). This would mean that Flemish Cap was initially located in the East Orphan Basin.

The hypothesis that Flemish Cap was once located in the East Orphan Basin also corresponds with seismic and stratigraphy information that suggests a prolonged rifting history for the Orphan Basin (Sibuet et al., 2007a). This includes possible initial rifting in the East Orphan Basin during the Late Triassic – Early Jurassic (e.g. Enachescu et al., 2004a; Enachescu et al., 2004c). The second Late Jurassic – Early Cretaceous rifting phase opened the West Orphan Basin, and reactivated faults in the East Orphan Basin (Enachescu et al., 2004a; Enachescu et al., 2004b; Enachescu et al., 2004c; Skogseid et al., 2004). Lastly, the Late Cretaceous rifting phase affected the western-most section of the West Orphan Basin.

4.5.3.2 Iberian and European Margins

As rifting and seafloor spreading progressed between the Newfoundland and western Iberia Margin, the Bay of Biscay simultaneously experienced extension and possibly seafloor spreading that opened the northern margin of Iberia. Various ideas are present regarding the timing and mechanisms that led to the opening of the Bay of

Biscay. Some authors evoke the idea that there was a dominantly left-lateral strike slip motion with an Iberia (IB)/Eurasia (EU) pole of rotation located in northern Europe (e.g. Le Pichon et al., 1970; Olivet, 1996). However the favored interpretation is that the Bay of Biscay opened with a scissors-type progressive opening (e.g. Sibuet and Collette, 1991; Srivastava et al., 2000; Sibuet et al., 2004). A study of Iberian paleomagnetic declination data led to the conclusion that Iberia underwent a fast counterclockwise rotation of about 25° (±5°) with respect to Europe during the Barremian/Aptian, with an additional 13° counterclockwise rotation sometime between the Albian and Maastrichtian (Dinarès-Turell and Garcia-Senz, 2000). This paleomagnetic data supports the interpretation of a scissors type opening of the Bay of Biscay (Sibuet et al., 2004), and this interpretation is likewise used to constrain the model presented in this paper.

The youngest seafloor spreading anomaly mapped in the Bay of Biscay is C33 (~80 Ma using Kent and Gradstein, 1986, and Gradstein and Ogg, 2004, time scale), marking the termination of seafloor spreading there (Sibuet and Collette, 1991). Recent identification of M0-M3 (~118-124 Ma using Kent and Gradstein, 1986, time scale; ~125-129 Ma using current Gradstein and Ogg, 2004, time scale) anomalies in the Bay of Biscay suggest that seafloor spreading commenced some time during this period (Sibuet et al., 2004).

The northeastern margin of Flemish Cap is conjugate with Goban Spur from the European margin (de Graciansky et al., 1985), marking the southernmost section of the NA/EU branch. The structure of the Goban Spur has been developed predominantly through rifting between NA and EU (de Graciansky and Poag, 1985), and is the location of the DSDP Leg 80. Barremian and possibly some Aptian syn-rift sediments were cored at DSDP Site 549, where rifting is assumed to have begun near the Jurassic-Cretaceous boundary (de Graciansky and Poag, 1985).

4.5.4 Constraints of Breakup and Spreading from Magnetics

Srivastava et al. (2000) have mapped the M-sequence anomalies south of the Flemish Cap region, but these anomalies are poorly lineated compared to anomalies east of C34 (Figure 4.11) (Srivastava and Tapscott, 1986). For example, interpretation of M0 and M3 anomalies (Srivastava et al., 2000) plotted in Figure 4.11 are very poorly constrained, if at all. Also, as discussed in Section 3.1.3.1, some of these M-sequence anomalies may be produced by serpentinization of exhumed mantle rather than by seafloor spreading processes (Sibuet et al., 2007b). Thus, identification of these anomalies cannot be used to distinguish between oceanic and transitional crust. The oldest magnetic strip anomaly that is clearly defined in this area is C34 (~84 Ma using Kent and Gradstein, 1986, and Gradstein and Ogg, 2004, time scale), and is located seaward of the southern margin of Flemish Cap. This anomaly also represents a time of seafloor spreading ridge-ridge-ridge (RRR) triple junction (Figure 1.3), with an arm extending along the Grand Banks (NA/IB branch), an arm into the Labrador Sea (NA/IB branch), and an arm into the Bay of Biscay (EU/IB branch) (Sibuet and Collette, 1991).

The youngest seafloor spreading anomaly mapped in the Bay of Biscay is C33 (~80 Ma using Kent and Gradstein, 1986, and Gradstein and Ogg, 2004, time scale), marking the termination of seafloor spreading on the EU/IB arm of the NA/EU/IB triple junction (Sibuet and Collette, 1991). Recent identification of M0-M3 anomalies in the

Bay of Biscay suggest that seafloor spreading commenced some time during this period (Sibuet et al., 2004).

Break-up later followed between the northeast margin of Flemish Cap and Goban Spur at about 110 Ma (Graciansky et al., 1985). This marks the initiation of seafloor spreading that progressed northward into the Labrador Sea (between NA and EU). Seafloor spreading continued in the Labrador Sea until its cessation sometime between C20 and C13 (45-36 Ma using Kent and Gradstein, 1986, ~42-34 Ma using current Gradstein and Ogg, 2004, time scale) (Roest and Srivastava, 1989).

Near the location of the observed bend in crustal boundaries (Figure 4.8) lie the Newfoundland Seamounts offshore, which line up with the Collector Anomaly onshore (Haworth and MacIntyre, 1975; Haworth and Keen, 1979; Figure 4.11). The Collector Anomaly is a strong positive magnetic and gravity anomaly, which extends across the Bay of Fundy, through Nova Scotia, and along the southern Grand Banks, representing the boundary between Avalon and Meguma terranes (Haworth and MacIntyre, 1975). In Nova Scotia the superposition of these two rock types occurs along the Cobequid-Chedabucto transcurrent fault (e.g., Eisbacher, 1969; Haworth and Keen, 1979). It has been suggested that the Avalon-Meguma boundary may have formed a line of weakness that extended into the ocean crust and accommodated movement along a transform fault (Haworth and Keen, 1979), and that the Newfoundland seamounts formed from volcanic activity along the leaky transform fault related to a change in the spreading direction. However, another interpretation is that migration of plumes or hot-spots, such as the Azores, Madeira, and Canary plumes, is the source of the volcanic activity (Duncan,

1984) that produced the Newfoundland Seamounts, and also the diabase sills recovered from ODP Site 1276 about 180 km north in the Newfoundland Basin (Karner and Shillington, 2005). Since the source of the volcanic activity that produced the Newfoundland Seamounts is uncertain, we do not account for this feature in the proposed model.

4.6 Proposed Rifting and Break-Up Model (Plan View)

For this model, the NA plate remains fixed, Flemish Cap acts as a micro-plate rigid block, and likewise the IB and EU plates act as rigid blocks. Extension occurred in the Flemish Pass and East Orphan Basin during the Late Triassic – Early Jurassic rifting phase (e.g. Enachescu et al., 1988; Enachescu et al., 2004a; Enachescu et al., 2004c). Reactivation of rifting in these basins is also recorded during the Late Jurassic – Early Cretaceous (Sibuet et al., 2007a). Assuming that Flemish Cap was once located in the East Orphan basin, and has rotated clockwise 43° relative to the North America during M25-M0 time (Sibuet et al., 2007a), then we postulate a minor triple junction was present during the onset of the Late Jurassic – Early Cretaceous rifting phase (~M25) (Figure 4.12 a). One branch extended into what is present-day East Orphan Basin, and another extends along the southern margin of Flemish Cap (I, Figure 4.12 a). The third branch extended approximately south into the Flemish Pass Basin (III, Figure 4.12 a). Extension and dextral strike-slip motion occured on all three branches of the triple junction. Simultaneous reactivation of northeast-southwest faulting in the western-most section of the East Orphan Basin accommodated rifting near Flemish Cap (I, Figure 4.12 a). We propose that separation along branches II and III of the triple junction and reactivation of Orphan Basin faults pulled and rotated Flemish Cap out of Orphan Basin.

Approaching M3 time (before ~ 129 Ma using current Gradstein and Ogg, 2004, time scale), the East Orphan – Flemish Cap – Flemish Pass triple junction became for the most part inactive (Figure 4.12 b). Extensional vectors re-aligned themselves forming a major triple junction between the NA, IB, and EU plates that is about to accommodate rifting along each three branches: 1) NA/IB oriented ~north-south, 2) IB/EU oriented ~east-west, and 3) NA/EU oriented ~ northwest-southeast. We assume that most of Flemish Cap's rotation and southeasterly displacement has occurred by this time, and that rotation from M3-M0 time is negligible. This is because the NA/IB and NA/EU rift branches will tend to pull Flemish Cap to the east rather than to the south. Thus for simplicity sake, we have modeled the full 43° clockwise rotation to have occurred prior to M3.

Leading up to and during the M3 period, we postulate a slight northeast translation in the EU plate, and a 20° anti-clockwise rotation of IB with respect to NA and EU (Figure 4.12 c). The GP101 seismic line along the Galicia Bank images a subcontinental peridotite ridge (Evans and Girardeau, 1988; Girardeau et al., 1988; Kornprobst and Tabit, 1988) thus marking the seaward edge formed through rifting. Assuming the landward edge of extended crust lies at the shelf break, this gives a zone of about 480 km wide that has been produced by rifting processes. Placing the IB pole of rotation near the northeast edge of the Bay of Biscay models a similar width of rifted crust off the Galicia margin. Also, these plate motions create a small zone of rifted crust between NA and EU, and a scissors type opening with rifted crust between IB and EU.

Seafloor spreading has commenced in the southern section of this model between

Figure 4.11: Magnetic map of the Newfoundland margin and western North Atlantic Ocean (modified after Oakey and Dehler, 2004). Anomalies M3 and M0 are taken from Srivastava et al. (2000). Note that these magnetic anomalies are poorly lineated compared to the C34 and C33 magnetic strip anomalies illustrated in the top right corner. Although not in this map view, the C34 and C33 anomalies are also clearly delineated to the southeast.

NA and IB by M3 time (~ 129 Ma using current Gradstein and Ogg, 2004, time scale) (as outlined by the solid blue line). Here timing of seafloor spreading is constrained by the overlap of the ocean crust domain with the M3 anomaly interpreted by Srivastava et al. (2000). Break-up is about to progress to the northwest along the southern margin of Flemish Cap, and into the Bay of Biscay (outlined by the blue dashed line) (Figure 4.12 c).

By M0 time, seafloor spreading has progressed northward along the southern margin of Flemish Cap and into the Bay of Biscay (Figure 4.12 d). This spreading has been accommodated by an additional 5° anti-clockwise rotation of Iberia, giving a total rotation of 25°.

Finally, break-up between the northeast margin of Flemish Cap and Goban Spur occurred at approximately 110 Ma (Graciansky et al., 1985) or C34, defining the RRR major triple junction opening the North Atlantic, Labrador Sea, and Bay of Biscay (Figure 4.12 e). Note that there is a good fit between the shape of the margin and rifted crust domain as modeled at C34 after continental break-up (Figure 4.12 e), and as mapped on the present day Newfoundland margin (Figure 4.12 f). Assumptions and results of this model are combined with the summary of geological events (Figure 4.10) and presented in Figure (4.13).

Note that post M3 time, we assume that the extensional vectors accommodating rifting between NA/IB are approximately east-west. In Figure 4.12 c (expanded view in Figure 4.14), the southern section of break-up (outlined by solid blue line) is oriented almost north and perpendicular to the extensional vectors as expected (1, Figure 4.14).

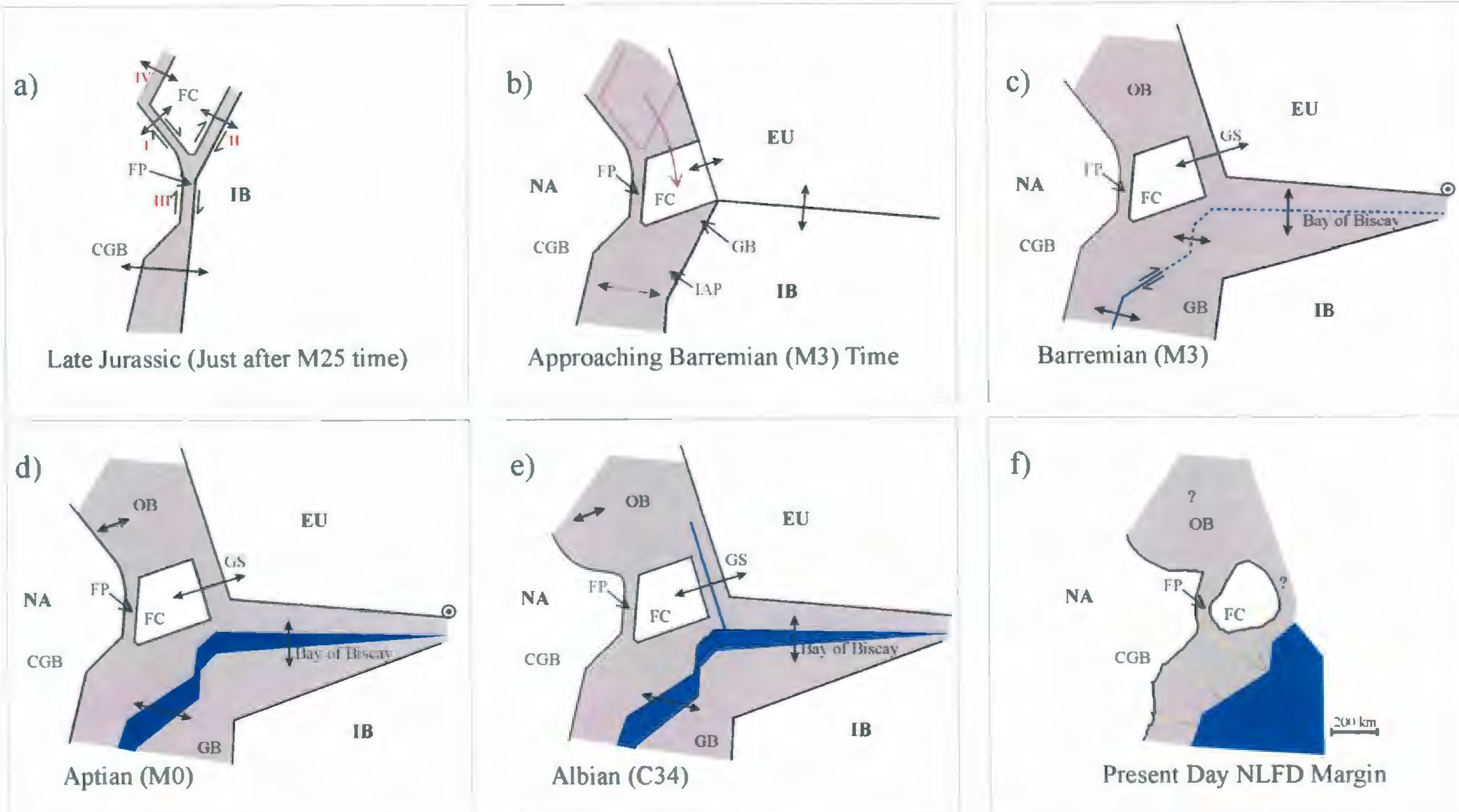

Figure 4.12: Plan-view model illustrating how rifting and break-up between Newfoundland and Iberia changes with time. CGB=Central Grand Banks, EU=Eurasia, FC=Flemish Cap, FP=Flemish Pass Basin, GB=Galicia Bank, GS=Goban Spur, IAP=Iberia Abyssal Plain, IB=Iberia, NFLD=Newfoundland, OB=Orphan Basin. Solid blue indicates formation of ocean crust, blue dashed line outlines where break-up is about to occur.

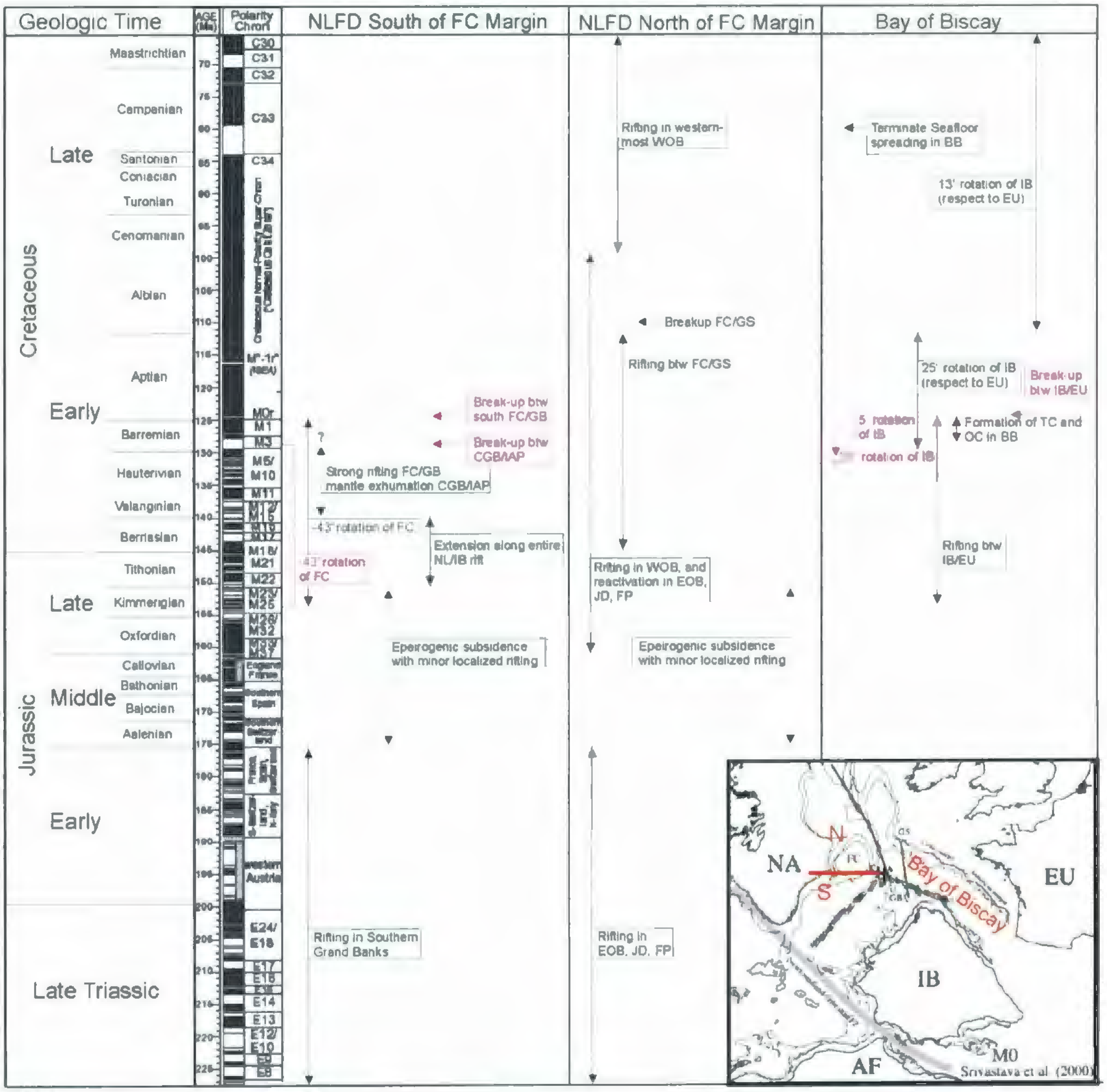

Figure 4.13: A summary of geological events as described throughout Section 4.5.3 using Gradstein and Ogg, 2004, time scale. Assumptions and results from the proposed rifting and break-up model (Figure 4.12) are overlain in purple text. BB=Bay of Biscay, CGB=Central Grand Banks, EOB=East Orphan Basin, EU=Eurasia, FC=Flemish Cap, FP=Flemish Pass Basin, GB=Galicia Bank, GS=Goban Spur, IAP=Iberia Abyssal Plain, IB=Iberia, JD= Jeanne d'Arc, NLFD=Newfoundland, OC= Ocean Crust, TC= Transitional Crust, WOB=West Orphan Basin. Arrows indicate a time range for the corresponding event, but the limits of the ranges are approximate. Geological events on the Newfoundland margin and within the Bay of Biscay are separated into columns based on location. Inset on both right corner is M0 reconstruction taken from Sibuet et al., 2004 (after Srivastava et al., 2000) to illustrate the location described in each column.

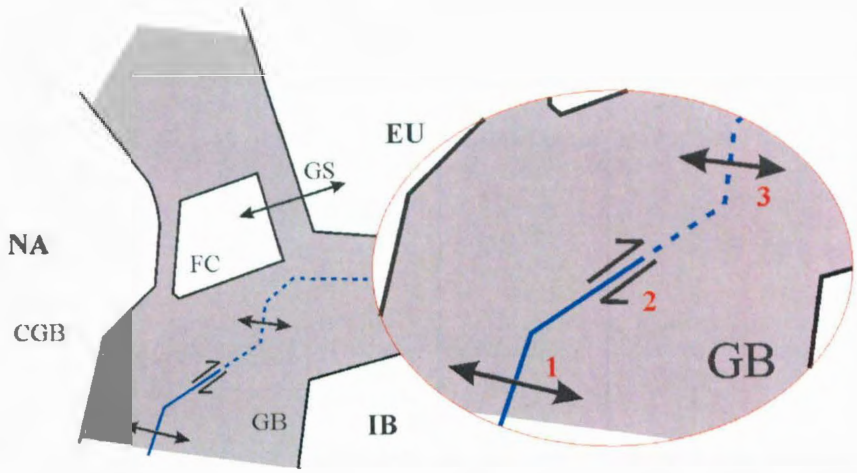

Figure 4.14: Expanded view of Figure 4.12 c, illustrating possible oblique shear motion along the southern margin of Flemish Cap.

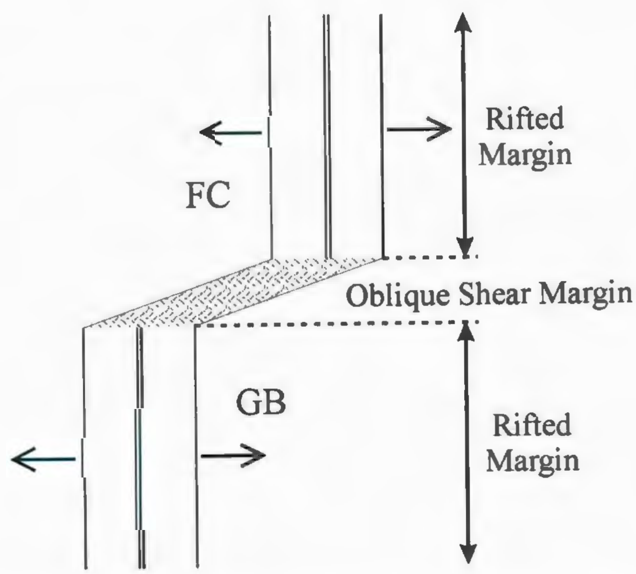

Figure 4.15: Oblique shear model modified after Todd and Reid (1989), where they proposed oblique shearing between the southern margin of Flemish Cap and the northern margin of Galicia Bank. This model was first proposed by Eldholm et al. (1987) for the Svalbard margin.

However, the line of breakup then takes a bend changing orientation to the northeast (2, Figure 4.14). Observing where the line of break-up is about to occur to the north of this (outlined by blue dashed line), the line reorients itself and once again trends almost north (3, Figure 4.14). It is possible that the two north-trending segments of the margin (1 and 3, Figure 4.14) represent rift and spreading segments that have been offset by an oblique transform margin.

The concept of a continental margin formed through oblique shearing was first introduced by Eldholm et al. (1987) for the Svalbard margin, and was adopted for the southern margin of Flemish Cap by Todd and Reid (1989) (Figure 4.15). They suggest that as Iberia moved eastward away from NA, an oblique shear zone formed between the southern margin of Flemish Cap and the northern margin of Galicia Bank.

A similar feature has been observed off Rio Muni in West Africa, where the Ascension Fracture Zone is modeled as an oblique transform that accommodates oblique-slip motion leading up to and following continental breakup (Turner et al., 2003). Here the oblique transform margin is described as having characteristics that are intermediate of two end-members: 1) rifted margins (exhibiting dip-slip kinematics, with a wide zone of rifted crust) and 2) normal transform margins (exhibiting strike-slip kinematics, with a steep continental slope).

The southern margin of Flemish Cap also exhibits characteristics intermediate to both end members. For example, in the northwest Atlantic, the Nova Scotia continental margin represents the rifted margin end member, where continental crust is thinned from 36 to 3 km thickness over a distance of 180 km (Funck et al., 2004). The Southwest

Newfoundland Fracture Zone represents the normal transform margin end member, where a transitional zone about 25 km wide contains a steep continental slope with crust that has thinned from 20 to 8 km thickness, and the seaward thinned continental crust seems to be overlain by a 3-5 km thick layer of volcanics (Todd et al., 1988). The continental crust on the southern margin of Flemish Cap thins from about 30 to 5 km thickness over a width of 70 km on the ER 54 profile, and 55 km on the ER56 profile.

Note that the model presented that approaches M3 time (Figure 4.12 b) positions the southern margin of Flemish Cap as conjugate with the western margin of Galicia Bank. However, during M0 time (Figure 4.12 d), the southern margin of Flemish Cap is conjugate with the northern margin of Galicia Bank, similar to reconstructions presented by Todd and Reid (1989). This solves the problem of a misfit with overlap in the Flemish Cap Galicia Bank area as encountered in other reconstructions (e.g., Keen and Barrett 1981; Masson and Miles 1984; Srivastava and Tapscott, 1986; Sibuet et al., 2004). But the model presented here is different from many past and recent M0 paleographic reconstructions that place the southern margin of Flemish Cap conjugate with the western margin of Galicia Bank (e.g., Verhoef and Srivastava, 1989; Sibuet and Collette, 1991; Srivastava et al., 2000; Sibuet et al., 2007a). This discrepancy may be a result of either the inability to properly identify the M0 anomaly on the Newfoundland margin, which has been used to place southern Flemish Cap conjugate to western Galicia Bank, or this model's inability to properly constrain motion of Flemish Cap, IB, and EU relative to North America.

4.7 Conclusions

Processing of two seismic reflection lines from the Erable survey has provided more extensive data coverage over the southern margin of Flemish Cap. Combining these data with SCREECH seismic profiles and two ODP drill sites have allowed the mapping of distinct zones of continental, transitional, and oceanic crust. These zones are compared to those on the conjugate Iberian margin to constrain the rifting and seafloor spreading processes.

Results show the presence of transitional crust (proposed to be exhumed subcontinental mantle) along the Central Grand Banks and the southwest margin of Flemish Cap that tapers to the northeast, so that no serpentinized mantle exists on the southeastern edge of Flemish Cap. The conjugate Iberian margin is characterized by a much wider zone of serpentinized exhumed mantle that narrows to the north moving into the Galicia Bank region. Also, the zone of extended continental crust on the Flemish Cap margin is much narrower than that on the Iberian Margin. The marked asymmetry of the Newfoundland and Iberian margins is likely a result of simple shear extension with a westward-dipping primary detachment, however both a simple shear model, and simple shear/pure shear combination model fit the data presented.

However, the Newfoundland Margin has a complex rifting history, and thus cannot be adequately described by two-dimensional rifting models only. The complexities involve the proposed rotation of Flemish Cap (Sibuet et al., 2007a), and possibly subsequent oblique shearing along the southern Flemish Cap margin (Todd and Reid, 1989). The plan-view rifting and break-up model presented in this paper attempts to account for the change in rifting and break-up processes throughout the Late Jurassic to Early Cretaceous that formed the south Flemish Cap margin.

Based on geochemical studies of ODP Site 1277 (Müntener and Manatschal, 2006) from the Newfoundland margin, and Sites 637 (Evans and Girardeau, 1988; Girardeau et al., 1988; Kornprobst and Tabit, 1988), 1068 and 1070 (Abe, 2001; Hébert et al., 2001) from the Iberian margin, it is proposed that the transitional region of the Newfoundland margin dominantly contains serpentinized exhumed subcontinental mantle formed during rifting. However, more drilling data is needed to constrain its composition with a high degree of confidence. It is possible that suboceanic mantle or melt products are present in some regions of transitional crust, and if present in large amounts would significantly reduce the region interpreted as being formed through rifting processes, and increase the region interpreted as being formed through seafloor spreading processes. This in turn would require modification of the model.

The model presented in this paper (Figure 4.12) leaves NA fixed. A rifting triple junction active during the Late Jurassic is proposed with three branches that extend into: 1) East Orphan Basin, 2) along the southern margin of Flemish Cap, and 3) into the (future) Flemish Pass Basin. In addition to extension, dextral strike slip motion occurs along all three branches, and accommodates rotation and southeast displacement of Flemish Cap and southeast translation of the IB plate with respect to NA. Thus, it is expected that the Flemish Pass Basin formed in a transtensional regime that accommodated movement and rotation of Flemish Cap (Sibuet et al., 2007a).

A new major triple junction forms between NA, IB, and EU, as rotation of Iberia and northeast translation of EU creates additional rifted crust. Breakup occurs along the Central Grand Banks during M3, progressing along the southern margin of Flemish Cap possibly through oblique shear mechanisms, and into the Bay of Biscay by M0 time. Finally, breakup occurs along the northeast edge of Flemish Cap during C34. At the M0 stage of the model, the southern margin of Flemish Cap is conjugate to the northern margin of Galicia Bank. It is uncertain whether this accurately represents plate positioning at the time since detailed geometries of crustal boundaries along the Iberian and European margins have not been taken into account for this model.

4.8 Recommendation for Future Work

New seismic surveys and processing of older seismic reflection data has provided coverage along transitional crust in the Newfoundland Basin, however seismic coverage remains sparse. Similarly, only one drilling site has penetrated basement within the transitional region. We recommend acquiring additional 2-D, or possibly 3-D seismic reflection data, and wide-angle reflection/refraction data to provide more extensive data coverage. Acquiring these data using longer offsets would make multiple removal more successful and allow well-constrained pre-stack depth migration thus improving the quality of data. We propose that the transitional region southwest of ER56 is formed through exhumed serpentinized mantle, and northeast of ER54 is formed through ultra-slow to slow seafloor spreading. Thus, we suggest the most critical location for acquiring new seismic data is between the ER56 and ER54 profiles. This would provide more detailed imaging to help determine how rifting and seafloor-spreading processes change within this area.

Drilling additional locations in both the flat (T1) and high relief (T2) transitional crust can provide information to confirm its composition, formation, and determine whether this zone is fairly homogeneous, or contains various rock types (thinned continental crust/serpentinized mantle/ocean crust).

Another recommendation is to do further work with modeling the complete rifting and break-up history of the Flemish Cap area, that incorporates and properly constrains the rifting events and resulting crustal boundaries in the Orphan Basin, Iberian margin, and European margin.

References

Abe, N. (2001), Petrochemistry of serpentinized peridotite from the Iberia Abyssal Plain (ODP Leg 173): its character intermediate between suboceanic and sub-continental upper mantle, *Geological Society London Special Publications, 187*(1), 143-159.

Balkwill, H. R. and F. D. Legall (1989), Chapter 15: Whale basin, offshore Newfoundland, extension and salt diapirism, in *Extensional Tectonics and Stratigraphy of the North Atlantic Margins, AAPG Memoir*, vol. 46 , pp. 233-245, American Association of Petroleum Geologist and the Canadian Geological Foundation, Tulsa, OK.

Beslier, M. O., M. Ask, and G. Boillot (1993), Ocean: continent boundary in the Iberia Abyssal Plain from multichannel seismic data, *Tectonophysics, 218*, 383-393.

Beslier, M. O., R. B. Whitmarsh, P. J. Wallace, and J. Girardeau (Eds.) (2001), *Proceedings of the Ocean Drilling Program, Scientific Results, 173*, 31 pp., Ocean Drilling Program, College Station, TX.

Boillot, G., J. Girardeau, and J. Kornprobst (1988), Rifting of the Galicia margin: Crustal thinning and emplacement of mantle rocks on the seafloor, in *Proceedings of the Ocean Drilling Program, Scientific Results*, vol. 103, edited by G. Boillot, E. L. Winterer, and et al., pp. 741-756, Ocean Drilling Program, College Station, TX.

Boillot, G., M. Recq, E. L. Winterer, A. W. Meyer, J. Applegate, M. Baltuck, J. A. Bergen, M. C. Comas, T. A. Davies, and K. Dunham (1987), Tectonic denudation of the upper mantle along passive margins: a model based on drilling results (ODP leg 103, western Galicia margin, Spain), *Tectonophysics, 132*(4), 335-342.

Boillot, G. and E. L. Winterer (1988), Drilling on the Galicia margin: Retrospect and prospect, in *Proceedings of the Ocean Drilling Program, Scientific Results*, vol. 103, edited by G. Boillot, E. L. Winterer, and et al., pp. 809-828, Ocean Drilling Program, College Station, TX.

Brun, J. P. and M. O. Beslier (1996), Mantle exhumation at passive margins, *Earth and Planetary Science Letters, 142*(1-2), 161-173.

Christensen, N. I. and W. D. Mooney (1995), Seismic velocity structure and composition of the continental crust: A global view, *Journal of Geophysical Research, 100*, 9761-9788.

Concheryo, A. and S. W. J. Wise (2001), Jurassic calcareous nannofossils from prerift sediments drilled during ODP leg 173, Iberia Abyssal Plain, and their implications for rift tectonics, in *Proceedings of the Ocean Drilling Program,* *Scientific Results*, vol. 173, edited by M. O. Beslier, R. B. Whitmarsh, P. J. Wallace, and J. and Girardeau, pp. 1-24, Ocean Drilling Program, College Station, TX.

Coward, M. P. (1986), Heterogeneous stretching, simple shear and basin development, *Earth and Planetary Science Letters, 80*(3-4), 325-336.

de Graciansky, P. C. and C. W. Poag (1985), Geologic history of Goban Spur, Northwest Europe continental margin, *Initial Reports of the Deep Sea Drilling Project, 80*, 1187-1216.

de Graciansky, P. C., C. W. Poag, R. Cunningham, P. Loubere, D. G. Masson, J. M. Mazzullo, L. Montadert, C. Mueller, K. Otsuka, and L. A. Reynolds (1985), The Goban Spur transect; geologic evolution of a sediment-starved passive continental margin, *Bulletin of the Geological Society of America, 96*(1), 58-76.

Dean, S. M., T. A. Minshull, R. B. Whitmarsh, and K. E. Louden (2000), Deep structure of the ocean-continent transition in the southern Iberia Abyssal Plain from seismic refraction profiles: The IAM-9 transect at 40 20'N, *Journal of Geophysical Research, 105*, 5859-5886.

Dinarès-Turell, J. and J. García-Senz (2000), Remagnetization of lower cretaceous limestones from the southern Pyrenees and relation to the Iberian plate geodynamic evolution, *Journal of Geophysical Research, 105*(B8), 19,405-19,418.

Duncan, R. A. (1984), Age Progressive Volcanism in the New England Seamounts and the opening of the Central Atlantic Ocean, *Journal of Geophysical Research, 89*, 9980-9990.

Dyment, J., J. Arkani-Hamed, and A. Ghods (1997), Contribution of serpentinized ultramafics to marine magnetic anomalies at slow and intermediate spreading centres: insights from the shape of the anomalies, *Geophysical Journal International, 129*, 691-701.

Eisbacher, G. H. (1969), Displacement and stress field along part of the Cobequid Fault, Nova Scotia, *Canadian Journal of Earth Sciences, 6*, 1095-1104.

Enachescu, M. (1987), Tectonic and structural framework of the northeast Newfoundland continental margin, *Sedimentary Basins and Basin-Forming Mechanisms, Canadian Society of Petroleum Geologists, Memoir, 12*, 117-146.

Enachescu, M. (1988), Extended basement beneath the intracratonic rifted basins of the Grand Banks of Newfoundland, *Canadian Journal of Exploration Geophysics, 24*(1), 48-65.

Enachescu, M., J. Hogg, and K. Meyer (2004a), East Orphan Basin, offshore Newfoundland and Labrador: a deep water super extended rift with potential petroleum system, CSPG Annual Convention, expanded abstracts.

Enachescu, M., S. Kearsey, J. Hogg, P. Einarsson, S. Nader, and J. Smee (2004b), Orphan Basin, offshore Newfoundland, Canada: structural and tectonic framework, petroleum systems and exploration potential, 74th SEG Annual Meeting and Exposition, expanded abstract.

Enachescu, M., K. Meyer, and J. Hogg (2004c), East Orphan Basin: structural setting and evolution with seismic and potential fields arguments, CSEG Annual Convention, expanded abstracts.

Enachescu, M. E. (1992), Enigmatic basins offshore Newfoundland, *Canadian Journal of Exploration Geophysics, 28*(1), 44-61.

Enachescu, M. E., S. Kearsey, V. Hardy, J. Sibuet, J. Hogg, S. A. Srivastava, A. Fagan, T. Thompson, and R. Ferguson (2005), Evolution and petroleum potential of Orphan Basin, offshore Newfoundlnad, and its relation to the movement and rotation of Flemish Cap based on plate kinematics of the North Atlantic, 25th Annual Bob F. Perkins Research Conference: Petroleum Systems of Divergent Continental Margin Basins.

Escartin, J., G. Hirth, and B. Evans (2001), Strength of slightly serpentinized peridotites: Implications for the tectonics of oceanic lithosphere, *Geology, 29*(11), 1023-1026.

Etheridge, M. A., P. A. Symonds, and G. S. Lister (1989), Application of the detachment model to reconstruction of conjugate passive margins, *Extension Tectonics and Stratigraphy of the North Atlantic Margins*, 23-40.

Evans, C. A. and J. Girardeau (1988), Galicia margin peridotites: Undepleted abyssal peridotites from the North Atlantic, in *Proceedings of the Ocean Drilling Program, Scientific Results*, vol. 103, edited by G. Boillot, E. L. Winterer, and et al., pp. 195-207, Ocean Drilling Program, College Station, TX.

Foster, D. J. and C. C. Mosher (1992), Suppression of multiple reflections using the Radon transform, *Geophysics, 57*, 386-395.

Fowler, C. M. R. (2005), *The Solid Earth: An Introduction to Global Geophysics*, The Solid Earth: An Introduction to Global Geophysics, 2nd ed., 685-3 pp., Cambridge University Press.

Funck, T., J. R. Hopper, H. C. Larsen, K. E. Louden, B. E. Tucholke, and W. S. Holbrook (2003), Crustal structure of the ocean-continent transition at Flemish Cap:

Seismic refraction results, *Journal of Geophysical Research, 108*(B11), EPM 10-1-EPM 10-20, doi: 10.1029/2003JB002434.

Funck, T., H. R. Jackson, K. E. Louden, S. A. Dehler, and Y. Wu (2004), Crustal structure of the northern Nova Scotia rifted continental margin (Eastern Canada), *Journal of Geophysical Research, 109*, B09102, doi: 10.1029/2004JB003008.

Girardeau, J., C. A. Evans, and M. O. Beslier (1988), Structural analysis of plagioclase-bearing peridotites emplaced at the end of continental rifting: Hole 637A, ODP leg 103 on the Galicia margin, in *Proceedings of the Ocean Drilling Program, Scientific Results*, vol. 103, edited by G. Boillot, E. L. Winterer, and et al., pp. 209-223, Ocean Drilling Program, College Station, TX.

Gradstein, F. M. and J. G. Ogg (2004), Geologic Time Scale 2004–why, how, and where next!, *Lethaia, 37*(2), 175-181.

Grant, A. C. (1973), Geological and geophysical results bearing upon the structural history of the Flemish Cap region; Earth Science Symposium on Offshore Eastern Canada, *Paper - Geological Survey of Canada, 71-23*, 373-387.

Grant, A. C. and K. D. McAlpine (1990), Chapter 6: The continental margin around Newfoundland, in *Geology of the Continental Margin of Eastern Canada*, edited by M. J. Keen and G. L. Williams, pp. 239-292, Geological Survey of Canada, Canada.

Hart, S. R. and J. Blusztajn (2006), Age and geochemistry of the mafic sills, ODP site 1276, Newfoundland margin, *Chemical Geology, 235*, 222-237.

Haworth, R. and C. E. Keen (1979), The Canadian Atlantic margin: a passive continental margin encompassing an active past, *Tectonophysics, 59*, 83-126.

Haworth, R. T. and J. B. MacIntyre (1975), The gravity and magnetic fields of Atlantic offshore Canada, *Geological Survey of Canada, 16*, 1-22.

Hébert, R., K. Gueddari, M. R. LaFleche, M. O. Beslier, and V. Gardien (2001), Petrology and geochemistry of exhumed peridotites and gabbros at non-volcanic margins: ODP Leg 173 West Iberia ocena-continent transition zone, *Geological Society London Special Publications, 187*(1), 161-189.

Hopper, J. R., T. Funck, B. E. Tucholke, H. C. Larsen, W. S. Holbrook, K. E. Louden, D. Shillington, and H. Lau (2004), Continental breakup and the onset of ultraslow seafloor spreading off Flemish Cap on the Newfoundland rifted margin, *Geology, 32*(1), 93-96.

Hopper, J. R., T. Funck, B. E. Tucholke, K. E. Louden, W. S. Holbrook, and H. Christian Larsen (2006), A deep seismic investigation of the Flemish Cap margin: implications for the origin of deep reflectivity and evidence for asymmetric break-up between Newfoundland and Iberia, *Geophysical Journal International, 164*(3), 501-515.

Karner, G. D. and D. J. Shillington (2005), Basalt sills of the U reflector, Newfoundland Basin: A serendipitous dating technique, *Geology, 33*(12), 985-988.

Keen, C., C. Peddy, B. de Voogd, and D. Matthews (1989), Conjugate margins of Canada and Europe: results from deep reflection profiling, *Geology, 17*, 173-176.

Keen, C. E. and D. L. Barrett (1981), Thinned and subsided continental crust on the rifted margin of eastern Canada: crustal structure, thermal evolution and subsidence history, *Geophysical Journal of the Royal Astronomical Society, 65*, 443-465.

Keen, C. E. and B. de Voogd (1988), The continent-ocean boundary at the rifted margin off eastern Canada: New results from deep seismic reflection studies, *Tectonics, 7*, 107-124.

Kent, D. V. and F. M. Gradstein (1986), A jurassic to recent chronology, in *The Western North Atlantic Region, the Geology of the North America*, vol. M, pp. 45-50, Geological Society of America, Boulder, CO.

King, L. H., G. B. Fader, W. H. Poole, and R. K. Wanless (1985), Geological setting and age of the Flemish Cap granodiorite, east of the Grand Banks of Newfoundland, *Canadian Journal of Earth Sciences, 22*, 1286-1298.

King, L. H., G. B. J. Fader, W. A. M. Jenkins, and E. L. King (1986), Occurrence and regional geological setting of Paleozoic rocks on the Grand Banks of Newfoundland, *Canadian Journal of Earth Sciences, 23*, 504-526.

Kornprobst, J. and A. Tabit (1988), Plagioclase-bearing ultramafic tectonites from the Galicia margin (leg 103, site 637): Comparison of their origin and evolution with low-pressure ultramafic bodies in western europe, in *Proceedings of the Ocean Drilling Program, Scientific Results,* vol. 103, edited by G. Boillot, E. L. Winterer, and et al., pp. 253-268, Ocean Drilling Program, College Station, TX.

Krawczyk, C. M., T. J. Reston, M. O. Beslier, and G. Boillot (1996), Evidence for detachment tectonics on the Iberia Abyssal Plain rifted margin, vol. 149, pp. 603-615, Ocean Drilling Program, College Station, TX.

Kusznir, N. J. and S. S. Egan (1989), Simple-shear and pure-shear models of extensional sedimentary basin formation: application to the Jeanne d'Arc Basin, Grand Banks of Newfoundland, *Extensional Tectonics and Stratigraphy of the North Atlantic Margins, American Association of Petroleum Geologists Memoirs, 46*, 305-322.

Larner, K., R. Chambers, M. Yang, W. Lynn, and W. Wai (1983), Coherent noise in marine seismic data, *Geophysics, 48*, 854-886.

Lau, K. W. H., K. E. Louden, S. Deemer, J. Hall, J. R. Hopper, B. E. Tucholke, W. S. Holbrook, and H. C. Larsen (2006), Crustal structure across the Grand Banks-Newfoundland Basin continental margin—II. Results from a seismic reflection profile, *Geophysical Journal International, 167*(1), 127-156.

Lau, K. W. H., K. E. Louden, T. Funck, B. E. Tucholke, W. S. Holbrook, J. R. Hopper, and H. C. Larsen (2006), Crustal structure across the Grand Banks–Newfoundland Basin Continental Margin–I. Results from a seismic refraction profile, *Geophysical Journal International, 167*(1), 157-170.

Le Pichon, X., J. Bonnin, and J. C. Sibuet (1970), La faille nord-pyrénéenne: Faille transformante liée al'ouverture du golfe de Gascogne, *CR Acad. Sci. Paris, 271*(1941), 1944.

Lister, G. S. and G. A. Davis (1989), The origin of metamorphic core complexes and detachment faults formed during Tertiary continental extension in the northern Colorado River region, U. S. A., *Journal of Structural Geology, 11*, 65-94.

Lister, G. S., M. A. Etheridge, and P. A. Symonds (1991), Detachment models for the formation of passive continental margins, *Tectonics, 10*, 1038-1064.

Lister, G. S., M. A. Etheridge, and P. A. Symonds (1986), Detachment faulting and the evolution of passive continental margins, *Geology, 14*, 246-250.

Masson, D. G. and P. R. Miles (1984), Mesozoic seafloor spreading between Iberia, Europe and North America, *Marine Geology, 56*(1-4), 279-287.

McKenzie, D. (1978), Some remarks on the development of sedimentary basins, *Earth and Planetary Science Letters, 40*, 25-32.

Müntener, O. and G. Manatschal (2006), High degrees of melt extraction recorded by spinel harzburgite of the Newfoundland margin: The role of inheritance and consequences for the evolution of the southern North Atlantic, *Earth and Planetary Science Letters, 252*(3-4), 437-452.

Nazarova, K. A. (1994), Serpentinized peridotites as a possible source for oceanic magnetic anomalies, *Marine Geophysical Researches, 16*(6), 455-462.

Oakey, G. N. and S. A. Delher (2004), Atlantic Canada Magnetic Map Series: Grand Banks and surrounds, *1:1 500 000.*

Olivet, J. L. (1996), La cinématique de la plaque IbériqueKinematics of the Iberian plate, *Bulletin des centres de recherches, exploration-production Elf, Aquitaine, 20*(1), 131-195.

Oufi, O., M. Cannat, and H. Horen (2002), Magnetic properties of variably serpentinized abyssal peridotites, *Journal of Geophysical Research, 107*, 1-17.

Pickup, S. L. B., R. B. Whitmarsh, C. M. R. Fowler, and T. J. Reston (1996), Insight into the nature of the ocean-continent transition off West Iberia from a deep multichannel seismic reflection profile, *Geology, 24*, 1079-1082.

Pinheiro, L. M., R. C. L. Wilson, R. P. dos Reis, R. B. Whitmarsh, and A. Ribeiro (1996), The western Iberia margin: A geophysical and geological overview, in *Proceedings of the Ocean Drilling Program, Scientific Results,* vol. 149, edited by R. B. Whitmarsh, D. S. Sawyer, A. Kalus, and D. G. Masson, pp. 3-23, Ocean Drilling Program, College Station, TX.

Reid, I. and C. E. Keen (1988), Upper crustal structure derived from seismic refraction experiments: Grand Banks of Eastern Canada, *Bulletin of Canadian Petroleum Geology, 36*, 388-396.

Reid, I. D. (1994), Crustal structure of a nonvolcanic rifted margin east of Newfoundland, *Journal of Geophysical Research, 99*(B8), 15161-15180.

Reid, I. D. and C. E. Keen (1990), High seismic velocities associated with reflections from within the lower oceanic crust near the continental margin of eastern Canada, *Earth and Planetary Science Letters, 99*, 118-126.

Reston, T. J. (1996), The S reflector west of Galicia: the seismic signature of a detachment fault, *Geophysical Journal International, 127*, 230-244.

Reston, T. J., C. M. Krawczyk, and D. Klaeschen (1996), The S reflector west of Galicia (Spain): Evidence from prestack depth migration for detachment faulting during continental breakup, *Journal of Geophysical Research, 101*, 8075-8092.

Roest, W. R. and S. P. Srivastava (1989), Sea-floor spreading in the Labrador Sea; a new reconstruction, *Geology, 17*(11), 1000-1003.

Schroeder, T., B. John, and B. R. Frost (2002), Geologic implications of seawater circulation through peridotite exposed at slow-spreading mid-ocean ridges, *Geology, 30*(4), 367-370.

Shillington, D. J., W. S. Holbrook, B. E. Tucholke, J. R. Hopper, K. E. Louden, H. C. Larsen, H. J. A. Van Avendonk, S. Deemer, and J. Hall (2004), Data report: Marine geophysical data on the Newfoundland nonvolcanic rifted margin around SCREECH transect 2, in *Proceedings of the Ocean Drilling Program, Initial Reports*, vol. 210, edited by B. E. Tucholke, J. C. Sibuet, A. Klaus, and et al., pp. 1-36, Ocean Drilling Program, College Station, TX.

Shillington, D. J., W. S. Holbrook, H. J. A. Van Avendonk, B. E. Tucholke, J. R. Hopper, K. E. Louden, H. C. Larsen, and G. T. Nunes (2006), Evidence for asymmetric nonvolcanic rifting and slow incipient oceanic accretion from seismic reflection data on the Newfoundland margin, *Journal of Geophysical Research, 111*(B9), B09402, doi: 10.1029/2005JB003981.

Shipboard Scientific Party (1987a), Introduction, objectives, and principal results: Ocean drilling program leg 103, west Galicia margin, in *Proceedings of the Ocean Drilling Program, Initial Reports*, vol. 103, edited by G. Boillot, E. L. Winterer, A. W. Meyer, and et al., pp. 3-17, Ocean Drilling Program, College Station, TX.

Shipboard Scientific Party (1987b), Site 637, in *Proceedings of the Ocean Drilling Program, Initial Reports,* vol. 103, edited by G. Boillot, E. L. Winterer, A. W. Meyer, and et al., pp. 123-219, Ocean Drilling Program, College Station, TX.

Shipboard Scientific Party (1998), Leg 173 introduction, in *Proceedings of the Ocean Drilling Program, Initial Reports,* vol. 173, edited by R. B. Whitmarsh, M. O. Beslier, P. J. Wallace, and et al., pp. 7-23, Ocean Drilling Program, College Station, TX.

Shipboard Scientific Party (2004a), Leg 210 summary, in *Proceedings of the Ocean Drilling Program, Initial Reports,* vol. 210, edited by B. E. Tucholke, J. C. Sibuet, A. Klaus, and et al., pp. 1-78, Ocean Drilling Program, College Station, TX.

Shipboard Scientific Party (2004b), Site 1277, in *Proceedings of the Ocean Drilling Program, Initial Reports,* vol. 210, edited by B. E. Tucholke, J. C. Sibuet, A. Klaus, and et al., pp. 1-39, Ocean Drilling Program, College Station, TX.

Sibuet, J. C. (1992), New constraints on the formation of the non-volcanic continental Galicia-Flemish Cap conjugate margins, *Journal of the Geological Society of London, 149*, 829-840.

Sibuet, J. C. and B. J. Collette (1991), Triple junctions of Bay of Biscay and North Atlantic; new constraints on the kinematic evolution, *Geology, 19*(5), 522-525.

Sibuet, J. C., S. Srivastava, M. Enachescu, and G. D. Karner (2007a), Early Cretaceous motion of Flemish Cap with respect to North America; implications on the formation of Orphan Basin and SE Flemish Cap-Galicia Bank conjugate margins; Imaging, mapping and modelling continental lithosphere extension and breakup, *Geological Society Special Publications, 282*, 63-76.

Sibuet, J. C., S. Srivastava, and G. Manatschal (2007b), Exhumed mantle-forming transitional crust in the Newfoundland-Iberia rift and associated magnetic anomalies, *Journal of Geophysical Research, 112*(B6), B06105, doi: 10.1029/2005JB003856.

Sibuet, J. C., S. P. Srivastava, M. E. Enachescu, and G. Karner (2005a), Lower cretataceous motion of the Flemish Cap in respect with North America: Implications for the formation of Orphan Basin and Flemish/Cap Galicia Bank conjugate margins, 6th Petroleum Geology Conference: North West Europe & Global Perspectives, NSF Intermargins workshop, Pontresina Conference.

Sibuet, J. C., S. P. Srivastava, and W. Spakman (2004), Pyrenean orogeny and plate kinematics, *Journal of Geophysical Research, 109*(B08104), 1-18, doi:10.1029/2003JB002514.

Skogseid, J., A. Barnwell, E. S. Aarseth, P. C. Alsgaard, H. C. Briseid, and C. Zwach (2004), Orphan Basin: multiple failed rifting during early opening of the North Atlantic., American Geophysical Union, Spring Meeting 2004, abstract T41B-03.

Srivastava, S. and C. R. Tapscott (1986), Plate kinematics of the North Atlantic, in *The Western North Atlantic Region, the Geology of the North America, Vol. M*, vol. M, edited by P. R. Vogt and B. E. Tucholke, pp. 379-404, Geological Society America, Boulder, CO.

Srivastava, S. P. and C. E. Keen (1995), A deep seismic reflection profile across the extinct Mid-Labrador Sea spreading center, *Tectonics, 14*, 372-389.

Srivastava, S. P., J. C. Sibuet, S. Cande, W. R. Roest, and I. D. Reid (2000), Magnetic evidence for slow seafloor spreading during the formation of the Newfoundland and Iberian margins, *Earth and Planetary Science Letters, 182*, 61-76.

Tankard, A. J. and H. J. Welsink (1989), Chapter 12: Mesozoic extension and styles of basin formation in Atlantic Canada, in *Extensional Tectonics and Stratigraphy of the North Atlantic Margins, AAPG Memoir*, vol. 46, edited by A. J. Tankard and H. R. Balkwill, pp. 175-195, American Association of Petroleum Geologist and the Canadian Geological Foundation, Tulsa, OK.

Todd, B. J. and I. Reid (1989), The continent-ocean boundary south of Flemish Cap: constraints from seismic refraction and gravity, *Canadian Journal of Earth Sciences, 26*(7), 1392-1407.

Todd, B. J., I. Reid, and C. E. Keen (1988), Crustal structure across the Southwest Newfoundland transform margin, *Canadian Journal of Earth Sciences, 25*, 744-759.

Todd, B. J., I. Reid, and C. E. Keen (1988), Crustal structure across the Southwest Newfoundland Transform Margin, *Canadian Journal of Earth Sciences, 25*(5), 744-759.

Tucholke, B. E., J. A. Austin, and E. Uchupi (1989), Chapter 16: Crustal structure and rift-drift evolution of the Newfoundland basin, in *Extensional Tectonics and Stratigraphy of the North Atlantic Margins, AAPG Memoir*, vol. 46, edited by A. J. Tankard and H. R. Balkwill, pp. 247-263, American Association of Petroleum Geologist and the Canadian Geological Foundation, Tulsa, OK.

Tucholke, B. E., D. S. Sawyer, and J. C. Sibuet (2006), Breakup of the Newfoundland-Iberia rift, *Extensional Deformation of the Lithosphere*.

Tucholke, B. E., D. S. Sawyer, and J. C. Sibuet (2007), Breakup of the Newfoundland-Iberia rift; Imaging, mapping and modelling continental lithosphere extension and breakup, *Geological Society Special Publications, 282*, 9-46.

Tucholke, B. E. and J. C. Sibuet (2007), Leg 210 synthesis: Tectonic, magmatic, and sedimentary evolution of the Newfoundland-Iberia rift, in *Proceedings of the Ocean Drilling Program, Scientific Results*, vol. 210, edited by B. E. Tucholke, J. C. Sibuet, and A. Klaus, pp. 1-56, Ocean Drilling Program, College Station, TX.

Turner, J. P., B. R. Rosendahl, and P. G. Wilson (2003), Structure and evolution of an obliquely sheared continental margin: Rio Muni, West Africa, *Tectonophysics, 374*(1-2), 41-55.

Van Avendonk, H. J. A., W. S. Holbrook, G. T. Nunes, D. J. Shillington, B. E. Tucholke, K. E. Louden, H. C. Larsen, and J. R. Hopper (2006), Seismic velocity structure of the rifted margin of the eastern Grand Banks of Newfoundland, Canada, *Journal of Geophysical Research, 111*(B11), B11404, doi: 10.1029/2005JB004156.

Verhoef, J. and S. Srivastava (1989), Chapter 9: Correlation of sedimentary basins across the North Atlantic as obtained from gravity and magnetic data, and its relation to the early evolution of the North Atlantic, in *Extensional Tectonics and Stratigraphy of the North Atlantic Margins, AAPG Memoir*, vol. 46, edited by A. J. Tankard and H. R. Balkwill, pp. 131-147, American Association of Petroleum Geologist and the Canadian Geological Foundation, Tulsa, OK.

Weichart, H. F. (1973), Acoustic waves along oil-filled streamer cables, *Geophysical Prospecting*, 21(2), 281-295.

Wernicke, B. P. (1985), Uniform-sense normal simple shear of the continental lithosphere, *Canadian Journal of Earth Sciences, 22*, 108-125.

White, R. S., D. McKenzie, and R. K. O'Nions (1992), Oceanic crustal thickness from seismic measurements and rare earth element inversions, *Journal of Geophysical Research, 97*(B13), 19683-19715.

Whitmarsh, R. B., S. M. Dean, T. A. Minshull, and M. Tompkins (2000), Tectonic implications of exposure of lower continental crust beneath the Iberia Abyssal Plain, Northeast Atlantic Ocean: Geophysical evidence, *Tectonics, 19*, 919-942.

Whitmarsh, R. B., P. R. Miles, and A. Mauffret (1990), The ocean-continent boundary off the western continental margin of Iberia, I. Crustal structure at 40 30'N, *Geophysical Journal International, 103*, 509-531.

Whitmarsh, R. B. and P. J. Wallace (2001), The rift-to-drift development of the west Iberia nonvolcanic continental margin: A summary and review of the contribution of ocean drilling program leg 173, in *Proceedings of the Ocean Drilling Program, Scientific Results*, vol. 173, edited by M. O. Beslier, R. B. Whitmarsh, P. J. Wallace, and J. Girardeau, pp. 1-36, Ocean Drilling Program, College Station, TX.

Whitmarsh, R. B., R. S. White, S. J. Horsefield, J. C. Sibuet, M. Recq, and V. Louvel. (1996), The ocean-continent boundary off the western continental margin of Iberia: crustal structure west of Galicia Bank, *Journal of Geophysical Research, 101*, 28291-28314.

Williams, H. and R. D. Hatcher (1982), Suspect terranes and accretionary history of the Appalachian Orogen, *Geology, 10*, 530-536.

Winterer, E. L., J. S. Gee, and R. J. Van Waasbergen (1988), The source area for lower Cretaceous clastic sediments of the Galicia margin: Geology and tectonic and erosional history, in *Proceedings of the Ocean Drilling Program, Scientific Results*, vol. 103, pp. 697-732, Ocean Drilling Program, College Station, TX.

Yilmaz, O. (2001), *Seismic Data Analysis : Processing, Inversion, and Interpretation of Seismic Data*, vol. 1, 2nd ed., Society of Exploration Geophysicists, Tulsa, OK.

Yilmaz, Ö (1987), *Seismic Data Processing*, Society of Exploration Geophysicists, Tulsa, OK.

Appendices

Appendix 1: Velocity versus TWT models derived from Velocity-depth models from a refraction experiment collected by the GSC during the CSS Hudson Cruise 85-025. These models have been overlain onto the Erable Line 54 profile as illustrated in Plate 2f.

Refraction Line	TWT (s)	Velocity (km/s)
HU-1	0.0	1.5
	6.3	1.5
	6.3	2.0
	7.5	2.6
	7.5	4.5
	8.2	5.0
	8.2	7.0
	9.5	7.2
HU-2	0.0	1.5
	6.3	1.5
	6.3	2.0
	7.6	2.4
	7.6	4.5
	8.4	5.0
	8.4	7.2
	9.5	7.4
HU-6	0.0	1.5
	6.0	1.5
	6.0	2.0
	7.9	2.2
	7.9	4.0
	9.1	4.5
	9.1	7.9
	11.6	8.0
HU-9&10	0.0	1.5
	3.9	1.5
	3.9	2.0
	4.6	2.5
	4.6	6.0
	9.9	6.3
HU-11 (E&W)	0.0	1.5
	5.3	1.5
	5.3	2.0
	6.4	2.3
	6.4	4.5
	6.8	4.9
	6.8	5.9
	10.2	6.0
HU-18 E	0.0	1.5
	5.6	1.5
	5.6	2.0
	7.5	2.4
	7.5	4.5
	8.0	5.1
	8.0	7.1
	9.3	7.3
HU-18 W	0.0	1.5
	5.6	1.5
	5.6	2.0
	7.5	2.4
	7.5	4.5
	8.2	5.0
	8.2	7.1
	9.6	7.3

Appendix 2: Latitude and longitude points for Line 54 converted to UTM and corresponding station numbers assigned to each FFID. These points were then interpolated to assign a UTM and station number to every FFID for setting up the geometry. No latitude and longitude point was given for FFID 6114 which is the last FFID for the line, so the UTM and station number was extrapolated for this FFID.

FFID	Latitude	Longitude	Northing (UTM)	Easting (UTM)	Station No.
3174	47.51637	-44.02635	5263008.394	573305.82	1000
3276	47.42513	-44.08482	5252814.98	569023.03	570023
3378	47.33553	-44.1412	5242809.005	564880.706	1134904
3481	47.24123	-44.20183	5232280.631	560407.526	1695311
3582	47.1486	-44.25845	5221944.431	556220.152	2251531
3683	47.055	-44.3191	5211501.023	551712.584	2803244
3711	47.03098	-44.3333	5208822.476	550656.867	3353901
3787	46.97242	-44.36337	5202295.928	548424.996	3902326
3931	46.83981	-44.45295	5187508.292	541713.891	4444040
4002	46.7694	-44.49233	5179664.01	538761.615	4982801
4055	46.72018	-44.52433	5174179.35	536351.426	5519153
4074	46.70162	-44.52317	5172117.486	536452.569	6055605
4296	46.52508	-44.382	5152575.678	547398.451	6603004
4518	46.35088	-44.2449	5133310.891	558098.376	7161102
4670	46.2302	-44.14986	5119976.02	565554.682	7726657
4747	46.1673	-44.1035	5113026.54	569208.443	8295865
4823	46.109	-44.05321	5106593.94	573167.926	8869033
4940	46.0151	-43.98395	5096227.028	578653.561	9447687
5058	45.9328	-43.91927	5087148.952	583784.521	10031471
5272	45.78663	-43.80948	5071030.196	592538.243	10624010
5383	45.71358	-43.75017	5062984.626	597275.18	11221285
5495	45.63695	-43.69544	5054539.026	601673.538	11822958
5748	45.45622	-43.55475	5034648.545	613000.059	12435958
5780	45.43323	-43.53703	5032119.525	614432.015	13050390
5864	45.37187	-43.49211	5025367.666	618073.37	13668464
5946	45.31042	-43.44464	5018611.699	621922.289	14290386
6029	45.24438	-43.39543	5011350.8	625925.799	14916312
6113	45.17925	-43.3447	5004195.879	630055.45	15546367
6114			5004110.701	630104.6125	16176472

Appendix 3: FFID and corresponding UTM and station numbers used for geometry set up of Line 54.

FFID	Easting (UTM)	Northing (UTM)	Station No.	FFID	Easting (UTM)	Northing (UTM)	Station No.
3174	573305.82	5263008.394	1000	3223	571248.4013	5258111.558	1425
3175	573263.8319	5262908.459	1009	3224	571206.4131	5258011.622	1434
3176	573221.8437	5262808.523	1017	3225	571164.425	5257911.687	1442
3177	573179.8556	5262708.588	1026	3226	571122.4369	5257811.752	1451
3178	573137.8675	5262608.652	1035	3227	571080.4487	5257711.816	1460
3179	573095.8793	5262508.717	1043	3228	571038.4606	5257611.881	1468
3180	573053.8912	5262408.781	1052	3229	570996.4725	5257511.945	1477
3181	573011.903	5262308.846	1061	3230	570954.4843	5257412.01	1486
3182	572969.9149	5262208.911	1069	3231	570912.4962	5257312.074	1494
3183	572927.9268	5262108.975	1078	3232	570870.508	5257212.139	1503
3184	572885.9386	5262009.04	1087	3233	570828.5199	5257112.204	1512
3185	572843.9505	5261909.104	1095	3234	570786.5318	5257012.268	1520
3186	572801.9624	5261809.169	1104	3235	570744.5436	5256912.333	1529
3187	572759.9742	5261709.233	1113	3236	570702.5555	5256812.397	1538
3188	572717.9861	5261609.298	1121	3237	570660.5674	5256712.462	1546
3189	572675.9979	5261509.363	1130	3238	570618.5792	5256612.526	1555
3190	572634.0098	5261409.427	1139	3239	570576.5911	5256512.591	1564
3191	572592.0217	5261309.492	1147	3240	570534.6029	5256412.656	1572
3192	572550.0335	5261209.556	1156	3241	570492.6148	5256312.72	1581
3193	572508.0454	5261109.621	1165	3242	570450.6267	5256212.785	1590
3194	572466.0573	5261009.685	1173	3243	570408.6385	5256112.849	1598
3195	572424.0691	5260909.75	1182	3244	570366.6504	5256012.914	1607
3196	572382.081	5260809.815	1191	3245	570324.6623	5255912.978	1616
3197	572340.0928	5260709.879	1199	3246	570282.6741	5255813.043	1624
3198	572298.1047	5260609.944	1208	3247	570240.686	5255713.108	1633
3199	572256.1166	5260510.008	1217	3248	570198.6978	5255613.172	1642
3200	572214.1284	5260410.073	1225	3249	570156.7097	5255513.237	1650
3201	572172.1403	5260310.137	1234	3250	570114.7216	5255413.301	1659
3202	572130.1522	5260210.202	1243	3251	570072.7334	5255313.366	1668
3203	572088.164	5260110.266	1251	3252	570030.7453	5255213.43	1676
3204	572046.1759	5260010.331	1260	3253	569988.7572	5255113.495	1685
3205	572004.1877	5259910.396	1269	3254	569946.769	5255013.559	1694
3206	571962.1996	5259810.46	1277	3255	569904.7809	5254913.624	1702
3207	571920.2115	5259710.525	1286	3256	569862.7927	5254813.689	1711
3208	571878.2233	5259610.589	1295	3257	569820.8046	5254713.753	1720
3209	571836.2352	5259510.654	1304	3258	569778.8165	5254613.818	1728
3210	571794.2471	5259410.718	1312	3259	569736.8283	5254513.882	1737
3211	571752.2589	5259310.783	1321	3260	569694.8402	5254413.947	1746
3212	571710.2708	5259210.848	1330	3261	569652.8521	5254314.011	1754
3213	571668.2826	5259110.912	1338	3262	569610.8639	5254214.076	1763
3214	571626.2945	5259010.977	1347	3263	569568.8758	5254114.141	1772
3215	571584.3064	5258911.041	1356	3264	569526.8876	5254014.205	1780
3216	571542.3182	5258811.106	1364	3265	569484.8995	5253914.27	1789
3217	571500.3301	5258711.17	1373	3266	569442.9114	5253814.334	1798
3218	571458.342	5258611.235	1382	3267	569400.9232	5253714.399	1806
3219	571416.3538	5258511.3	1390	3268	569358.9351	5253614.463	1815
3220	571374.3657	5258411.364	1399	3269	569316.947	5253514.528	1824
3221	571332.3775	5258311.429	1408	3270	569274.9588	5253414.593	1832
3222	571290.3894	5258211.493	1416	3271	569232.9707	5253314.657	1841

3272	569190.9825	5253214.722	1850	3328	566911.257	5247713.895	2326
3273	569148.9944	5253114.786	1859	3329	566870.646	5247615.797	2335
3274	569107.0063	5253014.851	1867	3330	566830.0349	5247517.699	2343
3275	569065.0181	5252914.915	1876	3331	566789.4239	5247419.601	2352
3276	569023.03	5252814.98	1885	3332	566748.8129	5247321.504	2360
3277	568982.419	5252716.882	1893	3333	566708.2019	5247223.406	2369
3278	568941.808	5252618.784	1902	3334	566667.5909	5247125.308	2377
3279	568901.1969	5252520.687	1910	3335	566626.9798	5247027.21	2386
3280	568860.5859	5252422.589	1919	3336	566586.3688	5246929.112	2394
3281	568819.9749	5252324.491	1927	3337	566545.7578	5246831.015	2403
3282	568779.3639	5252226.393	1935	3338	566505.1468	5246732.917	2411
3283	568738.7529	5252128.295	1944	3339	566464.5358	5246634.819	2420
3284	568698.1418	5252030.198	1952	3340	566423.9247	5246536.721	2428
3285	568657.5308	5251932.1	1961	3341	566383.3137	5246438.623	2437
3286	568616.9198	5251834.002	1969	3342	566342.7027	5246340.526	2445
3287	568576.3088	5251735.904	1978	3343	566302.0917	5246242.428	2454
3288	568535.6978	5251637.806	1986	3344	566261.4807	5246144.33	2462
3289	568495.0867	5251539.709	1995	3345	566220.8696	5246046.232	2471
3290	568454.4757	5251441.611	2003	3346	566180.2586	5245948.134	2479
3291	568413.8647	5251343.513	2012	3347	566139.6476	5245850.037	2488
3292	568373.2537	5251245.415	2020	3348	566099.0366	5245751.939	2496
3293	568332.6427	5251147.318	2029	3349	566058.4256	5245653.841	2505
3294	568292.0316	5251049.22	2037	3350	566017.8145	5245555.743	2513
3295	568251.4206	5250951.122	2046	3351	565977.2035	5245457.645	2522
3296	568210.8096	5250853.024	2054	3352	565936.5925	5245359.548	2530
3297	568170.1986	5250754.926	2063	3353	565895.9815	5245261.45	2539
3298	568129.5876	5250656.829	2071	3354	565855.3705	5245163.352	2547
3299	568088.9765	5250558.731	2080	3355	565814.7595	5245065.254	2556
3300	568048.3655	5250460.633	2088	3356	565774.1484	5244967.156	2564
3301	568007.7545	5250362.535	2097	3357	565733.5374	5244869.059	2573
3302	567967.1435	5250264.437	2105	3358	565692.9264	5244770.961	2581
3303	567926.5325	5250166.34	2114	3359	565652.3154	5244672.863	2590
3304	567885.9215	5250068.242	2122	3360	565611.7044	5244574.765	2598
3305	567845.3104	5249970.144	2131	3361	565571.0933	5244476.668	2606
3306	567804.6994	5249872.046	2139	3362	565530.4823	5244378.57	2615
3307	567764.0884	5249773.948	2148	3363	565489.8713	5244280.472	2623
3308	567723.4774	5249675.851	2156	3364	565449.2603	5244182.374	2632
3309	567682.8664	5249577.753	2165	3365	565408.6493	5244084.276	2640
3310	567642.2553	5249479.655	2173	3366	565368.0382	5243986.179	2649
3311	567601.6443	5249381.557	2182	3367	565327.4272	5243888.081	2657
3312	567561.0333	5249283.459	2190	3368	565286.8162	5243789.983	2666
3313	567520.4223	5249185.362	2199	3369	565246.2052	5243691.885	2674
3314	567479.8113	5249087.264	2207	3370	565205.5942	5243593.787	2683
3315	567439.2002	5248989.166	2216	3371	565164.9831	5243495.69	2691
3316	567398.5892	5248891.068	2224	3372	565124.3721	5243397.592	2700
3317	567357.9782	5248792.97	2233	3373	565083.7611	5243299.494	2708
3318	567317.3672	5248694.873	2241	3374	565043.1501	5243201.396	2717
3319	567276.7562	5248596.775	2250	3375	565002.5391	5243103.298	2725
3320	567236.1451	5248498.677	2258	3376	564961.928	5243005.201	2734
3321	567195.5341	5248400.579	2267	3377	564921.317	5242907.103	2742
3322	567154.9231	5248302.481	2275	3378	564880.706	5242809.005	2751
3323	567114.3121	5248204.384	2284	3379	564837.2771	5242706.788	2760
3324	567073.7011	5248106.286	2292	3380	564793.8481	5242604.571	2769
3325	567033.09	5248008.188	2301	3381	564750.4192	5242502.353	2778
3326	566992.479	5247910.09	2309	3382	564706.9903	5242400.136	2786
3327	566951.868	5247811.993	2318	3383	564663.5613	5242297.919	2795

3384	564620.1324	5242195.702	2804
3385	564576.7035	5242093.484	2813
3386	564533.2745	5241991.267	2822
3387	564489.8456	5241889.05	2831
3388	564446.4167	5241786.833	2840
3389	564402.9877	5241684.616	2849
3390	564359.5588	5241582.398	2858
3391	564316.1299	5241480.181	2866
3392	564272.701	5241377.964	2875
3393	564229.272	5241275.747	2884
3394	564185.8431	5241173.529	2893
3395	564142.4142	5241071.312	2902
3396	564098.9852	5240969.095	2911
3397	564055.5563	5240866.878	2920
3398	564012.1274	5240764.661	2929
3399	563968.6984	5240662.443	2937
3400	563925.2695	5240560.226	2946
3401	563881.8406	5240458.009	2955
3402	563838.4116	5240355.792	2964
3403	563794.9827	5240253.574	2973
3404	563751.5538	5240151.357	2982
3405	563708.1248	5240049.14	2991
3406	563664.6959	5239946.923	3000
3407	563621.267	5239844.706	3009
3408	563577.838	5239742.488	3017
3409	563534.4091	5239640.271	3026
3410	563490.9802	5239538.054	3035
3411	563447.5512	5239435.837	3044
3412	563404.1223	5239333.619	3053
3413	563360.6934	5239231.402	3062
3414	563317.2644	5239129.185	3071
3415	563273.8355	5239026.968	3080
3416	563230.4066	5238924.751	3089
3417	563186.9777	5238822.533	3097
3418	563143.5487	5238720.316	3106
3419	563100.1198	5238618.099	3115
3420	563056.6909	5238515.882	3124
3421	563013.2619	5238413.664	3133
3422	562969.833	5238311.447	3142
3423	562926.4041	5238209.23	3151
3424	562882.9751	5238107.013	3160
3425	562839.5462	5238004.796	3168
3426	562796.1173	5237902.578	3177
3427	562752.6883	5237800.361	3186
3428	562709.2594	5237698.144	3195
3429	562665.8305	5237595.927	3204
3430	562622.4015	5237493.709	3213
3431	562578.9726	5237391.492	3222
3432	562535.5437	5237289.275	3231
3433	562492.1147	5237187.058	3240
3434	562448.6858	5237084.84	3248
3435	562405.2569	5236982.623	3257
3436	562361.8279	5236880.406	3266
3437	562318.399	5236778.189	3275
3438	562274.9701	5236675.972	3284
3439	562231.5411	5236573.754	3293
3440	562188.1122	5236471.537	3302
3441	562144.6833	5236369.32	3311
3442	562101.2543	5236267.103	3320
3443	562057.8254	5236164.885	3328
3444	562014.3965	5236062.668	3337
3445	561970.9676	5235960.451	3346
3446	561927.5386	5235858.234	3355
3447	561884.1097	5235756.017	3364
3448	561840.6808	5235653.799	3373
3449	561797.2518	5235551.582	3382
3450	561753.8229	5235449.365	3391
3451	561710.394	5235347.148	3399
3452	561666.965	5235244.93	3408
3453	561623.5361	5235142.713	3417
3454	561580.1072	5235040.496	3426
3455	561536.6782	5234938.279	3435
3456	561493.2493	5234836.062	3444
3457	561449.8204	5234733.844	3453
3458	561406.3914	5234631.627	3462
3459	561362.9625	5234529.41	3471
3460	561319.5336	5234427.193	3479
3461	561276.1046	5234324.975	3488
3462	561232.6757	5234222.758	3497
3463	561189.2468	5234120.541	3506
3464	561145.8178	5234018.324	3515
3465	561102.3889	5233916.107	3524
3466	561058.96	5233813.889	3533
3467	561015.531	5233711.672	3542
3468	560972.1021	5233609.455	3551
3469	560928.6732	5233507.238	3559
3470	560885.2443	5233405.02	3568
3471	560841.8153	5233302.803	3577
3472	560798.3864	5233200.586	3586
3473	560754.9575	5233098.369	3595
3474	560711.5285	5232996.152	3604
3475	560668.0996	5232893.934	3613
3476	560624.6707	5232791.717	3622
3477	560581.2417	5232689.5	3630
3478	560537.8128	5232587.283	3639
3479	560494.3839	5232485.065	3648
3480	560450.9549	5232382.848	3657
3481	560407.526	5232280.631	3666
3482	560366.0669	5232178.292	3675
3483	560324.6077	5232075.954	3684
3484	560283.1486	5231973.615	3693
3485	560241.6894	5231871.277	3701
3486	560200.2303	5231768.938	3710
3487	560158.7711	5231666.599	3719
3488	560117.312	5231564.261	3728
3489	560075.8528	5231461.922	3737
3490	560034.3937	5231359.583	3746
3491	559992.9345	5231257.245	3754
3492	559951.4754	5231154.906	3763
3493	559910.0162	5231052.568	3772
3494	559868.5571	5230950.229	3781
3495	559827.0979	5230847.89	3790

3496	559785.6388	5230745.552	3799
3497	559744.1796	5230643.213	3807
3498	559702.7205	5230540.875	3816
3499	559661.2613	5230438.536	3825
3500	559619.8022	5230336.197	3834
3501	559578.343	5230233.859	3843
3502	559536.8839	5230131.52	3852
3503	559495.4247	5230029.181	3860
3504	559453.9656	5229926.843	3869
3505	559412.5064	5229824.504	3878
3506	559371.0473	5229722.166	3887
3507	559329.5881	5229619.827	3896
3508	559288.129	5229517.488	3905
3509	559246.6698	5229415.15	3913
3510	559205.2107	5229312.811	3922
3511	559163.7515	5229210.473	3931
3512	559122.2924	5229108.134	3940
3513	559080.8332	5229005.795	3949
3514	559039.3741	5228903.457	3958
3515	558997.915	5228801.118	3966
3516	558956.4558	5228698.78	3975
3517	558914.9967	5228596.441	3984
3518	558873.5375	5228494.102	3993
3519	558832.0784	5228391.764	4002
3520	558790.6192	5228289.425	4011
3521	558749.1601	5228187.086	4019
3522	558707.7009	5228084.748	4028
3523	558666.2418	5227982.409	4037
3524	558624.7826	5227880.071	4046
3525	558583.3235	5227777.732	4055
3526	558541.8643	5227675.393	4064
3527	558500.4052	5227573.055	4072
3528	558458.946	5227470.716	4081
3529	558417.4869	5227368.378	4090
3530	558376.0277	5227266.039	4099
3531	558334.5686	5227163.7	4108
3532	558293.1094	5227061.362	4117
3533	558251.6503	5226959.023	4125
3534	558210.1911	5226856.684	4134
3535	558168.732	5226754.346	4143
3536	558127.2728	5226652.007	4152
3537	558085.8137	5226549.669	4161
3538	558044.3545	5226447.33	4170
3539	558002.8954	5226344.991	4178
3540	557961.4362	5226242.653	4187
3541	557919.9771	5226140.314	4196
3542	557878.5179	5226037.976	4205
3543	557837.0588	5225935.637	4214
3544	557795.5996	5225833.298	4223
3545	557754.1405	5225730.96	4231
3546	557712.6813	5225628.621	4240
3547	557671.2222	5225526.282	4249
3548	557629.763	5225423.944	4258
3549	557588.3039	5225321.605	4267
3550	557546.8448	5225219.267	4276
3551	557505.3856	5225116.928	4284
3552	557463.9265	5225014.589	4293
3553	557422.4673	5224912.251	4302
3554	557381.0082	5224809.912	4311
3555	557339.549	5224707.574	4320
3556	557298.0899	5224605.235	4329
3557	557256.6307	5224502.896	4337
3558	557215.1716	5224400.558	4346
3559	557173.7124	5224298.219	4355
3560	557132.2533	5224195.881	4364
3561	557090.7941	5224093.542	4373
3562	557049.335	5223991.203	4382
3563	557007.8758	5223888.865	4390
3564	556966.4167	5223786.526	4399
3565	556924.9575	5223684.187	4408
3566	556883.4984	5223581.849	4417
3567	556842.0392	5223479.51	4426
3568	556800.5801	5223377.172	4435
3569	556759.1209	5223274.833	4443
3570	556717.6618	5223172.494	4452
3571	556676.2026	5223070.156	4461
3572	556634.7435	5222967.817	4470
3573	556593.2843	5222865.479	4479
3574	556551.8252	5222763.14	4488
3575	556510.366	5222660.801	4496
3576	556468.9069	5222558.463	4505
3577	556427.4477	5222456.124	4514
3578	556385.9886	5222353.785	4523
3579	556344.5294	5222251.447	4532
3580	556303.0703	5222149.108	4541
3581	556261.6111	5222046.77	4549
3582	556220.152	5221944.431	4558
3583	556175.5226	5221841.031	4567
3584	556130.8932	5221737.631	4576
3585	556086.2638	5221634.231	4585
3586	556041.6345	5221530.831	4594
3587	555997.0051	5221427.431	4603
3588	555952.3757	5221324.031	4612
3589	555907.7463	5221220.63	4621
3590	555863.1169	5221117.23	4630
3591	555818.4875	5221013.83	4639
3592	555773.8581	5220910.43	4648
3593	555729.2288	5220807.03	4657
3594	555684.5994	5220703.63	4666
3595	555639.97	5220600.23	4675
3596	555595.3406	5220496.83	4684
3597	555550.7112	5220393.43	4693
3598	555506.0818	5220290.03	4702
3599	555461.4524	5220186.63	4711
3600	555416.823	5220083.23	4720
3601	555372.1937	5219979.829	4729
3602	555327.5643	5219876.429	4738
3603	555282.9349	5219773.029	4747
3604	555238.3055	5219669.629	4756
3605	555193.6761	5219566.229	4765
3606	555149.0467	5219462.829	4774
3607	555104.4173	5219359.429	4783

3608	555059.788	5219256.029	4792	3664	552560.5423	5213465.625	5297
3609	555015.1586	5219152.629	4801	3665	552515.913	5213362.224	5306
3610	554970.5292	5219049.229	4810	3666	552471.2836	5213258.824	5315
3611	554925.8998	5218945.829	4819	3667	552426.6542	5213155.424	5324
3612	554881.2704	5218842.429	4828	3668	552382.0248	5213052.024	5333
3613	554836.641	5218739.029	4837	3669	552337.3954	5212948.624	5342
3614	554792.0116	5218635.628	4847	3670	552292.766	5212845.224	5351
3615	554747.3823	5218532.228	4856	3671	552248.1366	5212741.824	5360
3616	554702.7529	5218428.828	4865	3672	552203.5072	5212638.424	5369
3617	554658.1235	5218325.428	4874	3673	552158.8779	5212535.024	5378
3618	554613.4941	5218222.028	4883	3674	552114.2485	5212431.624	5387
3619	554568.8647	5218118.628	4892	3675	552069.6191	5212328.224	5396
3620	554524.2353	5218015.228	4901	3676	552024.9897	5212224.824	5405
3621	554479.6059	5217911.828	4910	3677	551980.3603	5212121.423	5414
3622	554434.9766	5217808.428	4919	3678	551935.7309	5212018.023	5423
3623	554390.3472	5217705.028	4928	3679	551891.1015	5211914.623	5432
3624	554345.7178	5217601.628	4937	3680	551846.4722	5211811.223	5441
3625	554301.0884	5217498.228	4946	3681	551801.8428	5211707.823	5450
3626	554256.459	5217394.828	4955	3682	551757.2134	5211604.423	5459
3627	554211.8296	5217291.427	4964	3683	551712.584	5211501.023	5468
3628	554167.2002	5217188.027	4973	3684	551674.8798	5211405.361	5476
3629	554122.5709	5217084.627	4982	3685	551637.1756	5211309.698	5485
3630	554077.9415	5216981.227	4991	3686	551599.4715	5211214.036	5493
3631	554033.3121	5216877.827	5000	3687	551561.7673	5211118.373	5501
3632	553988.6827	5216774.427	5009	3688	551524.0631	5211022.711	5509
3633	553944.0533	5216671.027	5018	3689	551486.3589	5210927.049	5518
3634	553899.4239	5216567.627	5027	3690	551448.6548	5210831.386	5526
3635	553854.7945	5216464.227	5036	3691	551410.9506	5210735.724	5534
3636	553810.1651	5216360.827	5045	3692	551373.2464	5210640.061	5542
3637	553765.5358	5216257.427	5054	3693	551335.5422	5210544.399	5550
3638	553720.9064	5216154.027	5063	3694	551297.838	5210448.737	5559
3639	553676.277	5216050.626	5072	3695	551260.1339	5210353.074	5567
3640	553631.6476	5215947.226	5081	3696	551222.4297	5210257.412	5575
3641	553587.0182	5215843.826	5090	3697	551184.7255	5210161.75	5583
3642	553542.3888	5215740.426	5099	3698	551147.0213	5210066.087	5592
3643	553497.7594	5215637.026	5108	3699	551109.3171	5209970.425	5600
3644	553453.1301	5215533.626	5117	3700	551071.613	5209874.762	5608
3645	553408.5007	5215430.226	5126	3701	551033.9088	5209779.1	5616
3646	553363.8713	5215326.826	5135	3702	550996.2046	5209683.438	5624
3647	553319.2419	5215223.426	5144	3703	550958.5004	5209587.775	5633
3648	553274.6125	5215120.026	5153	3704	550920.7962	5209492.113	5641
3649	553229.9831	5215016.626	5162	3705	550883.0921	5209396.45	5649
3650	553185.3537	5214913.226	5171	3706	550845.3879	5209300.788	5657
3651	553140.7244	5214809.826	5180	3707	550807.6837	5209205.126	5666
3652	553096.095	5214706.425	5189	3708	550769.9795	5209109.463	5674
3653	553051.4656	5214603.025	5198	3709	550732.2754	5209013.801	5682
3654	553006.8362	5214499.625	5207	3710	550694.5712	5208918.138	5690
3655	552962.2068	5214396.225	5216	3711	550656.867	5208822.476	5699
3656	552917.5774	5214292.825	5225	3713	550598.1336	5208650.725	5713
3657	552872.948	5214189.425	5234	3715	550539.4001	5208478.973	5728
3658	552828.3187	5214086.025	5243	3717	550480.6667	5208307.222	5742
3659	552783.6893	5213982.625	5252	3719	550421.9332	5208135.471	5757
3660	552739.0599	5213879.225	5261	3721	550363.1998	5207963.72	5771
3661	552694.4305	5213775.825	5270	3723	550304.4663	5207791.968	5786
3662	552649.8011	5213672.425	5279	3725	550245.7329	5207620.217	5800
3663	552605.1717	5213569.025	5288	3727	550186.9994	5207448.466	5815

3729	550128.266	5207276.715	5829	3814	547166.6638	5199523.246	6494
3731	550069.5325	5207104.963	5844	3815	547120.0589	5199420.554	6503
3733	550010.7991	5206933.212	5858	3816	547073.454	5199317.862	6512
3735	549952.0656	5206761.461	5873	3817	547026.8491	5199215.17	6521
3737	549893.3322	5206589.71	5887	3818	546980.2442	5199112.479	6530
3739	549834.5987	5206417.958	5902	3819	546933.6393	5199009.787	6539
3741	549775.8653	5206246.207	5916	3820	546887.0344	5198907.095	6548
3743	549717.1318	5206074.456	5931	3821	546840.4295	5198804.403	6557
3745	549658.3984	5205902.705	5945	3822	546793.8246	5198701.711	6566
3747	549599.6649	5205730.953	5960	3823	546747.2198	5198599.019	6575
3749	549540.9315	5205559.202	5974	3824	546700.6149	5198496.327	6584
3751	549482.1981	5205387.451	5989	3825	546654.01	5198393.635	6593
3753	549423.4646	5205215.699	6003	3826	546607.4051	5198290.943	6602
3755	549364.7312	5205043.948	6018	3827	546560.8002	5198188.251	6611
3757	549305.9977	5204872.197	6032	3828	546514.1953	5198085.559	6620
3759	549247.2643	5204700.446	6047	3829	546467.5904	5197982.867	6629
3761	549188.5308	5204528.694	6062	3830	546420.9855	5197880.176	6638
3763	549129.7974	5204356.943	6076	3831	546374.3806	5197777.484	6647
3765	549071.0639	5204185.192	6091	3832	546327.7757	5197674.792	6656
3767	549012.3305	5204013.441	6105	3833	546281.1708	5197572.1	6665
3769	548953.597	5203841.689	6120	3834	546234.5659	5197469.408	6674
3771	548894.8636	5203669.938	6134	3835	546187.961	5197366.716	6683
3773	548836.1301	5203498.187	6149	3836	546141.3561	5197264.024	6692
3775	548777.3967	5203326.436	6163	3837	546094.7512	5197161.332	6701
3777	548718.6632	5203154.684	6178	3838	546048.1463	5197058.64	6710
3779	548659.9298	5202982.933	6192	3839	546001.5414	5196955.948	6719
3781	548601.1963	5202811.182	6207	3840	545954.9365	5196853.256	6728
3783	548542.4629	5202639.431	6221	3841	545908.3316	5196750.564	6737
3785	548483.7294	5202467.679	6236	3842	545861.7267	5196647.873	6747
3787	548424.996	5202295.928	6250	3843	545815.1218	5196545.181	6756
3788	548378.3911	5202193.236	6259	3844	545768.5169	5196442.489	6765
3789	548331.7862	5202090.544	6268	3845	545721.912	5196339.797	6774
3790	548285.1813	5201987.852	6277	3846	545675.3071	5196237.105	6783
3791	548238.5764	5201885.16	6286	3847	545628.7023	5196134.413	6792
3792	548191.9715	5201782.468	6295	3848	545582.0974	5196031.721	6801
3793	548145.3666	5201679.777	6304	3849	545535.4925	5195929.029	6810
3794	548098.7617	5201577.085	6313	3850	545488.8876	5195826.337	6819
3795	548052.1568	5201474.393	6322	3851	545442.2827	5195723.645	6828
3796	548005.5519	5201371.701	6332	3852	545395.6778	5195620.953	6837
3797	547958.947	5201269.009	6341	3853	545349.0729	5195518.261	6846
3798	547912.3421	5201166.317	6350	3854	545302.468	5195415.57	6855
3799	547865.7373	5201063.625	6359	3855	545255.8631	5195312.878	6864
3800	547819.1324	5200960.933	6368	3856	545209.2582	5195210.186	6873
3801	547772.5275	5200858.241	6377	3857	545162.6533	5195107.494	6882
3802	547725.9226	5200755.549	6386	3858	545116.0484	5195004.802	6891
3803	547679.3177	5200652.857	6395	3859	545069.4435	5194902.11	6900
3804	547632.7128	5200550.165	6404	3860	545022.8386	5194799.418	6909
3805	547586.1079	5200447.474	6413	3861	544976.2337	5194696.726	6918
3806	547539.503	5200344.782	6422	3862	544929.6288	5194594.034	6927
3807	547492.8981	5200242.09	6431	3863	544883.0239	5194491.342	6936
3808	547446.2932	5200139.398	6440	3864	544836.419	5194388.65	6945
3809	547399.6883	5200036.706	6449	3865	544789.8141	5194285.958	6954
3810	547353.0834	5199934.014	6458	3866	544743.2092	5194183.267	6963
3811	547306.4785	5199831.322	6467	3867	544696.6043	5194080.575	6972
3812	547259.8736	5199728.63	6476	3868	544649.9994	5193977.883	6981
3813	547213.2687	5199625.938	6485	3869	544603.3945	5193875.191	6990

3870	544556.7896	5193772.499	6999	3926	541946.9155	5188021.752	7504
3871	544510.1848	5193669.807	7008	3927	541900.3106	5187919.06	7513
3872	544463.5799	5193567.115	7017	3928	541853.7057	5187816.368	7522
3873	544416.975	5193464.423	7026	3929	541807.1008	5187713.676	7531
3874	544370.3701	5193361.731	7035	3930	541760.4959	5187610.984	7540
3875	544323.7652	5193259.039	7044	3931	541713.891	5187508.292	7549
3876	544277.1603	5193156.347	7053	3932	541672.3096	5187397.809	7559
3877	544230.5554	5193053.655	7062	3933	541630.7283	5187287.326	7568
3878	544183.9505	5192950.964	7071	3934	541589.1469	5187176.843	7578
3879	544137.3456	5192848.272	7080	3935	541547.5656	5187066.361	7587
3880	544090.7407	5192745.58	7089	3936	541505.9842	5186955.878	7597
3881	544044.1358	5192642.888	7098	3937	541464.4029	5186845.395	7606
3882	543997.5309	5192540.196	7107	3938	541422.8215	5186734.912	7616
3883	543950.926	5192437.504	7116	3939	541381.2402	5186624.429	7625
3884	543904.3211	5192334.812	7125	3940	541339.6588	5186513.946	7634
3885	543857.7162	5192232.12	7134	3941	541298.0775	5186403.464	7644
3886	543811.1113	5192129.428	7143	3942	541256.4961	5186292.981	7653
3887	543764.5064	5192026.736	7152	3943	541214.9148	5186182.498	7663
3888	543717.9015	5191924.044	7162	3944	541173.3334	5186072.015	7672
3889	543671.2966	5191821.352	7171	3945	541131.7521	5185961.532	7682
3890	543624.6917	5191718.661	7180	3946	541090.1707	5185851.049	7691
3891	543578.0868	5191615.969	7189	3947	541048.5894	5185740.566	7701
3892	543531.4819	5191513.277	7198	3948	541007.008	5185630.084	7710
3893	543484.877	5191410.585	7207	3949	540965.4267	5185519.601	7719
3894	543438.2721	5191307.893	7216	3950	540923.8453	5185409.118	7729
3895	543391.6673	5191205.201	7225	3951	540882.264	5185298.635	7738
3896	543345.0624	5191102.509	7234	3952	540840.6826	5185188.152	7748
3897	543298.4575	5190999.817	7243	3953	540799.1013	5185077.669	7757
3898	543251.8526	5190897.125	7252	3954	540757.5199	5184967.187	7767
3899	543205.2477	5190794.433	7261	3955	540715.9385	5184856.704	7776
3900	543158.6428	5190691.741	7270	3956	540674.3572	5184746.221	7786
3901	543112.0379	5190589.049	7279	3957	540632.7758	5184635.738	7795
3902	543065.433	5190486.358	7288	3958	540591.1945	5184525.255	7804
3903	543018.8281	5190383.666	7297	3959	540549.6131	5184414.772	7814
3904	542972.2232	5190280.974	7306	3960	540508.0318	5184304.289	7823
3905	542925.6183	5190178.282	7315	3961	540466.4504	5184193.807	7833
3906	542879.0134	5190075.59	7324	3962	540424.8691	5184083.324	7842
3907	542832.4085	5189972.898	7333	3963	540383.2877	5183972.841	7852
3908	542785.8036	5189870.206	7342	3964	540341.7064	5183862.358	7861
3909	542739.1987	5189767.514	7351	3965	540300.125	5183751.875	7871
3910	542692.5938	5189664.822	7360	3966	540258.5437	5183641.392	7880
3911	542645.9889	5189562.13	7369	3967	540216.9623	5183530.91	7889
3912	542599.384	5189459.438	7378	3968	540175.381	5183420.427	7899
3913	542552.7791	5189356.746	7387	3969	540133.7996	5183309.944	7908
3914	542506.1742	5189254.055	7396	3970	540092.2183	5183199.461	7918
3915	542459.5693	5189151.363	7405	3971	540050.6369	5183088.978	7927
3916	542412.9644	5189048.671	7414	3972	540009.0556	5182978.495	7937
3917	542366.3595	5188945.979	7423	3973	539967.4742	5182868.013	7946
3918	542319.7546	5188843.287	7432	3974	539925.8929	5182757.53	7956
3919	542273.1498	5188740.595	7441	3975	539884.3115	5182647.047	7965
3920	542226.5449	5188637.903	7450	3976	539842.7302	5182536.564	7974
3921	542179.94	5188535.211	7459	3977	539801.1488	5182426.081	7984
3922	542133.3351	5188432.519	7468	3978	539759.5675	5182315.598	7993
3923	542086.7302	5188329.827	7477	3979	539717.9861	5182205.115	8003
3924	542040.1253	5188227.135	7486	3980	539676.4047	5182094.633	8012
3925	541993.5204	5188124.443	7495	3981	539634.8234	5181984.15	8022

3982	539593.242	5181873.667	8031
3983	539551.6607	5181763.184	8041
3984	539510.0793	5181652.701	8050
3985	539468.498	5181542.218	8059
3986	539426.9166	5181431.736	8069
3987	539385.3353	5181321.253	8078
3988	539343.7539	5181210.77	8088
3989	539302.1726	5181100.287	8097
3990	539260.5912	5180989.804	8107
3991	539219.0099	5180879.321	8116
3992	539177.4285	5180768.838	8126
3993	539135.8472	5180658.356	8135
3994	539094.2658	5180547.873	8144
3995	539052.6845	5180437.39	8154
3996	539011.1031	5180326.907	8163
3997	538969.5218	5180216.424	8173
3998	538927.9404	5180105.941	8182
3999	538886.3591	5179995.459	8192
4000	538844.7777	5179884.976	8201
4001	538803.1964	5179774.493	8211
4002	538761.615	5179664.01	8220
4003	538716.1397	5179560.526	8229
4004	538670.6645	5179457.042	8238
4005	538625.1892	5179353.558	8247
4006	538579.7139	5179250.073	8256
4007	538534.2387	5179146.589	8265
4008	538488.7634	5179043.105	8274
4009	538443.2882	5178939.621	8283
4010	538397.8129	5178836.137	8292
4011	538352.3376	5178732.653	8301
4012	538306.8624	5178629.168	8310
4013	538261.3871	5178525.684	8319
4014	538215.9118	5178422.2	8328
4015	538170.4366	5178318.716	8338
4016	538124.9613	5178215.232	8347
4017	538079.486	5178111.748	8356
4018	538034.0108	5178008.264	8365
4019	537988.5355	5177904.779	8374
4020	537943.0602	5177801.295	8383
4021	537897.585	5177697.811	8392
4022	537852.1097	5177594.327	8401
4023	537806.6345	5177490.843	8410
4024	537761.1592	5177387.359	8419
4025	537715.6839	5177283.875	8428
4026	537670.2087	5177180.39	8437
4027	537624.7334	5177076.906	8446
4028	537579.2581	5176973.422	8455
4029	537533.7829	5176869.938	8464
4030	537488.3076	5176766.454	8473
4031	537442.8323	5176662.97	8482
4032	537397.3571	5176559.485	8491
4033	537351.8818	5176456.001	8500
4034	537306.4065	5176352.517	8509
4035	537260.9313	5176249.033	8518
4036	537215.456	5176145.549	8527
4037	537169.9808	5176042.065	8536
4038	537124.5055	5175938.581	8546
4039	537079.0302	5175835.096	8555
4040	537033.555	5175731.612	8564
4041	536988.0797	5175628.128	8573
4042	536942.6044	5175524.644	8582
4043	536897.1292	5175421.16	8591
4044	536851.6539	5175317.676	8600
4045	536806.1786	5175214.192	8609
4046	536760.7034	5175110.707	8618
4047	536715.2281	5175007.223	8627
4048	536669.7528	5174903.739	8636
4049	536624.2776	5174800.255	8645
4050	536578.8023	5174696.771	8654
4051	536533.3271	5174593.287	8663
4052	536487.8518	5174489.802	8672
4053	536442.3765	5174386.318	8681
4054	536396.9013	5174282.834	8690
4055	536351.426	5174179.35	8699
4056	536356.7493	5174070.831	8708
4057	536362.0726	5173962.312	8717
4058	536367.3959	5173853.793	8725
4059	536372.7193	5173745.273	8734
4060	536378.0426	5173636.754	8743
4061	536383.3659	5173528.235	8751
4062	536388.6892	5173419.716	8760
4063	536394.0125	5173311.197	8769
4064	536399.3358	5173202.678	8777
4065	536404.6592	5173094.158	8786
4066	536409.9825	5172985.639	8795
4067	536415.3058	5172877.12	8804
4068	536420.6291	5172768.601	8812
4069	536425.9524	5172660.082	8821
4070	536431.2757	5172551.563	8830
4071	536436.5991	5172443.043	8838
4072	536441.9224	5172334.524	8847
4073	536447.2457	5172226.005	8856
4074	536452.569	5172117.486	8864
4075	536501.8748	5172029.46	8872
4076	536551.1805	5171941.434	8881
4077	536600.4863	5171853.408	8889
4078	536649.7921	5171765.381	8897
4079	536699.0979	5171677.355	8905
4080	536748.4036	5171589.329	8913
4081	536797.7094	5171501.303	8921
4082	536847.0152	5171413.277	8929
4083	536896.321	5171325.251	8937
4084	536945.6267	5171237.224	8945
4085	536994.9325	5171149.198	8953
4086	537044.2383	5171061.172	8961
4087	537093.5441	5170973.146	8969
4088	537142.8498	5170885.12	8977
4089	537192.1556	5170797.094	8985
4090	537241.4614	5170709.067	8994
4091	537290.7672	5170621.041	9002
4092	537340.0729	5170533.015	9010
4093	537389.3787	5170444.989	9018

4094	537438.6845	5170356.963	9026	4150	540199.8079	5165427.498	9478
4095	537487.9903	5170268.937	9034	4151	540249.1137	5165339.472	9486
4096	537537.296	5170180.91	9042	4152	540298.4194	5165251.445	9494
4097	537586.6018	5170092.884	9050	4153	540347.7252	5165163.419	9502
4098	537635.9076	5170004.858	9058	4154	540397.031	5165075.393	9510
4099	537685.2134	5169916.832	9066	4155	540446.3368	5164987.367	9518
4100	537734.5191	5169828.806	9074	4156	540495.6425	5164899.341	9526
4101	537783.8249	5169740.78	9082	4157	540544.9483	5164811.315	9534
4102	537833.1307	5169652.753	9090	4158	540594.2541	5164723.288	9542
4103	537882.4365	5169564.727	9098	4159	540643.5599	5164635.262	9550
4104	537931.7422	5169476.701	9107	4160	540692.8656	5164547.236	9559
4105	537981.048	5169388.675	9115	4161	540742.1714	5164459.21	9567
4106	538030.3538	5169300.649	9123	4162	540791.4772	5164371.184	9575
4107	538079.6596	5169212.623	9131	4163	540840.783	5164283.158	9583
4108	538128.9653	5169124.596	9139	4164	540890.0887	5164195.131	9591
4109	538178.2711	5169036.57	9147	4165	540939.3945	5164107.105	9599
4110	538227.5769	5168948.544	9155	4166	540988.7003	5164019.079	9607
4111	538276.8827	5168860.518	9163	4167	541038.0061	5163931.053	9615
4112	538326.1884	5168772.492	9171	4168	541087.3118	5163843.027	9623
4113	538375.4942	5168684.466	9179	4169	541136.6176	5163755.001	9631
4114	538424.8	5168596.44	9187	4170	541185.9234	5163666.974	9639
4115	538474.1058	5168508.413	9195	4171	541235.2292	5163578.948	9647
4116	538523.4115	5168420.387	9203	4172	541284.5349	5163490.922	9655
4117	538572.7173	5168332.361	9211	4173	541333.8407	5163402.896	9663
4118	538622.0231	5168244.335	9220	4174	541383.1465	5163314.87	9672
4119	538671.3289	5168156.309	9228	4175	541432.4523	5163226.844	9680
4120	538720.6346	5168068.283	9236	4176	541481.758	5163138.817	9688
4121	538769.9404	5167980.256	9244	4177	541531.0638	5163050.791	9696
4122	538819.2462	5167892.23	9252	4178	541580.3696	5162962.765	9704
4123	538868.552	5167804.204	9260	4179	541629.6754	5162874.739	9712
4124	538917.8577	5167716.178	9268	4180	541678.9811	5162786.713	9720
4125	538967.1635	5167628.152	9276	4181	541728.2869	5162698.687	9728
4126	539016.4693	5167540.126	9284	4182	541777.5927	5162610.66	9736
4127	539065.7751	5167452.099	9292	4183	541826.8985	5162522.634	9744
4128	539115.0808	5167364.073	9300	4184	541876.2042	5162434.608	9752
4129	539164.3866	5167276.047	9308	4185	541925.51	5162346.582	9760
4130	539213.6924	5167188.021	9316	4186	541974.8158	5162258.556	9768
4131	539262.9982	5167099.995	9324	4187	542024.1215	5162170.53	9776
4132	539312.3039	5167011.969	9333	4188	542073.4273	5162082.504	9785
4133	539361.6097	5166923.942	9341	4189	542122.7331	5161994.477	9793
4134	539410.9155	5166835.916	9349	4190	542172.0389	5161906.451	9801
4135	539460.2213	5166747.89	9357	4191	542221.3446	5161818.425	9809
4136	539509.527	5166659.864	9365	4192	542270.6504	5161730.399	9817
4137	539558.8328	5166571.838	9373	4193	542319.9562	5161642.373	9825
4138	539608.1386	5166483.812	9381	4194	542369.262	5161554.347	9833
4139	539657.4444	5166395.785	9389	4195	542418.5677	5161466.32	9841
4140	539706.7501	5166307.759	9397	4196	542467.8735	5161378.294	9849
4141	539756.0559	5166219.733	9405	4197	542517.1793	5161290.268	9857
4142	539805.3617	5166131.707	9413	4198	542566.4851	5161202.242	9865
4143	539854.6675	5166043.681	9421	4199	542615.7908	5161114.216	9873
4144	539903.9732	5165955.655	9429	4200	542665.0966	5161026.19	9881
4145	539953.279	5165867.628	9437	4201	542714.4024	5160938.163	9889
4146	540002.5848	5165779.602	9446	4202	542763.7082	5160850.137	9898
4147	540051.8906	5165691.576	9454	4203	542813.0139	5160762.111	9906
4148	540101.1963	5165603.55	9462	4204	542862.3197	5160674.085	9914
4149	540150.5021	5165515.524	9470	4205	542911.6255	5160586.059	9922

4206	542960.9313	5160498.033	9930
4207	543010.237	5160410.006	9938
4208	543059.5428	5160321.98	9946
4209	543108.8486	5160233.954	9954
4210	543158.1544	5160145.928	9962
4211	543207.4601	5160057.902	9970
4212	543256.7659	5159969.876	9978
4213	543306.0717	5159881.849	9986
4214	543355.3775	5159793.823	9994
4215	543404.6832	5159705.797	10002
4216	543453.989	5159617.771	10011
4217	543503.2948	5159529.745	10019
4218	543552.6006	5159441.719	10027
4219	543601.9063	5159353.692	10035
4220	543651.2121	5159265.666	10043
4221	543700.5179	5159177.64	10051
4222	543749.8237	5159089.614	10059
4223	543799.1294	5159001.588	10067
4224	543848.4352	5158913.562	10075
4225	543897.741	5158825.536	10083
4226	543947.0468	5158737.509	10091
4227	543996.3525	5158649.483	10099
4228	544045.6583	5158561.457	10107
4229	544094.9641	5158473.431	10115
4230	544144.2699	5158385.405	10124
4231	544193.5756	5158297.379	10132
4232	544242.8814	5158209.352	10140
4233	544292.1872	5158121.326	10148
4234	544341.493	5158033.3	10156
4235	544390.7987	5157945.274	10164
4236	544440.1045	5157857.248	10172
4237	544489.4103	5157769.222	10180
4238	544538.7161	5157681.195	10188
4239	544588.0218	5157593.169	10196
4240	544637.3276	5157505.143	10204
4241	544686.6334	5157417.117	10212
4242	544735.9392	5157329.091	10220
4243	544785.2449	5157241.065	10228
4244	544834.5507	5157153.038	10237
4245	544883.8565	5157065.012	10245
4246	544933.1623	5156976.986	10253
4247	544982.468	5156888.96	10261
4248	545031.7738	5156800.934	10269
4249	545081.0796	5156712.908	10277
4250	545130.3854	5156624.881	10285
4251	545179.6911	5156536.855	10293
4252	545228.9969	5156448.829	10301
4253	545278.3027	5156360.803	10309
4254	545327.6085	5156272.777	10317
4255	545376.9142	5156184.751	10325
4256	545426.22	5156096.724	10333
4257	545475.5258	5156008.698	10341
4258	545524.8316	5155920.672	10350
4259	545574.1373	5155832.646	10358
4260	545623.4431	5155744.62	10366
4261	545672.7489	5155656.594	10374
4262	545722.0547	5155568.568	10382
4263	545771.3604	5155480.541	10390
4264	545820.6662	5155392.515	10398
4265	545869.972	5155304.489	10406
4266	545919.2778	5155216.463	10414
4267	545968.5835	5155128.437	10422
4268	546017.8893	5155040.411	10430
4269	546067.1951	5154952.384	10438
4270	546116.5009	5154864.358	10446
4271	546165.8066	5154776.332	10454
4272	546215.1124	5154688.306	10463
4273	546264.4182	5154600.28	10471
4274	546313.724	5154512.254	10479
4275	546363.0297	5154424.227	10487
4276	546412.3355	5154336.201	10495
4277	546461.6413	5154248.175	10503
4278	546510.9471	5154160.149	10511
4279	546560.2528	5154072.123	10519
4280	546609.5586	5153984.097	10527
4281	546658.8644	5153896.07	10535
4282	546708.1702	5153808.044	10543
4283	546757.4759	5153720.018	10551
4284	546806.7817	5153631.992	10559
4285	546856.0875	5153543.966	10567
4286	546905.3933	5153455.94	10576
4287	546954.699	5153367.913	10584
4288	547004.0048	5153279.887	10592
4289	547053.3106	5153191.861	10600
4290	547102.6164	5153103.835	10608
4291	547151.9221	5153015.809	10616
4292	547201.2279	5152927.783	10624
4293	547250.5337	5152839.756	10632
4294	547299.8395	5152751.73	10640
4295	547349.1452	5152663.704	10648
4296	547398.451	5152575.678	10656
4297	547446.6489	5152488.9	10664
4298	547494.8467	5152402.121	10672
4299	547543.0446	5152315.343	10680
4300	547591.2424	5152228.565	10688
4301	547639.4403	5152141.786	10696
4302	547687.6382	5152055.008	10704
4303	547735.836	5151968.23	10712
4304	547784.0339	5151881.451	10720
4305	547832.2317	5151794.673	10728
4306	547880.4296	5151707.895	10736
4307	547928.6275	5151621.116	10744
4308	547976.8253	5151534.338	10752
4309	548025.0232	5151447.56	10760
4310	548073.221	5151360.782	10767
4311	548121.4189	5151274.003	10775
4312	548169.6168	5151187.225	10783
4313	548217.8146	5151100.447	10791
4314	548266.0125	5151013.668	10799
4315	548314.2103	5150926.89	10807
4316	548362.4082	5150840.112	10815
4317	548410.6061	5150753.333	10823

4318	548458.8039	5150666.555	10831	4374	551157.8841	5145806.969	11276
4319	548507.0018	5150579.777	10839	4375	551206.082	5145720.191	11284
4320	548555.1996	5150492.998	10847	4376	551254.2798	5145633.412	11292
4321	548603.3975	5150406.22	10855	4377	551302.4777	5145546.634	11300
4322	548651.5954	5150319.442	10863	4378	551350.6755	5145459.856	11307
4323	548699.7932	5150232.663	10871	4379	551398.8734	5145373.077	11315
4324	548747.9911	5150145.885	10879	4380	551447.0713	5145286.299	11323
4325	548796.189	5150059.107	10887	4381	551495.2691	5145199.521	11331
4326	548844.3868	5149972.328	10895	4382	551543.467	5145112.742	11339
4327	548892.5847	5149885.55	10902	4383	551591.6649	5145025.964	11347
4328	548940.7825	5149798.772	10910	4384	551639.8627	5144939.186	11355
4329	548988.9804	5149711.993	10918	4385	551688.0606	5144852.408	11363
4330	549037.1783	5149625.215	10926	4386	551736.2584	5144765.629	11371
4331	549085.3761	5149538.437	10934	4387	551784.4563	5144678.851	11379
4332	549133.574	5149451.658	10942	4388	551832.6542	5144592.073	11387
4333	549181.7718	5149364.88	10950	4389	551880.852	5144505.294	11395
4334	549229.9697	5149278.102	10958	4390	551929.0499	5144418.516	11403
4335	549278.1676	5149191.324	10966	4391	551977.2477	5144331.738	11411
4336	549326.3654	5149104.545	10974	4392	552025.4456	5144244.959	11419
4337	549374.5633	5149017.767	10982	4393	552073.6435	5144158.181	11427
4338	549422.7611	5148930.989	10990	4394	552121.8413	5144071.403	11435
4339	549470.959	5148844.21	10998	4395	552170.0392	5143984.624	11442
4340	549519.1569	5148757.432	11006	4396	552218.237	5143897.846	11450
4341	549567.3547	5148670.654	11014	4397	552266.4349	5143811.068	11458
4342	549615.5526	5148583.875	11022	4398	552314.6328	5143724.289	11466
4343	549663.7504	5148497.097	11030	4399	552362.8306	5143637.511	11474
4344	549711.9483	5148410.319	11037	4400	552411.0285	5143550.733	11482
4345	549760.1462	5148323.54	11045	4401	552459.2263	5143463.954	11490
4346	549808.344	5148236.762	11053	4402	552507.4242	5143377.176	11498
4347	549856.5419	5148149.984	11061	4403	552555.6221	5143290.398	11506
4348	549904.7397	5148063.205	11069	4404	552603.8199	5143203.619	11514
4349	549952.9376	5147976.427	11077	4405	552652.0178	5143116.841	11522
4350	550001.1355	5147889.649	11085	4406	552700.2156	5143030.063	11530
4351	550049.3333	5147802.87	11093	4407	552748.4135	5142943.285	11538
4352	550097.5312	5147716.092	11101	4408	552796.6114	5142856.506	11546
4353	550145.729	5147629.314	11109	4409	552844.8092	5142769.728	11554
4354	550193.9269	5147542.535	11117	4410	552893.0071	5142682.95	11562
4355	550242.1248	5147455.757	11125	4411	552941.2049	5142596.171	11570
4356	550290.3226	5147368.979	11133	4412	552989.4028	5142509.393	11577
4357	550338.5205	5147282.2	11141	4413	553037.6007	5142422.615	11585
4358	550386.7183	5147195.422	11149	4414	553085.7985	5142335.836	11593
4359	550434.9162	5147108.644	11157	4415	553133.9964	5142249.058	11601
4360	550483.1141	5147021.866	11165	4416	553182.1942	5142162.28	11609
4361	550531.3119	5146935.087	11172	4417	553230.3921	5142075.501	11617
4362	550579.5098	5146848.309	11180	4418	553278.59	5141988.723	11625
4363	550627.7076	5146761.531	11188	4419	553326.7878	5141901.945	11633
4364	550675.9055	5146674.752	11196	4420	553374.9857	5141815.166	11641
4365	550724.1034	5146587.974	11204	4421	553423.1835	5141728.388	11649
4366	550772.3012	5146501.196	11212	4422	553471.3814	5141641.61	11657
4367	550820.4991	5146414.417	11220	4423	553519.5793	5141554.831	11665
4368	550868.6969	5146327.639	11228	4424	553567.7771	5141468.053	11673
4369	550916.8948	5146240.861	11236	4425	553615.975	5141381.275	11681
4370	550965.0927	5146154.082	11244	4426	553664.1728	5141294.496	11689
4371	551013.2905	5146067.304	11252	4427	553712.3707	5141207.718	11697
4372	551061.4884	5145980.526	11260	4428	553760.5686	5141120.94	11705
4373	551109.6862	5145893.747	11268	4429	553808.7664	5141034.161	11712

4430	553856.9643	5140947.383	11720	4486	556556.0445	5136087.797	12165
4431	553905.1621	5140860.605	11728	4487	556604.2423	5136001.019	12173
4432	553953.36	5140773.827	11736	4488	556652.4402	5135914.241	12181
4433	554001.5579	5140687.048	11744	4489	556700.638	5135827.462	12189
4434	554049.7557	5140600.27	11752	4490	556748.8359	5135740.684	12197
4435	554097.9536	5140513.492	11760	4491	556797.0338	5135653.906	12205
4436	554146.1515	5140426.713	11768	4492	556845.2316	5135567.127	12213
4437	554194.3493	5140339.935	11776	4493	556893.4295	5135480.349	12221
4438	554242.5472	5140253.157	11784	4494	556941.6274	5135393.571	12229
4439	554290.745	5140166.378	11792	4495	556989.8252	5135306.792	12237
4440	554338.9429	5140079.6	11800	4496	557038.0231	5135220.014	12245
4441	554387.1408	5139992.822	11808	4497	557086.2209	5135133.236	12252
4442	554435.3386	5139906.043	11816	4498	557134.4188	5135046.457	12260
4443	554483.5365	5139819.265	11824	4499	557182.6167	5134959.679	12268
4444	554531.7343	5139732.487	11832	4500	557230.8145	5134872.901	12276
4445	554579.9322	5139645.708	11840	4501	557279.0124	5134786.122	12284
4446	554628.1301	5139558.93	11847	4502	557327.2102	5134699.344	12292
4447	554676.3279	5139472.152	11855	4503	557375.4081	5134612.566	12300
4448	554724.5258	5139385.373	11863	4504	557423.606	5134525.787	12308
4449	554772.7236	5139298.595	11871	4505	557471.8038	5134439.009	12316
4450	554820.9215	5139211.817	11879	4506	557520.0017	5134352.231	12324
4451	554869.1194	5139125.038	11887	4507	557568.1995	5134265.453	12332
4452	554917.3172	5139038.26	11895	4508	557616.3974	5134178.674	12340
4453	554965.5151	5138951.482	11903	4509	557664.5953	5134091.896	12348
4454	555013.7129	5138864.703	11911	4510	557712.7931	5134005.118	12356
4455	555061.9108	5138777.925	11919	4511	557760.991	5133918.339	12364
4456	555110.1087	5138691.147	11927	4512	557809.1888	5133831.561	12372
4457	555158.3065	5138604.369	11935	4513	557857.3867	5133744.783	12380
4458	555206.5044	5138517.59	11943	4514	557905.5846	5133658.004	12387
4459	555254.7022	5138430.812	11951	4515	557953.7824	5133571.226	12395
4460	555302.9001	5138344.034	11959	4516	558001.9803	5133484.448	12403
4461	555351.098	5138257.255	11967	4517	558050.1781	5133397.669	12411
4462	555399.2958	5138170.477	11975	4518	558098.376	5133310.891	12419
4463	555447.4937	5138083.699	11982	4519	558147.4306	5133223.162	12427
4464	555495.6915	5137996.92	11990	4520	558196.4853	5133135.432	12435
4465	555543.8894	5137910.142	11998	4521	558245.5399	5133047.703	12443
4466	555592.0873	5137823.364	12006	4522	558294.5946	5132959.973	12451
4467	555640.2851	5137736.585	12014	4523	558343.6492	5132872.244	12459
4468	555688.483	5137649.807	12022	4524	558392.7039	5132784.515	12467
4469	555736.6808	5137563.029	12030	4525	558441.7585	5132696.785	12475
4470	555784.8787	5137476.25	12038	4526	558490.8132	5132609.056	12484
4471	555833.0766	5137389.472	12046	4527	558539.8678	5132521.326	12492
4472	555881.2744	5137302.694	12054	4528	558588.9224	5132433.597	12500
4473	555929.4723	5137215.915	12062	4529	558637.9771	5132345.867	12508
4474	555977.6701	5137129.137	12070	4530	558687.0317	5132258.138	12516
4475	556025.868	5137042.359	12078	4531	558736.0864	5132170.409	12524
4476	556074.0659	5136955.58	12086	4532	558785.141	5132082.679	12532
4477	556122.2637	5136868.802	12094	4533	558834.1957	5131994.95	12540
4478	556170.4616	5136782.024	12102	4534	558883.2503	5131907.22	12548
4479	556218.6594	5136695.245	12110	4535	558932.305	5131819.491	12556
4480	556266.8573	5136608.467	12117	4536	558981.3596	5131731.762	12564
4481	556315.0552	5136521.689	12125	4537	559030.4142	5131644.032	12572
4482	556363.253	5136434.911	12133	4538	559079.4689	5131556.303	12580
4483	556411.4509	5136348.132	12141	4539	559128.5235	5131468.573	12588
4484	556459.6487	5136261.354	12149	4540	559177.5782	5131380.844	12596
4485	556507.8466	5136174.576	12157	4541	559226.6328	5131293.114	12604

4542	559275.6875	5131205.385	12612	4598	562022.7476	5126292.538	13062
4543	559324.7421	5131117.656	12620	4599	562071.8022	5126204.808	13071
4544	559373.7968	5131029.926	12628	4600	562120.8569	5126117.079	13079
4545	559422.8514	5130942.197	12636	4601	562169.9115	5126029.35	13087
4546	559471.9061	5130854.467	12644	4602	562218.9662	5125941.62	13095
4547	559520.9607	5130766.738	12652	4603	562268.0208	5125853.891	13103
4548	559570.0153	5130679.009	12660	4604	562317.0754	5125766.161	13111
4549	559619.07	5130591.279	12668	4605	562366.1301	5125678.432	13119
4550	559668.1246	5130503.55	12677	4606	562415.1847	5125590.703	13127
4551	559717.1793	5130415.82	12685	4607	562464.2394	5125502.973	13135
4552	559766.2339	5130328.091	12693	4608	562513.294	5125415.244	13143
4553	559815.2886	5130240.361	12701	4609	562562.3487	5125327.514	13151
4554	559864.3432	5130152.632	12709	4610	562611.4033	5125239.785	13159
4555	559913.3979	5130064.903	12717	4611	562660.458	5125152.055	13167
4556	559962.4525	5129977.173	12725	4612	562709.5126	5125064.326	13175
4557	560011.5071	5129889.444	12733	4613	562758.5672	5124976.597	13183
4558	560060.5618	5129801.714	12741	4614	562807.6219	5124888.867	13191
4559	560109.6164	5129713.985	12749	4615	562856.6765	5124801.138	13199
4560	560158.6711	5129626.256	12757	4616	562905.7312	5124713.408	13207
4561	560207.7257	5129538.526	12765	4617	562954.7858	5124625.679	13215
4562	560256.7804	5129450.797	12773	4618	563003.8405	5124537.95	13223
4563	560305.835	5129363.067	12781	4619	563052.8951	5124450.22	13231
4564	560354.8897	5129275.338	12789	4620	563101.9498	5124362.491	13239
4565	560403.9443	5129187.609	12797	4621	563151.0044	5124274.761	13247
4566	560452.9989	5129099.879	12805	4622	563200.0591	5124187.032	13255
4567	560502.0536	5129012.15	12813	4623	563249.1137	5124099.302	13264
4568	560551.1082	5128924.42	12821	4624	563298.1683	5124011.573	13272
4569	560600.1629	5128836.691	12829	4625	563347.223	5123923.844	13280
4570	560649.2175	5128748.961	12837	4626	563396.2776	5123836.114	13288
4571	560698.2722	5128661.232	12845	4627	563445.3323	5123748.385	13296
4572	560747.3268	5128573.503	12853	4628	563494.3869	5123660.655	13304
4573	560796.3815	5128485.773	12861	4629	563543.4416	5123572.926	13312
4574	560845.4361	5128398.044	12870	4630	563592.4962	5123485.197	13320
4575	560894.4907	5128310.314	12878	4631	563641.5509	5123397.467	13328
4576	560943.5454	5128222.585	12886	4632	563690.6055	5123309.738	13336
4577	560992.6	5128134.856	12894	4633	563739.6601	5123222.008	13344
4578	561041.6547	5128047.126	12902	4634	563788.7148	5123134.279	13352
4579	561090.7093	5127959.397	12910	4635	563837.7694	5123046.55	13360
4580	561139.764	5127871.667	12918	4636	563886.8241	5122958.82	13368
4581	561188.8186	5127783.938	12926	4637	563935.8787	5122871.091	13376
4582	561237.8733	5127696.208	12934	4638	563984.9334	5122783.361	13384
4583	561286.9279	5127608.479	12942	4639	564033.988	5122695.632	13392
4584	561335.9826	5127520.75	12950	4640	564083.0427	5122607.902	13400
4585	561385.0372	5127433.02	12958	4641	564132.0973	5122520.173	13408
4586	561434.0918	5127345.291	12966	4642	564181.1519	5122432.444	13416
4587	561483.1465	5127257.561	12974	4643	564230.2066	5122344.714	13424
4588	561532.2011	5127169.832	12982	4644	564279.2612	5122256.985	13432
4589	561581.2558	5127082.103	12990	4645	564328.3159	5122169.255	13440
4590	561630.3104	5126994.373	12998	4646	564377.3705	5122081.526	13448
4591	561679.3651	5126906.644	13006	4647	564426.4252	5121993.797	13457
4592	561728.4197	5126818.914	13014	4648	564475.4798	5121906.067	13465
4593	561777.4744	5126731.185	13022	4649	564524.5345	5121818.338	13473
4594	561826.529	5126643.456	13030	4650	564573.5891	5121730.608	13481
4595	561875.5836	5126555.726	13038	4651	564622.6437	5121642.879	13489
4596	561924.6383	5126467.997	13046	4652	564671.6984	5121555.149	13497
4597	561973.6929	5126380.267	13054	4653	564720.753	5121467.42	13505

4654	564769.8077	5121379.691	13513
4655	564818.8623	5121291.961	13521
4656	564867.917	5121204.232	13529
4657	564916.9716	5121116.502	13537
4658	564966.0263	5121028.773	13545
4659	565015.0809	5120941.044	13553
4660	565064.1356	5120853.314	13561
4661	565113.1902	5120765.585	13569
4662	565162.2448	5120677.855	13577
4663	565211.2995	5120590.126	13585
4664	565260.3541	5120502.396	13593
4665	565309.4088	5120414.667	13601
4666	565358.4634	5120326.938	13609
4667	565407.5181	5120239.208	13617
4668	565456.5727	5120151.479	13625
4669	565505.6274	5120063.749	13633
4670	565554.682	5119976.02	13641
4671	565602.1334	5119885.767	13650
4672	565649.5849	5119795.514	13658
4673	565697.0363	5119705.261	13666
4674	565744.4878	5119615.008	13674
4675	565791.9392	5119524.755	13682
4676	565839.3906	5119434.502	13690
4677	565886.8421	5119344.249	13699
4678	565934.2935	5119253.996	13707
4679	565981.745	5119163.743	13715
4680	566029.1964	5119073.49	13723
4681	566076.6479	5118983.237	13731
4682	566124.0993	5118892.984	13739
4683	566171.5507	5118802.731	13747
4684	566219.0022	5118712.478	13756
4685	566266.4536	5118622.225	13764
4686	566313.9051	5118531.972	13772
4687	566361.3565	5118441.719	13780
4688	566408.8079	5118351.466	13788
4689	566456.2594	5118261.213	13796
4690	566503.7108	5118170.96	13805
4691	566551.1623	5118080.707	13813
4692	566598.6137	5117990.454	13821
4693	566646.0652	5117900.201	13829
4694	566693.5166	5117809.948	13837
4695	566740.968	5117719.695	13845
4696	566788.4195	5117629.442	13854
4697	566835.8709	5117539.189	13862
4698	566883.3224	5117448.936	13870
4699	566930.7738	5117358.683	13878
4700	566978.2252	5117268.43	13886
4701	567025.6767	5117178.177	13894
4702	567073.1281	5117087.924	13902
4703	567120.5796	5116997.671	13911
4704	567168.031	5116907.418	13919
4705	567215.4825	5116817.165	13927
4706	567262.9339	5116726.912	13935
4707	567310.3853	5116636.659	13943
4708	567357.8368	5116546.406	13951
4709	567405.2882	5116456.154	13960
4710	567452.7397	5116365.901	13968
4711	567500.1911	5116275.648	13976
4712	567547.6425	5116185.395	13984
4713	567595.094	5116095.142	13992
4714	567642.5454	5116004.889	14000
4715	567689.9969	5115914.636	14009
4716	567737.4483	5115824.383	14017
4717	567784.8998	5115734.13	14025
4718	567832.3512	5115643.877	14033
4719	567879.8026	5115553.624	14041
4720	567927.2541	5115463.371	14049
4721	567974.7055	5115373.118	14057
4722	568022.157	5115282.865	14066
4723	568069.6084	5115192.612	14074
4724	568117.0598	5115102.359	14082
4725	568164.5113	5115012.106	14090
4726	568211.9627	5114921.853	14098
4727	568259.4142	5114831.6	14106
4728	568306.8656	5114741.347	14115
4729	568354.3171	5114651.094	14123
4730	568401.7685	5114560.841	14131
4731	568449.2199	5114470.588	14139
4732	568496.6714	5114380.335	14147
4733	568544.1228	5114290.082	14155
4734	568591.5743	5114199.829	14164
4735	568639.0257	5114109.576	14172
4736	568686.4771	5114019.323	14180
4737	568733.9286	5113929.07	14188
4738	568781.38	5113838.817	14196
4739	568828.8315	5113748.564	14204
4740	568876.2829	5113658.311	14212
4741	568923.7344	5113568.058	14221
4742	568971.1858	5113477.805	14229
4743	569018.6372	5113387.552	14237
4744	569066.0887	5113297.299	14245
4745	569113.5401	5113207.046	14253
4746	569160.9916	5113116.793	14261
4747	569208.443	5113026.54	14270
4748	569260.5415	5112941.901	14278
4749	569312.6399	5112857.261	14285
4750	569364.7384	5112772.622	14293
4751	569416.8368	5112687.982	14301
4752	569468.9353	5112603.343	14309
4753	569521.0338	5112518.703	14317
4754	569573.1322	5112434.064	14325
4755	569625.2307	5112349.424	14333
4756	569677.3291	5112264.785	14341
4757	569729.4276	5112180.145	14349
4758	569781.5261	5112095.506	14357
4759	569833.6245	5112010.866	14365
4760	569885.723	5111926.227	14373
4761	569937.8214	5111841.587	14381
4762	569989.9199	5111756.948	14389
4763	570042.0184	5111672.308	14397
4764	570094.1168	5111587.669	14405
4765	570146.2153	5111503.029	14413

4766	570198.3138	5111418.39	14421	4822	573115.8275	5106678.579	14866
4767	570250.4122	5111333.751	14429	4823	573167.926	5106593.94	14874
4768	570302.5107	5111249.111	14437	4824	573214.8118	5106505.334	14882
4769	570354.6091	5111164.472	14444	4825	573261.6975	5106416.728	14890
4770	570406.7076	5111079.832	14452	4826	573308.5833	5106328.122	14898
4771	570458.8061	5110995.193	14460	4827	573355.4691	5106239.516	14906
4772	570510.9045	5110910.553	14468	4828	573402.3548	5106150.91	14914
4773	570563.003	5110825.914	14476	4829	573449.2406	5106062.303	14922
4774	570615.1014	5110741.274	14484	4830	573496.1264	5105973.697	14930
4775	570667.1999	5110656.635	14492	4831	573543.0122	5105885.091	14938
4776	570719.2984	5110571.995	14500	4832	573589.8979	5105796.485	14946
4777	570771.3968	5110487.356	14508	4833	573636.7837	5105707.879	14954
4778	570823.4953	5110402.716	14516	4834	573683.6695	5105619.273	14962
4779	570875.5937	5110318.077	14524	4835	573730.5552	5105530.667	14970
4780	570927.6922	5110233.437	14532	4836	573777.441	5105442.061	14978
4781	570979.7907	5110148.798	14540	4837	573824.3268	5105353.455	14986
4782	571031.8891	5110064.158	14548	4838	573871.2125	5105264.849	14994
4783	571083.9876	5109979.519	14556	4839	573918.0983	5105176.243	15002
4784	571136.086	5109894.879	14564	4840	573964.9841	5105087.637	15010
4785	571188.1845	5109810.24	14572	4841	574011.8698	5104999.03	15018
4786	571240.283	5109725.601	14580	4842	574058.7556	5104910.424	15026
4787	571292.3814	5109640.961	14588	4843	574105.6414	5104821.818	15034
4788	571344.4799	5109556.322	14596	4844	574152.5272	5104733.212	15042
4789	571396.5783	5109471.682	14604	4845	574199.4129	5104644.606	15050
4790	571448.6768	5109387.043	14611	4846	574246.2987	5104556	15058
4791	571500.7753	5109302.403	14619	4847	574293.1845	5104467.394	15066
4792	571552.8737	5109217.764	14627	4848	574340.0702	5104378.788	15074
4793	571604.9722	5109133.124	14635	4849	574386.956	5104290.182	15082
4794	571657.0706	5109048.485	14643	4850	574433.8418	5104201.576	15090
4795	571709.1691	5108963.845	14651	4851	574480.7275	5104112.97	15098
4796	571761.2676	5108879.206	14659	4852	574527.6133	5104024.364	15106
4797	571813.366	5108794.566	14667	4853	574574.4991	5103935.757	15114
4798	571865.4645	5108709.927	14675	4854	574621.3848	5103847.151	15122
4799	571917.5629	5108625.287	14683	4855	574668.2706	5103758.545	15130
4800	571969.6614	5108540.648	14691	4856	574715.1564	5103669.939	15138
4801	572021.7599	5108456.008	14699	4857	574762.0422	5103581.333	15147
4802	572073.8583	5108371.369	14707	4858	574808.9279	5103492.727	15155
4803	572125.9568	5108286.729	14715	4859	574855.8137	5103404.121	15163
4804	572178.0553	5108202.09	14723	4860	574902.6995	5103315.515	15171
4805	572230.1537	5108117.451	14731	4861	574949.5852	5103226.909	15179
4806	572282.2522	5108032.811	14739	4862	574996.471	5103138.303	15187
4807	572334.3506	5107948.172	14747	4863	575043.3568	5103049.697	15195
4808	572386.4491	5107863.532	14755	4864	575090.2425	5102961.09	15203
4809	572438.5476	5107778.893	14763	4865	575137.1283	5102872.484	15211
4810	572490.646	5107694.253	14770	4866	575184.0141	5102783.878	15219
4811	572542.7445	5107609.614	14778	4867	575230.8998	5102695.272	15227
4812	572594.8429	5107524.974	14786	4868	575277.7856	5102606.666	15235
4813	572646.9414	5107440.335	14794	4869	575324.6714	5102518.06	15243
4814	572699.0399	5107355.695	14802	4870	575371.5572	5102429.454	15251
4815	572751.1383	5107271.056	14810	4871	575418.4429	5102340.848	15259
4816	572803.2368	5107186.416	14818	4872	575465.3287	5102252.242	15267
4817	572855.3352	5107101.777	14826	4873	575512.2145	5102163.636	15275
4818	572907.4337	5107017.137	14834	4874	575559.1002	5102075.03	15283
4819	572959.5322	5106932.498	14842	4875	575605.986	5101986.424	15291
4820	573011.6306	5106847.858	14850	4876	575652.8718	5101897.817	15299
4821	573063.7291	5106763.219	14858	4877	575699.7575	5101809.211	15307

4878	575746.6433	5101720.605	15315	4934	578372.2464	5096758.665	15764
4879	575793.5291	5101631.999	15323	4935	578419.1322	5096670.058	15772
4880	575840.4148	5101543.393	15331	4936	578466.0179	5096581.452	15780
4881	575887.3006	5101454.787	15339	4937	578512.9037	5096492.846	15788
4882	575934.1864	5101366.181	15347	4938	578559.7895	5096404.24	15796
4883	575981.0722	5101277.575	15355	4939	578606.6752	5096315.634	15804
4884	576027.9579	5101188.969	15363	4940	578653.561	5096227.028	15812
4885	576074.8437	5101100.363	15371	4941	578697.0437	5096150.095	15819
4886	576121.7295	5101011.757	15379	4942	578740.5264	5096073.162	15826
4887	576168.6152	5100923.151	15387	4943	578784.0091	5095996.229	15833
4888	576215.501	5100834.544	15395	4944	578827.4918	5095919.297	15840
4889	576262.3868	5100745.938	15403	4945	578870.9746	5095842.364	15847
4890	576309.2725	5100657.332	15411	4946	578914.4573	5095765.431	15855
4891	576356.1583	5100568.726	15419	4947	578957.94	5095688.498	15862
4892	576403.0441	5100480.12	15427	4948	579001.4227	5095611.565	15869
4893	576449.9298	5100391.514	15435	4949	579044.9054	5095534.632	15876
4894	576496.8156	5100302.908	15443	4950	579088.3881	5095457.7	15883
4895	576543.7014	5100214.302	15451	4951	579131.8708	5095380.767	15890
4896	576590.5872	5100125.696	15459	4952	579175.3535	5095303.834	15897
4897	576637.4729	5100037.09	15467	4953	579218.8363	5095226.901	15904
4898	576684.3587	5099948.484	15475	4954	579262.319	5095149.968	15911
4899	576731.2445	5099859.878	15483	4955	579305.8017	5095073.035	15918
4900	576778.1302	5099771.271	15491	4956	579349.2844	5094996.102	15925
4901	576825.016	5099682.665	15499	4957	579392.7671	5094919.17	15932
4902	576871.9018	5099594.059	15507	4958	579436.2498	5094842.237	15939
4903	576918.7875	5099505.453	15515	4959	579479.7325	5094765.304	15946
4904	576965.6733	5099416.847	15523	4960	579523.2152	5094688.371	15954
4905	577012.5591	5099328.241	15531	4961	579566.6979	5094611.438	15961
4906	577059.4448	5099239.635	15539	4962	579610.1807	5094534.505	15968
4907	577106.3306	5099151.029	15547	4963	579653.6634	5094457.573	15975
4908	577153.2164	5099062.423	15556	4964	579697.1461	5094380.64	15982
4909	577200.1022	5098973.817	15564	4965	579740.6288	5094303.707	15989
4910	577246.9879	5098885.211	15572	4966	579784.1115	5094226.774	15996
4911	577293.8737	5098796.604	15580	4967	579827.5942	5094149.841	16003
4912	577340.7595	5098707.998	15588	4968	579871.0769	5094072.908	16010
4913	577387.6452	5098619.392	15596	4969	579914.5596	5093995.975	16017
4914	577434.531	5098530.786	15604	4970	579958.0424	5093919.043	16024
4915	577481.4168	5098442.18	15612	4971	580001.5251	5093842.11	16031
4916	577528.3025	5098353.574	15620	4972	580045.0078	5093765.177	16038
4917	577575.1883	5098264.968	15628	4973	580088.4905	5093688.244	16045
4918	577622.0741	5098176.362	15636	4974	580131.9732	5093611.311	16053
4919	577668.9598	5098087.756	15644	4975	580175.4559	5093534.378	16060
4920	577715.8456	5097999.15	15652	4976	580218.9386	5093457.445	16067
4921	577762.7314	5097910.544	15660	4977	580262.4213	5093380.513	16074
4922	577809.6172	5097821.938	15668	4978	580305.9041	5093303.58	16081
4923	577856.5029	5097733.331	15676	4979	580349.3868	5093226.647	16088
4924	577903.3887	5097644.725	15684	4980	580392.8695	5093149.714	16095
4925	577950.2745	5097556.119	15692	4981	580436.3522	5093072.781	16102
4926	577997.1602	5097467.513	15700	4982	580479.8349	5092995.848	16109
4927	578044.046	5097378.907	15708	4983	580523.3176	5092918.916	16116
4928	578090.9318	5097290.301	15716	4984	580566.8003	5092841.983	16123
4929	578137.8175	5097201.695	15724	4985	580610.283	5092765.05	16130
4930	578184.7033	5097113.089	15732	4986	580653.7657	5092688.117	16137
4931	578231.5891	5097024.483	15740	4987	580697.2485	5092611.184	16144
4932	578278.4748	5096935.877	15748	4988	580740.7312	5092534.251	16151
4933	578325.3606	5096847.271	15756	4989	580784.2139	5092457.318	16159

4990	580827.6966	5092380.386	16166	5046	583262.7285	5088072.146	16562
4991	580871.1793	5092303.453	16173	5047	583306.2112	5087995.213	16569
4992	580914.662	5092226.52	16180	5048	583349.6939	5087918.28	16576
4993	580958.1447	5092149.587	16187	5049	583393.1766	5087841.348	16583
4994	581001.6274	5092072.654	16194	5050	583436.6593	5087764.415	16590
4995	581045.1102	5091995.721	16201	5051	583480.142	5087687.482	16597
4996	581088.5929	5091918.789	16208	5052	583523.6247	5087610.549	16604
4997	581132.0756	5091841.856	16215	5053	583567.1074	5087533.616	16611
4998	581175.5583	5091764.923	16222	5054	583610.5902	5087456.683	16618
4999	581219.041	5091687.99	16229	5055	583654.0729	5087379.751	16625
5000	581262.5237	5091611.057	16236	5056	583697.5556	5087302.818	16632
5001	581306.0064	5091534.124	16243	5057	583741.0383	5087225.885	16639
5002	581349.4891	5091457.191	16250	5058	583784.521	5087148.952	16646
5003	581392.9718	5091380.259	16258	5059	583825.4262	5087073.631	16653
5004	581436.4546	5091303.326	16265	5060	583866.3315	5086998.309	16660
5005	581479.9373	5091226.393	16272	5061	583907.2367	5086922.988	16667
5006	581523.42	5091149.46	16279	5062	583948.142	5086847.667	16674
5007	581566.9027	5091072.527	16286	5063	583989.0472	5086772.346	16681
5008	581610.3854	5090995.594	16293	5064	584029.9525	5086697.024	16688
5009	581653.8681	5090918.662	16300	5065	584070.8577	5086621.703	16694
5010	581697.3508	5090841.729	16307	5066	584111.7629	5086546.382	16701
5011	581740.8335	5090764.796	16314	5067	584152.6682	5086471.06	16708
5012	581784.3163	5090687.863	16321	5068	584193.5734	5086395.739	16715
5013	581827.799	5090610.93	16328	5069	584234.4787	5086320.418	16722
5014	581871.2817	5090533.997	16335	5070	584275.3839	5086245.097	16729
5015	581914.7644	5090457.064	16342	5071	584316.2892	5086169.775	16736
5016	581958.2471	5090380.132	16349	5072	584357.1944	5086094.454	16742
5017	582001.7298	5090303.199	16357	5073	584398.0996	5086019.133	16749
5018	582045.2125	5090226.266	16364	5074	584439.0049	5085943.811	16756
5019	582088.6952	5090149.333	16371	5075	584479.9101	5085868.49	16763
5020	582132.1779	5090072.4	16378	5076	584520.8154	5085793.169	16770
5021	582175.6607	5089995.467	16385	5077	584561.7206	5085717.847	16777
5022	582219.1434	5089918.535	16392	5078	584602.6259	5085642.526	16784
5023	582262.6261	5089841.602	16399	5079	584643.5311	5085567.205	16790
5024	582306.1088	5089764.669	16406	5080	584684.4363	5085491.884	16797
5025	582349.5915	5089687.736	16413	5081	584725.3416	5085416.562	16804
5026	582393.0742	5089610.803	16420	5082	584766.2468	5085341.241	16811
5027	582436.5569	5089533.87	16427	5083	584807.1521	5085265.92	16818
5028	582480.0396	5089456.937	16434	5084	584848.0573	5085190.598	16825
5029	582523.5224	5089380.005	16441	5085	584888.9626	5085115.277	16832
5030	582567.0051	5089303.072	16448	5086	584929.8678	5085039.956	16838
5031	582610.4878	5089226.139	16455	5087	584970.773	5084964.635	16845
5032	582653.9705	5089149.206	16463	5088	585011.6783	5084889.313	16852
5033	582697.4532	5089072.273	16470	5089	585052.5835	5084813.992	16859
5034	582740.9359	5088995.34	16477	5090	585093.4888	5084738.671	16866
5035	582784.4186	5088918.407	16484	5091	585134.394	5084663.349	16873
5036	582827.9013	5088841.475	16491	5092	585175.2993	5084588.028	16880
5037	582871.3841	5088764.542	16498	5093	585216.2045	5084512.707	16886
5038	582914.8668	5088687.609	16505	5094	585257.1097	5084437.386	16893
5039	582958.3495	5088610.676	16512	5095	585298.015	5084362.064	16900
5040	583001.8322	5088533.743	16519	5096	585338.9202	5084286.743	16907
5041	583045.3149	5088456.81	16526	5097	585379.8255	5084211.422	16914
5042	583088.7976	5088379.878	16533	5098	585420.7307	5084136.1	16921
5043	583132.2803	5088302.945	16540	5099	585461.636	5084060.779	16928
5044	583175.763	5088226.012	16547	5100	585502.5412	5083985.458	16934
5045	583219.2457	5088149.079	16554	5101	585543.4464	5083910.137	16941

5102	585584.3517	5083834.815	16948	5158	587875.0453	5079616.823	17332
5103	585625.2569	5083759.494	16955	5159	587915.9505	5079541.502	17339
5104	585666.1622	5083684.173	16962	5160	587956.8558	5079466.18	17346
5105	585707.0674	5083608.851	16969	5161	587997.761	5079390.859	17353
5106	585747.9727	5083533.53	16976	5162	588038.6663	5079315.538	17359
5107	585788.8779	5083458.209	16982	5163	588079.5715	5079240.217	17366
5108	585829.7831	5083382.888	16989	5164	588120.4768	5079164.895	17373
5109	585870.6884	5083307.566	16996	5165	588161.382	5079089.574	17380
5110	585911.5936	5083232.245	17003	5166	588202.2872	5079014.253	17387
5111	585952.4989	5083156.924	17010	5167	588243.1925	5078938.931	17394
5112	585993.4041	5083081.602	17017	5168	588284.0977	5078863.61	17401
5113	586034.3094	5083006.281	17024	5169	588325.003	5078788.289	17407
5114	586075.2146	5082930.96	17030	5170	588365.9082	5078712.968	17414
5115	586116.1199	5082855.638	17037	5171	588406.8135	5078637.646	17421
5116	586157.0251	5082780.317	17044	5172	588447.7187	5078562.325	17428
5117	586197.9303	5082704.996	17051	5173	588488.6239	5078487.004	17435
5118	586238.8356	5082629.675	17058	5174	588529.5292	5078411.682	17442
5119	586279.7408	5082554.353	17065	5175	588570.4344	5078336.361	17449
5120	586320.6461	5082479.032	17071	5176	588611.3397	5078261.04	17455
5121	586361.5513	5082403.711	17078	5177	588652.2449	5078185.719	17462
5122	586402.4566	5082328.389	17085	5178	588693.1502	5078110.397	17469
5123	586443.3618	5082253.068	17092	5179	588734.0554	5078035.076	17476
5124	586484.267	5082177.747	17099	5180	588774.9606	5077959.755	17483
5125	586525.1723	5082102.426	17106	5181	588815.8659	5077884.433	17490
5126	586566.0775	5082027.104	17113	5182	588856.7711	5077809.112	17497
5127	586606.9828	5081951.783	17119	5183	588897.6764	5077733.791	17503
5128	586647.888	5081876.462	17126	5184	588938.5816	5077658.469	17510
5129	586688.7933	5081801.14	17133	5185	588979.4869	5077583.148	17517
5130	586729.6985	5081725.819	17140	5186	589020.3921	5077507.827	17524
5131	586770.6037	5081650.498	17147	5187	589061.2973	5077432.506	17531
5132	586811.509	5081575.177	17154	5188	589102.2026	5077357.184	17538
5133	586852.4142	5081499.855	17161	5189	589143.1078	5077281.863	17545
5134	586893.3195	5081424.534	17167	5190	589184.0131	5077206.542	17551
5135	586934.2247	5081349.213	17174	5191	589224.9183	5077131.22	17558
5136	586975.13	5081273.891	17181	5192	589265.8236	5077055.899	17565
5137	587016.0352	5081198.57	17188	5193	589306.7288	5076980.578	17572
5138	587056.9404	5081123.249	17195	5194	589347.634	5076905.257	17579
5139	587097.8457	5081047.928	17202	5195	589388.5393	5076829.935	17586
5140	587138.7509	5080972.606	17209	5196	589429.4445	5076754.614	17593
5141	587179.6562	5080897.285	17215	5197	589470.3498	5076679.293	17599
5142	587220.5614	5080821.964	17222	5198	589511.255	5076603.971	17606
5143	587261.4667	5080746.642	17229	5199	589552.1603	5076528.65	17613
5144	587302.3719	5080671.321	17236	5200	589593.0655	5076453.329	17620
5145	587343.2771	5080596	17243	5201	589633.9707	5076378.008	17627
5146	587384.1824	5080520.679	17250	5202	589674.876	5076302.686	17634
5147	587425.0876	5080445.357	17257	5203	589715.7812	5076227.365	17641
5148	587465.9929	5080370.036	17263	5204	589756.6865	5076152.044	17647
5149	587506.8981	5080294.715	17270	5205	589797.5917	5076076.722	17654
5150	587547.8034	5080219.393	17277	5206	589838.497	5076001.401	17661
5151	587588.7086	5080144.072	17284	5207	589879.4022	5075926.08	17668
5152	587629.6138	5080068.751	17291	5208	589920.3074	5075850.759	17675
5153	587670.5191	5079993.429	17298	5209	589961.2127	5075775.437	17682
5154	587711.4243	5079918.108	17305	5210	590002.1179	5075700.116	17689
5155	587752.3296	5079842.787	17311	5211	590043.0232	5075624.795	17695
5156	587793.2348	5079767.466	17318	5212	590083.9284	5075549.473	17702
5157	587834.1401	5079692.144	17325	5213	590124.8337	5075474.152	17709

5214	590165.7389	5075398.831	17716	5270	592456.4325	5071180.839	18100
5215	590206.6441	5075323.51	17723	5271	592497.3378	5071105.517	18107
5216	590247.5494	5075248.188	17730	5272	592538.243	5071030.196	18114
5217	590288.4546	5075172.867	17737	5273	592580.9181	5070957.713	18120
5218	590329.3599	5075097.546	17743	5274	592623.5932	5070885.231	18127
5219	590370.2651	5075022.224	17750	5275	592666.2683	5070812.748	18134
5220	590411.1704	5074946.903	17757	5276	592708.9434	5070740.266	18141
5221	590452.0756	5074871.582	17764	5277	592751.6185	5070667.783	18147
5222	590492.9809	5074796.26	17771	5278	592794.2936	5070595.3	18154
5223	590533.8861	5074720.939	17778	5279	592836.9688	5070522.818	18161
5224	590574.7913	5074645.618	17785	5280	592879.6439	5070450.335	18168
5225	590615.6966	5074570.297	17791	5281	592922.319	5070377.852	18174
5226	590656.6018	5074494.975	17798	5282	592964.9941	5070305.37	18181
5227	590697.5071	5074419.654	17805	5283	593007.6692	5070232.887	18188
5228	590738.4123	5074344.333	17812	5284	593050.3443	5070160.405	18195
5229	590779.3176	5074269.011	17819	5285	593093.0194	5070087.922	18201
5230	590820.2228	5074193.69	17826	5286	593135.6945	5070015.439	18208
5231	590861.128	5074118.369	17833	5287	593178.3696	5069942.957	18215
5232	590902.0333	5074043.048	17839	5288	593221.0447	5069870.474	18221
5233	590942.9385	5073967.726	17846	5289	593263.7198	5069797.992	18228
5234	590983.8438	5073892.405	17853	5290	593306.3949	5069725.509	18235
5235	591024.749	5073817.084	17860	5291	593349.0701	5069653.026	18242
5236	591065.6543	5073741.762	17867	5292	593391.7452	5069580.544	18248
5237	591106.5595	5073666.441	17874	5293	593434.4203	5069508.061	18255
5238	591147.4647	5073591.12	17881	5294	593477.0954	5069435.579	18262
5239	591188.37	5073515.799	17887	5295	593519.7705	5069363.096	18269
5240	591229.2752	5073440.477	17894	5296	593562.4456	5069290.613	18275
5241	591270.1805	5073365.156	17901	5297	593605.1207	5069218.131	18282
5242	591311.0857	5073289.835	17908	5298	593647.7958	5069145.648	18289
5243	591351.991	5073214.513	17915	5299	593690.4709	5069073.165	18295
5244	591392.8962	5073139.192	17922	5300	593733.146	5069000.683	18302
5245	591433.8014	5073063.871	17929	5301	593775.8211	5068928.2	18309
5246	591474.7067	5072988.55	17935	5302	593818.4962	5068855.718	18316
5247	591515.6119	5072913.228	17942	5303	593861.1714	5068783.235	18322
5248	591556.5172	5072837.907	17949	5304	593903.8465	5068710.752	18329
5249	591597.4224	5072762.586	17956	5305	593946.5216	5068638.27	18336
5250	591638.3277	5072687.264	17963	5306	593989.1967	5068565.787	18343
5251	591679.2329	5072611.943	17970	5307	594031.8718	5068493.305	18349
5252	591720.1381	5072536.622	17977	5308	594074.5469	5068420.822	18356
5253	591761.0434	5072461.301	17983	5309	594117.222	5068348.339	18363
5254	591801.9486	5072385.979	17990	5310	594159.8971	5068275.857	18369
5255	591842.8539	5072310.658	17997	5311	594202.5722	5068203.374	18376
5256	591883.7591	5072235.337	18004	5312	594245.2473	5068130.891	18383
5257	591924.6644	5072160.015	18011	5313	594287.9224	5068058.409	18390
5258	591965.5696	5072084.694	18018	5314	594330.5975	5067985.926	18396
5259	592006.4748	5072009.373	18025	5315	594373.2726	5067913.444	18403
5260	592047.3801	5071934.051	18031	5316	594415.9478	5067840.961	18410
5261	592088.2853	5071858.73	18038	5317	594458.6229	5067768.478	18417
5262	592129.1906	5071783.409	18045	5318	594501.298	5067695.996	18423
5263	592170.0958	5071708.088	18052	5319	594543.9731	5067623.513	18430
5264	592211.0011	5071632.766	18059	5320	594586.6482	5067551.031	18437
5265	592251.9063	5071557.445	18066	5321	594629.3233	5067478.548	18443
5266	592292.8115	5071482.124	18073	5322	594671.9984	5067406.065	18450
5267	592333.7168	5071406.802	18079	5323	594714.6735	5067333.583	18457
5268	592374.622	5071331.481	18086	5324	594757.3486	5067261.1	18464
5269	592415.5273	5071256.16	18093	5325	594800.0237	5067188.618	18470

5326	594842.6988	5067116.135	18477	5382	597232.5049	5063057.109	18854
5327	594885.3739	5067043.652	18484	5383	597275.18	5062984.626	18861
5328	594928.0491	5066971.17	18491	5384	597314.4511	5062909.219	18867
5329	594970.7242	5066898.687	18497	5385	597353.7221	5062833.812	18874
5330	595013.3993	5066826.204	18504	5386	597392.9932	5062758.405	18881
5331	595056.0744	5066753.722	18511	5387	597432.2642	5062682.997	18888
5332	595098.7495	5066681.239	18517	5388	597471.5353	5062607.59	18895
5333	595141.4246	5066608.757	18524	5389	597510.8063	5062532.183	18901
5334	595184.0997	5066536.274	18531	5390	597550.0774	5062456.776	18908
5335	595226.7748	5066463.791	18538	5391	597589.3484	5062381.369	18915
5336	595269.4499	5066391.309	18544	5392	597628.6195	5062305.962	18922
5337	595312.125	5066318.826	18551	5393	597667.8905	5062230.555	18929
5338	595354.8001	5066246.344	18558	5394	597707.1616	5062155.147	18935
5339	595397.4752	5066173.861	18565	5395	597746.4326	5062079.74	18942
5340	595440.1504	5066101.378	18571	5396	597785.7037	5062004.333	18949
5341	595482.8255	5066028.896	18578	5397	597824.9747	5061928.926	18956
5342	595525.5006	5065956.413	18585	5398	597864.2458	5061853.519	18963
5343	595568.1757	5065883.931	18592	5399	597903.5169	5061778.112	18970
5344	595610.8508	5065811.448	18598	5400	597942.7879	5061702.705	18976
5345	595653.5259	5065738.965	18605	5401	597982.059	5061627.297	18983
5346	595696.201	5065666.483	18612	5402	598021.33	5061551.89	18990
5347	595738.8761	5065594	18618	5403	598060.6011	5061476.483	18997
5348	595781.5512	5065521.517	18625	5404	598099.8721	5061401.076	19004
5349	595824.2263	5065449.035	18632	5405	598139.1432	5061325.669	19010
5350	595866.9014	5065376.552	18639	5406	598178.4142	5061250.262	19017
5351	595909.5765	5065304.07	18645	5407	598217.6853	5061174.855	19024
5352	595952.2516	5065231.587	18652	5408	598256.9563	5061099.447	19031
5353	595994.9268	5065159.104	18659	5409	598296.2274	5061024.04	19038
5354	596037.6019	5065086.622	18666	5410	598335.4984	5060948.633	19044
5355	596080.277	5065014.139	18672	5411	598374.7695	5060873.226	19051
5356	596122.9521	5064941.657	18679	5412	598414.0406	5060797.819	19058
5357	596165.6272	5064869.174	18686	5413	598453.3116	5060722.412	19065
5358	596208.3023	5064796.691	18692	5414	598492.5827	5060647.005	19072
5359	596250.9774	5064724.209	18699	5415	598531.8537	5060571.597	19078
5360	596293.6525	5064651.726	18706	5416	598571.1248	5060496.19	19085
5361	596336.3276	5064579.243	18713	5417	598610.3958	5060420.783	19092
5362	596379.0027	5064506.761	18719	5418	598649.6669	5060345.376	19099
5363	596421.6778	5064434.278	18726	5419	598688.9379	5060269.969	19106
5364	596464.3529	5064361.796	18733	5420	598728.209	5060194.562	19112
5365	596507.0281	5064289.313	18740	5421	598767.48	5060119.155	19119
5366	596549.7032	5064216.83	18746	5422	598806.7511	5060043.747	19126
5367	596592.3783	5064144.348	18753	5423	598846.0221	5059968.34	19133
5368	596635.0534	5064071.865	18760	5424	598885.2932	5059892.933	19140
5369	596677.7285	5063999.383	18766	5425	598924.5642	5059817.526	19146
5370	596720.4036	5063926.9	18773	5426	598963.8353	5059742.119	19153
5371	596763.0787	5063854.417	18780	5427	599003.1064	5059666.712	19160
5372	596805.7538	5063781.935	18787	5428	599042.3774	5059591.305	19167
5373	596848.4289	5063709.452	18793	5429	599081.6485	5059515.897	19174
5374	596891.104	5063636.97	18800	5430	599120.9195	5059440.49	19180
5375	596933.7791	5063564.487	18807	5431	599160.1906	5059365.083	19187
5376	596976.4542	5063492.004	18814	5432	599199.4616	5059289.676	19194
5377	597019.1294	5063419.522	18820	5433	599238.7327	5059214.269	19201
5378	597061.8045	5063347.039	18827	5434	599278.0037	5059138.862	19208
5379	597104.4796	5063274.556	18834	5435	599317.2748	5059063.455	19214
5380	597147.1547	5063202.074	18840	5436	599356.5458	5058988.047	19221
5381	597189.8298	5063129.591	18847	5437	599395.8169	5058912.64	19228

5438	599435.0879	5058837.233	19235
5439	599474.359	5058761.826	19242
5440	599513.6301	5058686.419	19248
5441	599552.9011	5058611.012	19255
5442	599592.1722	5058535.605	19262
5443	599631.4432	5058460.197	19269
5444	599670.7143	5058384.79	19276
5445	599709.9853	5058309.383	19282
5446	599749.2564	5058233.976	19289
5447	599788.5274	5058158.569	19296
5448	599827.7985	5058083.162	19303
5449	599867.0695	5058007.755	19310
5450	599906.3406	5057932.347	19316
5451	599945.6116	5057856.94	19323
5452	599984.8827	5057781.533	19330
5453	600024.1537	5057706.126	19337
5454	600063.4248	5057630.719	19344
5455	600102.6959	5057555.312	19350
5456	600141.9669	5057479.905	19357
5457	600181.238	5057404.497	19364
5458	600220.509	5057329.09	19371
5459	600259.7801	5057253.683	19378
5460	600299.0511	5057178.276	19384
5461	600338.3222	5057102.869	19391
5462	600377.5932	5057027.462	19398
5463	600416.8643	5056952.055	19405
5464	600456.1353	5056876.647	19412
5465	600495.4064	5056801.24	19418
5466	600534.6774	5056725.833	19425
5467	600573.9485	5056650.426	19432
5468	600613.2196	5056575.019	19439
5469	600652.4906	5056499.612	19446
5470	600691.7617	5056424.205	19452
5471	600731.0327	5056348.797	19459
5472	600770.3038	5056273.39	19466
5473	600809.5748	5056197.983	19473
5474	600848.8459	5056122.576	19480
5475	600888.1169	5056047.169	19486
5476	600927.388	5055971.762	19493
5477	600966.659	5055896.355	19500
5478	601005.9301	5055820.947	19507
5479	601045.2011	5055745.54	19514
5480	601084.4722	5055670.133	19520
5481	601123.7432	5055594.726	19527
5482	601163.0143	5055519.319	19534
5483	601202.2854	5055443.912	19541
5484	601241.5564	5055368.505	19548
5485	601280.8275	5055293.097	19554
5486	601320.0985	5055217.69	19561
5487	601359.3696	5055142.283	19568
5488	601398.6406	5055066.876	19575
5489	601437.9117	5054991.469	19582
5490	601477.1827	5054916.062	19588
5491	601516.4538	5054840.655	19595
5492	601555.7248	5054765.247	19602
5493	601594.9959	5054689.84	19609
5494	601634.2669	5054614.433	19616
5495	601673.538	5054539.026	19622
5496	601718.3069	5054460.407	19630
5497	601763.0757	5054381.789	19637
5498	601807.8446	5054303.17	19644
5499	601852.6134	5054224.552	19651
5500	601897.3823	5054145.933	19659
5501	601942.1511	5054067.315	19666
5502	601986.92	5053988.696	19673
5503	602031.6889	5053910.078	19680
5504	602076.4577	5053831.459	19688
5505	602121.2266	5053752.841	19695
5506	602165.9954	5053674.222	19702
5507	602210.7643	5053595.604	19709
5508	602255.5332	5053516.985	19717
5509	602300.302	5053438.367	19724
5510	602345.0709	5053359.748	19731
5511	602389.8397	5053281.13	19738
5512	602434.6086	5053202.511	19745
5513	602479.3774	5053123.893	19753
5514	602524.1463	5053045.274	19760
5515	602568.9152	5052966.656	19767
5516	602613.684	5052888.037	19774
5517	602658.4529	5052809.419	19782
5518	602703.2217	5052730.8	19789
5519	602747.9906	5052652.182	19796
5520	602792.7594	5052573.563	19803
5521	602837.5283	5052494.945	19811
5522	602882.2972	5052416.326	19818
5523	602927.066	5052337.708	19825
5524	602971.8349	5052259.089	19832
5525	603016.6037	5052180.471	19840
5526	603061.3726	5052101.852	19847
5527	603106.1414	5052023.234	19854
5528	603150.9103	5051944.615	19861
5529	603195.6792	5051865.997	19869
5530	603240.448	5051787.378	19876
5531	603285.2169	5051708.76	19883
5532	603329.9857	5051630.141	19890
5533	603374.7546	5051551.523	19897
5534	603419.5235	5051472.904	19905
5535	603464.2923	5051394.286	19912
5536	603509.0612	5051315.667	19919
5537	603553.83	5051237.049	19926
5538	603598.5989	5051158.43	19934
5539	603643.3677	5051079.812	19941
5540	603688.1366	5051001.193	19948
5541	603732.9055	5050922.575	19955
5542	603777.6743	5050843.956	19963
5543	603822.4432	5050765.338	19970
5544	603867.212	5050686.719	19977
5545	603911.9809	5050608.101	19984
5546	603956.7497	5050529.482	19992
5547	604001.5186	5050450.864	19999
5548	604046.2875	5050372.245	20006
5549	604091.0563	5050293.627	20013

5550	604135.8252	5050215.008	20021	5606	606642.8812	5045812.372	20426
5551	604180.594	5050136.39	20028	5607	606687.6501	5045733.754	20433
5552	604225.3629	5050057.771	20035	5608	606732.4189	5045655.135	20440
5553	604270.1317	5049979.153	20042	5609	606777.1878	5045576.517	20448
5554	604314.9006	5049900.534	20049	5610	606821.9566	5045497.898	20455
5555	604359.6695	5049821.916	20057	5611	606866.7255	5045419.28	20462
5556	604404.4383	5049743.297	20064	5612	606911.4944	5045340.661	20469
5557	604449.2072	5049664.679	20071	5613	606956.2632	5045262.043	20477
5558	604493.976	5049586.06	20078	5614	607001.0321	5045183.424	20484
5559	604538.7449	5049507.442	20086	5615	607045.8009	5045104.806	20491
5560	604583.5138	5049428.823	20093	5616	607090.5698	5045026.187	20498
5561	604628.2826	5049350.205	20100	5617	607135.3386	5044947.569	20505
5562	604673.0515	5049271.586	20107	5618	607180.1075	5044868.95	20513
5563	604717.8203	5049192.968	20115	5619	607224.8764	5044790.332	20520
5564	604762.5892	5049114.349	20122	5620	607269.6452	5044711.713	20527
5565	604807.358	5049035.731	20129	5621	607314.4141	5044633.095	20534
5566	604852.1269	5048957.112	20136	5622	607359.1829	5044554.476	20542
5567	604896.8958	5048878.494	20144	5623	607403.9518	5044475.858	20549
5568	604941.6646	5048799.875	20151	5624	607448.7206	5044397.239	20556
5569	604986.4335	5048721.257	20158	5625	607493.4895	5044318.621	20563
5570	605031.2023	5048642.638	20165	5626	607538.2584	5044240.002	20571
5571	605075.9712	5048564.02	20173	5627	607583.0272	5044161.384	20578
5572	605120.74	5048485.401	20180	5628	607627.7961	5044082.765	20585
5573	605165.5089	5048406.783	20187	5629	607672.5649	5044004.147	20592
5574	605210.2778	5048328.164	20194	5630	607717.3338	5043925.528	20600
5575	605255.0466	5048249.546	20201	5631	607762.1026	5043846.91	20607
5576	605299.8155	5048170.927	20209	5632	607806.8715	5043768.291	20614
5577	605344.5843	5048092.309	20216	5633	607851.6404	5043689.673	20621
5578	605389.3532	5048013.69	20223	5634	607896.4092	5043611.054	20629
5579	605434.122	5047935.072	20230	5635	607941.1781	5043532.436	20636
5580	605478.8909	5047856.453	20238	5636	607985.9469	5043453.817	20643
5581	605523.6598	5047777.835	20245	5637	608030.7158	5043375.199	20650
5582	605568.4286	5047699.216	20252	5638	608075.4847	5043296.58	20657
5583	605613.1975	5047620.598	20259	5639	608120.2535	5043217.962	20665
5584	605657.9663	5047541.979	20267	5640	608165.0224	5043139.343	20672
5585	605702.7352	5047463.361	20274	5641	608209.7912	5043060.725	20679
5586	605747.5041	5047384.742	20281	5642	608254.5601	5042982.106	20686
5587	605792.2729	5047306.124	20288	5643	608299.3289	5042903.488	20694
5588	605837.0418	5047227.505	20296	5644	608344.0978	5042824.869	20701
5589	605881.8106	5047148.887	20303	5645	608388.8667	5042746.251	20708
5590	605926.5795	5047070.268	20310	5646	608433.6355	5042667.632	20715
5591	605971.3483	5046991.65	20317	5647	608478.4044	5042589.014	20723
5592	606016.1172	5046913.031	20325	5648	608523.1732	5042510.395	20730
5593	606060.8861	5046834.413	20332	5649	608567.9421	5042431.777	20737
5594	606105.6549	5046755.794	20339	5650	608612.7109	5042353.158	20744
5595	606150.4238	5046677.176	20346	5651	608657.4798	5042274.54	20752
5596	606195.1926	5046598.557	20353	5652	608702.2487	5042195.921	20759
5597	606239.9615	5046519.939	20361	5653	608747.0175	5042117.303	20766
5598	606284.7303	5046441.32	20368	5654	608791.7864	5042038.684	20773
5599	606329.4992	5046362.702	20375	5655	608836.5552	5041960.066	20780
5600	606374.2681	5046284.083	20382	5656	608881.3241	5041881.447	20788
5601	606419.0369	5046205.465	20390	5657	608926.0929	5041802.829	20795
5602	606463.8058	5046126.846	20397	5658	608970.8618	5041724.21	20802
5603	606508.5746	5046048.228	20404	5659	609015.6307	5041645.592	20809
5604	606553.3435	5045969.609	20411	5660	609060.3995	5041566.973	20817
5605	606598.1123	5045890.991	20419	5661	609105.1684	5041488.355	20824

5662	609149.9372	5041409.736	20831	5718	611656.9933	5037007.1	21236
5663	609194.7061	5041331.118	20838	5719	611701.7621	5036928.482	21244
5664	609239.475	5041252.499	20846	5720	611746.531	5036849.863	21251
5665	609284.2438	5041173.881	20853	5721	611791.2998	5036771.245	21258
5666	609329.0127	5041095.262	20860	5722	611836.0687	5036692.626	21265
5667	609373.7815	5041016.644	20867	5723	611880.8376	5036614.008	21273
5668	609418.5504	5040938.025	20875	5724	611925.6064	5036535.389	21280
5669	609463.3192	5040859.407	20882	5725	611970.3753	5036456.771	21287
5670	609508.0881	5040780.788	20889	5726	612015.1441	5036378.152	21294
5671	609552.857	5040702.17	20896	5727	612059.913	5036299.534	21302
5672	609597.6258	5040623.551	20904	5728	612104.6818	5036220.915	21309
5673	609642.3947	5040544.933	20911	5729	612149.4507	5036142.297	21316
5674	609687.1635	5040466.314	20918	5730	612194.2196	5036063.678	21323
5675	609731.9324	5040387.696	20925	5731	612238.9884	5035985.06	21331
5676	609776.7012	5040309.077	20932	5732	612283.7573	5035906.441	21338
5677	609821.4701	5040230.459	20940	5733	612328.5261	5035827.823	21345
5678	609866.239	5040151.84	20947	5734	612373.295	5035749.204	21352
5679	609911.0078	5040073.222	20954	5735	612418.0638	5035670.586	21360
5680	609955.7767	5039994.603	20961	5736	612462.8327	5035591.967	21367
5681	610000.5455	5039915.985	20969	5737	612507.6016	5035513.349	21374
5682	610045.3144	5039837.366	20976	5738	612552.3704	5035434.73	21381
5683	610090.0832	5039758.748	20983	5739	612597.1393	5035356.112	21388
5684	610134.8521	5039680.129	20990	5740	612641.9081	5035277.493	21396
5685	610179.621	5039601.511	20998	5741	612686.677	5035198.875	21403
5686	610224.3898	5039522.892	21005	5742	612731.4459	5035120.256	21410
5687	610269.1587	5039444.274	21012	5743	612776.2147	5035041.638	21417
5688	610313.9275	5039365.655	21019	5744	612820.9836	5034963.019	21425
5689	610358.6964	5039287.037	21027	5745	612865.7524	5034884.401	21432
5690	610403.4653	5039208.418	21034	5746	612910.5213	5034805.782	21439
5691	610448.2341	5039129.8	21041	5747	612955.2901	5034727.164	21446
5692	610493.003	5039051.181	21048	5748	613000.059	5034648.545	21454
5693	610537.7718	5038972.563	21056	5749	613044.8076	5034569.513	21461
5694	610582.5407	5038893.944	21063	5750	613089.5563	5034490.481	21468
5695	610627.3095	5038815.326	21070	5751	613134.3049	5034411.449	21475
5696	610672.0784	5038736.707	21077	5752	613179.0535	5034332.418	21483
5697	610716.8473	5038658.089	21084	5753	613223.8021	5034253.386	21490
5698	610761.6161	5038579.47	21092	5754	613268.5508	5034174.354	21497
5699	610806.385	5038500.852	21099	5755	613313.2994	5034095.322	21504
5700	610851.1538	5038422.233	21106	5756	613358.048	5034016.29	21512
5701	610895.9227	5038343.615	21113	5757	613402.7966	5033937.258	21519
5702	610940.6915	5038264.996	21121	5758	613447.5453	5033858.226	21526
5703	610985.4604	5038186.378	21128	5759	613492.2939	5033779.194	21534
5704	611030.2293	5038107.759	21135	5760	613537.0425	5033700.163	21541
5705	611074.9981	5038029.141	21142	5761	613581.7911	5033621.131	21548
5706	611119.767	5037950.522	21150	5762	613626.5398	5033542.099	21555
5707	611164.5358	5037871.904	21157	5763	613671.2884	5033463.067	21563
5708	611209.3047	5037793.285	21164	5764	613716.037	5033384.035	21570
5709	611254.0735	5037714.667	21171	5765	613760.7856	5033305.003	21577
5710	611298.8424	5037636.048	21179	5766	613805.5343	5033225.971	21584
5711	611343.6113	5037557.43	21186	5767	613850.2829	5033146.939	21592
5712	611388.3801	5037478.811	21193	5768	613895.0315	5033067.907	21599
5713	611433.149	5037400.193	21200	5769	613939.7801	5032988.876	21606
5714	611477.9178	5037321.574	21208	5770	613984.5288	5032909.844	21613
5715	611522.6867	5037242.956	21215	5771	614029.2774	5032830.812	21621
5716	611567.4556	5037164.337	21222	5772	614074.026	5032751.78	21628
5717	611612.2244	5037085.719	21229	5773	614118.7746	5032672.748	21635

5774	614163.5233	5032593.716	21643
5775	614208.2719	5032514.684	21650
5776	614253.0205	5032435.652	21657
5777	614297.7691	5032356.621	21664
5778	614342.5178	5032277.589	21672
5779	614387.2664	5032198.557	21679
5780	614432.015	5032119.525	21686
5781	614475.3645	5032039.146	21693
5782	614518.7139	5031958.766	21701
5783	614562.0634	5031878.387	21708
5784	614605.4129	5031798.008	21715
5785	614648.7623	5031717.629	21723
5786	614692.1118	5031637.249	21730
5787	614735.4613	5031556.87	21737
5788	614778.8107	5031476.491	21745
5789	614822.1602	5031396.112	21752
5790	614865.5096	5031315.732	21759
5791	614908.8591	5031235.353	21766
5792	614952.2086	5031154.974	21774
5793	614995.558	5031074.594	21781
5794	615038.9075	5030994.215	21788
5795	615082.257	5030913.836	21796
5796	615125.6064	5030833.457	21803
5797	615168.9559	5030753.077	21810
5798	615212.3054	5030672.698	21818
5799	615255.6548	5030592.319	21825
5800	615299.0043	5030511.94	21832
5801	615342.3538	5030431.56	21840
5802	615385.7032	5030351.181	21847
5803	615429.0527	5030270.802	21854
5804	615472.4021	5030190.422	21861
5805	615515.7516	5030110.043	21869
5806	615559.1011	5030029.664	21876
5807	615602.4505	5029949.285	21883
5808	615645.8	5029868.905	21891
5809	615689.1495	5029788.526	21898
5810	615732.4989	5029708.147	21905
5811	615775.8484	5029627.768	21913
5812	615819.1979	5029547.388	21920
5813	615862.5473	5029467.009	21927
5814	615905.8968	5029386.63	21935
5815	615949.2463	5029306.25	21942
5816	615992.5957	5029225.871	21949
5817	616035.9452	5029145.492	21956
5818	616079.2946	5029065.113	21964
5819	616122.6441	5028984.733	21971
5820	616165.9936	5028904.354	21978
5821	616209.343	5028823.975	21986
5822	616252.6925	5028743.596	21993
5823	616296.042	5028663.216	22000
5824	616339.3914	5028582.837	22008
5825	616382.7409	5028502.458	22015
5826	616426.0904	5028422.078	22022
5827	616469.4398	5028341.699	22029
5828	616512.7893	5028261.32	22037
5829	616556.1388	5028180.941	22044
5830	616599.4882	5028100.561	22051
5831	616642.8377	5028020.182	22059
5832	616686.1871	5027939.803	22066
5833	616729.5366	5027859.423	22073
5834	616772.8861	5027779.044	22081
5835	616816.2355	5027698.665	22088
5836	616859.585	5027618.286	22095
5837	616902.9345	5027537.906	22103
5838	616946.2839	5027457.527	22110
5839	616989.6334	5027377.148	22117
5840	617032.9829	5027296.769	22124
5841	617076.3323	5027216.389	22132
5842	617119.6818	5027136.01	22139
5843	617163.0313	5027055.631	22146
5844	617206.3807	5026975.251	22154
5845	617249.7302	5026894.872	22161
5846	617293.0796	5026814.493	22168
5847	617336.4291	5026734.114	22176
5848	617379.7786	5026653.734	22183
5849	617423.128	5026573.355	22190
5850	617466.4775	5026492.976	22198
5851	617509.827	5026412.597	22205
5852	617553.1764	5026332.217	22212
5853	617596.5259	5026251.838	22219
5854	617639.8754	5026171.459	22227
5855	617683.2248	5026091.079	22234
5856	617726.5743	5026010.7	22241
5857	617769.9238	5025930.321	22249
5858	617813.2732	5025849.942	22256
5859	617856.6227	5025769.562	22263
5860	617899.9721	5025689.183	22271
5861	617943.3216	5025608.804	22278
5862	617986.6711	5025528.425	22285
5863	618030.0205	5025448.045	22292
5864	618073.37	5025367.666	22300
5865	618120.308	5025285.276	22307
5866	618167.2461	5025202.886	22315
5867	618214.1841	5025120.496	22323
5868	618261.1221	5025038.107	22330
5869	618308.0602	5024955.717	22338
5870	618354.9982	5024873.327	22345
5871	618401.9363	5024790.937	22353
5872	618448.8743	5024708.547	22360
5873	618495.8123	5024626.157	22368
5874	618542.7504	5024543.768	22376
5875	618589.6884	5024461.378	22383
5876	618636.6264	5024378.988	22391
5877	618683.5645	5024296.598	22398
5878	618730.5025	5024214.208	22406
5879	618777.4405	5024131.818	22414
5880	618824.3786	5024049.429	22421
5881	618871.3166	5023967.039	22429
5882	618918.2547	5023884.649	22436
5883	618965.1927	5023802.259	22444
5884	619012.1307	5023719.869	22452
5885	619059.0688	5023637.479	22459

5886	619106.0068	5023555.089	22467	5942	621734.5369	5018941.258	22891
5887	619152.9448	5023472.7	22474	5943	621781.4749	5018858.869	22899
5888	619199.8829	5023390.31	22482	5944	621828.4129	5018776.479	22907
5889	619246.8209	5023307.92	22489	5945	621875.351	5018694.089	22914
5890	619293.759	5023225.53	22497	5946	621922.289	5018611.699	22922
5891	619340.697	5023143.14	22505	5947	621970.5241	5018524.218	22930
5892	619387.635	5023060.75	22512	5948	622018.7591	5018436.738	22938
5893	619434.5731	5022978.361	22520	5949	622066.9942	5018349.257	22946
5894	619481.5111	5022895.971	22527	5950	622115.2292	5018261.776	22954
5895	619528.4491	5022813.581	22535	5951	622163.4643	5018174.295	22962
5896	619575.3872	5022731.191	22543	5952	622211.6994	5018086.815	22970
5897	619622.3252	5022648.801	22550	5953	622259.9344	5017999.334	22978
5898	619669.2632	5022566.411	22558	5954	622308.1695	5017911.853	22986
5899	619716.2013	5022484.022	22565	5955	622356.4045	5017824.373	22994
5900	619763.1393	5022401.632	22573	5956	622404.6396	5017736.892	23002
5901	619810.0774	5022319.242	22580	5957	622452.8747	5017649.411	23010
5902	619857.0154	5022236.852	22588	5958	622501.1097	5017561.93	23018
5903	619903.9534	5022154.462	22596	5959	622549.3448	5017474.45	23026
5904	619950.8915	5022072.072	22603	5960	622597.5798	5017386.969	23034
5905	619997.8295	5021989.683	22611	5961	622645.8149	5017299.488	23042
5906	620044.7675	5021907.293	22618	5962	622694.05	5017212.008	23050
5907	620091.7056	5021824.903	22626	5963	622742.285	5017124.527	23058
5908	620138.6436	5021742.513	22634	5964	622790.5201	5017037.046	23066
5909	620185.5816	5021660.123	22641	5965	622838.7551	5016949.565	23074
5910	620232.5197	5021577.733	22649	5966	622886.9902	5016862.085	23082
5911	620279.4577	5021495.343	22656	5967	622935.2253	5016774.604	23090
5912	620326.3958	5021412.954	22664	5968	622983.4603	5016687.123	23098
5913	620373.3338	5021330.564	22672	5969	623031.6954	5016599.643	23106
5914	620420.2718	5021248.174	22679	5970	623079.9304	5016512.162	23114
5915	620467.2099	5021165.784	22687	5971	623128.1655	5016424.681	23122
5916	620514.1479	5021083.394	22694	5972	623176.4006	5016337.201	23130
5917	620561.0859	5021001.004	22702	5973	623224.6356	5016249.72	23138
5918	620608.024	5020918.615	22709	5974	623272.8707	5016162.239	23146
5919	620654.962	5020836.225	22717	5975	623321.1057	5016074.758	23154
5920	620701.9	5020753.835	22725	5976	623369.3408	5015987.278	23162
5921	620748.8381	5020671.445	22732	5977	623417.5759	5015899.797	23170
5922	620795.7761	5020589.055	22740	5978	623465.8109	5015812.316	23178
5923	620842.7142	5020506.665	22747	5979	623514.046	5015724.836	23186
5924	620889.6522	5020424.276	22755	5980	623562.281	5015637.355	23194
5925	620936.5902	5020341.886	22763	5981	623610.5161	5015549.874	23202
5926	620983.5283	5020259.496	22770	5982	623658.7512	5015462.393	23210
5927	621030.4663	5020177.106	22778	5983	623706.9862	5015374.913	23218
5928	621077.4043	5020094.716	22785	5984	623755.2213	5015287.432	23226
5929	621124.3424	5020012.326	22793	5985	623803.4563	5015199.951	23234
5930	621171.2804	5019929.936	22800	5986	623851.6914	5015112.471	23242
5931	621218.2185	5019847.547	22808	5987	623899.9265	5015024.99	23249
5932	621265.1565	5019765.157	22816	5988	623948.1615	5014937.509	23257
5933	621312.0945	5019682.767	22823	5989	623996.3966	5014850.028	23265
5934	621359.0326	5019600.377	22831	5990	624044.6317	5014762.548	23273
5935	621405.9706	5019517.987	22838	5991	624092.8667	5014675.067	23281
5936	621452.9086	5019435.597	22846	5992	624141.1018	5014587.586	23289
5937	621499.8467	5019353.208	22854	5993	624189.3368	5014500.106	23297
5938	621546.7847	5019270.818	22861	5994	624237.5719	5014412.625	23305
5939	621593.7227	5019188.428	22869	5995	624285.807	5014325.144	23313
5940	621640.6608	5019106.038	22876	5996	624334.042	5014237.663	23321
5941	621687.5988	5019023.648	22884	5997	624382.2771	5014150.183	23329

5998	624430.5121	5014062.702	23337
5999	624478.7472	5013975.221	23345
6000	624526.9823	5013887.741	23353
6001	624575.2173	5013800.26	23361
6002	624623.4524	5013712.779	23369
6003	624671.6874	5013625.298	23377
6004	624719.9225	5013537.818	23385
6005	624768.1576	5013450.337	23393
6006	624816.3926	5013362.856	23401
6007	624864.6277	5013275.376	23409
6008	624912.8627	5013187.895	23417
6009	624961.0978	5013100.414	23425
6010	625009.3329	5013012.934	23433
6011	625057.5679	5012925.453	23441
6012	625105.803	5012837.972	23449
6013	625154.038	5012750.491	23457
6014	625202.2731	5012663.011	23465
6015	625250.5082	5012575.53	23473
6016	625298.7432	5012488.049	23481
6017	625346.9783	5012400.569	23489
6018	625395.2133	5012313.088	23497
6019	625443.4484	5012225.607	23505
6020	625491.6835	5012138.126	23513
6021	625539.9185	5012050.646	23521
6022	625588.1536	5011963.165	23529
6023	625636.3886	5011875.684	23537
6024	625684.6237	5011788.204	23545
6025	625732.8588	5011700.723	23553
6026	625781.0938	5011613.242	23561
6027	625829.3289	5011525.761	23569
6028	625877.5639	5011438.281	23577
6029	625925.799	5011350.8	23585
6030	625974.9615	5011265.622	23593
6031	626024.124	5011180.445	23601
6032	626073.2865	5011095.267	23609
6033	626122.449	5011010.089	23617
6034	626171.6116	5010924.912	23624
6035	626220.7741	5010839.734	23632
6036	626269.9366	5010754.557	23640
6037	626319.0991	5010669.379	23648
6038	626368.2616	5010584.201	23656
6039	626417.4241	5010499.024	23664
6040	626466.5866	5010413.846	23672
6041	626515.7491	5010328.668	23680
6042	626564.9117	5010243.491	23687
6043	626614.0742	5010158.313	23695
6044	626663.2367	5010073.136	23703
6045	626712.3992	5009987.958	23711
6046	626761.5617	5009902.78	23719
6047	626810.7242	5009817.603	23727
6048	626859.8867	5009732.425	23735
6049	626909.0492	5009647.247	23743
6050	626958.2117	5009562.07	23750
6051	627007.3743	5009476.892	23758
6052	627056.5368	5009391.714	23766
6053	627105.6993	5009306.537	23774
6054	627154.8618	5009221.359	23782
6055	627204.0243	5009136.182	23790
6056	627253.1868	5009051.004	23798
6057	627302.3493	5008965.826	23805
6058	627351.5118	5008880.649	23813
6059	627400.6744	5008795.471	23821
6060	627449.8369	5008710.293	23829
6061	627498.9994	5008625.116	23837
6062	627548.1619	5008539.938	23845
6063	627597.3244	5008454.761	23853
6064	627646.4869	5008369.583	23861
6065	627695.6494	5008284.405	23868
6066	627744.8119	5008199.228	23876
6067	627793.9745	5008114.05	23884
6068	627843.137	5008028.872	23892
6069	627892.2995	5007943.695	23900
6070	627941.462	5007858.517	23908
6071	627990.6245	5007773.339	23916
6072	628039.787	5007688.162	23923
6073	628088.9495	5007602.984	23931
6074	628138.112	5007517.807	23939
6075	628187.2745	5007432.629	23947
6076	628236.4371	5007347.451	23955
6077	628285.5996	5007262.274	23963
6078	628334.7621	5007177.096	23971
6079	628383.9246	5007091.918	23979
6080	628433.0871	5007006.741	23986
6081	628482.2496	5006921.563	23994
6082	628531.4121	5006836.386	24002
6083	628580.5746	5006751.208	24010
6084	628629.7372	5006666.03	24018
6085	628678.8997	5006580.853	24026
6086	628728.0622	5006495.675	24034
6087	628777.2247	5006410.497	24041
6088	628826.3872	5006325.32	24049
6089	628875.5497	5006240.142	24057
6090	628924.7122	5006154.965	24065
6091	628973.8747	5006069.787	24073
6092	629023.0372	5005984.609	24081
6093	629072.1998	5005899.432	24089
6094	629121.3623	5005814.254	24097
6095	629170.5248	5005729.076	24104
6096	629219.6873	5005643.899	24112
6097	629268.8498	5005558.721	24120
6098	629318.0123	5005473.543	24128
6099	629367.1748	5005388.366	24136
6100	629416.3373	5005303.188	24144
6101	629465.4999	5005218.011	24152
6102	629514.6624	5005132.833	24160
6103	629563.8249	5005047.655	24167
6104	629612.9874	5004962.478	24175
6105	629662.1499	5004877.3	24183
6106	629711.3124	5004792.122	24191
6107	629760.4749	5004706.945	24199
6108	629809.6374	5004621.767	24207
6109	629858.8	5004536.59	24215

6110	629907.9625	5004451.412	24222
6111	629957.125	5004366.234	24230
6112	630006.2875	5004281.057	24238
6113	630055.45	5004195.879	24246
6114	630104.6125	5004110.701	24254

Appendix 4: Latitude and longitude points for Line 56 converted to UTM and corresponding station numbers assigned to each FFID. These points were then interpolated to assign a UTM and station number to every FFID for setting up the geometry.

FFID	Latitude	Longitude	Northing (UTM)	Easting (UTM)	Station No.
7633	44.46447	-43.76073	4924209.434	598579.145	1000
7859	44.65727	-43.8912	4945476.504	587909.892	599579
8083	44.84646	-44.02198	4966359.496	577288.555	1187489
8308	45.04202	-44.1563	4987964.513	566447.844	1764778
8533	45.23312	-44.28899	5009093.473	555810.75	2331225
8759	45.417	-44.42074	5029438.691	545322.165	2887036
8872	45.50816	-44.48371	5039532.68	540330.248	3432358
8984	45.5992	-44.55093	5049615.496	535022.733	3972689
9208	45.76743	-44.67258	5068260.023	525458.897	4507711
9320	45.84405	-44.72657	5076756.965	521231.716	5033170
9433	45.93576	-44.78947	5086931.574	516320.681	5554402
9546	46.02737	-44.85994	5097098.029	510839.823	6070723
9602	46.07407	-44.89188	5102282.912	508360.803	6581562
9659	46.12017	-44.92445	5107386.933	505837.351	7089923
9772	46.2003	-44.9832	5116302.724	501296.159	7595761
9886	46.27905	-45.0425	5125053.495	496725.709	8097057

Appendix 5: FFID and corresponding UTM and station numbers used for geometry set up of Line 56.

FFID	Easting (UTM)	Northing (UTM)	Station No.	FFID	Easting (UTM)	Northing (UTM)	Station No.
7634	598531.9359	4924303.536	1008	7683	596218.6908	4928914.538	1421
7635	598484.7268	4924397.638	1017	7684	596171.4817	4929008.64	1430
7636	598437.5177	4924491.74	1025	7685	596124.2726	4929102.742	1438
7637	598390.3087	4924585.842	1034	7686	596077.0635	4929196.844	1446
7638	598343.0996	4924679.944	1042	7687	596029.8545	4929290.946	1455
7639	598295.8905	4924774.046	1051	7688	595982.6454	4929385.048	1463
7640	598248.6814	4924868.149	1059	7689	595935.4363	4929479.15	1472
7641	598201.4723	4924962.251	1067	7690	595888.2272	4929573.253	1480
7642	598154.2632	4925056.353	1076	7691	595841.0181	4929667.355	1488
7643	598107.0542	4925150.455	1084	7692	595793.809	4929761.457	1497
7644	598059.8451	4925244.557	1093	7693	595746.6	4929855.559	1505
7645	598012.636	4925338.659	1101	7694	595699.3909	4929949.661	1514
7646	597965.4269	4925432.761	1109	7695	595652.1818	4930043.763	1522
7647	597918.2178	4925526.863	1118	7696	595604.9727	4930137.865	1531
7648	597871.0087	4925620.965	1126	7697	595557.7636	4930231.967	1539
7649	597823.7997	4925715.067	1135	7698	595510.5545	4930326.069	1547
7650	597776.5906	4925809.169	1143	7699	595463.3455	4930420.171	1556
7651	597729.3815	4925903.271	1152	7700	595416.1364	4930514.273	1564
7652	597682.1724	4925997.374	1160	7701	595368.9273	4930608.375	1573
7653	597634.9633	4926091.476	1168	7702	595321.7182	4930702.477	1581
7654	597587.7542	4926185.578	1177	7703	595274.5091	4930796.58	1590
7655	597540.5452	4926279.68	1185	7704	595227.3	4930890.682	1598
7656	597493.3361	4926373.782	1194	7705	595180.0909	4930984.784	1606
7657	597446.127	4926467.884	1202	7706	595132.8819	4931078.886	1615
7658	597398.9179	4926561.986	1211	7707	595085.6728	4931172.988	1623
7659	597351.7088	4926656.088	1219	7708	595038.4637	4931267.09	1632
7660	597304.4997	4926750.19	1227	7709	594991.2546	4931361.192	1640
7661	597257.2906	4926844.292	1236	7710	594944.0455	4931455.294	1649
7662	597210.0816	4926938.394	1244	7711	594896.8364	4931549.396	1657
7663	597162.8725	4927032.496	1253	7712	594849.6274	4931643.498	1665
7664	597115.6634	4927126.598	1261	7713	594802.4183	4931737.6	1674
7665	597068.4543	4927220.701	1270	7714	594755.2092	4931831.702	1682
7666	597021.2452	4927314.803	1278	7715	594708.0001	4931925.805	1691
7667	596974.0361	4927408.905	1286	7716	594660.791	4932019.907	1699
7668	596926.8271	4927503.007	1295	7717	594613.5819	4932114.009	1707
7669	596879.618	4927597.109	1303	7718	594566.3729	4932208.111	1716
7670	596832.4089	4927691.211	1312	7719	594519.1638	4932302.213	1724
7671	596785.1998	4927785.313	1320	7720	594471.9547	4932396.315	1733
7672	596737.9907	4927879.415	1328	7721	594424.7456	4932490.417	1741
7673	596690.7816	4927973.517	1337	7722	594377.5365	4932584.519	1750
7674	596643.5726	4928067.619	1345	7723	594330.3274	4932678.621	1758
7675	596596.3635	4928161.721	1354	7724	594283.1183	4932772.723	1766
7676	596549.1544	4928255.823	1362	7725	594235.9093	4932866.825	1775
7677	596501.9453	4928349.926	1371	7726	594188.7002	4932960.927	1783
7678	596454.7362	4928444.028	1379	7727	594141.4911	4933055.029	1792
7679	596407.5271	4928538.13	1387	7728	594094.282	4933149.132	1800
7680	596360.318	4928632.232	1396	7729	594047.0729	4933243.234	1809
7681	596313.109	4928726.334	1404	7730	593999.8638	4933337.336	1817
7682	596265.8999	4928820.436	1413	7731	593952.6548	4933431.438	1825

7732	593905.4457	4933525.54	1834
7733	593858.2366	4933619.642	1842
7734	593811.0275	4933713.744	1851
7735	593763.8184	4933807.846	1859
7736	593716.6093	4933901.948	1868
7737	593669.4003	4933996.05	1876
7738	593622.1912	4934090.152	1884
7739	593574.9821	4934184.254	1893
7740	593527.773	4934278.357	1901
7741	593480.5639	4934372.459	1910
7742	593433.3548	4934466.561	1918
7743	593386.1458	4934560.663	1926
7744	593338.9367	4934654.765	1935
7745	593291.7276	4934748.867	1943
7746	593244.5185	4934842.969	1952
7747	593197.3094	4934937.071	1960
7748	593150.1003	4935031.173	1969
7749	593102.8912	4935125.275	1977
7750	593055.6822	4935219.377	1985
7751	593008.4731	4935313.479	1994
7752	592961.264	4935407.581	2002
7753	592914.0549	4935501.684	2011
7754	592866.8458	4935595.786	2019
7755	592819.6367	4935689.888	2028
7756	592772.4277	4935783.99	2036
7757	592725.2186	4935878.092	2044
7758	592678.0095	4935972.194	2053
7759	592630.8004	4936066.296	2061
7760	592583.5913	4936160.398	2070
7761	592536.3822	4936254.5	2078
7762	592489.1732	4936348.602	2086
7763	592441.9641	4936442.704	2095
7764	592394.755	4936536.806	2103
7765	592347.5459	4936630.909	2112
7766	592300.3368	4936725.011	2120
7767	592253.1277	4936819.113	2129
7768	592205.9187	4936913.215	2137
7769	592158.7096	4937007.317	2145
7770	592111.5005	4937101.419	2154
7771	592064.2914	4937195.521	2162
7772	592017.0823	4937289.623	2171
7773	591969.8732	4937383.725	2179
7774	591922.6641	4937477.827	2188
7775	591875.4551	4937571.929	2196
7776	591828.246	4937666.031	2204
7777	591781.0369	4937760.133	2213
7778	591733.8278	4937854.236	2221
7779	591686.6187	4937948.338	2230
7780	591639.4096	4938042.44	2238
7781	591592.2006	4938136.542	2247
7782	591544.9915	4938230.644	2255
7783	591497.7824	4938324.746	2263
7784	591450.5733	4938418.848	2272
7785	591403.3642	4938512.95	2280
7786	591356.1551	4938607.052	2289
7787	591308.9461	4938701.154	2297

7788	591261.737	4938795.256	2305
7789	591214.5279	4938889.358	2314
7790	591167.3188	4938983.461	2322
7791	591120.1097	4939077.563	2331
7792	591072.9006	4939171.665	2339
7793	591025.6915	4939265.767	2348
7794	590978.4825	4939359.869	2356
7795	590931.2734	4939453.971	2364
7796	590884.0643	4939548.073	2373
7797	590836.8552	4939642.175	2381
7798	590789.6461	4939736.277	2390
7799	590742.437	4939830.379	2398
7800	590695.228	4939924.481	2407
7801	590648.0189	4940018.583	2415
7802	590600.8098	4940112.685	2423
7803	590553.6007	4940206.788	2432
7804	590506.3916	4940300.89	2440
7805	590459.1825	4940394.992	2449
7806	590411.9735	4940489.094	2457
7807	590364.7644	4940583.196	2465
7808	590317.5553	4940677.298	2474
7809	590270.3462	4940771.4	2482
7810	590223.1371	4940865.502	2491
7811	590175.928	4940959.604	2499
7812	590128.719	4941053.706	2508
7813	590081.5099	4941147.808	2516
7814	590034.3008	4941241.91	2524
7815	589987.0917	4941336.012	2533
7816	589939.8826	4941430.115	2541
7817	589892.6735	4941524.217	2550
7818	589845.4644	4941618.319	2558
7819	589798.2554	4941712.421	2567
7820	589751.0463	4941806.523	2575
7821	589703.8372	4941900.625	2583
7822	589656.6281	4941994.727	2592
7823	589609.419	4942088.829	2600
7824	589562.2099	4942182.931	2609
7825	589515.0009	4942277.033	2617
7826	589467.7918	4942371.135	2626
7827	589420.5827	4942465.237	2634
7828	589373.3736	4942559.34	2642
7829	589326.1645	4942653.442	2651
7830	589278.9554	4942747.544	2659
7831	589231.7464	4942841.646	2668
7832	589184.5373	4942935.748	2676
7833	589137.3282	4943029.85	2684
7834	589090.1191	4943123.952	2693
7835	589042.91	4943218.054	2701
7836	588995.7009	4943312.156	2710
7837	588948.4918	4943406.258	2718
7838	588901.2828	4943500.36	2727
7839	588854.0737	4943594.462	2735
7840	588806.8646	4943688.564	2743
7841	588759.6555	4943782.667	2752
7842	588712.4464	4943876.769	2760
7843	588665.2373	4943970.871	2769

7844	588618.0283	4944064.973	2777	7900	585965.808	4949298.837	3247
7845	588570.8192	4944159.075	2786	7901	585918.3913	4949392.065	3255
7846	588523.6101	4944253.177	2794	7902	585870.9746	4949485.293	3263
7847	588476.401	4944347.279	2802	7903	585823.5579	4949578.52	3272
7848	588429.1919	4944441.381	2811	7904	585776.1413	4949671.748	3280
7849	588381.9828	4944535.483	2819	7905	585728.7246	4949764.976	3288
7850	588334.7738	4944629.585	2828	7906	585681.3079	4949858.203	3297
7851	588287.5647	4944723.687	2836	7907	585633.8912	4949951.431	3305
7852	588240.3556	4944817.789	2845	7908	585586.4745	4950044.659	3313
7853	588193.1465	4944911.892	2853	7909	585539.0578	4950137.886	3322
7854	588145.9374	4945005.994	2861	7910	585491.6412	4950231.114	3330
7855	588098.7283	4945100.096	2870	7911	585444.2245	4950324.341	3339
7856	588051.5193	4945194.198	2878	7912	585396.8078	4950417.569	3347
7857	588004.3102	4945288.3	2887	7913	585349.3911	4950510.797	3355
7858	587957.1011	4945382.402	2895	7914	585301.9744	4950604.024	3364
7859	587909.892	4945476.504	2903	7915	585254.5578	4950697.252	3372
7860	587862.4753	4945569.732	2912	7916	585207.1411	4950790.48	3380
7861	587815.0586	4945662.959	2920	7917	585159.7244	4950883.707	3389
7862	587767.642	4945756.187	2929	7918	585112.3077	4950976.935	3397
7863	587720.2253	4945849.415	2937	7919	585064.891	4951070.163	3406
7864	587672.8086	4945942.642	2945	7920	585017.4743	4951163.39	3414
7865	587625.3919	4946035.87	2954	7921	584970.0577	4951256.618	3422
7866	587577.9752	4946129.098	2962	7922	584922.641	4951349.846	3431
7867	587530.5585	4946222.325	2970	7923	584875.2243	4951443.073	3439
7868	587483.1419	4946315.553	2979	7924	584827.8076	4951536.301	3447
7869	587435.7252	4946408.78	2987	7925	584780.3909	4951629.528	3456
7870	587388.3085	4946502.008	2996	7926	584732.9742	4951722.756	3464
7871	587340.8918	4946595.236	3004	7927	584685.5576	4951815.984	3472
7872	587293.4751	4946688.463	3012	7928	584638.1409	4951909.211	3481
7873	587246.0584	4946781.691	3021	7929	584590.7242	4952002.439	3489
7874	587198.6418	4946874.919	3029	7930	584543.3075	4952095.667	3498
7875	587151.2251	4946968.146	3037	7931	584495.8908	4952188.894	3506
7876	587103.8084	4947061.374	3046	7932	584448.4741	4952282.122	3514
7877	587056.3917	4947154.602	3054	7933	584401.0575	4952375.35	3523
7878	587008.975	4947247.829	3062	7934	584353.6408	4952468.577	3531
7879	586961.5583	4947341.057	3071	7935	584306.2241	4952561.805	3539
7880	586914.1417	4947434.285	3079	7936	584258.8074	4952655.033	3548
7881	586866.725	4947527.512	3088	7937	584211.3907	4952748.26	3556
7882	586819.3083	4947620.74	3096	7938	584163.974	4952841.488	3564
7883	586771.8916	4947713.967	3104	7939	584116.5574	4952934.715	3573
7884	586724.4749	4947807.195	3113	7940	584069.1407	4953027.943	3581
7885	586677.0582	4947900.423	3121	7941	584021.724	4953121.171	3590
7886	586629.6416	4947993.65	3129	7942	583974.3073	4953214.398	3598
7887	586582.2249	4948086.878	3138	7943	583926.8906	4953307.626	3606
7888	586534.8082	4948180.106	3146	7944	583879.4739	4953400.854	3615
7889	586487.3915	4948273.333	3154	7945	583832.0573	4953494.081	3623
7890	586439.9748	4948366.561	3163	7946	583784.6406	4953587.309	3631
7891	586392.5581	4948459.789	3171	7947	583737.2239	4953680.537	3640
7892	586345.1415	4948553.016	3180	7948	583689.8072	4953773.764	3648
7893	586297.7248	4948646.244	3188	7949	583642.3905	4953866.992	3657
7894	586250.3081	4948739.472	3196	7950	583594.9738	4953960.22	3665
7895	586202.8914	4948832.699	3205	7951	583547.5572	4954053.447	3673
7896	586155.4747	4948925.927	3213	7952	583500.1405	4954146.675	3682
7897	586108.058	4949019.154	3221	7953	583452.7238	4954239.902	3690
7898	586060.6414	4949112.382	3230	7954	583405.3071	4954333.13	3698
7899	586013.2247	4949205.61	3238	7955	583357.8904	4954426.358	3707

7956	583310.4737	4954519.585	3715	8012	580655.1395	4959740.333	4184
7957	583263.0571	4954612.813	3723	8013	580607.7228	4959833.561	4192
7958	583215.6404	4954706.041	3732	8014	580560.3061	4959926.789	4200
7959	583168.2237	4954799.268	3740	8015	580512.8894	4960020.016	4209
7960	583120.807	4954892.496	3749	8016	580465.4728	4960113.244	4217
7961	583073.3903	4954985.724	3757	8017	580418.0561	4960206.472	4226
7962	583025.9736	4955078.951	3765	8018	580370.6394	4960299.699	4234
7963	582978.557	4955172.179	3774	8019	580323.2227	4960392.927	4242
7964	582931.1403	4955265.407	3782	8020	580275.806	4960486.155	4251
7965	582883.7236	4955358.634	3790	8021	580228.3893	4960579.382	4259
7966	582836.3069	4955451.862	3799	8022	580180.9727	4960672.61	4267
7967	582788.8902	4955545.089	3807	8023	580133.556	4960765.837	4276
7968	582741.4735	4955638.317	3816	8024	580086.1393	4960859.065	4284
7969	582694.0569	4955731.545	3824	8025	580038.7226	4960952.293	4292
7970	582646.6402	4955824.772	3832	8026	579991.3059	4961045.52	4301
7971	582599.2235	4955918	3841	8027	579943.8893	4961138.748	4309
7972	582551.8068	4956011.228	3849	8028	579896.4726	4961231.976	4318
7973	582504.3901	4956104.455	3857	8029	579849.0559	4961325.203	4326
7974	582456.9735	4956197.683	3866	8030	579801.6392	4961418.431	4334
7975	582409.5568	4956290.911	3874	8031	579754.2225	4961511.659	4343
7976	582362.1401	4956384.138	3882	8032	579706.8058	4961604.886	4351
7977	582314.7234	4956477.366	3891	8033	579659.3892	4961698.114	4359
7978	582267.3067	4956570.594	3899	8034	579611.9725	4961791.342	4368
7979	582219.89	4956663.821	3908	8035	579564.5558	4961884.569	4376
7980	582172.4734	4956757.049	3916	8036	579517.1391	4961977.797	4385
7981	582125.0567	4956850.276	3924	8037	579469.7224	4962071.024	4393
7982	582077.64	4956943.504	3933	8038	579422.3057	4962164.252	4401
7983	582030.2233	4957036.732	3941	8039	579374.8891	4962257.48	4410
7984	581982.8066	4957129.959	3949	8040	579327.4724	4962350.707	4418
7985	581935.3899	4957223.187	3958	8041	579280.0557	4962443.935	4426
7986	581887.9733	4957316.415	3966	8042	579232.639	4962537.163	4435
7987	581840.5566	4957409.642	3974	8043	579185.2223	4962630.39	4443
7988	581793.1399	4957502.87	3983	8044	579137.8056	4962723.618	4451
7989	581745.7232	4957596.098	3991	8045	579090.389	4962816.846	4460
7990	581698.3065	4957689.325	4000	8046	579042.9723	4962910.073	4468
7991	581650.8898	4957782.553	4008	8047	578995.5556	4963003.301	4477
7992	581603.4732	4957875.781	4016	8048	578948.1389	4963096.529	4485
7993	581556.0565	4957969.008	4025	8049	578900.7222	4963189.756	4493
7994	581508.6398	4958062.236	4033	8050	578853.3055	4963282.984	4502
7995	581461.2231	4958155.463	4041	8051	578805.8889	4963376.211	4510
7996	581413.8064	4958248.691	4050	8052	578758.4722	4963469.439	4518
7997	581366.3897	4958341.919	4058	8053	578711.0555	4963562.667	4527
7998	581318.9731	4958435.146	4067	8054	578663.6388	4963655.894	4535
7999	581271.5564	4958528.374	4075	8055	578616.2221	4963749.122	4543
8000	581224.1397	4958621.602	4083	8056	578568.8054	4963842.35	4552
8001	581176.723	4958714.829	4092	8057	578521.3888	4963935.577	4560
8002	581129.3063	4958808.057	4100	8058	578473.9721	4964028.805	4569
8003	581081.8896	4958901.285	4108	8059	578426.5554	4964122.033	4577
8004	581034.473	4958994.512	4117	8060	578379.1387	4964215.26	4585
8005	580987.0563	4959087.74	4125	8061	578331.722	4964308.488	4594
8006	580939.6396	4959180.968	4133	8062	578284.3053	4964401.716	4602
8007	580892.2229	4959274.195	4142	8063	578236.8887	4964494.943	4610
8008	580844.8062	4959367.423	4150	8064	578189.472	4964588.171	4619
8009	580797.3895	4959460.65	4159	8065	578142.0553	4964681.398	4627
8010	580749.9729	4959553.878	4167	8066	578094.6386	4964774.626	4636
8011	580702.5562	4959647.106	4175	8067	578047.2219	4964867.854	4644

8068	577999.8052	4964961.081	4652
8069	577952.3886	4965054.309	4661
8070	577904.9719	4965147.537	4669
8071	577857.5552	4965240.764	4677
8072	577810.1385	4965333.992	4686
8073	577762.7218	4965427.22	4694
8074	577715.3051	4965520.447	4702
8075	577667.8885	4965613.675	4711
8076	577620.4718	4965706.903	4719
8077	577573.0551	4965800.13	4728
8078	577525.6384	4965893.358	4736
8079	577478.2217	4965986.585	4744
8080	577430.805	4966079.813	4753
8081	577383.3884	4966173.041	4761
8082	577335.9717	4966266.268	4769
8083	577288.555	4966359.496	4778
8084	577240.3741	4966455.518	4786
8085	577192.1931	4966551.541	4795
8086	577144.0122	4966647.563	4804
8087	577095.8312	4966743.585	4812
8088	577047.6503	4966839.607	4821
8089	576999.4694	4966935.63	4829
8090	576951.2884	4967031.652	4838
8091	576903.1075	4967127.674	4847
8092	576854.9266	4967223.697	4855
8093	576806.7456	4967319.719	4864
8094	576758.5647	4967415.741	4872
8095	576710.3837	4967511.764	4881
8096	576662.2028	4967607.786	4890
8097	576614.0219	4967703.808	4898
8098	576565.8409	4967799.83	4907
8099	576517.66	4967895.853	4915
8100	576469.4791	4967991.875	4924
8101	576421.2981	4968087.897	4932
8102	576373.1172	4968183.92	4941
8103	576324.9362	4968279.942	4950
8104	576276.7553	4968375.964	4958
8105	576228.5744	4968471.987	4967
8106	576180.3934	4968568.009	4975
8107	576132.2125	4968664.031	4984
8108	576084.0316	4968760.053	4993
8109	576035.8506	4968856.076	5001
8110	575987.6697	4968952.098	5010
8111	575939.4887	4969048.12	5018
8112	575891.3078	4969144.143	5027
8113	575843.1269	4969240.165	5036
8114	575794.9459	4969336.187	5044
8115	575746.765	4969432.21	5053
8116	575698.5841	4969528.232	5061
8117	575650.4031	4969624.254	5070
8118	575602.2222	4969720.276	5079
8119	575554.0412	4969816.299	5087
8120	575505.8603	4969912.321	5096
8121	575457.6794	4970008.343	5104
8122	575409.4984	4970104.366	5113
8123	575361.3175	4970200.388	5122
8124	575313.1366	4970296.41	5130
8125	575264.9556	4970392.433	5139
8126	575216.7747	4970488.455	5147
8127	575168.5937	4970584.477	5156
8128	575120.4128	4970680.499	5165
8129	575072.2319	4970776.522	5173
8130	575024.0509	4970872.544	5182
8131	574975.87	4970968.566	5190
8132	574927.689	4971064.589	5199
8133	574879.5081	4971160.611	5208
8134	574831.3272	4971256.633	5216
8135	574783.1462	4971352.655	5225
8136	574734.9653	4971448.678	5233
8137	574686.7844	4971544.7	5242
8138	574638.6034	4971640.722	5250
8139	574590.4225	4971736.745	5259
8140	574542.2415	4971832.767	5268
8141	574494.0606	4971928.789	5276
8142	574445.8797	4972024.812	5285
8143	574397.6987	4972120.834	5293
8144	574349.5178	4972216.856	5302
8145	574301.3369	4972312.878	5311
8146	574253.1559	4972408.901	5319
8147	574204.975	4972504.923	5328
8148	574156.794	4972600.945	5336
8149	574108.6131	4972696.968	5345
8150	574060.4322	4972792.99	5354
8151	574012.2512	4972889.012	5362
8152	573964.0703	4972985.035	5371
8153	573915.8894	4973081.057	5379
8154	573867.7084	4973177.079	5388
8155	573819.5275	4973273.101	5397
8156	573771.3465	4973369.124	5405
8157	573723.1656	4973465.146	5414
8158	573674.9847	4973561.168	5422
8159	573626.8037	4973657.191	5431
8160	573578.6228	4973753.213	5440
8161	573530.4419	4973849.235	5448
8162	573482.2609	4973945.258	5457
8163	573434.08	4974041.28	5465
8164	573385.899	4974137.302	5474
8165	573337.7181	4974233.324	5483
8166	573289.5372	4974329.347	5491
8167	573241.3562	4974425.369	5500
8168	573193.1753	4974521.391	5508
8169	573144.9944	4974617.414	5517
8170	573096.8134	4974713.436	5526
8171	573048.6325	4974809.458	5534
8172	573000.4515	4974905.481	5543
8173	572952.2706	4975001.503	5551
8174	572904.0897	4975097.525	5560
8175	572855.9087	4975193.547	5568
8176	572807.7278	4975289.57	5577
8177	572759.5468	4975385.592	5586
8178	572711.3659	4975481.614	5594
8179	572663.185	4975577.637	5603

8180	572615.004	4975673.659	5611	8236	569916.8715	4981050.908	6093
8181	572566.8231	4975769.681	5620	8237	569868.6906	4981146.93	6101
8182	572518.6422	4975865.703	5629	8238	569820.5096	4981242.952	6110
8183	572470.4612	4975961.726	5637	8239	569772.3287	4981338.974	6119
8184	572422.2803	4976057.748	5646	8240	569724.1478	4981434.997	6127
8185	572374.0993	4976153.77	5654	8241	569675.9668	4981531.019	6136
8186	572325.9184	4976249.793	5663	8242	569627.7859	4981627.041	6144
8187	572277.7375	4976345.815	5672	8243	569579.605	4981723.064	6153
8188	572229.5565	4976441.837	5680	8244	569531.424	4981819.086	6162
8189	572181.3756	4976537.86	5689	8245	569483.2431	4981915.108	6170
8190	572133.1947	4976633.882	5697	8246	569435.0621	4982011.131	6179
8191	572085.0137	4976729.904	5706	8247	569386.8812	4982107.153	6187
8192	572036.8328	4976825.926	5715	8248	569338.7003	4982203.175	6196
8193	571988.6518	4976921.949	5723	8249	569290.5193	4982299.197	6204
8194	571940.4709	4977017.971	5732	8250	569242.3384	4982395.22	6213
8195	571892.29	4977113.993	5740	8251	569194.1575	4982491.242	6222
8196	571844.109	4977210.016	5749	8252	569145.9765	4982587.264	6230
8197	571795.9281	4977306.038	5758	8253	569097.7956	4982683.287	6239
8198	571747.7472	4977402.06	5766	8254	569049.6146	4982779.309	6247
8199	571699.5662	4977498.083	5775	8255	569001.4337	4982875.331	6256
8200	571651.3853	4977594.105	5783	8256	568953.2528	4982971.354	6265
8201	571603.2043	4977690.127	5792	8257	568905.0718	4983067.376	6273
8202	571555.0234	4977786.149	5801	8258	568856.8909	4983163.398	6282
8203	571506.8425	4977882.172	5809	8259	568808.71	4983259.42	6290
8204	571458.6615	4977978.194	5818	8260	568760.529	4983355.443	6299
8205	571410.4806	4978074.216	5826	8261	568712.3481	4983451.465	6308
8206	571362.2997	4978170.239	5835	8262	568664.1671	4983547.487	6316
8207	571314.1187	4978266.261	5844	8263	568615.9862	4983643.51	6325
8208	571265.9378	4978362.283	5852	8264	568567.8053	4983739.532	6333
8209	571217.7568	4978458.306	5861	8265	568519.6243	4983835.554	6342
8210	571169.5759	4978554.328	5869	8266	568471.4434	4983931.576	6351
8211	571121.395	4978650.35	5878	8267	568423.2624	4984027.599	6359
8212	571073.214	4978746.372	5886	8268	568375.0815	4984123.621	6368
8213	571025.0331	4978842.395	5895	8269	568326.9006	4984219.643	6376
8214	570976.8522	4978938.417	5904	8270	568278.7196	4984315.666	6385
8215	570928.6712	4979034.439	5912	8271	568230.5387	4984411.688	6394
8216	570880.4903	4979130.462	5921	8272	568182.3578	4984507.71	6402
8217	570832.3093	4979226.484	5929	8273	568134.1768	4984603.733	6411
8218	570784.1284	4979322.506	5938	8274	568085.9959	4984699.755	6419
8219	570735.9475	4979418.528	5947	8275	568037.8149	4984795.777	6428
8220	570687.7665	4979514.551	5955	8276	567989.634	4984891.799	6437
8221	570639.5856	4979610.573	5964	8277	567941.4531	4984987.822	6445
8222	570591.4046	4979706.595	5972	8278	567893.2721	4985083.844	6454
8223	570543.2237	4979802.618	5981	8279	567845.0912	4985179.866	6462
8224	570495.0428	4979898.64	5990	8280	567796.9103	4985275.889	6471
8225	570446.8618	4979994.662	5998	8281	567748.7293	4985371.911	6480
8226	570398.6809	4980090.685	6007	8282	567700.5484	4985467.933	6488
8227	570350.5	4980186.707	6015	8283	567652.3674	4985563.956	6497
8228	570302.319	4980282.729	6024	8284	567604.1865	4985659.978	6505
8229	570254.1381	4980378.751	6033	8285	567556.0056	4985756	6514
8230	570205.9571	4980474.774	6041	8286	567507.8246	4985852.022	6522
8231	570157.7762	4980570.796	6050	8287	567459.6437	4985948.045	6531
8232	570109.5953	4980666.818	6058	8288	567411.4628	4986044.067	6540
8233	570061.4143	4980762.841	6067	8289	567363.2818	4986140.089	6548
8234	570013.2334	4980858.863	6076	8290	567315.1009	4986236.112	6557
8235	569965.0525	4980954.885	6084	8291	567266.9199	4986332.134	6565

8292	567218.739	4986428.156	6574	8348	564556.8051	4991720.773	7048
8293	567170.5581	4986524.179	6583	8349	564509.5291	4991814.679	7056
8294	567122.3771	4986620.201	6591	8350	564462.2531	4991908.586	7065
8295	567074.1962	4986716.223	6600	8351	564414.9771	4992002.492	7073
8296	567026.0153	4986812.245	6608	8352	564367.7012	4992096.399	7082
8297	566977.8343	4986908.268	6617	8353	564320.4252	4992190.305	7090
8298	566929.6534	4987004.29	6626	8354	564273.1492	4992284.211	7098
8299	566881.4724	4987100.312	6634	8355	564225.8733	4992378.118	7107
8300	566833.2915	4987196.335	6643	8356	564178.5973	4992472.024	7115
8301	566785.1106	4987292.357	6651	8357	564131.3213	4992565.931	7124
8302	566736.9296	4987388.379	6660	8358	564084.0453	4992659.837	7132
8303	566688.7487	4987484.402	6669	8359	564036.7694	4992753.744	7141
8304	566640.5678	4987580.424	6677	8360	563989.4934	4992847.65	7149
8305	566592.3868	4987676.446	6686	8361	563942.2174	4992941.557	7157
8306	566544.2059	4987772.468	6694	8362	563894.9414	4993035.463	7166
8307	566496.0249	4987868.491	6703	8363	563847.6655	4993129.37	7174
8308	566447.844	4987964.513	6712	8364	563800.3895	4993223.276	7183
8309	566400.568	4988058.419	6720	8365	563753.1135	4993317.183	7191
8310	566353.2921	4988152.326	6728	8366	563705.8375	4993411.089	7199
8311	566306.0161	4988246.232	6737	8367	563658.5616	4993504.996	7208
8312	566258.7401	4988340.139	6745	8368	563611.2856	4993598.902	7216
8313	566211.4641	4988434.045	6754	8369	563564.0096	4993692.809	7225
8314	566164.1882	4988527.952	6762	8370	563516.7337	4993786.715	7233
8315	566116.9122	4988621.858	6770	8371	563469.4577	4993880.622	7241
8316	566069.6362	4988715.765	6779	8372	563422.1817	4993974.528	7250
8317	566022.3602	4988809.671	6787	8373	563374.9057	4994068.435	7258
8318	565975.0843	4988903.578	6796	8374	563327.6298	4994162.341	7267
8319	565927.8083	4988997.484	6804	8375	563280.3538	4994256.248	7275
8320	565880.5323	4989091.391	6812	8376	563233.0778	4994350.154	7283
8321	565833.2563	4989185.297	6821	8377	563185.8018	4994444.061	7292
8322	565785.9804	4989279.204	6829	8378	563138.5259	4994537.967	7300
8323	565738.7044	4989373.11	6838	8379	563091.2499	4994631.874	7309
8324	565691.4284	4989467.017	6846	8380	563043.9739	4994725.78	7317
8325	565644.1525	4989560.923	6855	8381	562996.6979	4994819.687	7326
8326	565596.8765	4989654.83	6863	8382	562949.422	4994913.593	7334
8327	565549.6005	4989748.736	6871	8383	562902.146	4995007.5	7342
8328	565502.3245	4989842.643	6880	8384	562854.87	4995101.406	7351
8329	565455.0486	4989936.549	6888	8385	562807.5941	4995195.313	7359
8330	565407.7726	4990030.456	6897	8386	562760.3181	4995289.219	7368
8331	565360.4966	4990124.362	6905	8387	562713.0421	4995383.126	7376
8332	565313.2206	4990218.269	6913	8388	562665.7661	4995477.032	7384
8333	565265.9447	4990312.175	6922	8389	562618.4902	4995570.939	7393
8334	565218.6687	4990406.082	6930	8390	562571.2142	4995664.845	7401
8335	565171.3927	4990499.988	6939	8391	562523.9382	4995758.752	7410
8336	565124.1167	4990593.895	6947	8392	562476.6622	4995852.658	7418
8337	565076.8408	4990687.801	6955	8393	562429.3863	4995946.565	7426
8338	565029.5648	4990781.708	6964	8394	562382.1103	4996040.471	7435
8339	564982.2888	4990875.614	6972	8395	562334.8343	4996134.378	7443
8340	564935.0129	4990969.521	6981	8396	562287.5583	4996228.284	7452
8341	564887.7369	4991063.427	6989	8397	562240.2824	4996322.191	7460
8342	564840.4609	4991157.334	6998	8398	562193.0064	4996416.097	7469
8343	564793.1849	4991251.24	7006	8399	562145.7304	4996510.003	7477
8344	564745.909	4991345.147	7014	8400	562098.4545	4996603.91	7485
8345	564698.633	4991439.053	7023	8401	562051.1785	4996697.816	7494
8346	564651.357	4991532.96	7031	8402	562003.9025	4996791.723	7502
8347	564604.081	4991626.866	7040	8403	561956.6265	4996885.629	7511

8404	561909.3506	4996979.536	7519	8460	559261.8961	5002238.299	7990
8405	561862.0746	4997073.442	7527	8461	559214.6201	5002332.206	7998
8406	561814.7986	4997167.349	7536	8462	559167.3441	5002426.112	8007
8407	561767.5226	4997261.255	7544	8463	559120.0681	5002520.019	8015
8408	561720.2467	4997355.162	7553	8464	559072.7922	5002613.925	8024
8409	561672.9707	4997449.068	7561	8465	559025.5162	5002707.832	8032
8410	561625.6947	4997542.975	7569	8466	558978.2402	5002801.738	8040
8411	561578.4187	4997636.881	7578	8467	558930.9642	5002895.645	8049
8412	561531.1428	4997730.788	7586	8468	558883.6883	5002989.551	8057
8413	561483.8668	4997824.694	7595	8469	558836.4123	5003083.458	8066
8414	561436.5908	4997918.601	7603	8470	558789.1363	5003177.364	8074
8415	561389.3149	4998012.507	7612	8471	558741.8603	5003271.271	8083
8416	561342.0389	4998106.414	7620	8472	558694.5844	5003365.177	8091
8417	561294.7629	4998200.32	7628	8473	558647.3084	5003459.084	8099
8418	561247.4869	4998294.227	7637	8474	558600.0324	5003552.99	8108
8419	561200.211	4998388.133	7645	8475	558552.7565	5003646.897	8116
8420	561152.935	4998482.04	7654	8476	558505.4805	5003740.803	8125
8421	561105.659	4998575.946	7662	8477	558458.2045	5003834.71	8133
8422	561058.383	4998669.853	7670	8478	558410.9285	5003928.616	8141
8423	561011.1071	4998763.759	7679	8479	558363.6526	5004022.523	8150
8424	560963.8311	4998857.666	7687	8480	558316.3766	5004116.429	8158
8425	560916.5551	4998951.572	7696	8481	558269.1006	5004210.336	8167
8426	560869.2791	4999045.479	7704	8482	558221.8246	5004304.242	8175
8427	560822.0032	4999139.385	7712	8483	558174.5487	5004398.149	8183
8428	560774.7272	4999233.292	7721	8484	558127.2727	5004492.055	8192
8429	560727.4512	4999327.198	7729	8485	558079.9967	5004585.962	8200
8430	560680.1753	4999421.105	7738	8486	558032.7207	5004679.868	8209
8431	560632.8993	4999515.011	7746	8487	557985.4448	5004773.775	8217
8432	560585.6233	4999608.918	7754	8488	557938.1688	5004867.681	8226
8433	560538.3473	4999702.824	7763	8489	557890.8928	5004961.587	8234
8434	560491.0714	4999796.731	7771	8490	557843.6169	5005055.494	8242
8435	560443.7954	4999890.637	7780	8491	557796.3409	5005149.4	8251
8436	560396.5194	4999984.544	7788	8492	557749.0649	5005243.307	8259
8437	560349.2434	5000078.45	7797	8493	557701.7889	5005337.213	8268
8438	560301.9675	5000172.357	7805	8494	557654.513	5005431.12	8276
8439	560254.6915	5000266.263	7813	8495	557607.237	5005525.026	8284
8440	560207.4155	5000360.17	7822	8496	557559.961	5005618.933	8293
8441	560160.1395	5000454.076	7830	8497	557512.685	5005712.839	8301
8442	560112.8636	5000547.983	7839	8498	557465.4091	5005806.746	8310
8443	560065.5876	5000641.889	7847	8499	557418.1331	5005900.652	8318
8444	560018.3116	5000735.795	7855	8500	557370.8571	5005994.559	8326
8445	559971.0357	5000829.702	7864	8501	557323.5811	5006088.465	8335
8446	559923.7597	5000923.608	7872	8502	557276.3052	5006182.372	8343
8447	559876.4837	5001017.515	7881	8503	557229.0292	5006276.278	8352
8448	559829.2077	5001111.421	7889	8504	557181.7532	5006370.185	8360
8449	559781.9318	5001205.328	7897	8505	557134.4773	5006464.091	8368
8450	559734.6558	5001299.234	7906	8506	557087.2013	5006557.998	8377
8451	559687.3798	5001393.141	7914	8507	557039.9253	5006651.904	8385
8452	559640.1038	5001487.047	7923	8508	556992.6493	5006745.811	8394
8453	559592.8279	5001580.954	7931	8509	556945.3734	5006839.717	8402
8454	559545.5519	5001674.86	7940	8510	556898.0974	5006933.624	8411
8455	559498.2759	5001768.767	7948	8511	556850.8214	5007027.53	8419
8456	559450.9999	5001862.673	7956	8512	556803.5454	5007121.437	8427
8457	559403.724	5001956.58	7965	8513	556756.2695	5007215.343	8436
8458	559356.448	5002050.486	7973	8514	556708.9935	5007309.25	8444
8459	559309.172	5002144.393	7982	8515	556661.7175	5007403.156	8453

8516	556614.4415	5007497.063	8461	8572	554000.7729	5012604.373	8920
8517	556567.1656	5007590.969	8469	8573	553954.3633	5012694.397	8928
8518	556519.8896	5007684.876	8478	8574	553907.9536	5012784.42	8936
8519	556472.6136	5007778.782	8486	8575	553861.5439	5012874.443	8944
8520	556425.3377	5007872.689	8495	8576	553815.1343	5012964.466	8952
8521	556378.0617	5007966.595	8503	8577	553768.7246	5013054.489	8961
8522	556330.7857	5008060.502	8511	8578	553722.3149	5013144.512	8969
8523	556283.5097	5008154.408	8520	8579	553675.9053	5013234.535	8977
8524	556236.2338	5008248.315	8528	8580	553629.4956	5013324.558	8985
8525	556188.9578	5008342.221	8537	8581	553583.0859	5013414.581	8993
8526	556141.6818	5008436.128	8545	8582	553536.6763	5013504.604	9001
8527	556094.4058	5008530.034	8554	8583	553490.2666	5013594.627	9009
8528	556047.1299	5008623.941	8562	8584	553443.8569	5013684.651	9017
8529	555999.8539	5008717.847	8570	8585	553397.4473	5013774.674	9025
8530	555952.5779	5008811.754	8579	8586	553351.0376	5013864.697	9033
8531	555905.3019	5008905.66	8587	8587	553304.6279	5013954.72	9042
8532	555858.026	5008999.567	8596	8588	553258.2183	5014044.743	9050
8533	555810.75	5009093.473	8604	8589	553211.8086	5014134.766	9058
8534	555764.3403	5009183.496	8612	8590	553165.3989	5014224.789	9066
8535	555717.9307	5009273.519	8620	8591	553118.9892	5014314.812	9074
8536	555671.521	5009363.542	8628	8592	553072.5796	5014404.835	9082
8537	555625.1113	5009453.565	8636	8593	553026.1699	5014494.858	9090
8538	555578.7017	5009543.588	8645	8594	552979.7602	5014584.881	9098
8539	555532.292	5009633.612	8653	8595	552933.3506	5014674.904	9106
8540	555485.8823	5009723.635	8661	8596	552886.9409	5014764.928	9114
8541	555439.4727	5009813.658	8669	8597	552840.5312	5014854.951	9123
8542	555393.063	5009903.681	8677	8598	552794.1216	5014944.974	9131
8543	555346.6533	5009993.704	8685	8599	552747.7119	5015034.997	9139
8544	555300.2437	5010083.727	8693	8600	552701.3022	5015125.02	9147
8545	555253.834	5010173.75	8701	8601	552654.8926	5015215.043	9155
8546	555207.4243	5010263.773	8709	8602	552608.4829	5015305.066	9163
8547	555161.0146	5010353.796	8717	8603	552562.0732	5015395.089	9171
8548	555114.605	5010443.819	8726	8604	552515.6636	5015485.112	9179
8549	555068.1953	5010533.842	8734	8605	552469.2539	5015575.135	9187
8550	555021.7856	5010623.866	8742	8606	552422.8442	5015665.158	9195
8551	554975.376	5010713.889	8750	8607	552376.4346	5015755.182	9204
8552	554928.9663	5010803.912	8758	8608	552330.0249	5015845.205	9212
8553	554882.5566	5010893.935	8766	8609	552283.6152	5015935.228	9220
8554	554836.147	5010983.958	8774	8610	552237.2056	5016025.251	9228
8555	554789.7373	5011073.981	8782	8611	552190.7959	5016115.274	9236
8556	554743.3276	5011164.004	8790	8612	552144.3862	5016205.297	9244
8557	554696.918	5011254.027	8798	8613	552097.9765	5016295.32	9252
8558	554650.5083	5011344.05	8807	8614	552051.5669	5016385.343	9260
8559	554604.0986	5011434.073	8815	8615	552005.1572	5016475.366	9268
8560	554557.689	5011524.096	8823	8616	551958.7475	5016565.389	9277
8561	554511.2793	5011614.119	8831	8617	551912.3379	5016655.412	9285
8562	554464.8696	5011704.143	8839	8618	551865.9282	5016745.436	9293
8563	554418.46	5011794.166	8847	8619	551819.5185	5016835.459	9301
8564	554372.0503	5011884.189	8855	8620	551773.1089	5016925.482	9309
8565	554325.6406	5011974.212	8863	8621	551726.6992	5017015.505	9317
8566	554279.231	5012064.235	8871	8622	551680.2895	5017105.528	9325
8567	554232.8213	5012154.258	8879	8623	551633.8799	5017195.551	9333
8568	554186.4116	5012244.281	8888	8624	551587.4702	5017285.574	9341
8569	554140.0019	5012334.304	8896	8625	551541.0605	5017375.597	9349
8570	554093.5923	5012424.327	8904	8626	551494.6509	5017465.62	9358
8571	554047.1826	5012514.35	8912	8627	551448.2412	5017555.643	9366

8628	551401.8315	5017645.666	9374	8684	548802.8901	5022686.959	9827
8629	551355.4219	5017735.689	9382	8685	548756.4804	5022776.982	9836
8630	551309.0122	5017825.713	9390	8686	548710.0708	5022867.006	9844
8631	551262.6025	5017915.736	9398	8687	548663.6611	5022957.029	9852
8632	551216.1929	5018005.759	9406	8688	548617.2514	5023047.052	9860
8633	551169.7832	5018095.782	9414	8689	548570.8418	5023137.075	9868
8634	551123.3735	5018185.805	9422	8690	548524.4321	5023227.098	9876
8635	551076.9638	5018275.828	9430	8691	548478.0224	5023317.121	9884
8636	551030.5542	5018365.851	9439	8692	548431.6128	5023407.144	9892
8637	550984.1445	5018455.874	9447	8693	548385.2031	5023497.167	9900
8638	550937.7348	5018545.897	9455	8694	548338.7934	5023587.19	9909
8639	550891.3252	5018635.92	9463	8695	548292.3838	5023677.213	9917
8640	550844.9155	5018725.943	9471	8696	548245.9741	5023767.236	9925
8641	550798.5058	5018815.967	9479	8697	548199.5644	5023857.26	9933
8642	550752.0962	5018905.99	9487	8698	548153.1548	5023947.283	9941
8643	550705.6865	5018996.013	9495	8699	548106.7451	5024037.306	9949
8644	550659.2768	5019086.036	9503	8700	548060.3354	5024127.329	9957
8645	550612.8672	5019176.059	9511	8701	548013.9258	5024217.352	9965
8646	550566.4575	5019266.082	9520	8702	547967.5161	5024307.375	9973
8647	550520.0478	5019356.105	9528	8703	547921.1064	5024397.398	9981
8648	550473.6382	5019446.128	9536	8704	547874.6967	5024487.421	9990
8649	550427.2285	5019536.151	9544	8705	547828.2871	5024577.444	9998
8650	550380.8188	5019626.174	9552	8706	547781.8774	5024667.467	10006
8651	550334.4092	5019716.197	9560	8707	547735.4677	5024757.49	10014
8652	550287.9995	5019806.221	9568	8708	547689.0581	5024847.513	10022
8653	550241.5898	5019896.244	9576	8709	547642.6484	5024937.537	10030
8654	550195.1802	5019986.267	9584	8710	547596.2387	5025027.56	10038
8655	550148.7705	5020076.29	9593	8711	547549.8291	5025117.583	10046
8656	550102.3608	5020166.313	9601	8712	547503.4194	5025207.606	10054
8657	550055.9512	5020256.336	9609	8713	547457.0097	5025297.629	10062
8658	550009.5415	5020346.359	9617	8714	547410.6001	5025387.652	10071
8659	549963.1318	5020436.382	9625	8715	547364.1904	5025477.675	10079
8660	549916.7221	5020526.405	9633	8716	547317.7807	5025567.698	10087
8661	549870.3125	5020616.428	9641	8717	547271.3711	5025657.721	10095
8662	549823.9028	5020706.451	9649	8718	547224.9614	5025747.744	10103
8663	549777.4931	5020796.475	9657	8719	547178.5517	5025837.767	10111
8664	549731.0835	5020886.498	9665	8720	547132.1421	5025927.791	10119
8665	549684.6738	5020976.521	9674	8721	547085.7324	5026017.814	10127
8666	549638.2641	5021066.544	9682	8722	547039.3227	5026107.837	10135
8667	549591.8545	5021156.567	9690	8723	546992.9131	5026197.86	10143
8668	549545.4448	5021246.59	9698	8724	546946.5034	5026287.883	10152
8669	549499.0351	5021336.613	9706	8725	546900.0937	5026377.906	10160
8670	549452.6255	5021426.636	9714	8726	546853.684	5026467.929	10168
8671	549406.2158	5021516.659	9722	8727	546807.2744	5026557.952	10176
8672	549359.8061	5021606.682	9730	8728	546760.8647	5026647.975	10184
8673	549313.3965	5021696.705	9738	8729	546714.455	5026737.998	10192
8674	549266.9868	5021786.728	9746	8730	546668.0454	5026828.021	10200
8675	549220.5771	5021876.752	9755	8731	546621.6357	5026918.045	10208
8676	549174.1675	5021966.775	9763	8732	546575.226	5027008.068	10216
8677	549127.7578	5022056.798	9771	8733	546528.8164	5027098.091	10225
8678	549081.3481	5022146.821	9779	8734	546482.4067	5027188.114	10233
8679	549034.9385	5022236.844	9787	8735	546435.997	5027278.137	10241
8680	548988.5288	5022326.867	9795	8736	546389.5874	5027368.16	10249
8681	548942.1191	5022416.89	9803	8737	546343.1777	5027458.183	10257
8682	548895.7094	5022506.913	9811	8738	546296.768	5027548.206	10265
8683	548849.2998	5022596.936	9819	8739	546250.3584	5027638.229	10273

8740	546203.9487	5027728.252	10281
8741	546157.539	5027818.275	10289
8742	546111.1294	5027908.298	10297
8743	546064.7197	5027998.322	10306
8744	546018.31	5028088.345	10314
8745	545971.9004	5028178.368	10322
8746	545925.4907	5028268.391	10330
8747	545879.081	5028358.414	10338
8748	545832.6713	5028448.437	10346
8749	545786.2617	5028538.46	10354
8750	545739.852	5028628.483	10362
8751	545693.4423	5028718.506	10370
8752	545647.0327	5028808.529	10378
8753	545600.623	5028898.552	10387
8754	545554.2133	5028988.576	10395
8755	545507.8037	5029078.599	10403
8756	545461.394	5029168.622	10411
8757	545414.9843	5029258.645	10419
8758	545368.5747	5029348.668	10427
8759	545322.165	5029438.691	10435
8760	545277.9887	5029528.018	10443
8761	545233.8125	5029617.346	10451
8762	545189.6362	5029706.673	10459
8763	545145.46	5029796	10467
8764	545101.2837	5029885.328	10475
8765	545057.1075	5029974.655	10483
8766	545012.9312	5030063.982	10491
8767	544968.7549	5030153.31	10499
8768	544924.5787	5030242.637	10507
8769	544880.4024	5030331.964	10515
8770	544836.2262	5030421.292	10523
8771	544792.0499	5030510.619	10531
8772	544747.8737	5030599.946	10539
8773	544703.6974	5030689.274	10547
8774	544659.5212	5030778.601	10555
8775	544615.3449	5030867.928	10563
8776	544571.1686	5030957.256	10571
8777	544526.9924	5031046.583	10579
8778	544482.8161	5031135.91	10587
8779	544438.6399	5031225.238	10595
8780	544394.4636	5031314.565	10603
8781	544350.2874	5031403.892	10611
8782	544306.1111	5031493.22	10619
8783	544261.9348	5031582.547	10627
8784	544217.7586	5031671.874	10634
8785	544173.5823	5031761.202	10642
8786	544129.4061	5031850.529	10650
8787	544085.2298	5031939.856	10658
8788	544041.0536	5032029.184	10666
8789	543996.8773	5032118.511	10674
8790	543952.701	5032207.838	10682
8791	543908.5248	5032297.166	10690
8792	543864.3485	5032386.493	10698
8793	543820.1723	5032475.82	10706
8794	543775.996	5032565.148	10714
8795	543731.8198	5032654.475	10722
8796	543687.6435	5032743.802	10730
8797	543643.4672	5032833.13	10738
8798	543599.291	5032922.457	10746
8799	543555.1147	5033011.784	10754
8800	543510.9385	5033101.112	10762
8801	543466.7622	5033190.439	10770
8802	543422.586	5033279.766	10778
8803	543378.4097	5033369.094	10786
8804	543334.2335	5033458.421	10794
8805	543290.0572	5033547.748	10802
8806	543245.8809	5033637.076	10810
8807	543201.7047	5033726.403	10818
8808	543157.5284	5033815.73	10826
8809	543113.3522	5033905.058	10834
8810	543069.1759	5033994.385	10842
8811	543024.9997	5034083.712	10850
8812	542980.8234	5034173.04	10858
8813	542936.6471	5034262.367	10866
8814	542892.4709	5034351.694	10874
8815	542848.2946	5034441.022	10882
8816	542804.1184	5034530.349	10890
8817	542759.9421	5034619.677	10898
8818	542715.7659	5034709.004	10906
8819	542671.5896	5034798.331	10914
8820	542627.4133	5034887.659	10921
8821	542583.2371	5034976.986	10929
8822	542539.0608	5035066.313	10937
8823	542494.8846	5035155.641	10945
8824	542450.7083	5035244.968	10953
8825	542406.5321	5035334.295	10961
8826	542362.3558	5035423.623	10969
8827	542318.1795	5035512.95	10977
8828	542274.0033	5035602.277	10985
8829	542229.827	5035691.605	10993
8830	542185.6508	5035780.932	11001
8831	542141.4745	5035870.259	11009
8832	542097.2983	5035959.587	11017
8833	542053.122	5036048.914	11025
8834	542008.9458	5036138.241	11033
8835	541964.7695	5036227.569	11041
8836	541920.5932	5036316.896	11049
8837	541876.417	5036406.223	11057
8838	541832.2407	5036495.551	11065
8839	541788.0645	5036584.878	11073
8840	541743.8882	5036674.205	11081
8841	541699.712	5036763.533	11089
8842	541655.5357	5036852.86	11097
8843	541611.3594	5036942.187	11105
8844	541567.1832	5037031.515	11113
8845	541523.0069	5037120.842	11121
8846	541478.8307	5037210.169	11129
8847	541434.6544	5037299.497	11137
8848	541390.4782	5037388.824	11145
8849	541346.3019	5037478.151	11153
8850	541302.1256	5037567.479	11161
8851	541257.9494	5037656.806	11169

8852	541213.7731	5037746.133	11177	8908	538624.261	5042773.585	11623
8853	541169.5969	5037835.461	11185	8909	538576.8725	5042863.61	11631
8854	541125.4206	5037924.788	11193	8910	538529.484	5042953.635	11639
8855	541081.2444	5038014.115	11201	8911	538482.0955	5043043.661	11647
8856	541037.0681	5038103.443	11208	8912	538434.7069	5043133.686	11655
8857	540992.8918	5038192.77	11216	8913	538387.3184	5043223.711	11663
8858	540948.7156	5038282.097	11224	8914	538339.9299	5043313.736	11671
8859	540904.5393	5038371.425	11232	8915	538292.5413	5043403.761	11679
8860	540860.3631	5038460.752	11240	8916	538245.1528	5043493.786	11687
8861	540816.1868	5038550.079	11248	8917	538197.7643	5043583.811	11695
8862	540772.0106	5038639.407	11256	8918	538150.3758	5043673.837	11703
8863	540727.8343	5038728.734	11264	8919	538102.9872	5043763.862	11711
8864	540683.6581	5038818.061	11272	8920	538055.5987	5043853.887	11719
8865	540639.4818	5038907.389	11280	8921	538008.2102	5043943.912	11727
8866	540595.3055	5038996.716	11288	8922	537960.8217	5044033.937	11735
8867	540551.1293	5039086.043	11296	8923	537913.4331	5044123.962	11743
8868	540506.953	5039175.371	11304	8924	537866.0446	5044213.987	11751
8869	540462.7768	5039264.698	11312	8925	537818.6561	5044304.013	11759
8870	540418.6005	5039354.025	11320	8926	537771.2676	5044394.038	11767
8871	540374.4243	5039443.353	11328	8927	537723.879	5044484.063	11775
8872	540330.248	5039532.68	11336	8928	537676.4905	5044574.088	11782
8873	540282.8595	5039622.705	11344	8929	537629.102	5044664.113	11790
8874	540235.4709	5039712.73	11352	8930	537581.7134	5044754.138	11798
8875	540188.0824	5039802.755	11360	8931	537534.3249	5044844.163	11806
8876	540140.6939	5039892.781	11368	8932	537486.9364	5044934.189	11814
8877	540093.3054	5039982.806	11376	8933	537439.5479	5045024.214	11822
8878	540045.9168	5040072.831	11384	8934	537392.1593	5045114.239	11830
8879	539998.5283	5040162.856	11392	8935	537344.7708	5045204.264	11838
8880	539951.1398	5040252.881	11400	8936	537297.3823	5045294.289	11846
8881	539903.7513	5040342.906	11408	8937	537249.9938	5045384.314	11854
8882	539856.3627	5040432.931	11416	8938	537202.6052	5045474.339	11862
8883	539808.9742	5040522.957	11424	8939	537155.2167	5045564.365	11870
8884	539761.5857	5040612.982	11432	8940	537107.8282	5045654.39	11878
8885	539714.1972	5040703.007	11440	8941	537060.4397	5045744.415	11886
8886	539666.8086	5040793.032	11448	8942	537013.0511	5045834.44	11894
8887	539619.4201	5040883.057	11456	8943	536965.6626	5045924.465	11902
8888	539572.0316	5040973.082	11464	8944	536918.2741	5046014.49	11910
8889	539524.643	5041063.107	11472	8945	536870.8855	5046104.515	11918
8890	539477.2545	5041153.133	11480	8946	536823.497	5046194.541	11926
8891	539429.866	5041243.158	11488	8947	536776.1085	5046284.566	11934
8892	539382.4775	5041333.183	11495	8948	536728.72	5046374.591	11942
8893	539335.0889	5041423.208	11503	8949	536681.3314	5046464.616	11950
8894	539287.7004	5041513.233	11511	8950	536633.9429	5046554.641	11958
8895	539240.3119	5041603.258	11519	8951	536586.5544	5046644.666	11966
8896	539192.9234	5041693.283	11527	8952	536539.1659	5046734.691	11974
8897	539145.5348	5041783.309	11535	8953	536491.7773	5046824.717	11982
8898	539098.1463	5041873.334	11543	8954	536444.3888	5046914.742	11990
8899	539050.7578	5041963.359	11551	8955	536397.0003	5047004.767	11998
8900	539003.3692	5042053.384	11559	8956	536349.6117	5047094.792	12006
8901	538955.9807	5042143.409	11567	8957	536302.2232	5047184.817	12014
8902	538908.5922	5042233.434	11575	8958	536254.8347	5047274.842	12022
8903	538861.2037	5042323.459	11583	8959	536207.4462	5047364.867	12030
8904	538813.8151	5042413.485	11591	8960	536160.0576	5047454.893	12038
8905	538766.4266	5042503.51	11599	8961	536112.6691	5047544.918	12046
8906	538719.0381	5042593.535	11607	8962	536065.2806	5047634.943	12054
8907	538671.6496	5042683.56	11615	8963	536017.8921	5047724.968	12062

8964	535970.5035	5047814.993	12069	9020	533485.6879	5052611.938	12517
8965	535923.115	5047905.018	12077	9021	533442.9922	5052695.172	12524
8966	535875.7265	5047995.043	12085	9022	533400.2965	5052778.407	12532
8967	535828.338	5048085.069	12093	9023	533357.6008	5052861.641	12539
8968	535780.9494	5048175.094	12101	9024	533314.9051	5052944.876	12547
8969	535733.5609	5048265.119	12109	9025	533272.2094	5053028.11	12554
8970	535686.1724	5048355.144	12117	9026	533229.5138	5053111.345	12562
8971	535638.7838	5048445.169	12125	9027	533186.8181	5053194.579	12569
8972	535591.3953	5048535.194	12133	9028	533144.1224	5053277.814	12577
8973	535544.0068	5048625.219	12141	9029	533101.4267	5053361.048	12584
8974	535496.6183	5048715.245	12149	9030	533058.731	5053444.283	12592
8975	535449.2297	5048805.27	12157	9031	533016.0353	5053527.517	12599
8976	535401.8412	5048895.295	12165	9032	532973.3396	5053610.752	12607
8977	535354.4527	5048985.32	12173	9033	532930.6439	5053693.986	12614
8978	535307.0642	5049075.345	12181	9034	532887.9482	5053777.221	12622
8979	535259.6756	5049165.37	12189	9035	532845.2525	5053860.455	12629
8980	535212.2871	5049255.395	12197	9036	532802.5568	5053943.69	12637
8981	535164.8986	5049345.421	12205	9037	532759.8611	5054026.924	12644
8982	535117.5101	5049435.446	12213	9038	532717.1654	5054110.159	12652
8983	535070.1215	5049525.471	12221	9039	532674.4697	5054193.393	12659
8984	535022.733	5049615.496	12248	9040	532631.774	5054276.628	12667
8985	534980.0373	5049698.73	12255	9041	532589.0783	5054359.862	12674
8986	534937.3416	5049781.965	12263	9042	532546.3826	5054443.097	12682
8987	534894.6459	5049865.199	12270	9043	532503.6869	5054526.331	12689
8988	534851.9502	5049948.434	12278	9044	532460.9912	5054609.566	12697
8989	534809.2545	5050031.668	12285	9045	532418.2955	5054692.8	12704
8990	534766.5588	5050114.903	12292	9046	532375.5998	5054776.035	12712
8991	534723.8631	5050198.137	12300	9047	532332.9041	5054859.269	12719
8992	534681.1674	5050281.372	12307	9048	532290.2084	5054942.504	12727
8993	534638.4717	5050364.606	12315	9049	532247.5127	5055025.738	12734
8994	534595.776	5050447.841	12322	9050	532204.817	5055108.973	12742
8995	534553.0803	5050531.075	12330	9051	532162.1213	5055192.207	12749
8996	534510.3846	5050614.31	12337	9052	532119.4256	5055275.442	12756
8997	534467.6889	5050697.544	12345	9053	532076.7299	5055358.676	12764
8998	534424.9933	5050780.779	12352	9054	532034.0343	5055441.911	12771
8999	534382.2976	5050864.013	12360	9055	531991.3386	5055525.145	12779
9000	534339.6019	5050947.248	12367	9056	531948.6429	5055608.38	12786
9001	534296.9062	5051030.482	12375	9057	531905.9472	5055691.614	12794
9002	534254.2105	5051113.717	12382	9058	531863.2515	5055774.849	12801
9003	534211.5148	5051196.951	12390	9059	531820.5558	5055858.083	12809
9004	534168.8191	5051280.186	12397	9060	531777.8601	5055941.318	12816
9005	534126.1234	5051363.42	12405	9061	531735.1644	5056024.552	12824
9006	534083.4277	5051446.655	12412	9062	531692.4687	5056107.787	12831
9007	534040.732	5051529.889	12420	9063	531649.773	5056191.021	12839
9008	533998.0363	5051613.124	12427	9064	531607.0773	5056274.256	12846
9009	533955.3406	5051696.358	12435	9065	531564.3816	5056357.49	12854
9010	533912.6449	5051779.593	12442	9066	531521.6859	5056440.725	12861
9011	533869.9492	5051862.827	12450	9067	531478.9902	5056523.959	12869
9012	533827.2535	5051946.062	12457	9068	531436.2945	5056607.194	12876
9013	533784.5578	5052029.296	12465	9069	531393.5988	5056690.428	12884
9014	533741.8621	5052112.531	12472	9070	531350.9031	5056773.663	12891
9015	533699.1664	5052195.765	12480	9071	531308.2074	5056856.897	12899
9016	533656.4707	5052279	12487	9072	531265.5117	5056940.132	12906
9017	533613.775	5052362.234	12495	9073	531222.816	5057023.366	12914
9018	533571.0793	5052445.469	12502	9074	531180.1203	5057106.601	12921
9019	533528.3836	5052528.703	12510	9075	531137.4246	5057189.835	12929

9076	531094.7289	5057273.07	12936	9132	528703.7699	5061934.201	13355
9077	531052.0332	5057356.304	12944	9133	528661.0742	5062017.436	13363
9078	531009.3375	5057439.539	12951	9134	528618.3785	5062100.67	13370
9079	530966.6418	5057522.773	12959	9135	528575.6828	5062183.905	13378
9080	530923.9461	5057606.008	12966	9136	528532.9871	5062267.139	13385
9081	530881.2504	5057689.242	12974	9137	528490.2914	5062350.374	13393
9082	530838.5548	5057772.477	12981	9138	528447.5958	5062433.608	13400
9083	530795.8591	5057855.711	12988	9139	528404.9001	5062516.843	13408
9084	530753.1634	5057938.946	12996	9140	528362.2044	5062600.077	13415
9085	530710.4677	5058022.18	13003	9141	528319.5087	5062683.312	13423
9086	530667.772	5058105.415	13011	9142	528276.813	5062766.546	13430
9087	530625.0763	5058188.649	13018	9143	528234.1173	5062849.781	13438
9088	530582.3806	5058271.884	13026	9144	528191.4216	5062933.015	13445
9089	530539.6849	5058355.118	13033	9145	528148.7259	5063016.25	13452
9090	530496.9892	5058438.353	13041	9146	528106.0302	5063099.484	13460
9091	530454.2935	5058521.587	13048	9147	528063.3345	5063182.719	13467
9092	530411.5978	5058604.822	13056	9148	528020.6388	5063265.953	13475
9093	530368.9021	5058688.056	13063	9149	527977.9431	5063349.188	13482
9094	530326.2064	5058771.291	13071	9150	527935.2474	5063432.422	13490
9095	530283.5107	5058854.525	13078	9151	527892.5517	5063515.657	13497
9096	530240.815	5058937.759	13086	9152	527849.856	5063598.891	13505
9097	530198.1193	5059020.994	13093	9153	527807.1603	5063682.126	13512
9098	530155.4236	5059104.228	13101	9154	527764.4646	5063765.36	13520
9099	530112.7279	5059187.463	13108	9155	527721.7689	5063848.595	13527
9100	530070.0322	5059270.697	13116	9156	527679.0732	5063931.829	13535
9101	530027.3365	5059353.932	13123	9157	527636.3775	5064015.064	13542
9102	529984.6408	5059437.166	13131	9158	527593.6818	5064098.298	13550
9103	529941.9451	5059520.401	13138	9159	527550.9861	5064181.533	13557
9104	529899.2494	5059603.635	13146	9160	527508.2904	5064264.767	13565
9105	529856.5537	5059686.87	13153	9161	527465.5947	5064348.002	13572
9106	529813.858	5059770.104	13161	9162	527422.899	5064431.236	13580
9107	529771.1623	5059853.339	13168	9163	527380.2033	5064514.471	13587
9108	529728.4666	5059936.573	13176	9164	527337.5076	5064597.705	13595
9109	529685.7709	5060019.808	13183	9165	527294.8119	5064680.94	13602
9110	529643.0753	5060103.042	13191	9166	527252.1163	5064764.174	13610
9111	529600.3796	5060186.277	13198	9167	527209.4206	5064847.409	13617
9112	529557.6839	5060269.511	13206	9168	527166.7249	5064930.643	13625
9113	529514.9882	5060352.746	13213	9169	527124.0292	5065013.878	13632
9114	529472.2925	5060435.98	13220	9170	527081.3335	5065097.112	13640
9115	529429.5968	5060519.215	13228	9171	527038.6378	5065180.347	13647
9116	529386.9011	5060602.449	13235	9172	526995.9421	5065263.581	13655
9117	529344.2054	5060685.684	13243	9173	526953.2464	5065346.816	13662
9118	529301.5097	5060768.918	13250	9174	526910.5507	5065430.05	13669
9119	529258.814	5060852.153	13258	9175	526867.855	5065513.285	13677
9120	529216.1183	5060935.387	13265	9176	526825.1593	5065596.519	13684
9121	529173.4226	5061018.622	13273	9177	526782.4636	5065679.754	13692
9122	529130.7269	5061101.856	13280	9178	526739.7679	5065762.988	13699
9123	529088.0312	5061185.091	13288	9179	526697.0722	5065846.223	13707
9124	529045.3355	5061268.325	13295	9180	526654.3765	5065929.457	13714
9125	529002.6398	5061351.56	13303	9181	526611.6808	5066012.692	13722
9126	528959.9441	5061434.794	13310	9182	526568.9851	5066095.926	13729
9127	528917.2484	5061518.029	13318	9183	526526.2894	5066179.161	13737
9128	528874.5527	5061601.263	13325	9184	526483.5937	5066262.395	13744
9129	528831.857	5061684.498	13333	9185	526440.898	5066345.63	13752
9130	528789.1613	5061767.732	13340	9186	526398.2023	5066428.864	13759
9131	528746.4656	5061850.967	13348	9187	526355.5066	5066512.099	13767

9188	526312.8109	5066595.333	13774
9189	526270.1152	5066678.568	13782
9190	526227.4195	5066761.802	13789
9191	526184.7238	5066845.037	13797
9192	526142.0281	5066928.271	13804
9193	526099.3324	5067011.506	13812
9194	526056.6368	5067094.74	13819
9195	526013.9411	5067177.975	13827
9196	525971.2454	5067261.209	13834
9197	525928.5497	5067344.444	13842
9198	525885.854	5067427.678	13849
9199	525843.1583	5067510.913	13857
9200	525800.4626	5067594.147	13864
9201	525757.7669	5067677.382	13872
9202	525715.0712	5067760.616	13879
9203	525672.3755	5067843.851	13887
9204	525629.6798	5067927.085	13894
9205	525586.9841	5068010.32	13901
9206	525544.2884	5068093.554	13909
9207	525501.5927	5068176.789	13916
9208	525458.897	5068260.023	13924
9209	525421.1543	5068335.889	13931
9210	525383.4116	5068411.754	13937
9211	525345.6689	5068487.62	13944
9212	525307.9263	5068563.485	13951
9213	525270.1836	5068639.351	13958
9214	525232.4409	5068715.216	13965
9215	525194.6982	5068791.082	13971
9216	525156.9555	5068866.947	13978
9217	525119.2128	5068942.813	13985
9218	525081.4701	5069018.679	13992
9219	525043.7274	5069094.544	13999
9220	525005.9848	5069170.41	14005
9221	524968.2421	5069246.275	14012
9222	524930.4994	5069322.141	14019
9223	524892.7567	5069398.006	14026
9224	524855.014	5069473.872	14032
9225	524817.2713	5069549.737	14039
9226	524779.5286	5069625.603	14046
9227	524741.7859	5069701.469	14053
9228	524704.0433	5069777.334	14060
9229	524666.3006	5069853.2	14066
9230	524628.5579	5069929.065	14073
9231	524590.8152	5070004.931	14080
9232	524553.0725	5070080.796	14087
9233	524515.3298	5070156.662	14093
9234	524477.5871	5070232.527	14100
9235	524439.8444	5070308.393	14107
9236	524402.1018	5070384.259	14114
9237	524364.3591	5070460.124	14121
9238	524326.6164	5070535.99	14127
9239	524288.8737	5070611.855	14134
9240	524251.131	5070687.721	14141
9241	524213.3883	5070763.586	14148
9242	524175.6456	5070839.452	14154
9243	524137.9029	5070915.317	14161
9244	524100.1603	5070991.183	14168
9245	524062.4176	5071067.048	14175
9246	524024.6749	5071142.914	14182
9247	523986.9322	5071218.78	14188
9248	523949.1895	5071294.645	14195
9249	523911.4468	5071370.511	14202
9250	523873.7041	5071446.376	14209
9251	523835.9614	5071522.242	14215
9252	523798.2188	5071598.107	14222
9253	523760.4761	5071673.973	14229
9254	523722.7334	5071749.838	14236
9255	523684.9907	5071825.704	14243
9256	523647.248	5071901.57	14249
9257	523609.5053	5071977.435	14256
9258	523571.7626	5072053.301	14263
9259	523534.0199	5072129.166	14270
9260	523496.2773	5072205.032	14276
9261	523458.5346	5072280.897	14283
9262	523420.7919	5072356.763	14290
9263	523383.0492	5072432.628	14297
9264	523345.3065	5072508.494	14304
9265	523307.5638	5072584.36	14310
9266	523269.8211	5072660.225	14317
9267	523232.0784	5072736.091	14324
9268	523194.3358	5072811.956	14331
9269	523156.5931	5072887.822	14337
9270	523118.8504	5072963.687	14344
9271	523081.1077	5073039.553	14351
9272	523043.365	5073115.418	14358
9273	523005.6223	5073191.284	14365
9274	522967.8796	5073267.15	14371
9275	522930.1369	5073343.015	14378
9276	522892.3943	5073418.881	14385
9277	522854.6516	5073494.746	14392
9278	522816.9089	5073570.612	14398
9279	522779.1662	5073646.477	14405
9280	522741.4235	5073722.343	14412
9281	522703.6808	5073798.208	14419
9282	522665.9381	5073874.074	14426
9283	522628.1954	5073949.94	14432
9284	522590.4528	5074025.805	14439
9285	522552.7101	5074101.671	14446
9286	522514.9674	5074177.536	14453
9287	522477.2247	5074253.402	14459
9288	522439.482	5074329.267	14466
9289	522401.7393	5074405.133	14473
9290	522363.9966	5074480.998	14480
9291	522326.2539	5074556.864	14487
9292	522288.5113	5074632.73	14493
9293	522250.7686	5074708.595	14500
9294	522213.0259	5074784.461	14507
9295	522175.2832	5074860.326	14514
9296	522137.5405	5074936.192	14520
9297	522099.7978	5075012.057	14527
9298	522062.0551	5075087.923	14534
9299	522024.3124	5075163.788	14541

9300	521986.5698	5075239.654	14548
9301	521948.8271	5075315.519	14554
9302	521911.0844	5075391.385	14561
9303	521873.3417	5075467.251	14568
9304	521835.599	5075543.116	14575
9305	521797.8563	5075618.982	14581
9306	521760.1136	5075694.847	14588
9307	521722.3709	5075770.713	14595
9308	521684.6282	5075846.578	14602
9309	521646.8856	5075922.444	14609
9310	521609.1429	5075998.309	14615
9311	521571.4002	5076074.175	14622
9312	521533.6575	5076150.041	14629
9313	521495.9148	5076225.906	14636
9314	521458.1721	5076301.772	14642
9315	521420.4294	5076377.637	14649
9316	521382.6867	5076453.503	14656
9317	521344.9441	5076529.368	14663
9318	521307.2014	5076605.234	14670
9319	521269.4587	5076681.099	14676
9320	521231.716	5076756.965	14683
9321	521188.2555	5076847.006	14691
9322	521144.795	5076937.047	14699
9323	521101.3345	5077027.087	14707
9324	521057.8741	5077117.128	14715
9325	521014.4136	5077207.169	14723
9326	520970.9531	5077297.21	14731
9327	520927.4926	5077387.251	14739
9328	520884.0321	5077477.291	14747
9329	520840.5716	5077567.332	14755
9330	520797.1111	5077657.373	14763
9331	520753.6506	5077747.414	14771
9332	520710.1902	5077837.454	14779
9333	520666.7297	5077927.495	14787
9334	520623.2692	5078017.536	14795
9335	520579.8087	5078107.577	14803
9336	520536.3482	5078197.618	14811
9337	520492.8877	5078287.658	14819
9338	520449.4272	5078377.699	14827
9339	520405.9668	5078467.74	14835
9340	520362.5063	5078557.781	14843
9341	520319.0458	5078647.822	14851
9342	520275.5853	5078737.862	14859
9343	520232.1248	5078827.903	14867
9344	520188.6643	5078917.944	14875
9345	520145.2038	5079007.985	14883
9346	520101.7433	5079098.025	14891
9347	520058.2829	5079188.066	14899
9348	520014.8224	5079278.107	14907
9349	519971.3619	5079368.148	14915
9350	519927.9014	5079458.189	14923
9351	519884.4409	5079548.229	14931
9352	519840.9804	5079638.27	14939
9353	519797.5199	5079728.311	14947
9354	519754.0595	5079818.352	14955
9355	519710.599	5079908.393	14963
9356	519667.1385	5079998.433	14971
9357	519623.678	5080088.474	14979
9358	519580.2175	5080178.515	14987
9359	519536.757	5080268.556	14995
9360	519493.2965	5080358.597	15003
9361	519449.836	5080448.637	15011
9362	519406.3756	5080538.678	15019
9363	519362.9151	5080628.719	15027
9364	519319.4546	5080718.76	15035
9365	519275.9941	5080808.8	15043
9366	519232.5336	5080898.841	15051
9367	519189.0731	5080988.882	15059
9368	519145.6126	5081078.923	15067
9369	519102.1522	5081168.964	15075
9370	519058.6917	5081259.004	15083
9371	519015.2312	5081349.045	15091
9372	518971.7707	5081439.086	15099
9373	518928.3102	5081529.127	15107
9374	518884.8497	5081619.168	15115
9375	518841.3892	5081709.208	15123
9376	518797.9287	5081799.249	15131
9377	518754.4683	5081889.29	15139
9378	518711.0078	5081979.331	15147
9379	518667.5473	5082069.371	15155
9380	518624.0868	5082159.412	15163
9381	518580.6263	5082249.453	15171
9382	518537.1658	5082339.494	15179
9383	518493.7053	5082429.535	15187
9384	518450.2448	5082519.575	15195
9385	518406.7844	5082609.616	15203
9386	518363.3239	5082699.657	15211
9387	518319.8634	5082789.698	15219
9388	518276.4029	5082879.739	15227
9389	518232.9424	5082969.779	15235
9390	518189.4819	5083059.82	15243
9391	518146.0214	5083149.861	15251
9392	518102.561	5083239.902	15259
9393	518059.1005	5083329.942	15267
9394	518015.64	5083419.983	15275
9395	517972.1795	5083510.024	15283
9396	517928.719	5083600.065	15291
9397	517885.2585	5083690.106	15299
9398	517841.798	5083780.146	15307
9399	517798.3375	5083870.187	15315
9400	517754.8771	5083960.228	15323
9401	517711.4166	5084050.269	15331
9402	517667.9561	5084140.31	15339
9403	517624.4956	5084230.35	15347
9404	517581.0351	5084320.391	15355
9405	517537.5746	5084410.432	15363
9406	517494.1141	5084500.473	15371
9407	517450.6537	5084590.514	15379
9408	517407.1932	5084680.554	15387
9409	517363.7327	5084770.595	15395
9410	517320.2722	5084860.636	15403
9411	517276.8117	5084950.677	15411

9412	517233.3512	5085040.717	15419	9468	514623.0701	5090080.476	15873
9413	517189.8907	5085130.758	15427	9469	514574.5669	5090170.445	15881
9414	517146.4302	5085220.799	15435	9470	514526.0638	5090260.413	15890
9415	517102.9698	5085310.84	15443	9471	514477.5606	5090350.382	15898
9416	517059.5093	5085400.881	15451	9472	514429.0574	5090440.351	15906
9417	517016.0488	5085490.921	15459	9473	514380.5543	5090530.319	15914
9418	516972.5883	5085580.962	15467	9474	514332.0511	5090620.288	15922
9419	516929.1278	5085671.003	15475	9475	514283.5479	5090710.256	15930
9420	516885.6673	5085761.044	15483	9476	514235.0448	5090800.225	15939
9421	516842.2068	5085851.085	15491	9477	514186.5416	5090890.194	15947
9422	516798.7464	5085941.125	15499	9478	514138.0384	5090980.162	15955
9423	516755.2859	5086031.166	15507	9479	514089.5353	5091070.131	15963
9424	516711.8254	5086121.207	15515	9480	514041.0321	5091160.1	15971
9425	516668.3649	5086211.248	15523	9481	513992.5289	5091250.068	15979
9426	516624.9044	5086301.288	15531	9482	513944.0258	5091340.037	15988
9427	516581.4439	5086391.329	15539	9483	513895.5226	5091430.005	15996
9428	516537.9834	5086481.37	15547	9484	513847.0194	5091519.974	16004
9429	516494.5229	5086571.411	15555	9485	513798.5163	5091609.943	16012
9430	516451.0625	5086661.452	15563	9486	513750.0131	5091699.911	16020
9431	516407.602	5086751.492	15571	9487	513701.5099	5091789.88	16029
9432	516364.1415	5086841.533	15579	9488	513653.0068	5091879.849	16037
9433	516320.681	5086931.574	15587	9489	513604.5036	5091969.817	16045
9434	516272.1778	5087021.543	15595	9490	513556.0004	5092059.786	16053
9435	516223.6747	5087111.511	15603	9491	513507.4972	5092149.754	16061
9436	516175.1715	5087201.48	15612	9492	513458.9941	5092239.723	16069
9437	516126.6683	5087291.449	15620	9493	513410.4909	5092329.692	16078
9438	516078.1652	5087381.417	15628	9494	513361.9877	5092419.66	16086
9439	516029.662	5087471.386	15636	9495	513313.4846	5092509.629	16094
9440	515981.1588	5087561.354	15644	9496	513264.9814	5092599.598	16102
9441	515932.6557	5087651.323	15652	9497	513216.4782	5092689.566	16110
9442	515884.1525	5087741.292	15661	9498	513167.9751	5092779.535	16118
9443	515835.6493	5087831.26	15669	9499	513119.4719	5092869.503	16127
9444	515787.1462	5087921.229	15677	9500	513070.9687	5092959.472	16135
9445	515738.643	5088011.198	15685	9501	513022.4656	5093049.441	16143
9446	515690.1398	5088101.166	15693	9502	512973.9624	5093139.409	16151
9447	515641.6366	5088191.135	15701	9503	512925.4592	5093229.378	16159
9448	515593.1335	5088281.103	15710	9504	512876.9561	5093319.347	16168
9449	515544.6303	5088371.072	15718	9505	512828.4529	5093409.315	16176
9450	515496.1271	5088461.041	15726	9506	512779.9497	5093499.284	16184
9451	515447.624	5088551.009	15734	9507	512731.4466	5093589.252	16192
9452	515399.1208	5088640.978	15742	9508	512682.9434	5093679.221	16200
9453	515350.6176	5088730.947	15751	9509	512634.4402	5093769.19	16208
9454	515302.1145	5088820.915	15759	9510	512585.9371	5093859.158	16217
9455	515253.6113	5088910.884	15767	9511	512537.4339	5093949.127	16225
9456	515205.1081	5089000.852	15775	9512	512488.9307	5094039.096	16233
9457	515156.605	5089090.821	15783	9513	512440.4275	5094129.064	16241
9458	515108.1018	5089180.79	15791	9514	512391.9244	5094219.033	16249
9459	515059.5986	5089270.758	15800	9515	512343.4212	5094309.002	16257
9460	515011.0955	5089360.727	15808	9516	512294.918	5094398.97	16266
9461	514962.5923	5089450.696	15816	9517	512246.4149	5094488.939	16274
9462	514914.0891	5089540.664	15824	9518	512197.9117	5094578.907	16282
9463	514865.586	5089630.633	15832	9519	512149.4085	5094668.876	16290
9464	514817.0828	5089720.601	15840	9520	512100.9054	5094758.845	16298
9465	514768.5796	5089810.57	15849	9521	512052.4022	5094848.813	16307
9466	514720.0765	5089900.539	15857	9522	512003.899	5094938.782	16315
9467	514671.5733	5089990.507	15865	9523	511955.3959	5095028.751	16323

9524	511906.8927	5095118.719	16331
9525	511858.3895	5095208.688	16339
9526	511809.8864	5095298.656	16347
9527	511761.3832	5095388.625	16356
9528	511712.88	5095478.594	16364
9529	511664.3769	5095568.562	16372
9530	511615.8737	5095658.531	16380
9531	511567.3705	5095748.5	16388
9532	511518.8674	5095838.468	16397
9533	511470.3642	5095928.437	16405
9534	511421.861	5096018.405	16413
9535	511373.3578	5096108.374	16421
9536	511324.8547	5096198.343	16429
9537	511276.3515	5096288.311	16437
9538	511227.8483	5096378.28	16446
9539	511179.3452	5096468.249	16454
9540	511130.842	5096558.217	16462
9541	511082.3388	5096648.186	16470
9542	511033.8357	5096738.154	16478
9543	510985.3325	5096828.123	16486
9544	510936.8293	5096918.092	16495
9545	510888.3262	5097008.06	16503
9546	510839.823	5097098.029	16511
9547	510795.5548	5097190.616	16519
9548	510751.2866	5097283.203	16527
9549	510707.0184	5097375.791	16536
9550	510662.7501	5097468.378	16544
9551	510618.4819	5097560.965	16552
9552	510574.2137	5097653.552	16560
9553	510529.9455	5097746.139	16568
9554	510485.6773	5097838.727	16577
9555	510441.4091	5097931.314	16585
9556	510397.1409	5098023.901	16593
9557	510352.8726	5098116.488	16601
9558	510308.6044	5098209.075	16609
9559	510264.3362	5098301.663	16618
9560	510220.068	5098394.25	16626
9561	510175.7998	5098486.837	16634
9562	510131.5316	5098579.424	16642
9563	510087.2634	5098672.011	16651
9564	510042.9951	5098764.599	16659
9565	509998.7269	5098857.186	16667
9566	509954.4587	5098949.773	16675
9567	509910.1905	5099042.36	16683
9568	509865.9223	5099134.947	16692
9569	509821.6541	5099227.535	16700
9570	509777.3859	5099320.122	16708
9571	509733.1176	5099412.709	16716
9572	509688.8494	5099505.296	16724
9573	509644.5812	5099597.883	16733
9574	509600.313	5099690.47	16741
9575	509556.0448	5099783.058	16749
9576	509511.7766	5099875.645	16757
9577	509467.5084	5099968.232	16765
9578	509423.2401	5100060.819	16774
9579	509378.9719	5100153.406	16782
9580	509334.7037	5100245.994	16790
9581	509290.4355	5100338.581	16798
9582	509246.1673	5100431.168	16807
9583	509201.8991	5100523.755	16815
9584	509157.6309	5100616.342	16823
9585	509113.3626	5100708.93	16831
9586	509069.0944	5100801.517	16839
9587	509024.8262	5100894.104	16848
9588	508980.558	5100986.691	16856
9589	508936.2898	5101079.278	16864
9590	508892.0216	5101171.866	16872
9591	508847.7534	5101264.453	16880
9592	508803.4851	5101357.04	16889
9593	508759.2169	5101449.627	16897
9594	508714.9487	5101542.214	16905
9595	508670.6805	5101634.802	16913
9596	508626.4123	5101727.389	16921
9597	508582.1441	5101819.976	16930
9598	508537.8759	5101912.563	16938
9599	508493.6076	5102005.15	16946
9600	508449.3394	5102097.738	16954
9601	508405.0712	5102190.325	16963
9602	508360.803	5102282.912	16971
9603	508316.5319	5102372.456	16979
9604	508272.2608	5102462	16987
9605	508227.9897	5102551.545	16995
9606	508183.7186	5102641.089	17003
9607	508139.4476	5102730.633	17011
9608	508095.1765	5102820.177	17019
9609	508050.9054	5102909.722	17027
9610	508006.6343	5102999.266	17035
9611	507962.3632	5103088.81	17043
9612	507918.0921	5103178.354	17051
9613	507873.821	5103267.899	17059
9614	507829.5499	5103357.443	17067
9615	507785.2789	5103446.987	17075
9616	507741.0078	5103536.531	17083
9617	507696.7367	5103626.075	17091
9618	507652.4656	5103715.62	17099
9619	507608.1945	5103805.164	17107
9620	507563.9234	5103894.708	17115
9621	507519.6523	5103984.252	17123
9622	507475.3812	5104073.797	17131
9623	507431.1102	5104163.341	17139
9624	507386.8391	5104252.885	17147
9625	507342.568	5104342.429	17155
9626	507298.2969	5104431.973	17163
9627	507254.0258	5104521.518	17171
9628	507209.7547	5104611.062	17179
9629	507165.4836	5104700.606	17187
9630	507121.2125	5104790.15	17194
9631	507076.9415	5104879.695	17202
9632	507032.6704	5104969.239	17210
9633	506988.3993	5105058.783	17218
9634	506944.1282	5105148.327	17226
9635	506899.8571	5105237.872	17234

9636	506855.586	5105327.416	17242	9692	504511.1622	5109990.66	17660
9637	506811.3149	5105416.96	17250	9693	504470.9746	5110069.56	17667
9638	506767.0438	5105506.504	17258	9694	504430.7871	5110148.461	17674
9639	506722.7728	5105596.048	17266	9695	504390.5996	5110227.362	17681
9640	506678.5017	5105685.593	17274	9696	504350.412	5110306.263	17688
9641	506634.2306	5105775.137	17282	9697	504310.2245	5110385.164	17695
9642	506589.9595	5105864.681	17290	9698	504270.0369	5110464.064	17703
9643	506545.6884	5105954.225	17298	9699	504229.8494	5110542.965	17710
9644	506501.4173	5106043.77	17306	9700	504189.6619	5110621.866	17717
9645	506457.1462	5106133.314	17314	9701	504149.4743	5110700.767	17724
9646	506412.8751	5106222.858	17322	9702	504109.2868	5110779.668	17731
9647	506368.6041	5106312.402	17330	9703	504069.0992	5110858.568	17738
9648	506324.333	5106401.946	17338	9704	504028.9117	5110937.469	17745
9649	506280.0619	5106491.491	17346	9705	503988.7242	5111016.37	17752
9650	506235.7908	5106581.035	17354	9706	503948.5366	5111095.271	17759
9651	506191.5197	5106670.579	17362	9707	503908.3491	5111174.172	17766
9652	506147.2486	5106760.123	17370	9708	503868.1615	5111253.072	17773
9653	506102.9775	5106849.668	17378	9709	503827.974	5111331.973	17780
9654	506058.7064	5106939.212	17386	9710	503787.7865	5111410.874	17788
9655	506014.4354	5107028.756	17394	9711	503747.5989	5111489.775	17795
9656	505970.1643	5107118.3	17402	9712	503707.4114	5111568.676	17802
9657	505925.8932	5107207.845	17410	9713	503667.2238	5111647.576	17809
9658	505881.6221	5107297.389	17418	9714	503627.0363	5111726.477	17816
9659	505837.351	5107386.933	17426	9715	503586.8488	5111805.378	17823
9660	505797.1635	5107465.834	17433	9716	503546.6612	5111884.279	17830
9661	505756.9759	5107544.735	17440	9717	503506.4737	5111963.18	17837
9662	505716.7884	5107623.635	17447	9718	503466.2862	5112042.081	17844
9663	505676.6008	5107702.536	17455	9719	503426.0986	5112120.981	17851
9664	505636.4133	5107781.437	17462	9720	503385.9111	5112199.882	17858
9665	505596.2258	5107860.338	17469	9721	503345.7235	5112278.783	17865
9666	505556.0382	5107939.239	17476	9722	503305.536	5112357.684	17873
9667	505515.8507	5108018.139	17483	9723	503265.3485	5112436.585	17880
9668	505475.6631	5108097.04	17490	9724	503225.1609	5112515.485	17887
9669	505435.4756	5108175.941	17497	9725	503184.9734	5112594.386	17894
9670	505395.2881	5108254.842	17504	9726	503144.7858	5112673.287	17901
9671	505355.1005	5108333.743	17511	9727	503104.5983	5112752.188	17908
9672	505314.913	5108412.643	17518	9728	503064.4108	5112831.089	17915
9673	505274.7254	5108491.544	17525	9729	503024.2232	5112909.989	17922
9674	505234.5379	5108570.445	17532	9730	502984.0357	5112988.89	17929
9675	505194.3504	5108649.346	17540	9731	502943.8481	5113067.791	17936
9676	505154.1628	5108728.247	17547	9732	502903.6606	5113146.692	17943
9677	505113.9753	5108807.147	17554	9733	502863.4731	5113225.593	17950
9678	505073.7877	5108886.048	17561	9734	502823.2855	5113304.493	17958
9679	505033.6002	5108964.949	17568	9735	502783.098	5113383.394	17965
9680	504993.4127	5109043.85	17575	9736	502742.9104	5113462.295	17972
9681	504953.2251	5109122.751	17582	9737	502702.7229	5113541.196	17979
9682	504913.0376	5109201.652	17589	9738	502662.5354	5113620.097	17986
9683	504872.85	5109280.552	17596	9739	502622.3478	5113698.997	17993
9684	504832.6625	5109359.453	17603	9740	502582.1603	5113777.898	18000
9685	504792.475	5109438.354	17610	9741	502541.9727	5113856.799	18007
9686	504752.2874	5109517.255	17618	9742	502501.7852	5113935.7	18014
9687	504712.0999	5109596.156	17625	9743	502461.5977	5114014.601	18021
9688	504671.9123	5109675.056	17632	9744	502421.4101	5114093.501	18028
9689	504631.7248	5109753.957	17639	9745	502381.2226	5114172.402	18035
9690	504591.5373	5109832.858	17646	9746	502341.035	5114251.303	18043
9691	504551.3497	5109911.759	17653	9747	502300.8475	5114330.204	18050

9748	502260.66	5114409.105	18057
9749	502220.4724	5114488.005	18064
9750	502180.2849	5114566.906	18071
9751	502140.0973	5114645.807	18078
9752	502099.9098	5114724.708	18085
9753	502059.7223	5114803.609	18092
9754	502019.5347	5114882.51	18099
9755	501979.3472	5114961.41	18106
9756	501939.1596	5115040.311	18113
9757	501898.9721	5115119.212	18120
9758	501858.7846	5115198.113	18128
9759	501818.597	5115277.014	18135
9760	501778.4095	5115355.914	18142
9761	501738.2219	5115434.815	18149
9762	501698.0344	5115513.716	18156
9763	501657.8469	5115592.617	18163
9764	501617.6593	5115671.518	18170
9765	501577.4718	5115750.418	18177
9766	501537.2842	5115829.319	18184
9767	501497.0967	5115908.22	18191
9768	501456.9092	5115987.121	18198
9769	501416.7216	5116066.022	18205
9770	501376.5341	5116144.922	18213
9771	501336.3465	5116223.823	18220
9772	501296.159	5116302.724	18227
9773	501256.0673	5116379.485	18234
9774	501215.9757	5116456.246	18241
9775	501175.884	5116533.007	18247
9776	501135.7923	5116609.769	18254
9777	501095.7007	5116686.53	18261
9778	501055.609	5116763.291	18268
9779	501015.5173	5116840.052	18275
9780	500975.4257	5116916.813	18282
9781	500935.334	5116993.574	18289
9782	500895.2423	5117070.335	18296
9783	500855.1507	5117147.097	18303
9784	500815.059	5117223.858	18310
9785	500774.9673	5117300.619	18317
9786	500734.8757	5117377.38	18324
9787	500694.784	5117454.141	18331
9788	500654.6923	5117530.902	18338
9789	500614.6007	5117607.664	18344
9790	500574.509	5117684.425	18351
9791	500534.4173	5117761.186	18358
9792	500494.3257	5117837.947	18365
9793	500454.234	5117914.708	18372
9794	500414.1423	5117991.469	18379
9795	500374.0507	5118068.23	18386
9796	500333.959	5118144.992	18393
9797	500293.8673	5118221.753	18400
9798	500253.7757	5118298.514	18407
9799	500213.684	5118375.275	18414
9800	500173.5923	5118452.036	18421
9801	500133.5007	5118528.797	18428
9802	500093.409	5118605.558	18435
9803	500053.3173	5118682.32	18441
9804	500013.2257	5118759.081	18448
9805	499973.134	5118835.842	18455
9806	499933.0423	5118912.603	18462
9807	499892.9507	5118989.364	18469
9808	499852.859	5119066.125	18476
9809	499812.7673	5119142.887	18483
9810	499772.6757	5119219.648	18490
9811	499732.584	5119296.409	18497
9812	499692.4923	5119373.17	18504
9813	499652.4007	5119449.931	18511
9814	499612.309	5119526.692	18518
9815	499572.2173	5119603.453	18525
9816	499532.1257	5119680.215	18532
9817	499492.034	5119756.976	18538
9818	499451.9423	5119833.737	18545
9819	499411.8507	5119910.498	18552
9820	499371.759	5119987.259	18559
9821	499331.6673	5120064.02	18566
9822	499291.5757	5120140.781	18573
9823	499251.484	5120217.543	18580
9824	499211.3923	5120294.304	18587
9825	499171.3007	5120371.065	18594
9826	499131.209	5120447.826	18601
9827	499091.1173	5120524.587	18608
9828	499051.0257	5120601.348	18615
9829	499010.934	5120678.109	18622
9830	498970.8423	5120754.871	18629
9831	498930.7507	5120831.632	18635
9832	498890.659	5120908.393	18642
9833	498850.5673	5120985.154	18649
9834	498810.4757	5121061.915	18656
9835	498770.384	5121138.676	18663
9836	498730.2923	5121215.438	18670
9837	498690.2007	5121292.199	18677
9838	498650.109	5121368.96	18684
9839	498610.0173	5121445.721	18691
9840	498569.9257	5121522.482	18698
9841	498529.834	5121599.243	18705
9842	498489.7423	5121676.004	18712
9843	498449.6507	5121752.766	18719
9844	498409.559	5121829.527	18726
9845	498369.4673	5121906.288	18732
9846	498329.3757	5121983.049	18739
9847	498289.284	5122059.81	18746
9848	498249.1923	5122136.571	18753
9849	498209.1007	5122213.332	18760
9850	498169.009	5122290.094	18767
9851	498128.9173	5122366.855	18774
9852	498088.8257	5122443.616	18781
9853	498048.734	5122520.377	18788
9854	498008.6423	5122597.138	18795
9855	497968.5507	5122673.899	18802
9856	497928.459	5122750.661	18809
9857	497888.3673	5122827.422	18816
9858	497848.2757	5122904.183	18823
9859	497808.184	5122980.944	18829

9860	497768.0923	5123057.705	18836	9873	497246.9007	5124055.6	18926
9861	497728.0007	5123134.466	18843	9874	497206.809	5124132.361	18933
9862	497687.909	5123211.227	18850	9875	497166.7173	5124209.122	18940
9863	497647.8173	5123287.989	18857	9876	497126.6257	5124285.884	18947
9864	497607.7257	5123364.75	18864	9877	497086.534	5124362.645	18954
9865	497567.634	5123441.511	18871	9878	497046.4423	5124439.406	18961
9866	497527.5423	5123518.272	18878	9879	497006.3507	5124516.167	18968
9867	497487.4507	5123595.033	18885	9880	496966.259	5124592.928	18975
9868	497447.359	5123671.794	18892	9881	496926.1673	5124669.689	18982
9869	497407.2673	5123748.555	18899	9882	496886.0757	5124746.45	18989
9870	497367.1757	5123825.317	18906	9883	496845.984	5124823.212	18996
9871	497327.084	5123902.078	18913	9884	496805.8923	5124899.973	19003
9872	497286.9923	5123978.839	18919	9885	496765.8007	5124976.734	19010

Appendix 6: Time windows used to apply Ormsby bandpass filter (4-8-20-35) to Line 56.

CDP	Time Window
1	9500-12000
4000	9500-12000
6500	9000-12000
14500	8500-12000
15500	8500-12000
17000	6400-12000
18096	5000-12000

Appendix 7: Time windows used for applying a time variant scalar gain to the shelf and slope region on Line 54 to create a more balanced section. The gain values applied to each time window are outlined in Appendix 8. TW = time window.

CDP	TW 1	TW 2	TW 3	TW 4
15500	0-6400	6500-9800	10000-11950	12000-12500
16000	0-6000	6200-9000	9500-11700	12000-12500
16500	0-4600	5800-8700	9100-10800	11100-12500
17250	0-4700	5000-7000	7500-9500	10000-12500
18096	0-3800	4000-5700	5900-7300	7700-12500

Appendix 8: Gain values used for applying a time variant scalar gain to the shelf and slope region on Line 54 to create a more balanced section. Each time window is outlined in Appendix 7.

CDP	Gain 1	Gain 2	Gain 3	Gain 2
15500	1	1.5	1	1
16000	1	1.5	1	1
16500	1	1.6	1	1.6
17250	1	2.5	1	2.5
18096	1	2.5	1.5	2.5

Appendix 9: Time windows used to apply Ormsby bandpass filter (4-8-20-35) to slope and deep water region Line 54.

CDP	Time Window
7000	2350-17000
7530	4500-17000
8015	5900-17000
8240	6300-17000
9080	6900-17000
9500	6860-17000
10300	7500-17000
10500	7840-17000
11115	12000-17000

Appendix 10: Velocity versus depth models from the SCR2 profile at CDPs 224800 (VD T1), 232800 (VD T2), and 239000 (VD OC) derived from refraction data (after Van Avendonk et al., 2006). Velocity models presented here are straight lines used to approximate the original models presented by Van Avendonk et al. (2006) that are curved functions. Original velocity-depth models are presented in Figures 3.2 and 3.3. These straight-lined velocity-depth models are converted to velocity-TWT (Appendix 11) and are overlain on the SCR2 seismic reflection profile in Plate 2b.

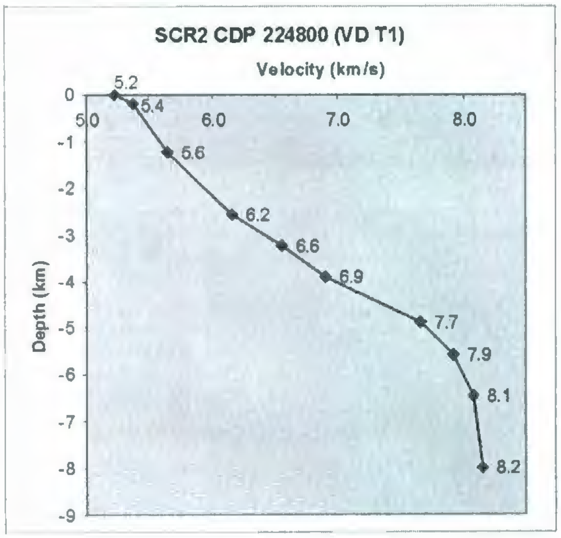

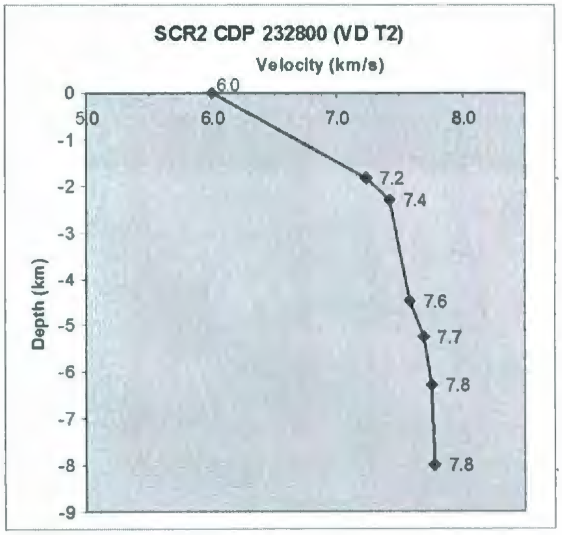

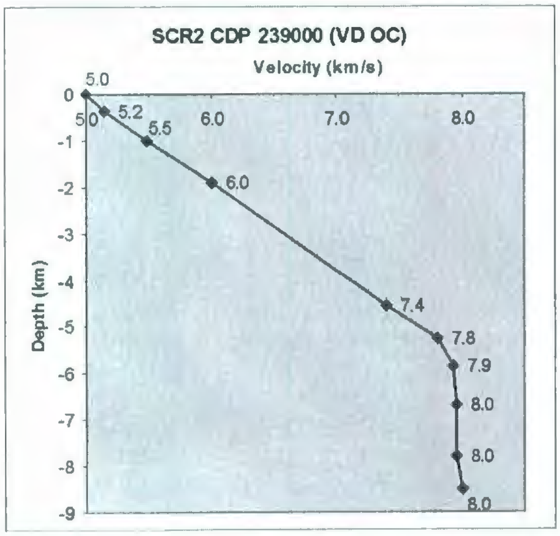

Appendix 11: Velocity versus TWT models derived from velocity-depth models illustrated in Appendix 10 (after Van Avendonk et al., 2006). These models have been overlain on the SCR2 seismic reflection profile in Plate 2b.

Location	TWT (s)	Velocity (km/s)
SCR2 - VD T1	7.5	5.2
CDP 224800	7.6	5.4
	7.9	5.6
	8.4	6.2
	8.6	6.6
	8.8	6.9
	9.1	7.7
	9.3	7.9
	9.5	8.1
	9.9	8.2
SCR2 - VD T2	7.6	6.0
CDP 232800	8.2	7.2
	8.3	7.4
	8.9	7.6
	9.1	7.7
	9.3	7.8
	9.8	7.8
SCR2 - VD OC	7.9	5.0
CDP 239000	8.0	5.2
	8.3	5.5
	8.6	6.0
	9.4	7.4
	9.6	7.8
	9.7	7.9
	9.9	8.0
	10.2	8.0
	10.4	8.0

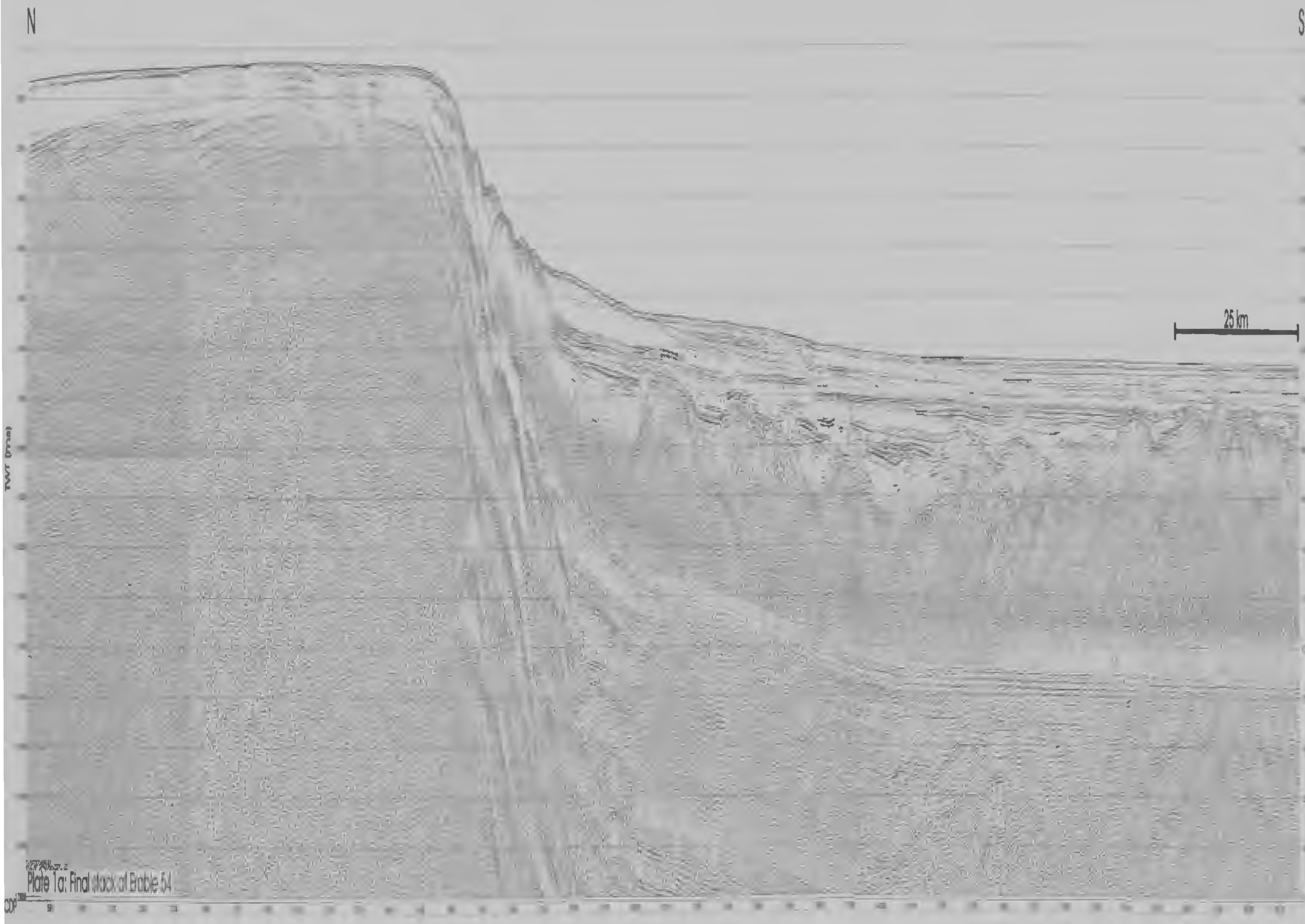

Plate 1a: Final stack of Brable 54

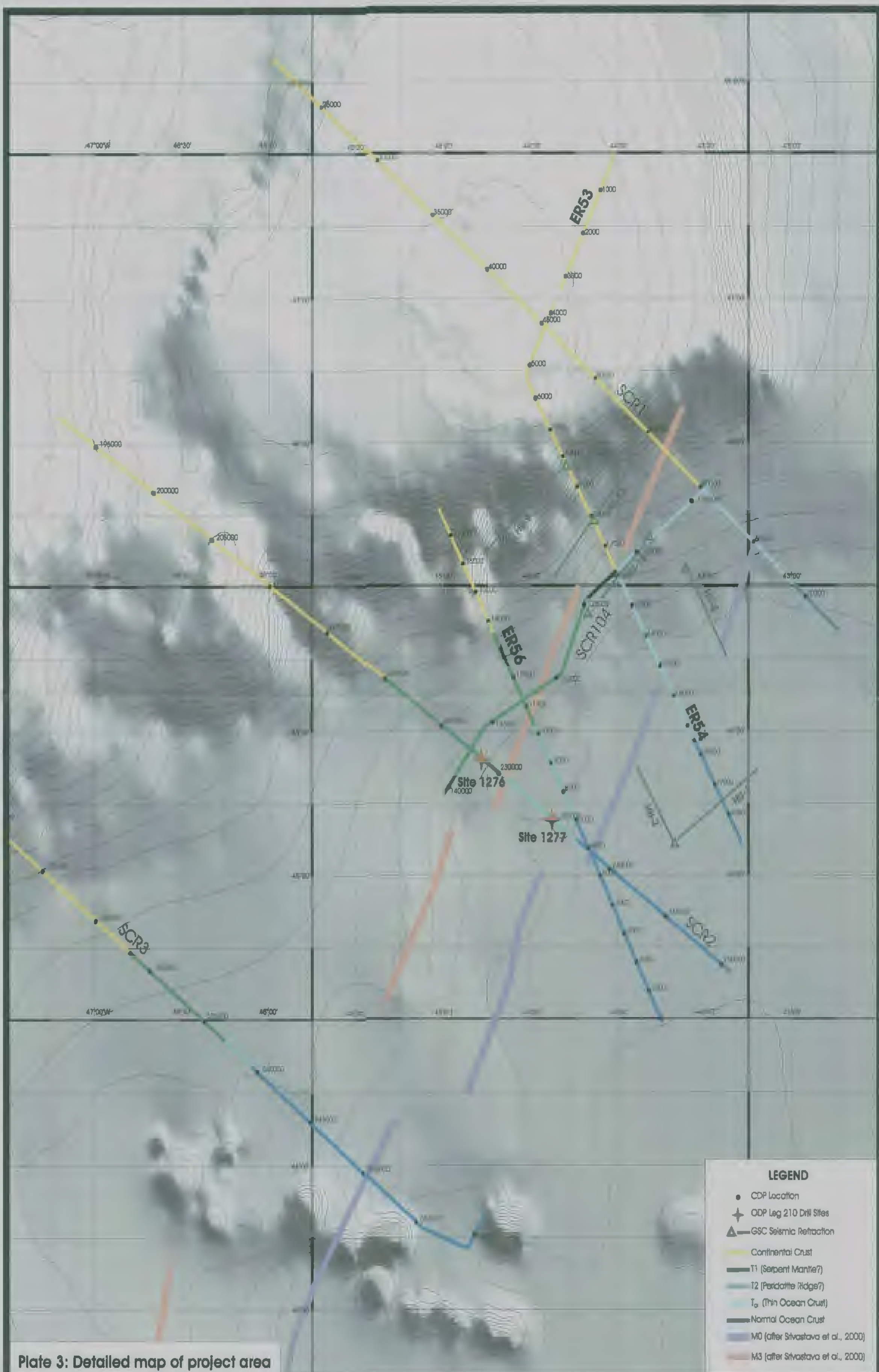

Plate 3: Detailed map of project area

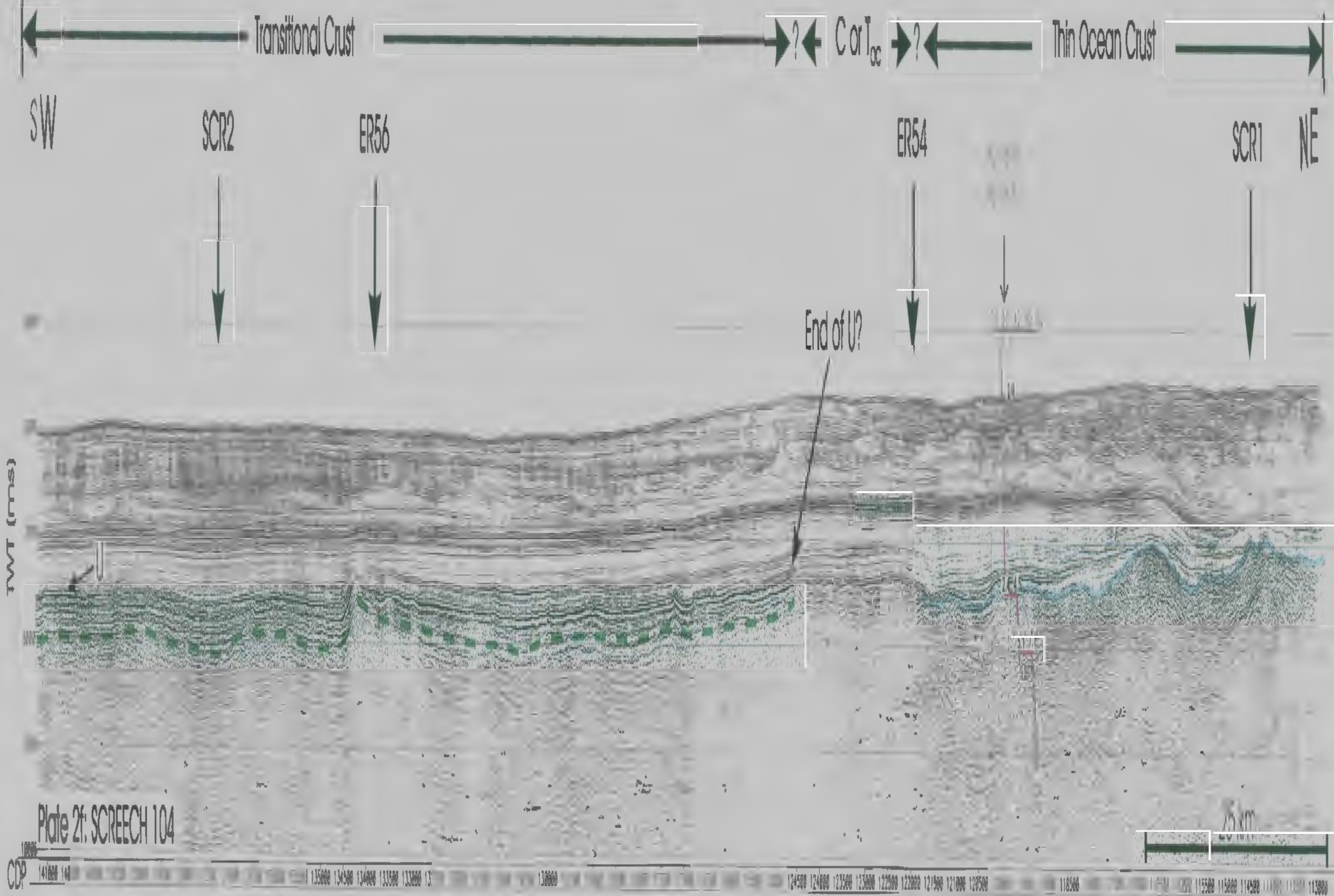

Plate 2f: Time migration of the SCREECH Line 104 seismic reflection profile. Intersection with other seismic lines are marked with black arrows. The HU-18 velocity model (modified from Todd and Reid, 1989) is projected onto the profile as outlined by black arrow. CC=continental crust,C2=unreflective continental crust, T1=unreflective transitional crust (exhumed serpentinized mantle?), T_{oc}=thin ocean crust, U=U-reflection.

LEGEND

Top acoustic basement interpreted as:

T1

T_{oc}

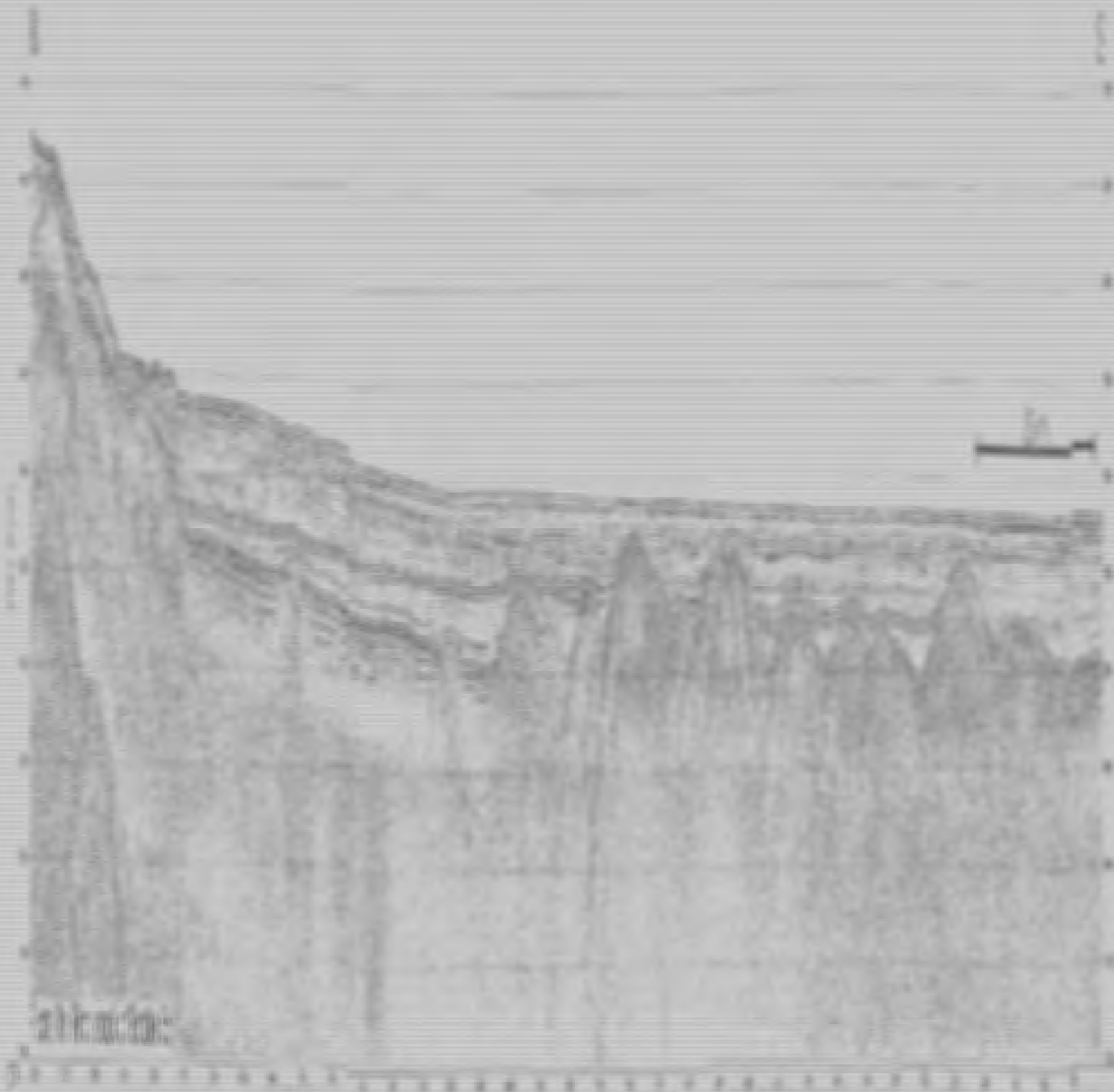

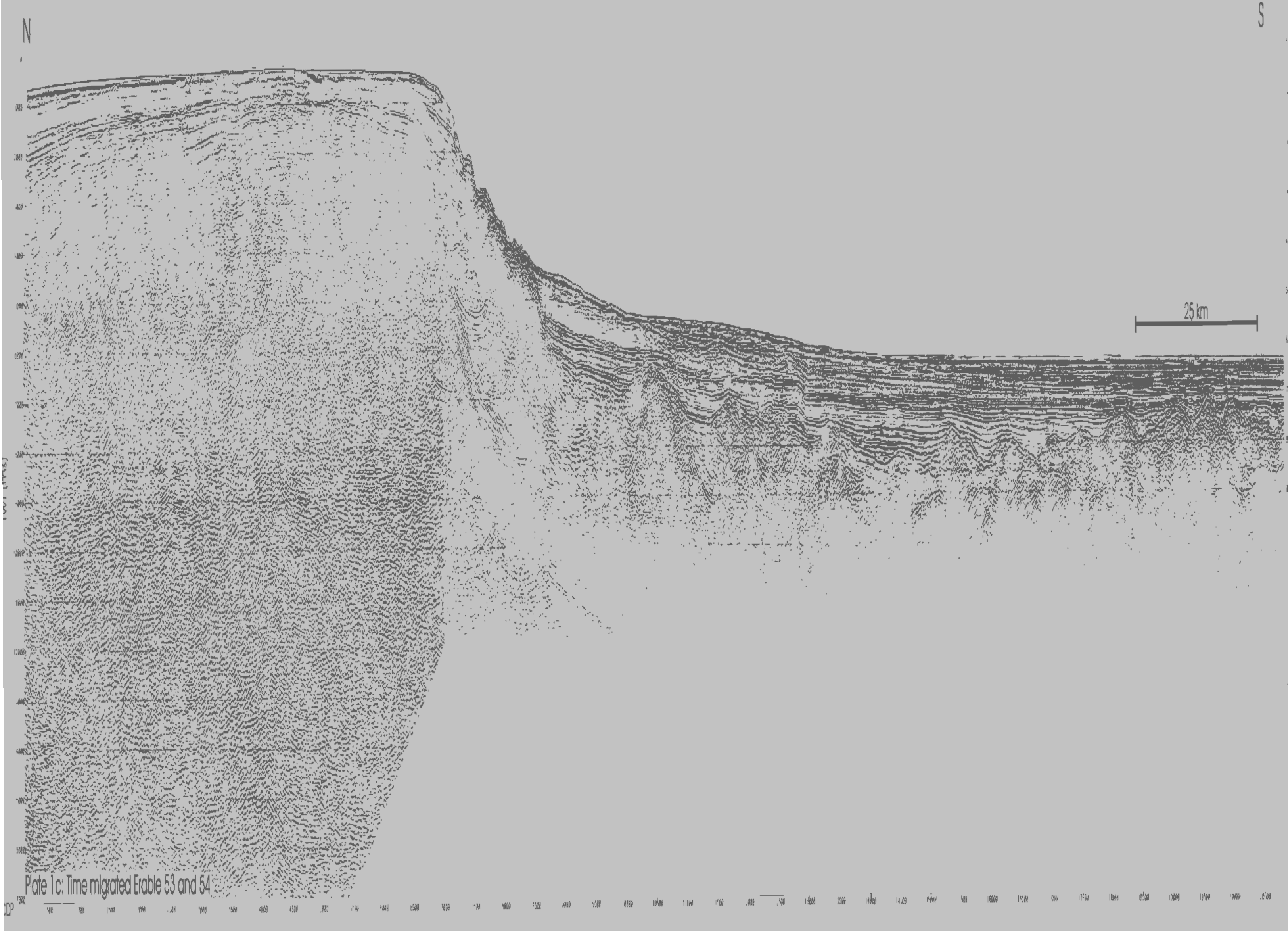

Plate 1c: Time migrated Erable 53 and 54

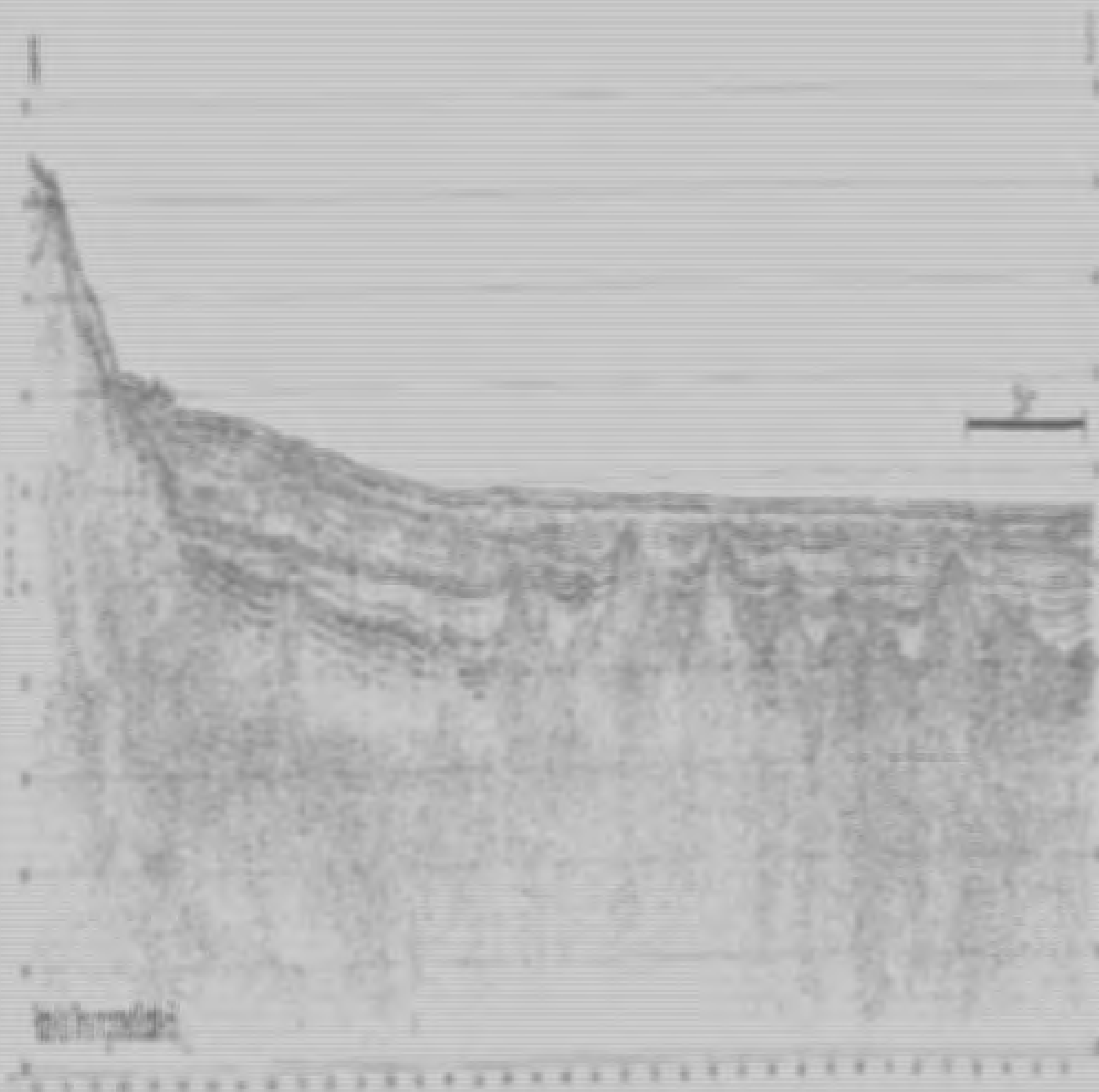

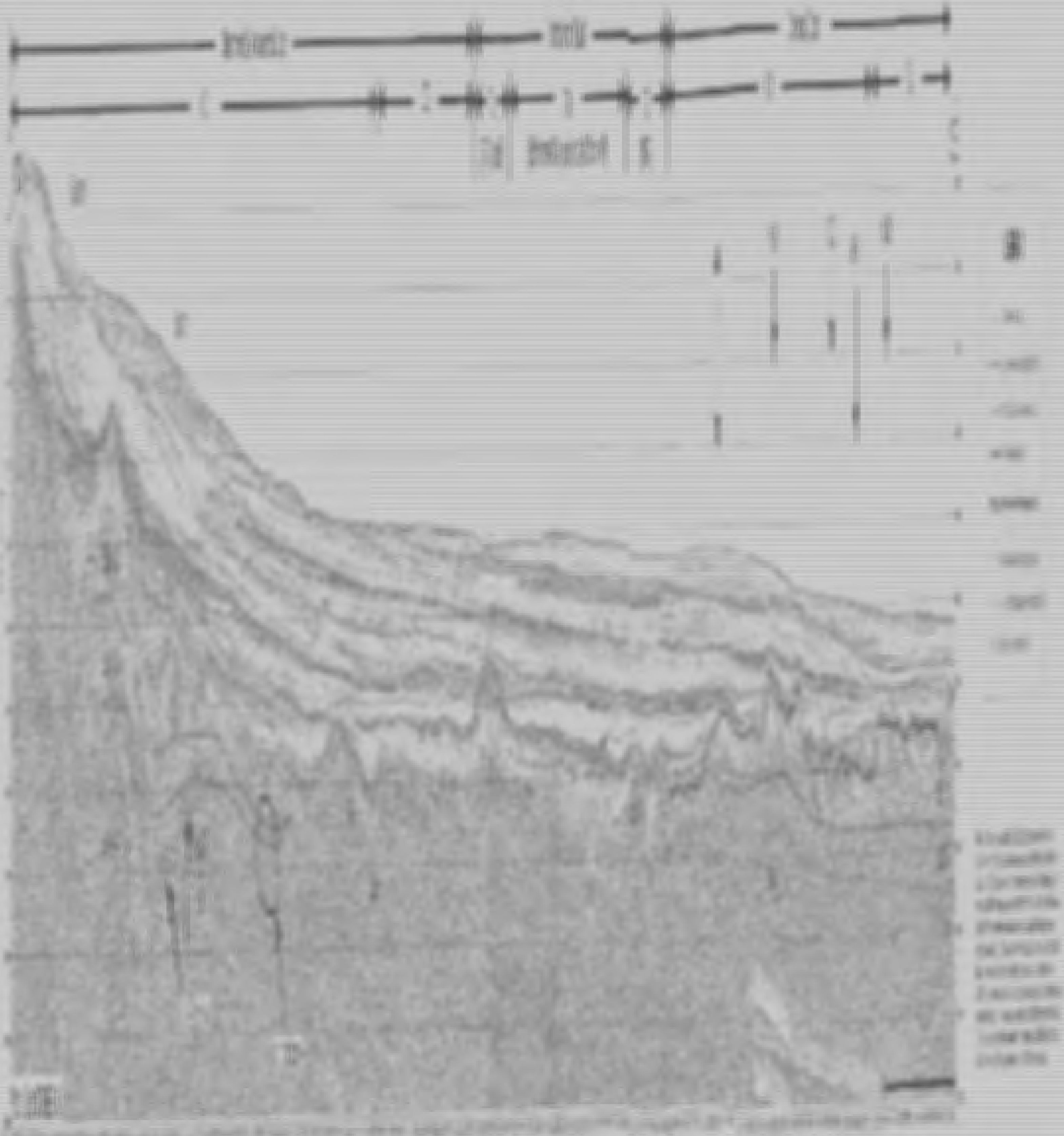

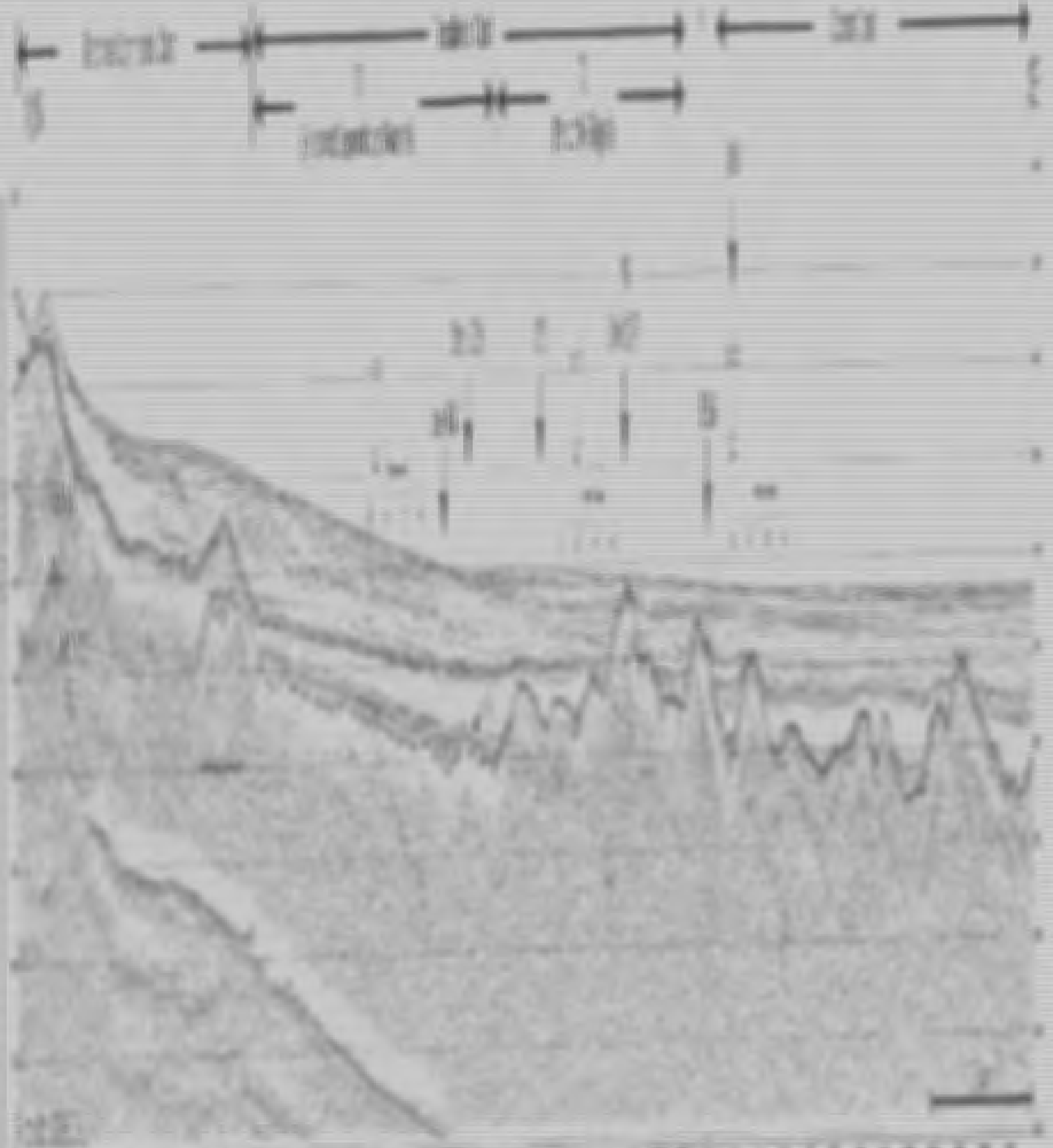

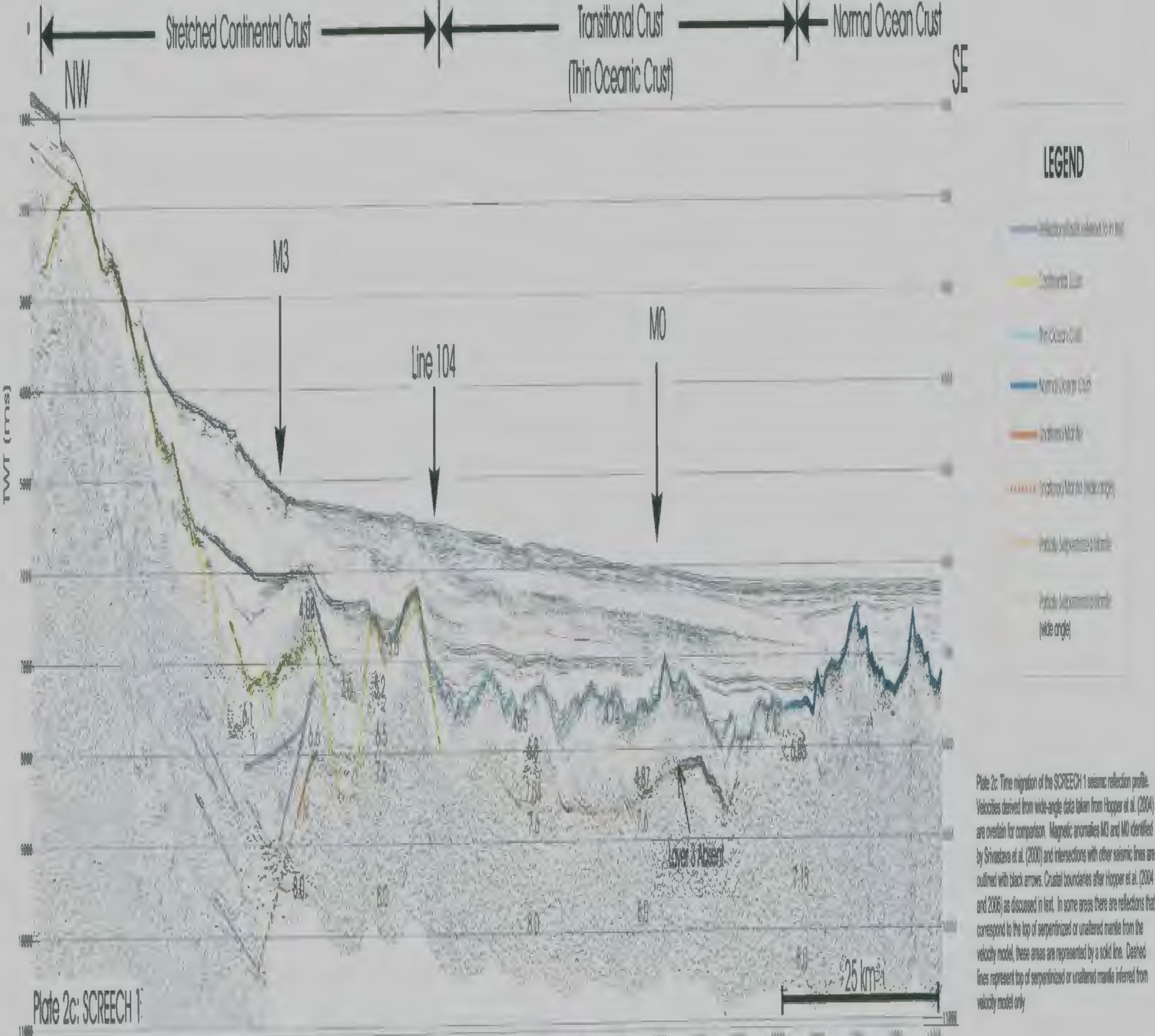

Plate 2c: Time migration of the SCREECH 1 seismic reflection profile. Velocities derived from wide-angle data taken from Hopper et al. (2004) are overlain for comparison. Magnetic anomalies M3 and M0 identified by Srivastava et al. (2000) and intersections with other seismic lines are outlined with black arrows. Crustal boundaries after Hopper et al. (2004 and 2006) as discussed in text. In some areas there are reflections that correspond to the top of serpentinized or unaltered mantle from the velocity model, these areas are represented by a solid line. Dashed lines represent top of serpentinized or unaltered mantle inferred from velocity model only

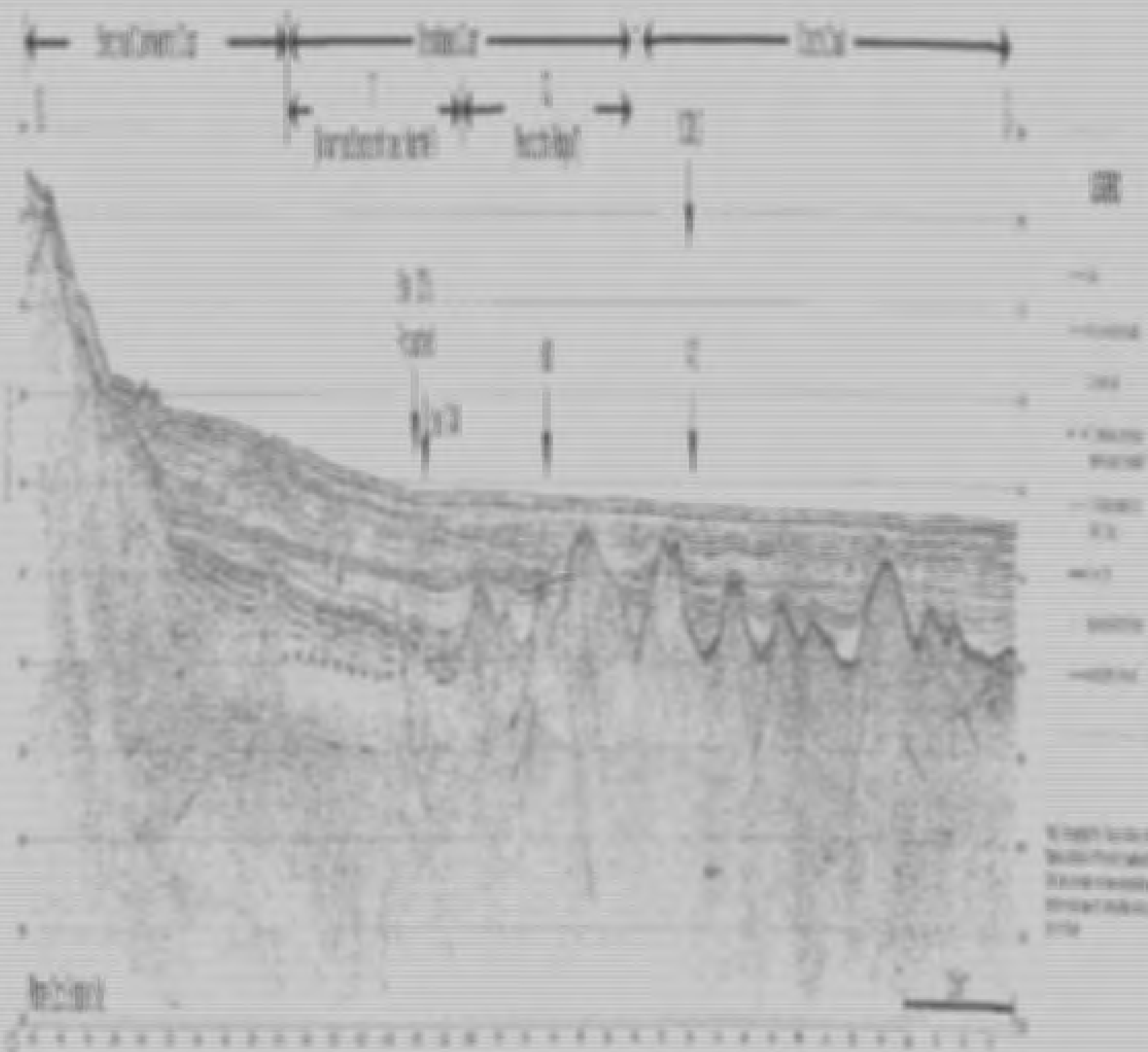

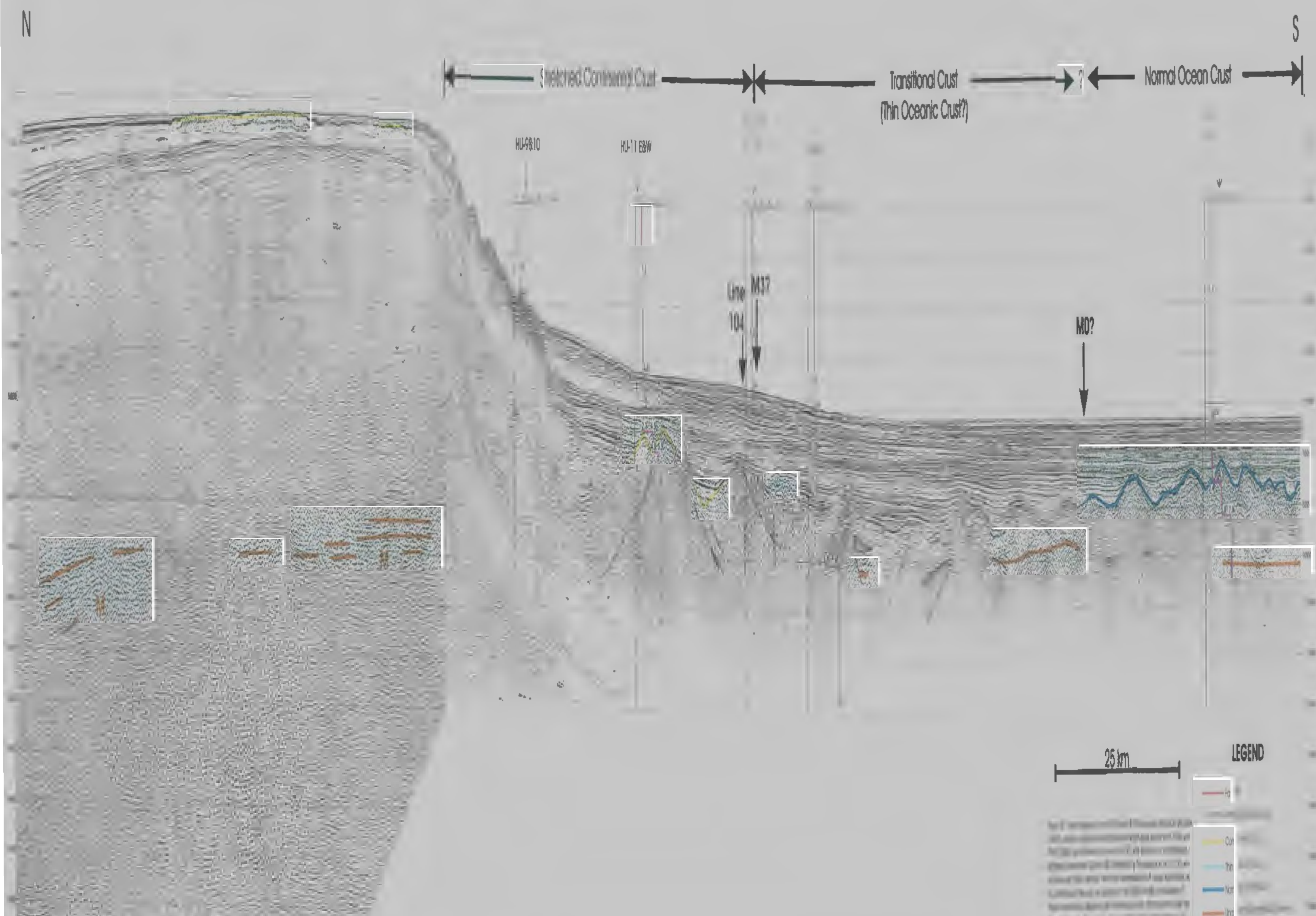

Plate 2e: Exhibit 63 and 54